

Structure formation during phase transitions in strongly interacting matter

D. N. Voskresensky,^{1,2}

¹BLTP, Joint Institute for Nuclear Research, RU-141980 Dubna, Russia

²National Research Nuclear University (MEPhI), Kashirskoe shosse 31,
115409 Moscow, Russia

December 27, 2022

Abstract

A broad range of problems associated with phase transitions in systems characterized by the strong interaction between particles and with formation of structures is reviewed. A general phenomenological mean-field model is constructed describing phase transitions of the first and the second order to the homogeneous, $k_0 = 0$, and inhomogeneous, $\vec{k}_0 \neq 0$, states, the latter may occur even in case, when the interaction is translation-invariant. Due to fluctuations, the phase transition to the state, $\vec{k}_0 \neq 0$, becomes the transition of the first order. Various specific features of the phase transitions to the state $\vec{k}_0 \neq 0$ are considered such as the anisotropic spectrum of excitations, a possibility of the formation of various structures including running and standing waves, three-axis structures, the chiral waves, pasta mixed phases, etc. Next, a formal transition to hydrodynamical variables is performed. Then focus is made on description of the dynamics of the order parameter at the phase transitions to the states with $\vec{k}_0 = 0$ and $\vec{k}_0 \neq 0$. In case of the phase transition to the inhomogeneous state the dynamics has specific features. Next the non-ideal hydrodynamical description of the phase transitions of the liquid–gas type in nuclear systems is performed. The ordinary Ginzburg–Landau model proves to be not applicable for description of an initial inertial stage of the seeds. Surface tension and viscosity are the driving forces of the phase transitions. Quasi-periodic structures are developed during the transitions. Next, the specific example of the pion condensation phase transition to the $\vec{k}_0 \neq 0$ state in dense, cold or warm nuclear matter is considered and then the nuclear system at high temperature and small baryon chemical potential is studied, when baryons become completely blurred and light bosons, e.g., pions, may condense either in $\vec{k}_0 = 0$ or $\vec{k}_0 \neq 0$ states. Then, for the scalar collective modes the phenomena of the Pomeranchuk instability and the Bose condensation in $\vec{k}_0 = 0$ or $\vec{k}_0 \neq 0$ states are studied and a possibility of a metastable dilute nuclear state is discussed. Next, possibility of the condensation of Bose excitations in the $\vec{k}_0 \neq 0$ state in the moving media is considered. Then Bose-Einstein condensation of pions with dynamically fixed number of particles is studied. Finally, specific purely non-equilibrium effects are demonstrated on an example of the sudden breaking up of the box filled by nucleons.

Contents

1 Introduction

2	Phenomenological description of phase transitions and structure formation	10
2.1	Phenomenological description of dissipative dynamics at phase transitions	10
2.1.1	The phase transition to the state $k_0 = 0$. Mean field approximation	10
2.1.2	Fluctuations of the order parameter, case $k_0 = 0$	11
2.1.3	Effective Lagrangian, equation of motion, phase transition to the state $k_0 \neq 0$. .	12
2.2	Description of Bose excitations	13
2.2.1	The ω, k expansion of Green function	13
2.2.2	Spectrum of excitations	15
2.3	Static inhomogeneous configurations and finite size effects	17
2.3.1	One-axis-like structures	18
2.3.2	Three-axis structures	20
2.3.3	Chiral waves	22
2.4	Mean field versus fluctuations	22
2.4.1	Critical temperature in the mean field approximation	22
2.4.2	Fluctuations in case of the phase transition to the state $k_0 \neq 0$	22
2.5	Transition from the order parameter to hydrodynamical variables	24
2.5.1	Schrödinger equation in hydrodynamical variables	24
2.5.2	Phase transition to the state $k_0 = 0$	25
2.5.3	Phase transition to the state $k_0 \neq 0$. One-axis periodic system	25
2.5.4	Phase transition to state $k_0 \neq 0$. Anisotropic three-axis crystal	26
2.5.5	Normal liquid	26
3	First-order phase transitions in slowly evolving systems	27
3.1	Typical pressure–density behavior at first-order phase transitions	27
3.1.1	Transition of liquid–vapor type	27
3.1.2	Mixed phases and pasta	29
3.2	Transition between homogeneous configurations	30
3.2.1	Phenomenological model	30
3.2.2	Limit $h = 0$ (second-order phase transition)	31
3.2.3	Transition from metastable to stable state	32
3.3	Transitions between inhomogeneous configurations	34
3.3.1	Simple phenomenological model of phase transition to the state $k_0 \neq 0$	34
3.3.2	Transition between two one-axis configurations	34
3.4	Transitions between homogeneous and inhomogeneous phases	36
4	Hydrodynamics of liquid–gas-type transition at small overcriticality. Nuclear liquid–gas and hadron–quark transitions	38
4.1	Stationary solutions	41
4.2	Dynamics of seeds at first-order phase transition from metastable state to stable state .	42
4.3	Evolution of bands ($d_{\text{sol}} = 1$) and two-dimensional seeds ($d_{\text{sol}} = 2$)	43
4.4	Dynamics of fluctuations in unstable region	44
4.4.1	Growth of fluctuations of small amplitude	44
4.4.2	Limit of a rather high thermal conductivity	46
4.4.3	First-order phase transition in the process of cooling	48
4.4.4	Sticking of domains	49

5	Pion condensation in dense and not too hot nuclear matter	49
5.1	Fermi liquid description of NN and πN interactions	49
5.2	Pion softening and pion condensation	53
5.3	Fluctuations with $k_0 \neq 0$ and where soft pions are in atomic nuclei	55
5.3.1	Pion fluctuations	55
5.3.2	Where soft pions are in atomic nuclei	57
5.4	Dynamics of pion-condensate phase transition	58
6	Fermion blurring and hot Bose condensation	60
6.1	System of strongly interacting light bosons – heavy fermions at $\mu_f = 0$	60
6.2	Scalar boson – fermion coupling	62
6.2.1	Approximation of a soft thermal loop	63
6.2.2	Intensity of multiple scattering	64
6.2.3	Density of fermion-antifermion pairs	65
6.2.4	Boson quasiparticles	66
6.2.5	Hot Bose condensation	67
6.3	Pseudo-vector boson – fermion coupling	67
6.3.1	Hot pion-nucleon vacuum. Nucleon blurring	67
6.3.2	$\Delta\bar{\Delta}$ resonance matter	69
6.3.3	Towards the description of the state of hot hadron porridge	69
7	Non-pionic excitations in Fermi liquids and possible condensation of scalar quanta	70
7.1	Particle-hole amplitude and Landau-Migdal parameters	70
7.2	Scalar excitations and condensation	71
7.2.1	Spectrum of scalar excitations	71
7.2.2	Condensation of scalar field	73
7.2.3	Possibility of dilute metastable scalar condensate states	74
8	Condensation of Bose excitations in nonuniform state in uniformly moving media	76
8.1	Physical picture and general phenomenological treatment	76
8.2	Condensation of zero-sound-like excitations with a non-zero momentum and frequency in a moving Fermi liquid	78
8.2.1	Condensation in rectilinearly moving Fermi liquid	78
8.2.2	Condensation in two interpenetrating dilute streams of fermions	79
8.2.3	Vortices	80
9	Quantum and finite size effects in nonequilibrium particle distributions	81
9.1	Bose–Einstein condensation of relativistic bosons at a dynamically fixed particle number	81
9.2	Breaking of potential box filled by particles	85
9.3	Nucleon distributions	85
9.4	Pion distributions	86
10	Conclusion	87

1 Introduction

It is commonly believed that the strong interaction theory on fundamental level deals with quarks and gluons described by the QCD Lagrangian and the Lagrange equations of motion. The specific property of the QCD interactions is the presence of the so called asymptotic freedom at short distances

(associated with vanishing of the running QCD coupling, $\alpha_s(q)$, at high momenta) and the confinement at large distances, $d \gtrsim r_\Lambda \sim (0.2 - 0.4)$ fm, related to small momenta.

In the laboratory the quark-gluon interactions are studied in hadron-hadron, hadron-nucleus and nucleus-nucleus collisions at high collision energies. Even at highest energies in nucleus-nucleus collisions at the Large Hadron Collider (LHC) in TeV region of the momenta of colliding particles, $\alpha_s(q) \gtrsim 10^{-1}$ and the region of the asymptotic freedom is not yet reached. In dense baryon matter a perturbative QCD description is expected to be valid only for baryon densities $n \gtrsim 40n_0$, where $n_0 \simeq 0.16\text{fm}^{-3} \simeq 0.5m_\pi^3$ is the nuclear saturation density, $m_\pi \simeq 140$ MeV is the pion mass, $\hbar = c = 1$. Nevertheless most of the researchers believe that the deconfinement regime has been reached in the violent heavy-ion collisions at the Super Proton Synchrotron (SPS) at CERN, the Relativistic Heavy-Ion Collider (RHIC) at Brookhaven, and at the LHC at CERN energies, when typical temperature of excited matter is $T \gtrsim m_\pi$ and the particle density may vary from $n \ll n_0$ to n significantly exceeding n_0 . However the state of the matter is not weakly interacting quark-gluon plasma, as it was believed during a long time [1], but the strongly interacting quark-gluon plasma, being not badly described by the relativistic non-ideal hydrodynamics at very small but finite value of the shear viscosity, cf. [2, 3]. Being formed in the nucleus-nucleus collision, the nuclear fireball is expanded into vacuum, distance between quarks increases, they are hadronized at certain expansion stage and then the system breaks up. The last stage is already well described in terms of the purely hadronic degrees of freedom, cf. [4]. At lower collision energies, \lesssim several GeV /A (per nucleon), one deals with the hadron matter when the baryon density is $n \lesssim 3n_0$ and $T < m_\pi$, cf. [5, 6, 7, 8].

Calculations show that in the heaviest compact stars the baryon density in the center may reach up to $(6 - 8)n_0$, e.g. cf. [9]. Again typical distances between particles are such that asymptotic freedom regime is not realized. Various possibilities are considered: purely hadronic neutron stars, hybrid stars, where a part of the interior consists of the strongly interacting quark-gluon plasma, quark nuclearites (strange-quark objects of sizes of meteorites) and smaller size quark nuggets consisting of strange quark matter, cf. [10, 11, 12]. New branch of compact object astrophysics is related with the gravitational wave detections by LIGO and VIRGO Collaborations from mergers of compact stars. The Neutron Star Interior Composition Explorer (NICER) observations of rotation-powered millisecond pulsars get information about the mass-radius relation of compact stars and the equation of state of the dense matter in their cores, cf. [13]. Future gravitational wave measurements may help to constrain the onset densities of the strong phase transitions [14]. The future laboratory experiments at Nuclotron-based Ion Collider Facility (NICA) at Dubna and Antiproton and Ion Research (FAIR) at Darmstadt will complement actively continuing astronomical observations, cf. [15].

In case of the quark-gluon plasma one deals with quarks and gluons as the building blocks of matter, whereas in the description of hadronic matter with baryons and mesons as the building blocks glued together. In condensed matter physics the building blocks of matter are the atoms and electrons. Physicists are interested in how these basic building blocks, glued together by quantum forces, form new possible states of the matter. For example, they can form crystalline solids, liquid crystals, amorphous media, liquids, gases, magnets, superfluids and superconductors, etc. The success of the condensed matter and the particle physics in the previous and this centuries is associated with usage of the principle of spontaneous symmetry breaking [16]. For example, a crystalline solid breaks translation symmetry, although the interaction among the building blocks is translation invariant. The pattern of the symmetry breaking (below the critical point of the transition) is described by order parameters having non-vanishing expectation values in the ordered state, and anomalous dispersion characterized by strong long-range correlations. In superconductors the gauge symmetry is broken. The effective field theory, is generally called the Landau theory in case of the real scalar order parameter and the Ginzburg–Landau theory in case of the complex order parameter. The latter was developed to describe superconductivity in metallic superconductors and the Ginzburg–Pitaevskii theory was constructed in application to neutral superfluids, as ^4He , cf. [17, 18, 19, 20]. More complex phases may exist in

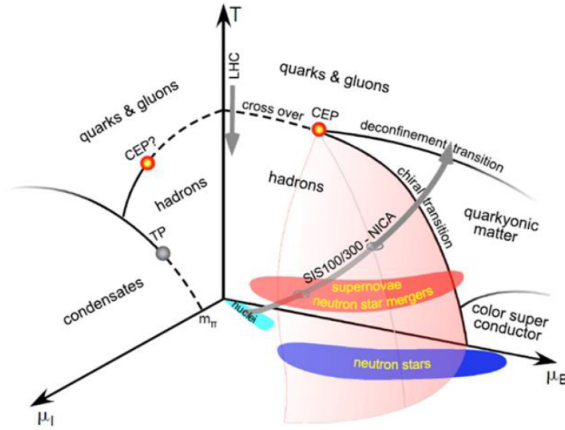


Figure 1: Sketch of the phase diagram for nuclear matter taken from [34].

superfluid ^3He , cold gases, liquid crystals, solids, anomalous superconductors and other substances, cf. [21, 22, 23, 24, 25, 26]. These phenomenological models give universal description of various phase transitions. In discovered new topological insulators, the bulk of two-dimensional samples is insulating, and the electric current is carried only along the edge of the sample [27]. The flow of this unidirectional current avoids dissipation and gives rise to a quantized Hall effect. These states are possible due to a combination of spin orbit interactions and time reversal symmetry [28]. A somewhat similar possibility of existence of a superconducting surface pion current in the piece of the dense nuclear matter in the ground state was found in [29].

Even ordinary water at different conditions may exist in 12 crystalline, 3 glass states, as well as in liquid and vapor phases. The phase diagram of strongly interacting matter also contains many possible phases with phase transitions between them [10, 30, 31, 32, 33]. A part of various possibilities is shown in Fig. 1 from [34] as the temperature dependence on the baryon- and isospin- chemical potentials. One bounds the critical endpoint (CEP) of a possible deconfinement phase transition at finite density by $\mu_B \gtrsim 2.5T$ and $T \lesssim m_\pi$, where μ_B is the baryon chemical potential. Within the Schwinger–Dyson approach from the temperature dependent quark propagator one extracts the order parameter for the chiral transition, the quark condensate value, and order parameters for the deconfinement transition, the dressed Polyakov loop and the dual scalar quark dressing [35, 36].

At small baryon-chemical potentials and high temperatures QCD predicts a smooth crossover transition from hadronic matter to the quark-gluon plasma at a pseudo-critical temperature. Fit of the particle production at top RHIC and LHC energies done with the help of the hadron resonance model [37] yields the value for the pseudo-critical temperature $T_c \simeq (155 - 160)$ MeV. Chemical nonequilibrium approach [38, 39] yields a smaller value T_c . The value of the critical temperature predicted by the Lattice QCD calculations [40] for a chiral phase transition is still smaller, $T_{\text{chir}} < 135$ MeV. A primordial hadron-quark particle-antiparticle soup [34] (or a hadron-quark porridge, as dubbed in [41]), existed in the early Universe during microseconds after the Big Bang and is produced in the laboratory at high energy heavy-ion collision experiments at RHIC and at LHC. One [42, 43] suggests that chiral quarks are bound by color-electric flux tubes in a regime, which has been dubbed a “stringy liquid”. When temperature increases beyond $T_s \sim 3T_c$, the color-electric interactions between quarks get screened and the symmetry reduces to the expected chiral symmetry corresponding to a quark gluon plasma.

At a hot quasi-equilibrium stage very specific phenomena of the baryon blurring [44, 41, 45] and, might be, a hot Bose condensation for effectively light bosons are possible, since the strong coupling effects dominate over thermal disordering, cf. [41, 45]. For pions the hot Bose condensation may appear either in the s-wave state or in p-wave state at finite pion momentum, $k_0 \neq 0$, owing to a strong p-wave pion-nucleon interaction. In the latter case the condensate matter may form a glass-like state.

On the other hand, as it was shown in [46] and in a number of subsequent works, cf. [47, 48, 49, 50, 51, 52, 53, 54, 55], the Bose-Einstein condensation of pions can occur at a small baryon chemical potential in a nonequilibrium stage characterized by the dynamically fixed pion number provided an initial nonequilibrium state was overpopulated. Similarly, the Bose-Einstein condensation of gluons may arise [56, 57, 58, 59, 60].

Dynamics of the first-order phase transition has many specific features [61]. At a low temperature $T \lesssim (15 - 20)\text{MeV}$, in the interval of the nucleon density $0.3n_0 \lesssim n \lesssim 0.7n_0$, there may occur the first-order gas-liquid phase transition, which signatures were already observed in low-energy heavy-ion collisions, cf. [62, 63, 64, 65, 66, 67, 68, 69, 8]. References [70, 71] suggested a possibility of the condensation of the scalar quanta, as the result of the Pomeranchuk instability arising in some region of densities at $n < n_0$ in approximately isospin-symmetric matter. This phenomenon may also result in appearance of a metastable nuclear state at $n \ll n_0$. The clusterization and α Bose condensation have been also studied, cf. [72, 73, 74, 75] and references there.

Many effective models predict a first-order phase transition with a critical end-point (CEP), cf. [76]. Most dense and not too hot matter is expected to be formed in the heavy-ion collisions at NICA energies, as it is shown in Fig. 1. The hadron-quark phase transition may have similar signatures, as the liquid-gas one [61, 77, 78, 80, 81]. Passing of the spinodal instability region, the matter forms structures, which effects might be easier to observe than those associated with passing of the vicinity of the CEP, due to the slowing down effects in the latter case. Spinodal instabilities are also relevant for consideration of the pasta phase in neutron stars, cf. [82, 83].

Many other phases of QCD and hadron matter have been proposed, such as quarkyonic matter, which can be considered as a Fermi gas of quarks with confined thermal excitations [84], and a parity doubled baryon matter as a candidate for a chiral spin-symmetric regime of cold and dense QCD, which can be naturally embedded into the quarkyonic matter. The existence of a first-order phase transition ending in a critical point, as indicated in Fig. 1, is still under debate. For example, following the concept of the quark-hadron continuity, it is conjectured [85] that quark degrees of freedom may emerge gradually with increasing density and a partial restoration of the chiral symmetry.

The theory of normal Fermi liquids was built up by Landau and Migdal in Ref. [86, 87, 88, 89, 90], see in textbooks [18, 22, 23]. The Fermi liquid approach to the description of nuclear systems was developed by Migdal in [91, 92], see also [93]. In the Fermi liquid theory the low-lying excitations are treated explicitly whereas the short-range correlations are described with the help of several phenomenological Landau parameters. Pomeranchuk has shown in Ref. [94] that Fermi liquids are stable only, if certain inequalities on the values of the Landau parameters are fulfilled. The Fermi-liquid approach with the explicit separation of the in-medium pion exchange was formulated by A. B. Migdal for description of the cold nuclear matter, cf. [95], and then it was generalized for equilibrium systems at finite temperatures, cf. [96, 97, 98], and for nonequilibrium systems, cf. [99, 100, 6, 96, 7, 101]. It was shown that in nuclear matter soft modes with pion quantum numbers and the momenta $k \neq 0$ become efficiently occupied by pion-like excitations at non-zero temperature forming so called liquid phase of the pion condensate for $n > n_c^{(1)} \sim (0.5 - 0.8)n_0$, cf. [98, 7]. With increase of the baryon density these modes may become unstable to formation of the liquid-crystal-like or solid-like pion condensate. This pion condensation in a warm and dense nuclear matter predicted to occur for $n > n_c^\pi \sim (2 - 3)n_0$ is the example of the phase transition to the inhomogeneous state $k_0 \neq 0$, cf. [95, 102, 96]. In some models the pion condensation in the isospin symmetric matter may arise also in the s-wave state [103], whereas in neutron star matter $\pi^{\pm,0}$ may condense only in states with $k_0 \neq 0$, cf. [95, 96], due to the presence of the repulsive Weinberg-Tomazawa pion-nucleon interaction term.

Many different structures can be formed in the process of formation of the inhomogeneous condensate state $k_0 \neq 0$, cf. [104, 96, 105, 106, 107]. The most energetically profitable proved to be the alternating-layer structure [108, 109], in the dynamics a polycrystal is probably formed [105].

Antikaon K^- and \bar{K}^0 condensations may arise as in the s-wave state, cf. [110], as in the p-wave one

[111, 112, 113]. If the effective ρ meson mass decreases with increasing density, the s-wave non-abelian ρ^- meson condensation in interiors of the neutron stars may occur [114, 115, 116].

Being studied in the mean-field approximation the critical temperature of the pion condensation phase transition to the inhomogeneous state $k_0 \neq 0$ is rather high (typically $\gtrsim \epsilon_{F,N}$, where $\epsilon_{F,N}$ is the nucleon Fermi energy), cf. [117, 118]. Even in case of the second-order phase transition at $k_0 = 0$ fluctuations may significantly modify the phase diagram of the strongly interacting matter, cf. [19, 119]. In the mean-field theory, three phases meet at what is known as a Lifshitz point. One of the phases that meet at the tricritical point is an inhomogeneous phase. In the context of the Cooper pairing phases in dilute isospin-asymmetric nucleon matter discussion of the Lifshitz three-critical point can be found in [120]. Fluctuations smear the Lifshitz point [121]. Strong color superconducting fluctuations in dense nuclear matter are expected to occur even significantly above CEP, cf. [122, 123]. In heavy-ion collisions they might be manifested at $T \lesssim (1.5 - 2)T_c$, provided the critical temperature of color superconductivity, T_c , is sufficiently large (e.g., if $T_c \gtrsim (50 - 70)\text{MeV}$). Reference [124] supported these estimates of [122, 123]. Di-lepton and photon yields in heavy-ion collisions can be affected by pre-critical fluctuations [124, 125]. Note here also the geometrical effect on fluctuations near the critical point, cf. [122, 123]. Effectively one deals with the 3d geometry, if the coherence length $l \sim 1/\sqrt{|T - T_c|}$ (estimated here in the mean-field approximation) fulfills inequalities $l < R_{\parallel}, l < R_{\perp}$; one deals with 2d geometry, if $R_{\perp} > l > R_{\parallel}$; and with the 1d geometry, if $R_{\parallel} > l > R_{\perp}$, where R_{\parallel} and R_{\perp} are typical sizes of the system in parallel and perpendicular directions. For $l > R_{\parallel}, l > R_{\perp}$ the geometry is so called 0-dimensional. These effects reflect, e.g., in the temperature dependence of the specific heat (associated with the variance of the energy), $C_V \sim 1/\sqrt{|T - T_c|}$ for 3d and $C_V \sim 1/(T - T_c)^2$ for d=0. So, in principle, such a geometrical effects can be manifested in not-central heavy-ion collisions.

Note here that even if in the mean-field consideration the phase transition to the state $k_0 = 0$ is of the second-order, inclusion of electromagnetic fluctuations results in a weakly first-order phase transition in superconductors, cf. [126]. Fluctuations near the critical point of the phase transition to the state $k_0 \neq 0$ prove to be so strong that they necessarily lead to the change of the order of the phase transition from the second-order to the first-order, cf. [127, 128, 129, 97, 98, 130, 131, 132, 133, 104, 6, 96, 7, 134, 135].

The matter with a large baryon chemical potential is reached in compact stars such as neutron stars and hypothetical hybrid and strange stars, cf. [110, 136, 137, 138, 139, 140, 141] and references therein. Thereby, figure 1 indicates also the regions of cosmic nuclear matter realized in neutron stars, neutron star mergers, and hypothetical hybrid stars and strange stars, and nuclearites and smaller size strange quark nuggets, located at large baryon chemical potentials, low temperatures, and finite isospin chemical potentials. The idea of nuclearites and strange stars [11, 12] was preceded by the idea of pion condensate superheavy nuclei [142, 143] and nuclei-stars [144, 96] glued by the inhomogeneous $k_0 \neq 0$ charged pion condensate and electrons. Recent paper [145] studied consequences for neutron star phenomenology that would follow from the existence of a possible stable sexaquark (S) state with the quark content $uuddss$. The authors showed that the hypothesis does not contradict to the current astrophysical constraints. If in the nature existed very heavy (with the mass $m_{DM} \gg m_N$, where m_N is the nucleon mass) stable charged dark matter (DM) particles, there would also exist nuclearites and nuclei-stars consisting of ordinary approximately isospin-symmetric nuclear matter at $n \simeq n_0$ stabilized by heavy charged dark matter particles [146].

Nucleons in nuclear matter form Cooper pairs but with small gaps, typically $T \lesssim$ several MeV, cf. [147, 101, 26]. Paired neutrons form neutron superfluid phases, paired protons form superconducting phases. In presence of not a strong deviation of proton and neutron Fermi seas the nucleons may form np pairs and the gap may form a one-dimensional wave (Fulde-Ferrell-Larkin-Ovchinnikov state [148, 149, 150]).

At densities above $(2 - 3)n_0$ Fermi seas of the hyperons [151] and Δ isobars [152, 153, 154, 155, 156] can be occupied. It typically occurs by the third-order phase transition (in the sense of Ehrenfest at the

third-order phase transition a thermodynamic potential turns out to have a discontinuity in the third derivative in n or T in critical point, whereas first and second derivatives are continuous.

Hybrid stars and strange stars should be color superconductors at $T < T_c$, cf. [157, 158]. Value of the pairing gap and the critical temperature depend on the phase under consideration. Many phases of the color superconducting matter were suggested, cf. [159, 160, 161, 162]. Estimates for the gaps vary from $T \sim 1\text{MeV}$ for spin-color-locking phase till hundred MeV or more for color-flavor-locked phase. Description of color superconductors by the generalized Ginzburg–Landau model was suggested in [163] and it was applied to description of fluctuations in [164, 122, 123, 165, 124, 125]. An inhomogeneous di-quark condensation may develop when the gap energy is comparable with m_s^2/μ_q , where $m_s \simeq (90-150)$ MeV is the strange quark mass and $\mu_q = \mu_B/3$ is the quark chemical potential. Such an inhomogeneous color superconducting state gives rise to a crystal structure, cf. [161, 150, 166].

The phase structure at high baryon densities and moderate temperatures can be considerably modified by the presence of the inhomogeneous QCD phases. Pion and kaon condensates may appear not only in the hadron matter but also in the quark matter, cf. [167]. Basing on the consideration of the $\sigma - \pi^0$ condensation [107] in nucleon matter characterized by the chiral wave with $k_0 \neq 0$, many models were suggested, cf. [168, 169, 170, 171, 134, 172]. Reference [173] derived inhomogeneous configurations of pion fields characterized by a non-vanishing topological charge that can be identified with baryons. Quark and pion condensates at finite isospin density studied in chiral perturbation theory may result in existence of pion stars [174].

Another interesting feature of the first-order phase transition in isospin-asymmetric matter characterized by more than one conserved charge is the possibility of the existence of so-called pasta phases [175]. In case of the compact stars the conserving charges are the baryon and electric charges. The interplay between Coulomb and surface tension leads to the possibility of the appearance of structures of different geometry as droplets, rods and slabs and configurations of a more whimsical form, cf. [176, 177, 178]. Important role is played by the Debye screening effects, cf. [179, 180]. Only with taking into account of finite size effects one is able to construct a correct description of the pasta phases [179, 180, 181, 182, 183, 138, 139, 140]. Nuclear pasta may exist in the inner crusts of neutron stars at $n \lesssim 0.7n_0$, cf. [176, 177, 181, 141]. In dense interiors there may exist regions of the hadron-quark [179, 180, 183] and pion and kaon [182] pasta phases. In heavy-ion collisions the conserving quantities are the baryon number and isospin. Specifics of the first-order phase transitions in collisions of asymmetric nuclei has been discussed in [65, 66, 67, 68, 69, 8]. It would be interesting to seek possible manifestations of the formation of the pasta structures in heavy-ion reactions [8].

Another part of problems is associated with the behavior of the quark-gluon and hadron media in external fields. First estimates [184] of the value of the strength of the magnetic field reached in peripheral heavy-ion collisions at energies \lesssim few GeV/A yielded $H \sim (10^{17} - 10^{18})$ G, that was later supported by numerical calculations [185]. Presence of strong magnetic fields and the rotation (with frequencies $\omega \lesssim 10^{22}\text{Hz}$ in case of heavy-ion collisions) influences the superfluids. Strong magnetic fields $\gtrsim 10^{15}\text{G}$ exist at the surface of magnetars. Fields $H \sim 10^{17}\text{G}$ influence the pasta phase in the inner core, cf. [82, 83]. In interiors of neutron stars the magnetic field may reach even higher values, $H \sim 10^{18}\text{G}$, cf. [184, 96]. Superconductors and superfluids specifically react on the magnetic field and the rotation, respectively. Abrikosov mixed phases can be formed. Forms of the vortices in case of inhomogeneous ($k_0 \neq 0$) and homogeneous ($k_0 = 0$) condensates prove to be different, cf. [184, 96].

Most of the problems touched above were studied for the equilibrium systems. Models describing inhomogeneous condensates are much less developed than those considering homogeneous condensates. Dynamics of the formation of various phases is still less studied. To partially cover this gap, the present review discusses besides effects of the condensation at $k_0 = 0$, the condensation at $k_0 \neq 0$ at equilibrium and nonequilibrium conditions.

The paper is organized as follows. Section 2 discusses a general phenomenological model for description of phase transitions. First we introduce a phenomenological description of dissipative dynamics of

phase transitions at $k_0 = 0$. Then Green function of the Bose excitations in matter is introduced and its expansion in frequencies and momenta is performed. Next, the spectrum of over-condensate excitations is found and its peculiarities in case of the running wave condensate with $k_0 \neq 0$ are discussed. Then various static configurations of the condensate field at $k_0 \neq 0$, one-axis and three-axis structures, chiral waves etc, are described. The specific role of fluctuations at the phase transition to the $k_0 \neq 0$ state is discussed. Then transition from the equation for the order parameter to hydrodynamical variables is performed as in case of the phase transition to the state $k_0 = 0$ as for $k_0 \neq 0$. In Section 3 the phase transitions in slowly evolving systems are studied. The congruent first-order phase transition of the gas–liquid type and the non-congruent transition to the pasta phase are considered. The dynamics of the first-order phase transition to the state $k_0 = 0$ is described. It depends on whether the initial seed of the stable phase is formed in the metastable region or within the spinodal region. Besides spherical droplets, dynamics of strongly non-spherical configurations is considered. Then focus is made on the description of dynamics of configurations at the first-order phase transition to the state $k_0 \neq 0$. Dynamical descriptions of the transitions between inhomogeneous phases and between homogeneous and inhomogeneous phases are performed. Formation of polycrystal and glass phases are discussed. In Section 4 the hydrodynamical description of the first-order and the second-order phase transitions of the liquid-gas type in terms of the local density-temperature variables is performed at assumption of a small over-criticality. From non-ideal hydrodynamical equations, the equation for the order parameter is derived. The initial (inertial) stage of the evolution of seeds differs from that described by the ordinary Ginzburg–Landau theory whereas the long-time tail is described by the Ginzburg–Landau equation. The dynamics of the growth of seeds formed in metastable phase is studied. At a low viscosity quasi-periodic oscillations occur. Then, the dynamics of fluctuations in the spinodal region is considered and again during time evolution, quasi-periodic configurations appear. In Section 5 we focus on the explicit example of the pion condensate phase transition to the state $k_0 \neq 0$ in cold and warm nuclear matter. The liquid/amorphous phase of the condensate appears already for $n > n_c^{(1)} \sim (0.5 - 0.7)n_0$ and the solid-like phase of the pion condensate may arise for $n > n_c^\pi \sim (1.5 - 3)n_0$. Peculiarities of the dynamical description of the pion condensate phase transition are reviewed. Section 6 studies issues of the fermion blurring and hot Bose condensation at conditions of a small or zero baryon chemical potential. For pions obeying a strong p-wave pion-baryon interaction, the hot Bose condensation may occur either in the state with $k_0 = 0$ or in the state $k_0 \neq 0$. Section 7 describes non-pionic excitations in a Fermi liquid and a possibility of the condensation of the scalar quanta in the region of the low densities, $n < n_0$, where there arises the Pomeranchuk instability. Section 8 discusses peculiarities of the condensation of Bose excitations in the state $k_0 \neq 0$ in the uniformly moving media. Section 9 demonstrates the role of quantum and finite size effects in nonequilibrium distributions. First, the Bose–Einstein condensation of bosons in nonequilibrium systems is considered at the stage when inelastic processes are not efficient. The possibility of the Bose–Einstein condensation of pions in ultrarelativistic heavy-ion collisions is discussed. Then, a toy model of the breaking up of a box filled by nucleons is considered. Nucleon distributions prove to be oscillating and the pion distributions follow a power law. Main results are discussed in the Conclusion.

2 Phenomenological description of phase transitions and structure formation

2.1 Phenomenological description of dissipative dynamics at phase transitions

Dissipative dynamics of the phase transitions is usually described by the phenomenological Ginzburg–Landau equation, cf. [17, 186, 187],

$$\partial_t \psi = -\hat{\Gamma}(\hat{\Delta}) \frac{\delta \delta F}{\delta \psi} + \xi(t, \vec{r}), \quad \hat{\Delta} = \partial_i^2, \quad i = 1, 2, 3, \quad (1)$$

where δF is the part of the free-energy density dependent on the order parameter ψ . The order parameters can be of the scalar, vector, tensor origin in dependence of the system under consideration. For description of the quantum liquids one uses the macroscopic wave function as the complex order parameter, cf. [18, 20, 21]. In case of smooth distributions the relaxation rate $\hat{\Gamma} = \Gamma_0 + \Gamma_1 \hat{\Delta} + \dots$ is expanded in the series of the operator $\hat{\Delta}$, Γ_i are coefficients of the expansion. For $\Gamma_0 > 0$, $\Gamma_1 = 0$ one deals with long-wavelength behavior of the non-conserving order parameter ψ . For $\Gamma_0 = 0$, $\Gamma_1 > 0$, the long-wavelength behavior of the conserved order parameter is well described by the stochastic diffusion equation. The meaning of Eq. (1) is that in a weakly nonequilibrium configuration a small rate of the relaxation of the system to the equilibrium is proportional to the thermodynamic force describing deviation from the equilibrium. In the linear response theory the kinetic coefficients Γ_i are related to correlators of the fluctuations of thermodynamic quantities in the hydrodynamical limit, cf. [188, 189]. The stochastic noise term $\xi(t, \vec{r})$ is assumed to be Gaussian and white. Its width is determined by the fluctuation-dissipation relation

$$\langle \xi(t, \vec{r}) \xi(t', \vec{r}') \rangle = a \delta(t - t') \delta(\vec{r} - \vec{r}'), \quad (2)$$

where the value a , dependent on the diffusion coefficient and the temperature T , cf. [18], as well as coefficients Γ_i , are supposed to be smoother t, \vec{r} variables compared to the order parameter $\psi(t, \vec{r})$. Recent applications of diffusive dynamics of critical fluctuations to heavy ion collisions see, e.g., in [190, 191]. Within the mean field consideration one may put the ξ term zero.

2.1.1 The phase transition to the state $k_0 = 0$. Mean field approximation

In case of the phase transition to the state $k_0 = 0$, the ψ dependent part of the free energy is usually also expanded in the order parameter and the operator $\hat{\Delta}$ up to a linear term. Expansion in ψ is performed at least up to ψ^4 term. For consideration of the phase transitions in non-uniform state $k_0 \neq 0$ expansion is done at least up to a quadratic term. In the simplest case for description of quasi-uniform quasi-equilibrium configurations one chooses the order-parameter dependent part of the free-energy density in the form [17]

$$\delta \mathcal{F} = \frac{1}{2} (\nabla \psi)^2 + \frac{1}{2} m^2 \psi^2 + \frac{1}{4} \Lambda \psi^4 - h \psi, \quad (3)$$

with temperature and density dependent coefficients m^2 , h and Λ . In the mean-field approximation the coefficients are expanded in the Taylor series near the critical point, e.g., in $T - T_c$. To describe the second-order phase transition in the simplest case one chooses $m^2 = \alpha_0(T - T_c)$, i.e. changing the sign in the critical point of the second-order phase transition, $\alpha_0 > 0$ to get nontrivial solution for ψ at $T < T_c$. The value Λ is chosen to be positive for the stability of the resulting state, $h = 0$ in case of the second-order phase transition and $h \neq 0$ in case of the first-order phase transition.

To describe superfluidity and superconductivity, when the flux/current can be nonzero, one should use the complex order parameter such as the macroscopic wave function. In these cases one deals with the second-order phase transitions and one uses [18],

$$\delta\mathcal{F} = \frac{1}{2}|\nabla\psi|^2 + \frac{1}{2}m^2|\psi|^2 + \frac{1}{4}\Lambda|\psi|^4. \quad (4)$$

2.1.2 Fluctuations of the order parameter, case $k_0 = 0$

Taking into account fluctuations of the order parameter in the vicinity of the critical point of the second-order phase transition results in a non-analyticity of the thermodynamical potentials and in divergences in the critical point of their second derivatives, such as the specific heat and magnetic susceptibility. Therefore Taylor expansion of the thermodynamical potential in $T - T_c$, being employed within the mean-field approximation, fails in the fluctuation region near the critical point, cf. [19].

In classical systems and also at not too small temperatures in quantum systems, quantum fluctuations are suppressed compared to thermal fluctuations. Fluctuation theory of phase transitions is a well developed field, cf. [119]. The width of the fluctuation region near the critical point is estimated from the so called Ginzburg criterion: the probability of the fluctuation $W \sim e^{-\delta F(V_{\text{fl}})/T}$ becomes ~ 1 for $\delta F(V_{\text{fl}}) \sim T_{\text{fl}}$ where $\delta F(V_{\text{fl}})$ is the work necessary to prepare the fluctuation in the minimal volume $V_{\text{fl}} \sim l_0^3$ for fluctuation, where l_0 is the typical length of the change of the order parameter. In case of the phase transition to the state $k_0 = 0$ one may estimate $l_0 \sim 1/|m|$, where m is the coefficient in (3), (4). As it was mentioned, dealing with the second-order phase transition in the mean field approximation one usually takes $m^2 = \alpha_0(T - T_c)$ and α_0, Λ are positive constants. Then the coherence length behaves as $l_0 \sim 1/\sqrt{|T - T_c|}$ and one easily estimates the value T_{fl} .

Cooper pairing fluctuations are associated with the formation and breaking of excitations of Cooper pairs out of the condensate. In case of clean metallic superconductors the region $|T_c - T_{\text{fl}}|$ proves to be very narrow and thereby the mean field approximation works very well. In case of the superfluid with a strong interaction between particles, as ^4He , fluctuations prove to be strong up to $T = 0$. The width of the energy region near the critical temperature, where fluctuations essentially contribute, is characterized by the Ginzburg number, $Gi = |T_{\text{fl}} - T_c|/T_c$. Gi proves to be tiny for clean conventional superconductors but might be ~ 1 for strongly interacting systems.

To take into account fluctuations more carefully one either uses the methods of scale invariance and ϵ -expansion or, as in case of the description of superfluid ^4He , in (4) one presents coefficients $m^2 = \alpha_0(T - T_c)|T - T_c|^{\alpha-1}$ and $\Lambda = \beta_0|T - T_c|^\beta$ with algebraic values α and β , cf. [19]. In the latter case one may find the coefficients α and β from the condition that the Ginzburg number should not depend on the quantity $T_{\text{fl}} - T_c$ and from the experimental fact that the specific heat in this case may diverge not stronger than logarithmically, cf. [192]. Thus one finds $\alpha = 4/3$ and $\beta = 2/3$, these values are in agreement with the data, see [19].

In interiors of most massive compact stars a color superconducting matter may exist. Temperatures are not as high and mean-field consideration is relevant for many purposes. To produce a color superconducting matter in the laboratory one needs to cook a dense but not too hot Cooper-paired quark matter. For that most relevant are probably the NICA and FAIR facilities. Although the temperatures at relevant densities permitted in heavy-ion collisions are most likely larger than the critical temperature T_c of the color superconductivity, one may rise the question about a possible manifestation of the precursor phenomena of the color superconducting phase transition, if the value T_c is rather high (for $T_c \gtrsim (50 - 70)$ MeV). Reference [164] considered such a possibility within the Nambu–Jona-Lasinio model and estimated $|T_{\text{fl}} - T_c| \lesssim (0.1 - 0.2)T_c$. References [122, 123] employed estimate [119] $Gi \sim A(T_c/\mu_q)^4$, with $A \sim 500$ for the case of color superconductors. To compare, for clean metals [119] one has $A \sim 100, \mu_q \rightarrow \mu_e$, where μ_q and μ_e are the quark and electron chemical potentials. Thus in case under consideration $Gi \sim 1$, if T_c is rather high, $T_c \sim (1/3 - 1/5)\mu_q$, and we expect a broad

region of temperatures, where fluctuation effects might be important. Thus Refs. [122, 123] estimated $T_{\text{fl},<} \lesssim 0.5T_c$ for $T < T_c$ and $T_{\text{fl},>} \sim 2T_c$ for $T > T_c$ and Ref. [124] also estimated $|T_{\text{fl}} - T_c| \sim 0.5T_c$. These estimates are rather optimistic to seek at least some signatures of the color superconducting fluctuations of the di-quark gap in the course of the heavy ion collisions. The color superconducting fluctuations might be also relevant for an initial stage of the hybrid star evolution, if T_c is $\gtrsim 50$ MeV. They may affect the neutrino radiation of the most massive hot hybrid stars and the heat transport at an initial stage of their evolution.

2.1.3 Effective Lagrangian, equation of motion, phase transition to the state $k_0 \neq 0$.

Let us first consider a complex classical condensate field. In case of the pair interaction including the retardation effects, the equation of motion for the order parameter describing a second-order phase transition, like that occurring in ^4He , can be presented as follows [105]:

$$\hat{D}^{-1}(\partial_t, \nabla)\psi(t, \vec{r}) - \psi(t, \vec{r}) \int |\psi(t+t', \vec{r}+\vec{r}')|^2 U(t', \vec{r}') dt' d\vec{r}' = 0, \quad (5)$$

where $D(\omega, k)$ is the boson Green function related to the ψ field in the medium, $\hat{\omega} = i\partial_t$, $\hat{\vec{k}} = -i\nabla$, cf. the Gross-Pitaevskii equation that follows for the static local potential U , cf. [18, 24].

Expanding $\psi(t+t', \vec{r}+\vec{r}')$ in the series in t', \vec{r}' one presents Eq. (5) as

$$\hat{D}^{-1}(\partial_t, \nabla)\psi(t, \vec{r}) - \psi(t, \vec{r}) \hat{\Lambda} |\psi(t, \vec{r})|^2 = 0, \quad (6)$$

with $\Lambda = \Lambda_0 + \Lambda_{12}\partial_t + \Lambda_{21}\Delta + \dots$, where $\Lambda_0 > 0$ for stability of the ground state and $\Lambda_{12}, \Lambda_{21}, \dots$ are some complex constants. The equation describing weakly non-ideal Bose gas placed in an external static field [18] follows from Eq. (6) as

$$i\partial_t\psi = -\left(\frac{1}{2m}\Delta + \mu\right)\psi + \psi \int |\psi(t, \vec{r}')|^2 U(\vec{r} - \vec{r}') d\vec{r}'. \quad (7)$$

For $\mu < 0$ and $U > 0$ it describes the phase transition to the homogeneous condensate state, $k = 0$, since the kinetic k^2 term enters the free energy with the positive sign.

Pions undergo a strong pion-nucleon attraction in the p-wave that may cause pion condensation in sufficiently dense nucleon matter [95, 96]. To describe the pion condensate phase transition to the state $k \neq 0$ in a dense ($n > n_c$) equilibrium nuclear matter one may employ the following Fourier representation of the Fourier transform of the Landau free energy, cf. [130],

$$\delta F[\phi] = \sum_{\vec{k}} [\omega_0^2 - \alpha_4(\vec{k}^2 - k_0^2)^2] \vec{\phi}_{\vec{k}} \vec{\phi}_{-\vec{k}} + \Lambda_1 (\sum_{\vec{k}} \vec{\phi}_{\vec{k}} \vec{\phi}_{-\vec{k}})^2 + \sum_{\vec{k}_i} \Lambda_2 (\vec{k}_i) \vec{\phi}_{\vec{k}_1} \vec{\phi}_{\vec{k}_2} \vec{\phi}_{\vec{k}_3} \vec{\phi}_{\vec{k}_4} \quad (8)$$

with positive Λ_1 and Λ_2 , $\vec{\phi} = (\phi_1, \phi_2, \phi_3)$ is the isospin-vector pion field. Differences between various crystalline and liquid structures are mainly determined by the term $\propto \Lambda_2$, which is usually rather small, $\Lambda_2 \ll \Lambda_1$. The phase transition occurs for $\omega_0^2 = -D^{-1}(\omega_c, k_0) < 0$, ω_c is the critical frequency and $k_0 \neq 0$ is the value of the momentum of the condensate corresponding to the minimum of $-D^{-1}(\omega_c, k)$, $\vec{\phi} = (\phi_1, \phi_2, \phi_3)$ is the isospin-vector pion field.

Further to be specific let us consider the case of the two-component (complex) classical field interacting with the medium consisting of heavy fermions. The part of the effective Lagrangian density depending on the condensate field, the fermion density n and the temperature T , can be expanded in the condensate field and time-space gradients as

$$\begin{aligned} \langle \mathcal{L} \rangle = & \left[\psi^* \hat{D}^{-1}(\hat{\omega}, \hat{\vec{k}}, n, T) \psi - \frac{1}{2} |\psi|^2 \hat{\Lambda}(\hat{\omega}, \hat{\vec{k}}, n, T) |\psi|^2 \right] \\ & + h\psi \left(\frac{\psi^* e^{2im\pi}}{\psi} \right)^{1/2} + h\psi^* \left(\frac{\psi e^{2im\pi}}{\psi^*} \right)^{1/2}. \end{aligned} \quad (9)$$

Here and further we use notations $\Re Z = \text{Re}Z$, $\Im Z = \text{Im}Z$. Averaging is assumed to be done over all degrees of freedom besides the given boson field described by the complex ψ variable.

The last two terms in (9), with $h > 0$, permit to describe first order phase transitions from metastable to stable homogeneous, $k_0 = 0$, or inhomogeneous, $k_0 \neq 0$, states. We have chosen a simplified form of the $|\psi|^4$ term. The multiplier $e^{2im\pi} = 1$ is introduced to recover two signs of the square root for $m = 0, 1$; and -1 is treated as $e^{i\pi}$, so $\psi \sqrt{\frac{\psi^* e^{2im\pi}}{\psi}}$ for $\psi = -1$ yields $-\sqrt{e^{-2i\pi} e^{2im\pi}} = \pm 1$ for $m = 0$ and $m = 1$ respectively, i.e., the same as for $\psi = 1$. As we shall see, the continues solutions will correspond to $m = 0$ within the volume of the stable phase, for $\vec{r} \in V_<$, and to $m = 1$ within the volume of the metastable phase, for $\vec{r} \notin V_<$. For the real field ψ , e.g., for π^0 or σ meson fields,

$$\langle \mathcal{L} \rangle = \left[\psi \Re \hat{D}^{-1}(\hat{\omega}, \hat{\vec{k}}, n, T) \psi - \frac{1}{2} \psi^2 \Re \hat{\Lambda}(\hat{\omega}, \hat{\vec{k}}, n, T) \psi^2 \right] + 2h\psi. \quad (10)$$

To get this expression from (9) for positive ψ describing the stable phase we should use $m = 0$ and for negative ψ describing the metastable phase, $m = -1$.

Equation of motion for the condensate field related to (9) can be presented as [95]:

$$\hat{D}^{-1}(\hat{\omega}, \hat{\vec{k}}, n, T) \psi - \psi \hat{\Lambda}(\hat{\omega}, \hat{\vec{k}}, n, T) |\psi|^2 + h e^{im\pi} (\psi/\psi^*)^{1/2} = 0. \quad (11)$$

Here

$$D^{-1}(\omega, \vec{k}) = \omega^2 - m^2 - \vec{k}^2 - \Sigma^R(\omega, \vec{k}, n, T), \quad (12)$$

$\Sigma^R(\omega, \vec{k}, n, T)$ is the boson retarded polarization operator. In case of the real field ψ at $k_0 = 0$, the last term simply yields h . In example of the pions interacting with the baryons n is the baryon density, $\langle \mathcal{L} \rangle$ is effective pion Lagrangian density, $\Sigma^R(\omega, \vec{k}, n, T)$ is the retarded polarization operator of particles heaving the pion quantum numbers, cf. [95, 96].

In case of the infinite matter for $n > n_c$, for $\hat{\Lambda} \simeq \Lambda_0$, for $\omega_0^2 = -D^{-1}(\omega_c, k_0) < 0$, equation of motion (11) has the running-wave classical solution

$$\psi = a \exp[-i\omega_c t + i\vec{k}_0 \vec{r}]. \quad (13)$$

Here ω_c and \vec{k}_0 are the condensate frequency and momentum, a is the amplitude of the condensate field.

Local charge neutrality in the infinite system suggests that

$$n_p + e (\partial \delta \mathcal{F} / \partial \omega)_{\omega_c} = 0,$$

where n_p is the non-condensate contribution to the charged density, e.g., the positive charge density of the baryon sub-system plus negative charge density of the lepton sub-system in case of the neutron star. This condition determines the critical frequency of the condensate ω_c . The condition of the absence of the current in the equilibrium state,

$$(\partial \delta \mathcal{F} / \partial \vec{k})_{\vec{k}_0} = 0,$$

determines the value of the condensate momentum k_0 .

2.2 Description of Bose excitations

2.2.1 The ω, k expansion of Green function

Let us study small variations from the equilibrium state. Then $D^{-1}(\omega, \vec{k})$ can be expanded in the series of $k^2 - k_0^2$ and $\omega - \omega_c$, cf [29, 104, 96]:

$$D^{-1}(\omega, \vec{k}) \simeq -\omega_0^2(\omega_c, k_0) + \alpha_0(\omega - \omega_c) + \alpha_1(\omega - \omega_c)^2 + \alpha_2(k_0^2 - k^2)(\omega - \omega_c) + \alpha_3(k_0^2 - k^2) + \alpha_4(k_0^2 - k^2)^2 + \dots, \quad (14)$$

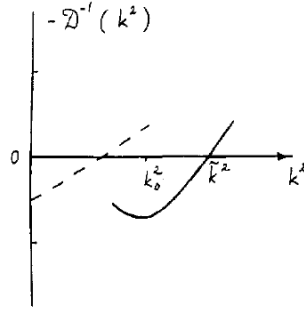


Figure 2: Dependence $-D^{-1}(k^2) = -\Re D^{-1}(\omega_c, \vec{k}^2, n, T)$ for $n > n_c$ for the case of the phase transition to inhomogeneous state $k_0 \neq 0$ (solid line) and to homogeneous state $k_0 = 0$ (dashed line).

$$\begin{aligned} \omega_0^2(\omega_c, k_0) &= m^2 + k_0^2 + \Re \Sigma^R(\omega_c, k_0) - \omega_c^2, \quad \alpha_0 = \left(2\omega - \frac{\partial \Sigma^R}{\partial \omega}\right)_{\omega_c, k_0}, \quad \alpha_1 = 1 - \left(\frac{\partial^2 \Sigma^R}{2\partial \omega^2}\right)_{\omega_c, k_0}, \\ \alpha_2 &= \left(\frac{\partial^2 \Sigma^R}{\partial k^2 \partial \omega}\right)_{\omega_c, k_0}, \quad \alpha_3 = 1 + \left(\frac{\partial \Sigma^R}{\partial k^2}\right)_{\omega_c, k_0}, \quad \alpha_4 = -\frac{\gamma}{2} = -\frac{1}{2} \left(\frac{\partial^2 \Sigma^R}{\partial (k^2)^2}\right)_{\omega_c, k_0}. \end{aligned} \quad (15)$$

In general case $\alpha_i = \alpha_{i1} + i\alpha_{i2}$, where α_{i1} and α_{i2} are real quantities, $\Im \Sigma^R(\omega_c, k_0) = 0$. In case of the phase transition to inhomogeneous state, $k_0 \neq 0$, from the condition of the absence of the current in the ground state follows that $\alpha_3 = 0$ and $\alpha_4 < 0$ for stability of the state. In case of the condensation in homogeneous state, $k_0 = 0$, we have $\alpha_3 > 0$, $\alpha_4 = 0$.

Similar expansion exists for Λ . Simplifying the consideration we use

$$\Lambda = \Lambda_0 + \Lambda_1(\omega - \omega_c) + \dots, \quad (16)$$

where $\Lambda_0 = \Lambda(\omega_c, \vec{k}_0) > 0$ to provide stability of the condensate state.

Expansion (14) holds also for the case of the non-relativistic bosons, $D^{-1} = \omega - k^2/(2m) - \Sigma^R$, but now with coefficients given by [105],

$$\begin{aligned} \alpha_0 &= 1 - \left(\frac{\partial \Sigma^R}{\partial \omega}\right)_{\omega_c, k_0} + \frac{\omega_c}{m} \simeq 1 - \left(\frac{\partial \Sigma^R}{\partial \omega}\right)_{\omega_c, k_0}, \quad \alpha_1 = \frac{1}{2m} - \left(\frac{\partial^2 \Sigma^R}{2\partial \omega^2}\right)_{\omega_c, k_0} \simeq -\left(\frac{\partial^2 \Sigma^R}{2\partial \omega^2}\right)_{\omega_c, k_0}, \\ \alpha_2 &= \left(\frac{\partial^2 \Sigma^R}{\partial k^2 \partial \omega}\right)_{\omega_c, k_0}, \quad \alpha_3 = \frac{1}{2m} + \left(\frac{\partial \Sigma^R}{\partial k^2}\right)_{\omega_c, k_0} \simeq \left(\frac{\partial \Sigma^R}{\partial k^2}\right)_{\omega_c, k_0}, \quad \alpha_4 = -\frac{\gamma}{2} = \left(\frac{\partial^2 \Sigma^R}{\partial (k^2)^2}\right)_{\omega_c, k_0}. \end{aligned} \quad (17)$$

The existence of gapless phases in “Bose-Luttinger liquids”, which in some respects can be regarded as bosonic versions of Fermi liquids, becomes now a hot topic [193]. The model considered in [193] is the limit case of (14) at $\alpha_0 = \alpha_2 = \alpha_3 = 0$. Similarly, the condensates with $k_0 \neq 0$ arise, when the spectra of the sigma mesons and pions have a “moat”, where the minimum of the energy lies over a sphere of nonzero radius in momentum. A moat spectrum can arise in a large region of the phase diagram, as in QCD and in different 1+1 dimensional models [194, 195, 196, 170, 135, 197, 198]. The spectrum of excitations is degenerate along a sphere of radius k_0 in momentum space, which is referred to as a “Bose surface” in [193].

For the case $\alpha_3 = 0$ the function $\Re D^{-1}(\omega_c, \vec{k}^2)$ has the form shown in Fig. 2 and we deal with the phase transition to the inhomogeneous state $k_0 \neq 0$. Also, simplifying consideration let us put for a while $h = 0$, then we deal with the second-order phase transition. Interaction of the condensate with the own electromagnetic field is introduced with the help of the minimal coupling. The part of the effective Lagrangian density depending on the order parameter related to the equation of motion (11) with D^{-1} presented in the form (14) it is convenient to present in a symmetric form

$$\begin{aligned} \delta \mathcal{L}[\psi] &= [-\omega_0^2 + \alpha_4 k_0^4] |\psi|^4 + \frac{1}{2}(\alpha_{01} + \alpha_{21} k_0^2) [\psi^*(i\partial_t - V)\psi + c.c.] - \alpha_{11}(i\partial_t + V)\psi^*(i\partial_t - V)\psi \\ &- 2\alpha_4 k_0^2 (\nabla + ie\vec{A})\psi^*(\nabla - ie\vec{A})\psi + \frac{1}{4}\alpha_{21} [(\nabla + ie\vec{A})^2 \psi^*(i\partial_t - V)\psi + \psi^*(\nabla - ie\vec{A})^2 (i\partial_t - V)\psi + c.c.] \\ &- \alpha_{41} [(\nabla + ie\vec{A})^2 \psi^*(\nabla - ie\vec{A})^2 \psi + (\nabla + ie\vec{A})^3 \psi^*(\nabla - ie\vec{A})\psi + (\nabla - ie\vec{A})\psi(\nabla + ie\vec{A})^3 \psi^*] \\ &- \frac{1}{2}\Re \hat{\Lambda} |\psi|^4 + h e^{im\pi} \psi (\psi^*/\psi)^{1/2} + e^{im\pi} h \psi^* (\psi/\psi^*)^{1/2} - \frac{1}{4} F_{\mu\nu} F^{\mu\nu}. \end{aligned} \quad (18)$$

Interaction with electromagnetic field A_μ is included with the help of the gauge replacement, $F_{\mu\nu} = \partial_\mu A_\nu - \partial_\nu A_\mu$, e is the electron charge, $V = eA_0$, $\mu, \nu = 0, 1, 2, 3$. This expression was extensively used in the problem of the pion condensation in nuclear matter [199, 184, 96] and in some condensed matter problems [104, 105]. For static case a similar extension of the ordinary Ginzburg–Landau expression was suggested to describe so called superdiamagnets, a class of materials with strong diamagnetism but differing from conventional superconductors [200].

2.2.2 Spectrum of excitations

We further assume $\alpha_3 = 0$, $\alpha_1, -\alpha_4 > 0$, and also α_0 and α_2 to be real that is satisfied for the case of the charged pion propagation in neutron star matter but not fulfilled for the case of isospin-symmetric matter. Besides that let us assume that $|\alpha_i| \sim 1$, $|\omega_0^2| \ll 1$ in units $m = 1$. Also, consider excitations dropping small $\propto \hbar$ terms.

To be specific let us bear in mind the case of charged pion condensate in neutron star matter. Then one should add to the Lagrangian density $\delta\mathcal{L}[\psi]$ the contribution of other relevant fields: of the nucleons and electrons, and, in case of sufficiently high density, also of muons and other baryons, and other mean meson fields. Note that in case of the pion condensation in nuclear matter $k_0 \sim p_{F,N}$, where $p_{F,N}$ is the nucleon Fermi momentum, $p_{F,N}(n_0) \simeq 1.9m_\pi$, m_π is the pion mass, and one expects $|\omega_0| \lesssim m_\pi$. Simplifying consideration with demonstration aim let us consider only interaction of the classical charged field with the positively charged particles (protons) assuming their density, n_p , to be constant inside the system. The proton charge is compensated in the medium by the π^- condensate charge. Then the spectrum of excitations is found from the equations of motion for the classical field ϕ and electromagnetic fields V, \vec{A} , which follow from the variation of the action in the fields. We choose solution in the form

$$\psi = a(1 + \rho')\exp[-i\omega_c t + i\vec{k}_0 \vec{r} + i\chi]. \quad (19)$$

Performing the variable replacements $\vec{A} \rightarrow \vec{A} - \nabla\chi/e$, $V \rightarrow V + \partial_t\chi$, $e^2/(4\pi) = 1/137$ we see that the Goldstone variable χ is absorbed by these transformations. The linearized equations of motion for the fields $\rho' \ll 1$, $V' = V - \omega_c$ and $\vec{A}' = \vec{A}$ for $|V'| \ll \omega_c$, $|e\vec{A}'| \ll m_\pi$ render

$$\begin{aligned} & 2\omega_0^2 \rho' - \alpha_1 \ddot{\rho}' - 2\alpha_2 \vec{k}_0 \nabla \dot{\rho}' + \alpha_4 \Delta^2 \rho' - 4\alpha_4 (\vec{k}_0 \nabla)^2 \rho' - \alpha_0 V' - \frac{\alpha_2}{2} \Delta V' \\ & + i\alpha_0 \dot{\rho}' + i\alpha_2 \Delta \dot{\rho}' + 4\alpha_4 i\vec{k}_0 \nabla \Delta \rho' - i\alpha_1 \dot{V}' - i\alpha_2 \vec{k}_0 \nabla V' + i\alpha_2 \vec{k}_0 e \vec{A}' - \alpha_4 \Delta \nabla e \vec{A}' \\ & + \frac{\alpha_2}{2} \nabla e \vec{A}' + 2\alpha_4 \vec{k}_0 \Delta e \vec{A}' + 2\alpha_4 (\vec{k}_0 \nabla)(\nabla e \vec{A}') + 4\alpha_4 (\vec{k}_0 \nabla)(\vec{k}_0 e \vec{A}') = 0, \end{aligned} \quad (20)$$

$$\partial_\mu F^{\mu\nu} = j^\nu, \quad j^\nu = (\rho, \vec{j}), \quad \rho = en_p + \rho_\pi, \quad (21)$$

$$\rho_\pi = e\partial\delta\mathcal{L}/\partial V = [-\alpha_0 - 2\alpha_0\rho' - \alpha_2\Delta\rho' + 2\alpha_1 V' - 2\alpha_2 \vec{k}_0 e \vec{A}']ea^2, \quad (22)$$

$$\vec{j} = \partial\delta\mathcal{L}/\partial\vec{A} = [\alpha_2 \nabla \dot{\rho}' + 4\alpha_4 \vec{k}_0 \Delta \rho' + 4\alpha_4 (\vec{k}_0 \nabla) \nabla \rho' - 2\alpha_2 \vec{k}_0 V' + 8\alpha_4 (\vec{k}_0 e \vec{A}')\vec{k}_0]ea^2. \quad (23)$$

Here we dropped small contributions of the type $e^2 a^2 (\ddot{A}'_\mu - \Delta A'_\mu)$ since such terms also appear in higher-order terms in the expansion of $D^{-1}(\omega, k^2)$ in $\omega - \omega_c$ and $k^2 - k_0^2$. The condition of the local charge neutrality yields $\rho_p = \alpha_0 a^2$.

The spectrum of excitations is found employing the Lorenz gauge $\partial_t V + \text{div}\vec{A} = 0$. It proves to be strongly anisotropic. We seek fluctuating fields $\rho', \chi, V', \vec{A}'$ in the form $\cos(\vec{q}\vec{r} - \omega t)$. Using expansion in small $|\vec{q}|$, for $\vec{A}' \perp \vec{k}_0$, one finds the branches [29, 96]:

$$(I): \quad \omega^2 = \vec{q}^2; \quad (24)$$

and

$$(IIa): \quad \omega^2 = \frac{2|\omega_0^2|}{\alpha_1} - \frac{\alpha_0^2 e^2}{\Lambda} - \frac{\alpha_1 \alpha_0^2 e^2}{2\Lambda|\omega_0^2|} \vec{q}^2 - \left(\frac{\alpha_4}{\alpha_1} + \frac{\alpha_1^2 \alpha_0^2 e^2}{4\Lambda\omega_0^4} \right) \vec{q}^4 + \dots, \quad (25)$$

for $\alpha_0 \neq 0$, $\vec{k}_0\vec{q} = 0$, $1 \gg |\omega_0^2|/m_\pi^2 \gg e^2/\Lambda$;

$$(IIb) : \quad \omega = \sqrt{\frac{2|\omega_0^2|}{\alpha_1}} - \frac{\alpha_0^2 e^2}{2\Lambda} \sqrt{\frac{\alpha_1}{|\omega_0^2|}} + \frac{\alpha_2}{\alpha_1} \vec{k}_0\vec{q} + \dots, \quad (26)$$

for $\alpha_2 \neq 0$ and $\vec{k}_0\vec{q} \neq 0$; and

$$(IIIa) : \quad \omega^2 = \frac{\alpha_0^2 e^2}{\Lambda} + \vec{q}^2, \quad (27)$$

for $\alpha_0 \neq 0$, $\vec{k}_0\vec{q} = 0$; and

$$(IIIb) : \quad \omega = \frac{|\alpha_0|e}{\Lambda} - \frac{\alpha_2 \alpha_0^2 e^2}{2\Lambda |\omega_0^2|} \vec{k}_0\vec{q} + \dots, \quad (28)$$

for $\alpha_2 \neq 0$, $\vec{k}_0\vec{q} \neq 0$.

For oscillations at $\vec{A}\vec{k}_0 \neq 0$ the spectrum is as follows

$$(Ia) : \quad \omega^2 = -8\alpha_4 k_0^2 a^2 e^2 + \frac{4|\omega_0^2| \alpha_2^2}{\alpha_0^2} a^2 e^2 k_0^2 + \vec{q}^2 + \dots, \quad (29)$$

for $\alpha_0 \neq 0$ and $\vec{k}_0\vec{q} = 0$; and

$$(Ib) : \quad \omega = 2\sqrt{-2\alpha_4} k_0 a e + \frac{|\omega_0^2| \alpha_2^2}{\sqrt{-2\alpha_4} \alpha_0^2} a e k_0 + \frac{\alpha_2^2 (\alpha_0 + 4\alpha_2 k_0^2)}{2\alpha_0^2} a^2 e^2 \vec{k}_0\vec{q} + \dots, \quad (30)$$

for $\alpha_0 \neq 0$ and $\vec{k}_0\vec{q} \neq 0$. The branches IIa,b and IIIa,b are the same as for the case $\vec{A}\vec{k}_0 = 0$. All excitations except branch I at $\vec{A}\vec{k}_0 = 0$, are gapped. The former branch describes Goldstone excitations. The spectrum is strongly anisotropic. For $\alpha_2 \neq 0$ “magnetic” excitations have a minimal mass $2\sqrt{-2\alpha_4} k_0 a e$, “electric” excitations have a higher mass $|\alpha_0|e/\sqrt{\Lambda}$, and “meson” excitations have still larger mass $|\omega_0|\sqrt{2/\alpha_1}$. The system is superfluid and superconducting.

It is curious to find spectrum of over-condensate excitations for the case of the complex condensate field of the form (19) but for $e^2 = 0$, cf. [29]. This consideration generalizes to the case $k_0 \neq 0$ the consideration of the excitations in He-II. For $\vec{k}_0\vec{q} = 0$ one finds for $\omega, |\vec{q}| \ll m_\pi$ the branches

$$(Ia) : \quad \omega^2 = \frac{\alpha_0^2}{\alpha_1^2} - \frac{2\omega_0^2}{\alpha_1} - \frac{2\alpha_0 \alpha_2}{\alpha_1^2} \vec{q}^2 + \dots, \quad (31)$$

$$(IIa) : \quad \omega^2 = + \frac{2\alpha_4 \omega_0^2}{\alpha_0^2 - 2\alpha_1 \omega_0^2} \vec{q}^4 + \dots, \quad (32)$$

whereas for $\vec{k}_0\vec{q} \neq 0$,

$$(Ib) : \quad \omega = \frac{\alpha_0}{\alpha_1} + \frac{2\alpha_2}{\alpha_1} \vec{k}_0\vec{q} - \frac{\alpha_2}{\alpha_1} \vec{q}^2 - \frac{\alpha_4}{\alpha_0} (\vec{k}_0\vec{q})^2 + \dots, \quad (33)$$

$$(IIb) : \quad \omega = \frac{\sqrt{-8\alpha_4}}{\alpha_0} |\omega_0 \vec{k}_0\vec{q}| + \dots \quad (34)$$

Thus there is the gappless non-Goldstone mode $\omega \propto \vec{q}^2$ and the gapped mode for $\vec{k}_0\vec{q} = 0$ and there is the Goldstone and the gapped anisotropic modes for $\vec{k}_0\vec{q} \neq 0$.

Knowledge of the spectrum of over-condensate excitations is important for description of the transport processes, e.g., in π condensate regions of the neutron stars.

2.3 Static inhomogeneous configurations and finite size effects

There are many configurations of the condensate field, which at the fixed volume V_3 correspond to the same volume energy $\delta F = -\frac{\omega_0^4}{2\Lambda_0}V_3$ and different surface energies. For example, these solutions are:

slabs

$$\psi = ae^{i\vec{k}_0\vec{r}}, \quad (35)$$

rods

$$\psi = ae^{ik_0\rho}, \quad (36)$$

spherical drops

$$\psi = ae^{ik_0r}, \quad (37)$$

disordered phase

$$\psi \simeq \frac{1}{N} \left\{ \sum_1^{N_1} a_i \exp[ik_0 \sqrt{(x-x_i)^2 + (y-y_i)^2 + (z-z_i)^2}] + \sum_{N_1+1}^N a_i \exp[ik_0 \sqrt{(x-x_i)^2 + (y-y_i)^2}] + a_0 e^{ik_0 x} \right\}, \quad \frac{1}{N} \sum_0^N a_i^2 = a^2. \quad (38)$$

The phase transition to the inhomogeneous state $k_0 \neq 0$ is always of the first-order due to strong fluctuations with $\vec{k} \sim \vec{k}_0 \neq 0$, cf. [127, 128, 129, 97, 98, 130, 132]. If the system is initially in the metastable state, the transition to the stable phase occurs by the growth of seeds of stable phase of an overcritical size, being formed in fluctuations. The system first reaches the state with different structures in different domains and only after a passage of a long time it may reach the equilibrium state with the most energetically profitable structure of the condensate field in the whole system [96, 105]. If the system in its evolution crosses the isothermal spinodal line, the fluctuations with different directions of \vec{k}_0 grow rapidly and the system arrives at the glass-like state disordered at distances $r \gg 1/k_0$.

Consider inhomogeneous phase characterized by the wave vector \vec{k}_0 and frequency ω_c . To describe surface effects one needs to consider deviations of \vec{k} from \vec{k}_0 . Setting $\psi \propto e^{-i\omega_c t}$ in equation of motion (11) one gets

$$[-\omega_0^2 + \alpha_4(k_0^2 + \Delta)^2]\psi - \psi \hat{\Lambda}(\Delta, |\psi|^4, |\psi|^2)|\psi|^2 + h e^{im\pi}(\psi/\psi^*)^{1/2} = 0. \quad (39)$$

For the static field one should put $\omega_c = 0$. Here we use simplified presentation of (14) for $\alpha_1 = \alpha_2 = \alpha_3 = 0$ and put $\hat{\Lambda} = \Lambda_0$, which value however may depend on the structure of the condensate field.

Let us again consider the case $h = 0$ corresponding to the description of the second-order phase transition. The free-energy density associated with the static classical field ψ is as follows,

$$\delta\mathcal{F} = -\psi^* D^{-1}(0, \hat{k}^2)\psi + \Lambda_0 |\psi|^4/2. \quad (40)$$

Let us consider the case of the sharp boundary between the medium and the vacuum. Inside the medium (to be specific let it be region $x < 0$) we have $-D^{-1}(0, \hat{k}^2) = \omega_0^2 - \alpha_4(k_0^2 + \Delta)^2$. In the vacuum (for $x > 0$) we have $-D^{-1}(0, \hat{k}^2) = m^2 - \hat{k}^2$. The equation of motion is as follows

$$(\beta_1 - \beta_2 \hat{k}^2 + \beta_3 \hat{k}^4)\psi - \Lambda_0 |\psi|^2 \psi = 0, \quad (41)$$

with $D^{-1}(\omega_c, \hat{k}^2) = \beta_1 - \beta_2 \hat{k}^2 + \beta_3 \hat{k}^4$ at $\beta_1 = -\omega_0^2 + \alpha_4 k_0^4$, $\beta_2 = -2\alpha_4 k_0^2$, $\beta_3 = \alpha_4$ for $x < 0$ and respectively $-m^2, -1, 0$ in the vacuum, for $x > 0$.

In the vacuum (for $x > 0$) the field is described by the differential equation of the second order in derivatives, whereas inside the medium by the 4-th order one. To derive necessary boundary conditions, cf. [104], one may consider single differential equation of the 4-th order for all x , with coefficients in front of the third- and fourth- derivative terms tending to zero in the sharp boundary layer (of the typical length $l_{b.l.} \ll l_<, l_>$, where $l_<, l_>$ are typical length scales, respectively for $x < 0$ and $x > 0$, characterizing

$\psi(x)$ obeying the equation of motion (41) with constant coefficients. One boundary condition is the continuity of ψ at $x = 0$. Other conditions are derived by one, two and three integrations of the equation of motion for the smoothed boundary subsequently letting the boundary layer width tend to zero. This procedure yields, as the boundary conditions, the continuity of the quantities

$$\beta_2 \nabla \psi + \beta_3 \Delta \nabla \psi, \quad \beta_3 \Delta \psi, \quad \beta_3 \nabla \psi, \quad \psi. \quad (42)$$

In case of the Maxwell equations describing two dielectric media, two latter conditions (42) coincide with the ordinary conditions of the continuity of the electric potential, Φ , and the electric displacement, $\epsilon \nabla \Phi$, where ϵ is the dielectric constant. In case of the semi-infinite three-dimensional system with the flat (x, y) boundary between the medium and the vacuum, provided $l_< = l_0 \sim 1/|\omega_0| \gg 1/k_0$ and $l_< \gg l_> \sim 1/m$, one may use more simple conditions $\phi(x=0) = \phi'_x(x=0) = 0$.

2.3.1 One-axis-like structures

There are two types of one-dimensional modulations. One is of the Fulde–Ferrell type [148], characterized by modulations of the phase of a complex order parameter with constant amplitude, the other is of the Larkin–Ovchinnikov type [149], where the amplitude of the condensate field is modulated.

One-axis structures are of interest for description of A-smectic liquid crystals and the charged pion condensate. With the field in the form of the running wave,

$$\psi = a\chi(\vec{r})e^{i\vec{k}_0\vec{r}}, \quad (43)$$

placed in Eq. (41) one obtains equation of motion for the χ amplitude

$$\alpha_4 \Delta^2 \chi - 4\alpha_4 (\vec{k}_0 \nabla)^2 - \omega_0^2 \chi + \omega_0^2 |\chi|^2 \chi = 0, \quad a^2 = (-\omega_0^2/\Lambda_0)\theta(-\omega_0^2), \quad (44)$$

where $\theta(x)$ is the step-function and we assumed that χ is a smooth function and we dropped $(\vec{k}_0 \nabla) \Delta \chi$ term but retained $\Delta^2 \chi$ term, being the main term in case $\vec{r} \perp \vec{k}_0$. Substituting (43) in (40) one obtains $\delta\mathcal{F} = -(\omega_0^4/(2\Lambda_0))\theta(-\omega_0^2)$.

After performing the transformation $x_i \rightarrow \tilde{x}_i = x_i 2k_{0i} \sqrt{\alpha_4/\omega_0^2}$, where $x_i = (x, y, z)$, in dimensionless variables ($\nabla \rightarrow \tilde{\nabla}$), Eq. (44) renders

$$-\alpha \tilde{\Delta}^2 \chi + (\vec{n} \tilde{\nabla})^2 \chi + \chi - |\chi|^2 \chi = 0, \quad \vec{n} = \vec{k}_0/k_0, \quad \alpha = \omega_0^2/(16k_0^4 \alpha_4). \quad (45)$$

For a smooth function χ , this is the second-order derivative equation in the directions $\vec{r} \cdot \vec{k}_0 \neq 0$ and the fourth-order one for $\vec{r} \perp \vec{k}_0$.

There are systems, which are ordered in the longitudinal direction, but react as a liquid in the transverse direction [201]. Note that Eq. (45) does not coincide with the Landau–De’Gennes equation [25], which is often used to describe A-phase of smectic liquid crystals. In the latter case the inter-plane distance d is fixed. The molecules are perpendicular to the layer planes and molecular centers are disordered. The density wave has the form

$$\rho(z) = \bar{\rho}[1 + 2^{-1/2}|\psi| \cos(k_0 z - \phi)], \quad (46)$$

where $\bar{\rho}$ is the averaged density, $|\psi|$ is the amplitude, k_0 is the wave number, ϕ is the phase. The order parameter $\psi = |\psi|e^{i\phi}$ obeys the Landau–De’Gennes equation

$$\frac{\partial_z^2 \psi}{2M_V} + \frac{(\partial_x^2 + \partial_y^2) \psi}{2M_T} + \alpha_0 \psi - \Lambda |\psi|^2 \psi = 0, \quad (47)$$

for $\alpha_0, \Lambda > 0$, M_V and M_T play roles of the effective longitudinal and transverse masses, $M_V \neq M_T$. The solution for the infinite system is given by $|\psi|^2 = \alpha_0/\Lambda > 0$. The free-energy density associated with ψ is as follows

$$\mathcal{F} = -\alpha_0|\psi|^2 + \frac{\Lambda|\psi|^4}{2} + \frac{|\partial_z\psi|^2}{2M_V} + \frac{(|\partial_x\psi|^2 + |\partial_y\psi|^2)}{2M_T}. \quad (48)$$

Note also that Landau-De'Gennes model does not describe the phase transition from the isotropic uniform phase to the A smectic phase since $k_{0x}^2 = k_{0y}^2 \neq k_{0z}^2$ in this model. In order to describe both mentioned phases one may use Eq. (44), which follows from the free energy depending on k_0^2 rather than on k_{0z}^2 and $k_{0x}^2 = k_{0y}^2 \neq k_{0z}^2$. In case of the model described by Eq. (44) the direction \vec{k}_0 arises by the spontaneous symmetry breaking.

Let $-\omega_0^2 > 0$ in the half-plane $z < 0$ and $\omega_0^2 = m^2$ for $z > 0$. Solutions of Eq. (44) are characterized by two length scales, $l_{\parallel} = (-2\alpha_4 k_0^2/|\omega_0^2|)^{1/2}$ in the directions $\vec{r}\vec{k}_0 \neq 0$ and $l_{\perp} = (-2\alpha_4/|\omega_0^2|)^{1/4}$ in the direction $\vec{r}\vec{k}_0 = 0$. The solution for $\vec{k}_0 \parallel z$ satisfying boundary conditions $\chi(z \rightarrow -\infty) \rightarrow 1$ and $\chi(z \rightarrow 0) \rightarrow 0$ is as follows,

$$\psi \simeq ae^{ik_0 z} \tanh[(z - z_0)/(\sqrt{2}l_{\parallel})]. \quad (49)$$

To find solution for $\vec{k}_0 \perp z$ one presents $\chi = 1 - \chi_1 - \chi_2 - \dots$ with $1 \gg |\chi_1| \gg |\chi_2| \dots$. Thus one obtains [199, 184, 96],

$$\psi \simeq ae^{ik_0 y} \left[1 - C_1 e^{z/l_{\perp}} \cos\left(\frac{z}{l_{\perp}} + C_2\right) + O(\chi_1^2, \chi_2) \right]. \quad (50)$$

Question on the boundary conditions is not trivial, as it has been mentioned, since for $z < 0$ we deal with the differential equation of the forth-order, whereas for $z > 0$ with the differential equation of the second-order [184, 104]. For $l_{\perp} \propto 1/|\omega_0|^{1/2} \gg 1/k_0$ and one may apply simpler boundary conditions $\psi(0) = \psi'_z = 0$ and one finds $C_1 = \sqrt{2}$, $C_2 = \pi/4$. Solution (50) yields the same volume part of the free energy as (49) but a smaller surface part, since $l_{\perp} < l_{\parallel}$ (provided $|\omega_0^2| \ll m^2$). Thereby, choice of the direction \vec{k}_0 parallel to the medium boundary is energetically profitable. Generalization to the case of the slab $-z_0 < z < z_0$, for $z_0 \gg l_{\perp}, l_{\parallel}$, is given with the help of the replacement $z \rightarrow |z|$ in Eqs. (49), (50). It is curious to notice that the relation $l_{\perp}^2 \sim l_{\parallel}/k_0$ indeed holds for A-smectic crystals [202].

For the spherical system of the radius R there is the following solution of Eq. (44), cf. [203, 105],

$$\psi \simeq ae^{ik_0 z} \tanh[(|z| - \sqrt{R^2 - x^2 - y^2})/(\sqrt{2}l_{\parallel})] \quad (51)$$

for $x^2 + y^2 < R^2$. Also, this solution holds for weakly deformed systems. Following this solution the condensate part of the surface energy decreases with increasing deformation and an elongation is energetically profitable. The equilibrium deformation is found from competition of the condensate and non-condensate parts of the free energy. Solution (51) holds only for weak deformations. Its value depends on the length scales $1/k_0$ and l_{\parallel} . With increasing deformation, there appears the dependence on the scale l_{\perp} . To demonstrate this dependence we may construct solution for the condensate field in the parallelepiped, cf. [184, 104],

$$\psi = ae^{ik_0 y} \left[\tanh \frac{y_0 - |y|}{\sqrt{2}l_{\parallel}} - \frac{(1-i)\sinh((1+i)x_0/l_{\perp})\cosh((1-i)x/l_{\perp}) + \text{c.c.}}{\sinh(2x_0/l_{\perp}) + \sin(2x_0/l_{\perp})} + x \leftrightarrow z, x_0 \leftrightarrow z_0 \right]. \quad (52)$$

The gain in the condensate part of the free energy renders

$$\delta F = - \int \frac{\Lambda_0 |\psi|^4}{2} d^3x = - \frac{\omega_0^4}{2\Lambda_0} \left[1 - \frac{4l_{\parallel}}{3y_0} - 4l_{\perp} \left(\frac{1}{x_0} + \frac{1}{z_0} \right) \right] V_3, \quad V_3 = 8x_0 y_0 z_0. \quad (53)$$

Let us assume that the non-condensate part of the surface energy is negligibly small. Then optimal sizes of the system at fixed volume V_3 are given by [29, 96]:

$$x_0 = z_0 = (3l_{\perp}/(l_{\parallel}))y_0 \ll y_0. \quad (54)$$

Therefore in presence of the condensate, an initially spherical nucleus becomes elongated in the direction \vec{k}_0 . Now optimal deformation exists, even if the non-condensate part of the surface energy is negligibly small.

The spherical solutions $\vec{k}_0 \parallel \vec{r}$ render [105]:

$$\psi \simeq a e^{i k_0 r} \tanh[(r - r_0)/(\sqrt{2} l_{\parallel})], \quad (55)$$

for $r_0 \gg l_{\parallel}$.

Cylindric solutions are

$$\psi \simeq a e^{i k_0 \rho} \tanh[(\rho - \rho_0)/(\sqrt{2} l_{\parallel})], \quad (56)$$

for $\rho_0 \gg l_{\parallel}$, $\rho = \sqrt{x^2 + y^2}$, and there are many other configurations of the same surface energy at different surface energies.

A polycrystal configuration constructed from domains is as follows

$$\begin{aligned} \psi = & a \sum_{i=1}^{N_1} e^{i k_0 |\vec{r} - \vec{r}_i|} \tanh[(|\vec{r} - \vec{r}_i| - R_i)/(\sqrt{2} l_{\parallel})] \theta(R_i - |\vec{r} - \vec{r}_i|) \\ & + a \sum_{N_1+1}^{N_2} e^{i k_0 z} \tanh[(|z| - \sqrt{R_i^2 - x^2 - y^2})/(\sqrt{2} l_{\parallel})] \theta(\sqrt{R_i^2 - x^2 - y^2} - |z|) \\ & + \sum_{N_2+1}^{N_3} \{\text{rod}\} + \sum_{N_3+1}^{N_4} \{\text{slab}\} + \dots, \quad \sum_i N_i = N, \end{aligned} \quad (57)$$

$R_i \gg l_{\parallel}$ is the domain radius, $\sum_i V_i \simeq V_{\text{tot}}$ up to a surface term, where V_i is the volume of the i -domain, V_{tot} is the volume of the condensate system.

In case when by some reason one deals with the real condensate field, e.g., as for neutral pions, equation of motion has the same form (41), but now for the real ψ . Choosing the field in the form of the standing wave,

$$\psi = a_{\text{stan}} \chi(\vec{r}) \cos(\vec{k}_0 \vec{r}) \quad (58)$$

and substituting it in (41) one finds $a_{\text{stan}}^2 = -4\omega_0^2/(3\Lambda_0)$. Substituting this solution in (40) one obtains $\delta\mathcal{F} = -\omega_0^4/(3\Lambda_0)$ and instead of Eq. (57) we get

$$\begin{aligned} \psi = & a_{\text{stan}} \sum_{i=1}^{N_1} \Re\{e^{i k_0 |\vec{r} - \vec{r}_i|}\} \tanh[(|\vec{r} - \vec{r}_i| - R_i)/(\sqrt{2} l_{\parallel})] \theta(R_i - |\vec{r} - \vec{r}_i|) \\ & + a_{\text{stan}} \sum_{N_1+1}^{N_2} \Re\{e^{i k_0 z}\} \tanh[(|z| - \sqrt{R_i^2 - x^2 - y^2})/(\sqrt{2} l_{\parallel})] \theta(\sqrt{R_i^2 - x^2 - y^2} - |z|) \\ & + \sum_{N_2+1}^{N_3} \{\text{two-dim.}\} + \dots, \quad \sum_i N_i = N. \end{aligned} \quad (59)$$

It is important to notice that in case of a complex field for $\Lambda = \text{const}$ the solution (43) produces a smaller free energy than (58).

2.3.2 Three-axis structures

Assume that the lattice structure has the form

$$\psi = a \chi \cos(k_{0x} x) \cos(k_{0y} y) \cos(k_{0z} z) \quad (60)$$

with $k_0^2 = k_{0x}^2 + k_{0y}^2 + k_{0z}^2$. Minimization of the free energy at $\chi = 1$ yields $a^2 = -(4/3)^3 \omega_0^2/\Lambda_0 > 0$. Then setting (60) in Eq. (41) one derives equation for χ :

$$\alpha_4 (\Delta^2 - 4k_{0x}^2 \partial_x^2 - 4k_{0y}^2 \partial_y^2 - 4k_{0z}^2 \partial_z^2) \chi - \omega_0^2 (\chi - \chi^3) = 0. \quad (61)$$

The free-energy density becomes

$$\delta\mathcal{F} = \delta\mathcal{F}_1 + \delta\mathcal{F}_2, \quad (62)$$

where

$$\delta\mathcal{F}_1 = \mathcal{F}_0 \left[\frac{\chi^2}{2} - \frac{\chi^4}{4} + \frac{2\alpha_4}{\omega_0^2} (k_{0x}^2 (\partial_x \chi)^2 + k_{0y}^2 (\partial_y \chi)^2 + k_{0z}^2 (\partial_z \chi)^2) \right], \quad (63)$$

$\mathcal{F}_0 = -\frac{16}{27}\frac{\omega_0^4}{\Lambda_0}$, $\delta\mathcal{F}_2$ is associated with higher derivatives of χ and thereby $|\delta\mathcal{F}_2| \ll |\delta\mathcal{F}_1|$. Note that although Eq. (61) describes the three-dimensional lattice, it coincides (up to higher derivative terms) with Eq. (47) of the Landau-De'Gennes model of the one-axis A-smectic liquid crystal.

Assuming lattice structure in the form

$$\psi = a\chi[\cos(k_{0x}x) + \cos(k_{0y}y) + \cos(k_{0z}z)] \quad (64)$$

one finds $a^2 = -(4/15)\omega_0^2/\Lambda_0 > 0$. Equation of motion for χ becomes

$$\alpha_4(\partial_x^4 + \partial_y^4 + \partial_z^4 - 4k_{0x}^2\partial_x^2 - 4k_{0y}^2\partial_y^2 - 4k_{0z}^2\partial_z^2)\chi - \omega_0^2(\chi - \chi^3) = 0. \quad (65)$$

The free-energy density is given by

$$\delta\mathcal{F} = \delta\tilde{\mathcal{F}}_1 + \delta\tilde{\mathcal{F}}_2, \quad (66)$$

where

$$\delta\tilde{\mathcal{F}}_1 = \tilde{\mathcal{F}}_0 \left[\frac{\chi^2}{2} - \frac{\chi^4}{4} + \frac{2\alpha_4}{\omega_0^2}(k_{0x}^2(\partial_x\chi)^2 + k_{0y}^2(\partial_y\chi)^2 + k_{0z}^2(\partial_z\chi)^2) \right], \quad (67)$$

$\tilde{\mathcal{F}}_0 = -\frac{4}{5}\frac{\omega_0^4}{\Lambda_0} < \mathcal{F}_0$, $\delta\tilde{\mathcal{F}}_2$ is associated with higher derivatives of χ and thereby $|\delta\tilde{\mathcal{F}}_2| \ll |\delta\tilde{\mathcal{F}}_1|$. Note that the value k_0^2 is determined by minimization of the free energy, whereas separate values k_{0i} remain not fixed. This circumstance might be of interest for description of phase transitions in various materials, e.g., like glassing transition, martensite structures in alloys, domain structures, etc. Although, as we see, solution (64) yields a smaller free energy than (60) at the same value Λ_0 , we pay attention that value Λ_0 may depend on the form of the solution.

Neglecting fourth-order derivative terms, after transformation $x_i \rightarrow x_i 2k_{0i}\sqrt{\alpha_4/\omega_0^2}$, where $x_i = (x, y, z)$, Eqs. (61), (65) require a simple form

$$\tilde{\Delta}\chi + \chi - \chi^3 = 0. \quad (68)$$

In these dimensionless variables equation for χ is the same as that describing the second-order phase transition to the homogeneous state $k_0 = 0$. In this sense, the consideration of the second-order phase transition to the three-dimensional lattice states is similar to that for the phase transition to the state $k_0 = 0$. Thereby, in general there is a principal difference in description of the three-axis and the one-axis-like structures. Note that the Landau-De'Gennes model used for description of A-phase of smectic liquid crystals employs simplified Eq. (68) rather than a more general Eq. (45).

Note again that the values of the coefficients Λ_i depend on the structure of the condensate field. Thereby they are different for various one-axis, two-axis and three-axis structures. Moreover instead of one real or complex order parameter there may exist many order parameters, e.g., the pion condensate order parameter is the vector in the isospin space. Some possible structures of the pion condensate were studied within the Thomas-Fermi approximation $k_0^2/4p_{F,N}^2 \ll 1$, cf. [95, 96]. Examples of such structures are

$$\vec{\phi} = (a \cos(k_0x), -a \sin(k_0x), 0), \quad (69)$$

$$\vec{\phi} = (2^{-1/2}a \cos(k_0x), 2^{-1/2}a \cos(k_0x), a \sin(k_0x)), \quad (70)$$

$$\vec{\phi} = (0, 0, (2/3)^{1/2}a[\sin(k_0x) + \sin(k_0y) + \sin(k_0z)]). \quad (71)$$

Then the isotopic and spatial structures of the pion condensate were considered in the so called alternating-layer-structure model, cf. [108]. It was demonstrated that the most energetically preferable structure likely corresponds to the standing π^0 wave with $\phi^0 \propto \Re e^{ik_0z}$ and the running π^\pm wave $\phi^\pm \propto e^{i\vec{k}_{0\perp}\vec{\rho}}$. Simplifying consideration, we further do not consider these complications supposing each Λ_i to be constant corresponding to the given structure of the condensate field.

Ultracold atoms with strong dipole-dipole interactions allow to study many-body systems with long-range anisotropic interactions [204]. Reference [205] demonstrated that such systems enable one to realize in the laboratory analogs of meson condensation in nuclear matter, due to similarities of the electric and magnetic dipole interactions and the nuclear tensor force, with the same r -dependence of the interaction potential as for the p wave πNN interaction. Consideration of these systems goes beyond the framework of the present study.

2.3.3 Chiral waves

Within the sigma model the pion and sigma mesons are unified in the Euclidean 4-vector: $\phi_i = (\sigma, \vec{\phi})$. Studies of pion condensates with $k_0 \neq 0$ within the sigma model were began in [206, 207, 208, 117, 97]. The chiral spiral structures are also possible [107, 168], where the sigma-pion condensate $(\sigma, \vec{\phi})$ forms a structure, e.g., like

$$\phi_i = (\phi_0 \cos(k_0 z), 0, 0, \phi_0 \sin(k_0 z)).$$

In the large N_c limit to QCD the early studies suggested the emergence of the chiral density wave [209, 210]. The phase structure at high baryon densities and moderate temperatures can be modified considerably also by the presence of the inhomogeneous QCD phases, cf. [168, 169, 170, 171, 134]. The chiral spiral structures were extensively discussed, where the sigma-pion condensate $(\sigma, \vec{\phi})$ forms a structure, e.g., like

$$(\phi_0 \cos(k_0 z), 0, 0, \phi_0 \sin(k_0 z)),$$

the quarkyonic chiral spiral, cf. [84, 211], and other systems with the moat-like spectrum, cf. [135, 197, 198]. Various inhomogeneous chiral condensed phases have been proposed, cf. [170, 134] and references therein. These features appear in mean-field calculations in the Nambu–Jona-Lasinio, the quark-meson models [168, 212] and the Dyson–Schwinger approach to the dense QCD [213].

2.4 Mean field versus fluctuations

2.4.1 Critical temperature in the mean field approximation

In relativistic mean-field models [214, 10, 115] one assumes that the T dependence enters only the fermion distribution functions. In the Schwinger–Dyson approach to the fermion-boson system the temperature dependence enters the particle Green functions. In the mean field approximation one takes into account the T dependence of the fermion Green functions but ignores it in the boson Green functions. In simplest case of the one fermion – one boson system, like for nucleons and pions in isospin-symmetric matter, the parameter characterizing the temperature dependence of the fermion Green function is $(T/\epsilon_F)^2$, as it follows from the known Fermi integral expansions at low T , cf. [17]. As the result $\langle |\psi|^2 \rangle = -\omega_0^2(T)/\Lambda_0(T) \simeq -\omega_0^2(0)/\Lambda_0(0) + C(T/\epsilon_{F,N})^2$, $C = const$, $\epsilon_{F,N}$ is the nucleon Fermi energy. Thus in the mean-field (MF) approximation, cf. [117], $\langle |\psi|^2 \rangle = 0$ at

$$T = T_c^{\text{MF}} \sim \epsilon_{F,N}(n - n_c)/n_c, \quad (72)$$

provided $(n - n_c)/n_c \ll 1$. In mentioned case of the pion condensation also Δ isobars give essential contribution, and the typical temperature destroying the Δ -particle – nucleon hole contribution is $T \sim m_\Delta - m_N \simeq 2.1m_\pi$. It proves to be that with taking into account of Δ -particle – nucleon hole diagrams the value T_c^{MF} increases, cf. [117, 97, 96].

2.4.2 Fluctuations in case of the phase transition to the state $k_0 \neq 0$

As we have discussed in Section 2.1.2, fluctuations of the order parameter become strong in the vicinity of the critical point of the phase transition to the state $k_0 = 0$. In case of the phase transition to the

state $k_0 \neq 0$ fluctuations play even more important role than in case $k_0 = 0$ because of their large phase space volume. As the result, with taking into account of fluctuations the phase transition to the state $k_0 \neq 0$ proves to be of the first order, even if in the mean field approximation it was of the second order [127, 128, 129, 97, 130, 132, 96, 6, 7]. A liquid/amorphous phase of the pion condensate characterized by strong correlations with $k \sim k_0 \neq 0$ may arise in nuclear matter already at $n \gtrsim n_c^{(1)} \simeq (0.5 - 0.8)n_0$, cf. [132, 96, 6, 7], i.e., at smaller densities compared to the critical density n_c^π for the pion condensation of the liquid-crystal-like or crystal-like type.

The correlation function of two fluctuating complex fields reads, cf. [129, 104],

$$N(\vec{r}) = \langle \psi(\tau_1, \vec{r}_1) \psi^*(\tau_2, \vec{r}_2) \rangle|_{\tau_2=\tau_1-0} = -T \sum_{n=-\infty}^{\infty} \int \frac{d^3 k}{(2\pi)^3} D_M(E_n, \vec{k}^2) e^{-E_n 0 + i \vec{k} \vec{r}}, \quad \vec{r} = \vec{r}_1 - \vec{r}_2, \quad (73)$$

where $D_M(E_n, \vec{k})$ is the Matsubara boson Green function determined for discrete frequencies $E_n = 2\pi nT$, $n = 0, \pm 1, \dots$

For non-relativistic systems the high temperature limit $|E_1| \gg |\omega_0^2|$ is usually realized. In this case one can put $n = 0$ in the sum (73) and for $k_0 \neq 0$, $\omega_0^2 > 0$, $\omega_0^2 \ll m^2$ one obtains [104]

$$N(r) = N(0) e^{-r/(\sqrt{2}l_\parallel)} \frac{\sin k_0 r}{k_0 r}, \quad N(0) \simeq k_0 T / [(4\pi)(-\alpha_4)^{1/2} |\omega_0|]. \quad (74)$$

After the replacement $\omega_0^2 \rightarrow -2\omega_0^2$ the same result holds for $\omega_0^2 < 0$. $N(r)$ is characterized by two length scales: it oscillates on a short scale $l_k \sim 1/k_0$ and smoothly falls off on a coherence length scale l_\parallel , and $l_\parallel \gg l_k$ at least in the vicinity of the critical point when $|\omega_0^2| \ll m_b^2$. In case of the pion condensation both classical and quantum limits are relevant, see below Section 5.3.1.

A good approximation to take into account fluctuation contribution in the boson Green function D is inclusion of the diagram



(75)

calculated with the full Green function of the boson (iD^R is shown by the bold wavy line). The bold block shows the effective boson-boson vertex that contains the vacuum part $-i\Lambda_{\text{vac}}$ and an in-medium contribution. This term is given by the correlator $N(0)$ times the vertex.

The equation for the effective gap $\tilde{\omega}^2$ that after taking into account of fluctuations replaces the value ω_0^2 is given by [104]

$$\tilde{\omega}^2 = \omega_0^2 + \Lambda N(0, \omega_0 \rightarrow \tilde{\omega}), \quad (76)$$

where now $N(0) \propto 1/\tilde{\omega}$ and does not reach zero. In the critical point there arises jump from the branch with $\tilde{\omega}^2 > 0$ to $\tilde{\omega}^2 < 0$ that is interpreted as the first-order phase transition to the state with the liquid-crystal or solid-like structured condensate. Only provided the value of the jump is not as large, with some accuracy one may continue to speak about the second order phase transition.

Note that the fluctuations at the phase transition to the state $k_0 \neq 0$ can be considered as one of the reasons for the appearance of the $\propto \hbar$ terms in the effective Lagrangian (9), (10) and in $\hat{D}^{-1}\psi$ in equation of motion, since for $\omega_0 \rightarrow 0$ one has $\Lambda N(0, \omega_0 \rightarrow \tilde{\omega})\psi \sim \psi/(\psi^*\psi)^{1/2}$.

Note that even the superconducting phase transition to the state $k_0 = 0$ proves to be of a weakly first order transition because of effects of the intrinsic fluctuating magnetic field, cf. [126]. In the Lagrangian there appears the term $\propto e^3 \phi^3$. Similar results hold for the phase transition from the A-smectic to a nematic liquid crystal.

For $k_0 \neq 0$ the specific heat gets a contribution $C_V \propto 1/|\tilde{\omega}|^3$, i.e. it diverges stronger than in case of $k_0 = 0$, cf. [129, 97], whereas the magnetic susceptibility proves to be convergent, $\chi_H \sim |\tilde{\omega}|$, cf. [104].

Besides the fluctuations of the amplitude of the order parameter, there exist fluctuations of the phase related to presence of the Goldstone modes. For $T \neq 0$ these modes destroy the ordering in one-dimensional condensates at very long distances. For condensates at $k_0 = 0$ it was shown by Peierls and Landau, cf. [17]. References [215, 216] demonstrated that at very large distances for condensates at $k_0 \neq 0$ also $\langle \psi \rangle = 0$. However quasi-one dimensional condensates are not prohibited. Thereby, either $k_0(x)$ should vary with the distance at large length scale [216], or due to the phase fluctuations the domains are formed [104, 96].

2.5 Transition from the order parameter to hydrodynamical variables

2.5.1 Schrödinger equation in hydrodynamical variables

First, consider approximate solutions of the Schrödinger equation

$$i\hbar\partial_t\Psi = -\frac{\hbar^2\Delta\Psi}{2m} + U\Psi, \quad (77)$$

with $U(t, \vec{r})$ to be a very smooth function of t and \vec{r} . In this case U can be either a scalar field or a zero-component of electromagnetic field eA_0 . Dependence on \hbar is recovered in order to track quantum corrections, which would vanish in the limit $\hbar \rightarrow 0$.

Let us search solution in the form

$$\Psi = Ae^{iS/\hbar}, \quad (78)$$

where the amplitude $A(t, \vec{r})$ and the phase $S(t, \vec{r})$ are real quantities, being smooth functions of t, \vec{r} . Substituting (78) in (77) and separating the real and imaginary parts we have

$$-\partial_t S = \frac{(\nabla S)^2}{2m} + U - \frac{\hbar^2\Delta A}{2mA}, \quad (79)$$

$$\hbar\partial_t A = -\frac{\hbar\Delta S}{2m}A - \frac{\hbar\nabla A \cdot \nabla S}{m}. \quad (80)$$

Introducing mass-density $\rho_\psi = mA^2$, and the quantity $\vec{v} = \nabla S/m$ and multiplying (80) by A we derive the continuity equation

$$\partial_t \rho_\psi + \text{div}(\rho_\psi \vec{v}) = 0. \quad (81)$$

Applying the operator ∇ to Eq. (79) we obtain

$$\partial_t \vec{v} + (\vec{v}\nabla)\vec{v} = -\frac{\nabla P_{\text{ext}}}{\rho_\psi} = -\frac{\nabla U}{m} + \frac{\hbar^2}{2m^2}\nabla\frac{\Delta\sqrt{\rho_\psi}}{\sqrt{\rho_\psi}}. \quad (82)$$

A note is in order: Ψ function is in general a complex function and it is not directly measurable thereby. However according to Eq. (78) it can be presented via two real functions. The amplitude A is directly measurable, since it is expressed via the mass-density ($A = \pm\sqrt{\rho_\psi/m}$, “ $-$ ” sign can be hidden in a constant phase). Flux, associated with the velocity, $\rho_\psi \vec{v} = \rho \nabla S/m$, and, thereby, ∇S are also measurable.

The term

$$\frac{\nabla P_{\text{quant}}}{\rho_\psi} = -\frac{\hbar^2}{2m^2}\nabla\frac{\Delta\sqrt{\rho_\psi}}{\sqrt{\rho_\psi}} \quad (83)$$

is called the Laplace pressure. This surface term is a purely quantum contribution $\propto \hbar^2$. Neglecting it we formally arrive at the Euler equation of ideal hydrodynamics.

2.5.2 Phase transition to the state $k_0 = 0$

Let us simplifying consideration take $k_0 = \alpha_1 = \alpha_2 = \alpha_{32} = \alpha_{02} = \alpha_4 = 0$, whereas $\alpha_{01} \neq 0$, $\alpha_{31} > 0$, $\Lambda_{12} \neq 0$, $\Lambda_{11} = 0$, $\Lambda_3 = 0$, $\Lambda_0 \neq 0$. i.e.,

$$D_R^{-1} = -\omega_0^2 + \alpha_{01}(i\partial_t - \omega_c) + \alpha_{31}\Delta, \quad \psi^* \hat{\Lambda} \psi = \Lambda_0 |\psi|^2 + \Lambda_{12} i \partial_t |\psi|^2. \quad (84)$$

A more general consideration can be found in [105].

Put $\psi = \psi_0 e^{iS}$ in equation of motion, where ψ_0 and S are real quantities. Separating real and imaginary parts one obtains:

$$-\alpha_{01}\psi_0(\partial_t S + \omega_c) + \Lambda_{12}\psi_0\partial_t\psi_0^2 - \omega_0^2\psi_0 - \Lambda_0\psi_0^3 + \alpha_{31}\Delta\psi_0 - \alpha_{31}\psi_0(\nabla S)^2 = 0, \quad (85)$$

$$\alpha_{01}\psi_0\partial_t\psi_0 + \alpha_{31}\text{div}[\nabla S\psi_0^2] = 0. \quad (86)$$

Introducing a mass-density-like variable, $\rho_\psi = \alpha_{01}m_{\text{ef}}\psi_0^2$, velocity $\vec{v} = \nabla S/m_{\text{ef}}$, and an effective mass, $m_{\text{ef}} = \alpha_{01}/(2\alpha_{31})$, after applying the gradient operator to Eq. (85) one arrives at equation

$$\partial_t \vec{v} + \nabla \frac{\vec{v}^2}{2} = -\frac{\nabla P}{\rho_\psi} + \nabla \left[\frac{(4\eta/3 + \zeta)}{\rho_\psi} \frac{\text{div}(\rho_\psi \vec{v})}{\rho_\psi} \right], \quad (87)$$

which coincides formally with the ordinary Navier–Stokes equation provided ρ_ψ is a very smooth function of t and \vec{r} . From Eq. (86) one arrives at the ordinary continuity equation

$$\partial_t \rho_\psi + \text{div}(\rho_\psi \vec{v}) = 0. \quad (88)$$

Here we introduced the shear, η , and bulk, ζ , viscosity-like notations

$$(4\eta/3 + \zeta)/\rho_\psi^2 = -\Lambda_{12}/(\alpha_{01}m_{\text{ef}})^2, \quad (89)$$

and

$$\nabla P = -\frac{\rho_\psi}{\alpha_{01}m_{\text{ef}}} \nabla \left[-\omega_0^2 - \frac{\Lambda_0 \rho}{\alpha_{01}m_{\text{ef}}} - \alpha_{01}\omega_c + \frac{\alpha_{31}\Delta\sqrt{\rho_\psi}}{\sqrt{\rho_\psi}} \right]. \quad (90)$$

Since the coefficient $4\eta/3 + \zeta$ plays a role of the effective viscosity, it should be positive and thereby one should take $\Lambda_{12} < 0$. To avoid a possible misunderstanding we should stress that derived equations only formally coincide with the hydrodynamical equations.

2.5.3 Phase transition to the state $k_0 \neq 0$. One-axis periodic system

Take now $\psi = \psi_0(t, \vec{r}) e^{-i\omega_c t + \vec{k}_0 \vec{r} + iS(t, \vec{r})}$ and assume $\vec{k}_0 \parallel z$. Let

$$\hat{D}_R^{-1} = -\omega_0^2 + \alpha_{01}(i\partial_t - \omega_c) + \alpha_{41}(\Delta + k_0^2)^2, \quad (91)$$

$$\hat{\Lambda}|\psi|^2 = (\Lambda_0 + \Lambda_1 i \partial_t)|\psi|^2. \quad (92)$$

We arrive at the equation of motion for $\chi = \psi_0(t, \vec{r}) e^{iS(t, \vec{r})}$, cf. [105],

$$\alpha_{01}(i\partial_t - \omega_c)\chi - 4\alpha_4(\vec{k}_0 \nabla)^2 \chi + \alpha_4 \Delta^2 \chi - \omega_0^2 \chi - \Lambda_0 |\chi|^2 \chi + \Lambda_{12} \chi \partial_t |\chi|^2 = 0. \quad (93)$$

Neglecting $\Delta^2 \psi_0$ term compared to $(\vec{k}_0 \nabla)^2 \psi_0$ we obtain (for $\vec{k}_0 \parallel z$)

$$\partial_t \rho_\psi + \partial_z(\rho_\psi v_z) \simeq 0 \quad (94)$$

with $\rho_\psi = \alpha_{01}\tilde{m}_{\text{ef}}\psi_0^2$, $\vec{v} = \nabla S/\tilde{m}_{\text{ef}}$, where now the effective mass $\tilde{m}_{\text{ef}} = \alpha_{01}/(-8\alpha_{41}k_0^2)$, $\alpha_{01} > 0$, $\alpha_{41} < 0$ and

$$\partial_t \vec{v} + \nabla \frac{v_z^2}{2} \simeq -\frac{\nabla P}{\rho_\psi} + \nabla \left[\frac{(4\eta/3 + \zeta)}{\rho_\psi} \frac{\partial_z(\rho_\psi v_z)}{\rho_\psi} \right], \quad (95)$$

with the kinetic coefficient $(4\eta/3 + \zeta)$ from (89) but with $m_{\text{ef}} \rightarrow \tilde{m}_{\text{ef}}$ and

$$\nabla P = -\frac{\rho_\psi}{\alpha_{01}\tilde{m}_{\text{ef}}} \nabla \left[-\omega_0^2 - \frac{\Lambda_0 \rho_\psi}{\alpha_{01}\tilde{m}_{\text{ef}}} - \alpha_{01}\omega_c - 4\frac{\alpha_{41}k_0^2 \partial_z^2 \sqrt{\rho_\psi}}{\sqrt{\rho_\psi}} \right]. \quad (96)$$

2.5.4 Phase transition to state $k_0 \neq 0$. Anisotropic three-axis crystal

Now, employing (60) let us take $\psi = \psi_0 e^{-i\omega_c + iS} \cos(k_{0x}x) \cos(k_{0y}y) \cos(k_{0z}z)$. We arrive at equation of motion for $\chi = \psi_0(t, \vec{r}) e^{iS(t, \vec{r})}$, cf. [105],

$$\alpha_{01}(i\partial_t - \omega_c)\chi - 4\alpha_4(\vec{k}_{0x}^2 \partial_x^2 + \vec{k}_{0y}^2 \partial_y^2 + \vec{k}_{0z}^2 \partial_z^2)\chi + \alpha_4 \Delta^2 \chi - \omega_0^2 \chi - \left(\frac{3}{4}\right)^3 \Lambda_0 |\chi|^2 \chi + \left(\frac{3}{4}\right)^3 \Lambda_{12} \chi \partial_t |\chi|^2 = 0. \quad (97)$$

Neglecting $\Delta^2 \psi_0$ compared to $(\vec{k}_0 \nabla)^2 \psi_0$ we obtain the continuity equation

$$\partial_t \rho_\psi + \tilde{\nabla}(\rho_\psi \vec{v}) = 0, \quad (98)$$

where $\tilde{\nabla} = (k_{0x}\partial_x, k_{0y}\partial_y, k_{0z}\partial_z)/k_0$, $\vec{v} = \tilde{\nabla}S/\tilde{m}_{\text{ef}}$, and the Navier–Stokes equation

$$\partial_t \vec{v} + \tilde{\nabla} \frac{\vec{v}^2}{2} = -\frac{\tilde{\nabla}P}{\rho_\psi} + \tilde{\nabla} \left[\frac{(4\tilde{\eta}/3 + \tilde{\zeta})}{\rho_\psi} \frac{\tilde{\nabla}(\rho_\psi \vec{v})}{\rho_\psi} \right], \quad (99)$$

compare Eqs. (99), (98) with Eqs. (87) and (88), derived in the homogeneous case. Here

$$(4\tilde{\eta}/3 + \tilde{\zeta})/\rho_\psi^2 = -(3/4)^3 \Lambda_{12}/(\alpha_{01} \tilde{m}_{\text{ef}})^2$$

and

$$\tilde{\nabla}P = -\frac{\rho_\psi}{\alpha_{01} \tilde{m}_{\text{ef}}} \tilde{\nabla} \left[-\omega_0^2 - \frac{(3/4)^3 \Lambda_0 \rho_\psi}{\alpha_{01} \tilde{m}_{\text{ef}}} - \alpha_{01} \omega_c - 4 \frac{\alpha_{41} k_0^2 \tilde{\nabla}^2 \sqrt{\rho_\psi}}{\sqrt{\rho_\psi}} \right]. \quad (100)$$

Note that in difference with the isotropic case, here enters the operator $\tilde{\nabla}$ rather than ∇ .

Summarizing, one can consider dynamics of the order parameter employing the hydrodynamical variables and solving then the equations formally coinciding with the equations of the non-ideal hydrodynamics.

2.5.5 Normal liquid

Standard hydrodynamical equations for the potential motion ($\text{curl } \vec{v} = 0$) of the normal liquid can be derived in a similar fassion, cf. [105]. For that we may introduce a physically small volume characterized by the common collective coordinates of its center of inertia \vec{r} considered at the time moment t . So, the N -particle Ψ function characterizing particles of this volume can be presented as

$$\Psi_N = \psi_0(t, \vec{r}) \psi(t, |\vec{r}_i - \vec{r}_j|) e^{iS(t, \vec{r}) + i\xi(t, |\vec{r}_i - \vec{r}_j|)}, \quad (101)$$

where i, j run $1, \dots, N$, ψ_0 and S are smooth real functions of (t, \vec{r}) and ψ and ξ are sharp real functions characterizing particles within the physically small volume. Then with the expansion (84) for the \hat{D}_R^{-1} and Λ , instead of (85), (86) we obtain the equations of motion, where operators \hat{D}_R^{-1} and $\hat{\Lambda}$ act on the function (101). Multiplying these equations of motion from the left on $\psi(t, |\vec{r}_i - \vec{r}_j|) e^{i\xi(t, |\vec{r}_i - \vec{r}_j|)}$ and averaging over $\int d^3\vec{r}_1 \dots d^3\vec{r}_N$, in case of the isotropic system we recover the equations, which have the same form as (85), (86), but with the coefficients α_i , Λ_i replaced to the short-range averaged quantities $\bar{\alpha}_i$, $\bar{\Lambda}_i$. Finally we arrive at the same Eqs. (88), (89), (90) but with $\alpha_i \rightarrow \bar{\alpha}_i$, $\Lambda_i \rightarrow \bar{\Lambda}_i$, $\rho_\psi \rightarrow \rho = \bar{\alpha}_{01}^2 \psi_0^2 / (2\bar{\alpha}_{31})$. Similarly, for the one-axis crystal we arrive at Eqs. (94), (95), (96) and in case of the lattice (60) at Eqs. (98), (99), (100) with the modifications $\alpha_i \rightarrow \bar{\alpha}_i$, $\Lambda_i \rightarrow \bar{\Lambda}_i$, $\rho_\psi \rightarrow \rho$. The coefficients should be found from the comparison of the model predictions with the data.

3 First-order phase transitions in slowly evolving systems

3.1 Typical pressure–density behavior at first-order phase transitions

3.1.1 Transition of liquid–vapor type

The first-order phase transitions may occur in various systems. These are the ordinary liquid–vapor phase transition in water and other liquid- and gaseous systems, the nuclear liquid–vapor phase transition, whose signatures are manifested in low-energy heavy-ion collisions, cf. [64, 77, 78, 79], feasibly the quark–hadron phase transition in baryon-rich matter, cf. [77], possible transition to the Δ -rich matter in the heavy-ion collisions [153], all phase transitions occurring to the states $k_0 \neq 0$, such as phase transitions to p wave pion- and kaon- condensate states [96, 111, 112], may be phase transition to the charged ρ^- condensate state in rather massive neutron stars [114, 115, 116], etc.

In compact stars, appearance of a strong phase transition may result in a second neutrino burst, if the transition occurred right after a supernova explosion at a hot stage of the compact star evolution. A possibility of the delayed second neutrino burst in the event supernova SN 1987A has been considered in [217, 218, 96]. It might be associated with a significant delay of the heat transport to the neutron-star surface, if the system is close to the pion–condensate phase transition. Recently, new arguments have been expressed for that namely two neutrino bursts were measured during 1987A explosion, one delayed respectively the other one by 4.7 h, cf. [219]. The second neutrino burst could then be related to the phase transition of the neutron star to the pion condensate state. In addition, a phase transition to the pion- or to the kaon–condensate state could also occur during tens-second-period of the neutron star formation or later resulting in a blowing off a star matter [220, 96]. In old neutron stars, the first-order phase transitions could also result in a strong star-quakes [96, 221].

In the cases of such systems as the liquid water – vapor and the nuclear fireball formed at low-energy collisions of isospin-symmetric nuclei one deals with the same species, in the latter case with nucleons, although at different densities. So, in both cases one deals with the one conserved charge: the number of particles in the first case and the baryon number in the second case. Such transitions in statistical physics are named the congruent transitions, cf. [222, 223]. So we will speak about the liquid–vapor (or differently saying liquid–gas) transition, if the variation of the density can be considered as the order parameter. Then one may deal with the equations of the non-ideal hydrodynamics to describe the dynamics of the phase transition. We will also conjecture, cf. [77], that the hadron–quark phase transition, as the ordinary liquid water–vapor transition, can be described in $n(t, \vec{r}), T(t, \vec{r})$ local variables.

The typical pressure–density behaviour has a van der Waals form. The pressure isotherms as functions of the density are shown in Fig. 3, cf., e.g., [17]. In the thermodynamical equilibrium, a necessary condition for the stability is that pressure P does not increase with the volume V_3 . The interval AB corresponds to a metastable supercooled vapor (SV), when on any horizontal line $\mu_V > \mu_L$, and the interval CD, relates to a metastable overheated liquid (OL), when on any horizontal line the chemical potential in liquid state enlarges that one in vapor phase, $\mu_L > \mu_V$. The interval BC labels an unstable spinodal region, where excitations grow exponentially. At the first-order phase transition in case of one conserved charge, thermally equilibrium configurations belong to the Maxwell construction (MC) shown by the horizontal dashed line, on which the chemical potentials μ_A and μ_D are equal to each other. The areas separated by the curve $P(1/n)$ and the MC horizontal line prove to be equal [17].

Fig. 4 shows the plot of $T/T_{\text{cr}} = f(n/n_{\text{cr}})$ for the van der Waals equation of state. Trajectories of the system undergoing an approximately adiabatic cooling are shown by the short dashed lines s_{cr} and s_{max} , where $\tilde{s} \equiv s/n \simeq \text{const}$, s is the entropy density. The upper convex curve (MC, bold solid line) demonstrates the boundary of the MC. The bold dashed line, ITS, shows the boundary of the isothermal spinodal region, and the bold dash-dotted curve, AS, indicates the boundary of the adiabatic spinodal region. The supercooled vapor (SV) and the overheated liquid (OL) regions are situated between the

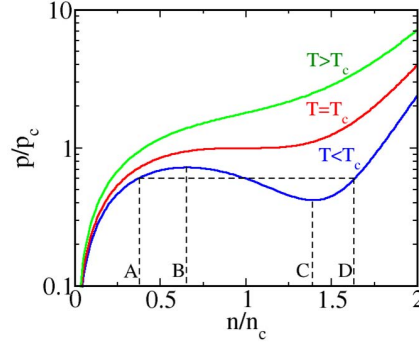


Figure 3: Schematic pressure isotherms as functions of the number density at a liquid–vapor-like phase transition. P_c , n_c and T_c are the pressure, number density and temperature at the critical point. Horizontal dashed line shows the Maxwell construction.

MC and the ITS curves, on the left and on the right, respectively. For $\tilde{s}_{cr} > \tilde{s} > \tilde{s}_{MC2}$, where \tilde{s}_{cr} is the value of the specific entropy \tilde{s} at the critical point, and (in the given example) the line with \tilde{s}_{MC2} passes through the point $n/n_{cr} = 3$ at $T = 0$, the system traverses the OL state (the region OL in Fig. 4), the ITS region (below the ITS line) and the AS region (below the AS line). For $\tilde{s} > \tilde{s}_{cr}$ the system trajectory passes through the SV state (the region SV in Fig. 4) and the ITS region. At the ITS line

$$u_T^2 = (\partial P / \partial \rho)_T = 0$$

and at AS line

$$u_{\tilde{s}}^2 = (\partial P / \partial \rho)_{\tilde{s}} = 0,$$

where u_T and $u_{\tilde{s}}$ have the meaning of the isothermal and adiabatic sound velocities, respectively, n is the number density. Below the ITS line (and above the AS line) one has $u_T^2 < 0$, $u_{\tilde{s}}^2 > 0$. After the

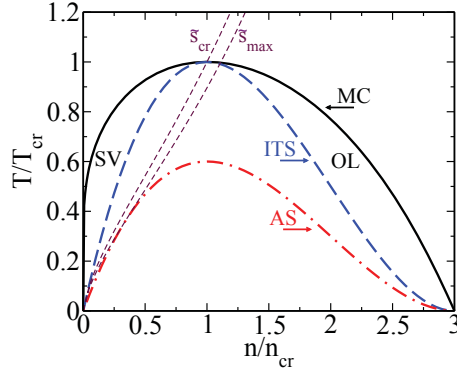


Figure 4: The phase diagram of the van der Waals equation of state on $T(n)$ -plane. The bold solid, dashed and dash-dotted curves show boundaries of the MC, the spinodal region at $T = \text{const}$ and $\tilde{s} = \text{const}$, respectively. The short dashed lines show two adiabatic trajectories of the system evolution: the curve labeled \tilde{s}_{cr} passes through the critical point; the curve \tilde{s}_{max} , through the maximum pressure point $P(n_{P,max})$ on the $P(n)$ plane, cf. [78].

system enters the region of the first-order phase transition of the liquid–vapor type the approximation of constant entropy fails and the description of the dynamics of the system needs solution of non-ideal hydrodynamical equations [77, 78]. Similarly, the description of the dynamics of the second-order phase transition needs solution of non-ideal hydrodynamical equations in the case, when the density and the temperature (or entropy) can be considered as appropriate order parameters. Moreover, let us note that

at the expansion of the nuclear fireball prepared in a heavy-ion collision first the trajectory of the system crosses the ITS and only at lower T it crosses the AS line. Thus, the vapor – liquid phase transition calculated within the non-ideal hydrodynamics starts at a higher T than the transition calculated within the ideal hydrodynamics. In the latter case, e.g., in the so called three-fluid ideal hydrodynamics in order to somehow simulate the viscosity effects one introduces the effective friction forces [224].

3.1.2 Mixed phases and pasta

The liquid – vapor congruent phase transition, which we discussed, is well known issue in condensed matter physics as well as the non-congruent first-order phase transitions. In the latter case two or more charges are conserved. In case of the asymmetric nuclear matter occurring in collisions of heavy nuclei the proton and neutron fractions are different in both phases due to significant density dependence of the symmetry energy. Thereby two conserving charges, the baryon charge and isospin, are relevant quantities. In case of the compact stars the conserving charges are the baryon and electric charges. The Coulomb force is long-distant one. As the consequence, the Coulomb contribution to the energy of the nucleus grows with the mass number A and the charge Z stronger (as $\propto Z^2/A^{1/3}$) than the surface energy term $\propto A^{2/3}$ that leads to the preference of the non-spherical form and fission of heavy nuclei. Interplay between the surface tension and the Coulomb interaction, which is screened in the matter on the Debye length, results in a possibility of appearance of structures of different geometry, as droplets, rods and slabs and configurations of a more whimsical form, cf. [176, 177, 178, 179, 180].

It is commonly accepted that the outer crust of the neutron star, at $\rho < 4 \cdot 10^{11}$ g/cm³, contains the Coulomb lattice of Fe nuclei and electrons compensating the charge. At the neutron density $\rho > 4 \cdot 10^{11}$ g/cm³ neutrons drip out of nuclei. Nuclei organized in the lattice are surrounded by the neutron gas, cf. [225, 226]. With increasing baryon density in an interval, $0.1n_0 \lesssim n < n_m \simeq 0.7n_0$, the pasta phase may arise [176, 177, 178, 181]. In some interval of densities above n_m the state consists of the neutron Fermi liquid, and a shallow proton Fermi sea with the charge compensated by electrons and μ^- . Then for $n \gtrsim (2 - 3)n_0$ there may appear the pion and anti-kaon condensates in states with $k_0 \neq 0$, cf. [95, 96, 111, 112], as well as K^- condensate in the state with $k_0 = 0$, cf. [227, 228, 229, 230], and probably for a somewhat larger density the phase transition to the quark matter state may occur, cf. [231, 180, 232, 183, 139, 140]. It has been argued that all mentioned transitions are, most likely, the first-order transitions.

Glendenning rised the issue, whether systems composed of charged particles consist mixed phases instead of the configuration described by the Maxwell construction [175]. In particular, the possibilities of the hadron (npe) - kaon condensate ($npeK_{cond}$) and hadron - quark mixed phases were discussed. The existence of such kind of mixed phases in dense neutron star interiors would have important consequences for the equation of state, glitch phenomena and neutrino transport and emissivity, cf. [233, 110, 234, 235, 236]. Reference [235] suggested that at the neutrino trapping stage in compact stars the pasta phase may behave similarly to amorphous matter. Already very low temperatures (typically $T \gtrsim 0.1$ MeV) may simulate transitions between different geometrical structures in the pasta phase of the neutron star crusts [237]. Recall here that the isospin-symmetric nuclear matter at $T \neq 0$ already for $n \gtrsim n_c^{(1)} \sim (0.5 - 0.8)n_0$ begins to behave as an amorphous matter due to strong pion fluctuations with $k_0 \neq 0$, cf. [132, 96, 6, 7].

First works [175, 229, 230, 110] assumed that the MC is always unstable due to the inequality of the local electron chemical potentials of two phases $\mu_e^I(n^I)$ and $\mu_e^{II}(n^{II})$ and, thus, a possibility for particles to fall down from the level characterized by the higher electron chemical potential of the one phase to the lower level of the other phase. It was thought that existence of a wide region of the mixed phase determined by fulfilment of the Gibbs conditions is inevitable. However it has been observed that in some models the Gibbs condition of equality of electron chemical potentials of two phases can't be fulfilled at all [238, 239, 160], whereas conditions for the MC are fulfilled. Moreover [176] demonstrated

the possibility of existence of the structures of different geometry determined by competition between the Coulomb energy and the surface energy of droplets. Then [240] and [241] applied these ideas to the description of the mixed phase for the hadron–quark and kaon phase transitions, respectively. It was demonstrated that there should exist a critical value of the surface tension, above which structures are not permitted.

References [179, 180] clarified that the Gibbs condition of equality of the charged chemical potentials in two phases $\mu_e^I = \mu_e^{II}$, as it was formulated for spatially homogeneous configurations, has no meaning in the application to charged systems of a small size, if one does not incorporate properly the electric field effects. It only fixes the level, from which one counts the electric potential. Only the gauge invariant quantity $\mu_e - V$ should enter the equations of motion including the Poisson equation for the electric potential V . References [179, 180, 181, 182, 183, 242] demonstrated that the careful consideration of the electric field including the Debye screening effects allows to resolve the mentioned contradiction. For the quark–hadron first-order phase transition, it was found that $\sigma_c \simeq 60 \text{ MeV/fm}^2$, so for $\sigma > \sigma_c$ the mixed quark–hadron phase is not realized. It was shown that, in cases of the quark-hadron and kaon condensate pastas, the $P(n)$ behaviour is close to that given by the MC, cf. [182, 183, 242, 243].

It is interesting to notice that elastic properties of the pasta phases might be similar to those of liquid crystals, cf. [244, 245]. Proton superconductivity still complicates structure of the pasta phase in neutron star crusts [246]. A possibility of a manifestation of some features of the pasta phase in heavy-ion collisions was recently discussed in [8].

The dynamics of the pasta phase transition was studied with the help of the formalism of molecular dynamics, cf. [247, 248, 249, 250, 251, 252, 253]. References [249, 250] demonstrated that in supernova matter a lattice of rod-like nuclei is formed from a bcc lattice by compression. It was demonstrated that in the transition process the system undergoes a zigzag configuration of elongated nuclei, which are formed by a fusion of original spherical nuclei. Artificial stretching rates were employed, cf. [251], whereas more realistic calculations are still required.

In a more straight way the dynamics of the formation of the pasta structures can be studied using Eq. (1). Within relativistic mean-field models the mean meson fields and the electric potential can be considered as the order parameters. Such a way (at ignorance of the white noise terms) was sketched in [181]. However the kinetic rates Γ_i cannot be found within the mean-field approach. They are expressed via the transport coefficients. The latter should follow from the analysis of experimental information and the study of relevant microscopic processes. In application to heavy-ion collisions, different estimates have been done, cf. [254, 255, 256, 257, 258, 259, 260, 261, 262] and refs therein. Various evaluations of the shear and bulk viscosities have been also performed in case of the neutron star matter, cf. [263, 264] and refs. therein. Their knowledge is important, e.g., for the description of the neutrino transport and the r -mode relaxation. In case of the pion condensate phase transition the Γ -rate is determined by the imaginary part of the pion polarization operator, cf. [265]. However this ambitious program still needs much more effort.

3.2 Transition between homogeneous configurations

3.2.1 Phenomenological model

Let us assume $k_0 = 0$, $\alpha_{02} = \alpha_1 = \alpha_2 = \alpha_{32} = \alpha_4 = 0$, $\alpha_{31} > 0$. Then the part of the free energy dependent on the order parameter is as follows [105]

$$\delta F[\psi] = \int d^3x [\alpha_{31} |\nabla \psi|^2 + \omega_0^2 |\psi|^2 + \Lambda_0 |\psi|^4 / 2 - h e^{im\pi} \psi (\psi^* / \psi)^{1/2} - h e^{im\pi} \psi^* (\psi / \psi^*)^{1/2}]. \quad (102)$$

Equation (1) yields

$$-\alpha_{31} \Delta \psi + \omega_0^2 \psi + \Lambda_0 |\psi|^2 \psi - h e^{im\pi} (\psi / \psi^*)^{1/2} = -\Gamma^{-1} \partial_t \psi. \quad (103)$$

Introducing dimensionless variables

$$\psi = e^{i\phi}\psi_0\chi,$$

$\psi_0 = \sqrt{-\omega_0^2/\Lambda_0}$, ϕ is arbitrary real constant phase, $\tilde{\Delta} = \Delta/l_0^2$, $\tilde{h} = -2h/(\omega_0^2\psi_0)$, $|\tilde{h}| \ll 1$, $l_0 = \sqrt{2\alpha_{31}/(-\omega_0^2)}$, $t_0 = -2/(\Gamma\omega_0^2)$, for $\omega_0^2 < 0$ we get equation

$$\chi'_\tau = \tilde{\Delta}\chi + 2\chi(1 - |\chi|^2) + \tilde{h}, \quad (104)$$

where $\tau = t/t_0$, $\tilde{r} = \vec{r}/l_0$.

3.2.2 Limit $h = 0$ (second-order phase transition)

In case of the second-order phase transition (for $h = 0$) Eq. (104) simplifies as

$$\chi'_\tau = \tilde{\Delta}\chi + 2\chi(1 - |\chi|^2). \quad (105)$$

For $|\chi| \ll 1$ it can be linearized and gets the solution of the form (in dimensionless variables)

$$\chi = \chi_0 e^{i\tilde{k}\tilde{x} + (2 - \tilde{k}^2)\tau}, \quad (106)$$

for arbitrary $\chi_0 \neq 0$.

Equation (105) has also the spatially uniform solution

$$\chi^2(\tau > 0) = \frac{\chi_0^2}{\chi_0^2 + (1 - \chi_0^2)e^{-4\tau}}, \quad (107)$$

where χ_0 is the real constant quantity describing an initial uniform distribution $\chi(0) = \chi_0$. If $\chi(0) > 0$, then the solution $\chi(\tau > 0)$ reaches the equilibrium value $\chi(\tau \rightarrow \infty) = 1$, and $\chi(\tau \rightarrow \infty) = -1$ for $\chi(0) < 0$. Both solutions correspond to the same energy. We see that spatially inhomogeneous small perturbations satisfying Eq. (106) with $\tilde{k}^2 < 2$ grow in time with a smaller rate compared to the spatially uniform fluctuations. For $\tilde{k}^2 > 2$ excitations are damped. Note that solutions (106) and (107) are limiting cases of a more general solution

$$\chi(\tau > 0) = e^{i\tilde{k}\tilde{x}} \sqrt{\frac{(2 - \tilde{k}^2)\chi_0^2}{2\chi_0^2 + (2 - \tilde{k}^2 - 2\chi_0^2)e^{-2\tau(2 - \tilde{k}^2)}}}. \quad (108)$$

Equation (107) continues to hold for $h \neq 0$ provided $|\chi_0| \gg |h|$. In this case it describes growth of the initially spatially-uniform configurations within the spinodal region at the first-order phase transition to the state $k_0 = 0$.

In case of the real order parameter we could start with Eq. (10) yielding the equation of motion in the form

$$-\alpha_{31}\Delta\psi + \omega_0^2\psi + \Lambda_0\psi^3 - h = -\Gamma^{-1}\partial_t\psi. \quad (109)$$

For $h = 0$ this equation, being expressed in appropriate dimensionless variables, has the same uniform solution (107).

Note here that, as it will be shown in Section 4, equations describing the phase transition of the gas-liquid type within the non-ideal hydrodynamics, cf. Eqs. (162), (164) below, are in general case not reduced to the Ginzburg-landau Eqs. (104), (109).

3.2.3 Transition from metastable to stable state

Angle-independent solutions. For spherically symmetric configurations assuming $\omega_0^2 < 0$ and using dimensionless variables $\psi = e^{i\phi}\psi_0\chi$, $\psi_0 = \sqrt{-\omega_0^2/\Lambda_0}$, ϕ is arbitrary real constant phase, $\tilde{h} = -2h/(\omega_0^2\psi_0)$, for $|\tilde{h}| \ll 1$, $l_0 = \sqrt{2\alpha_{31}/(-\omega_0^2)}$, $t_0 = -2/(\Gamma\omega_0^2)$, we derive equation

$$\chi'_\tau = \chi''_{\tilde{r}} + \frac{n-1}{\tilde{r}}\chi'_{\tilde{r}} + 2\chi(1-\chi^2) + \tilde{h}, \quad (110)$$

where $\tau = t/t_0$, $\tilde{r} = r/l_0$, $r = x$ for $n = 1$; $r = \sqrt{x^2 + y^2}$ for $n = 2$ and $r = \sqrt{x^2 + y^2 + z^2}$ for $n = 3$. As we have discussed, to get this equation we took $m = 0$ for $\chi(r) > 0$ and $m = 1$ for $\chi(r) < 0$. In this case the same equation follows from variation of the functional (10) introduced from the very initial for the purely real field.

The free energy of the seed of the stable phase inside the metastable medium counted from the volume free energy, $F_V = -\frac{\omega_0^4}{2\Lambda_0}V_3$, is as follows

$$\delta F_{\text{seed}} = E_0 \int d^3x \left[\frac{(\nabla_{\tilde{r}}\chi)^2 + (\chi^2 - 1)^2}{2} - \tilde{h}\chi \right], \quad E_0 = \Lambda_0\psi_0^4. \quad (111)$$

Solution of Eq. (110), $\chi = 1 + \tilde{h}/4$, describes stable phase, $\delta F_{\text{seed}} = [-E_0\tilde{h} + O(\tilde{h}^2)]V_{\text{seed}}$, and $\chi = -1 + \tilde{h}/4$ describes metastable phase, $\delta F = [E_0\tilde{h} + O(\tilde{h}^2)](V_3 - V_{\text{seed}})$. Here V_3 is the total volume, V_{seed} is the volume of the seed, $V_{\text{seed}} = 4\pi r_0^3(t)/3$ for spherical droplets. Let us seek solution of Eq. (110) in the form

$$\chi = -\tanh(\tilde{r} - \tilde{r}_0(\tau)) + \tilde{h}/4, \quad (112)$$

such that solution for $\tilde{r}_0(\tau) - \tilde{r} \gg 1$ describes the stable phase ($\chi = 1 + \tilde{h}/4$) and for $\tilde{r} - \tilde{r}_0(\tau) \gg 1$, the metastable phase. Substituting Eq. (112) in Eq. (110), where we approximate the curvature term as $\frac{n-1}{\tilde{r}}\chi'_{\tilde{r}} \simeq \frac{n-1}{\tilde{r}_0}\chi'_{\tilde{r}}$, we arrive at the equation

$$\frac{d\tilde{r}_0(\tau)}{d\tau} = \frac{3\tilde{h}}{2} - \frac{n-1}{\tilde{r}_0(\tau)}. \quad (113)$$

For $n = 1$ solution

$$\chi = -\tanh(\tilde{r} - \tilde{r}_0(0) - 3\tilde{h}\tau/2) + \tilde{h}/4 \quad (114)$$

describes growth of the seed heaving the form of a slab, where now $\tilde{r} = |x|/l_0$, $\tilde{r}_0(0) = |x_0(0)|/l_0$, $2|x_0(0)|$ is the initial size of the slab-seed. A slab of the stable phase (region $\chi > 0$, $\tilde{r} - \tilde{r}_0(0) - 3\tilde{h}\tau/2 < 0$) of arbitrary initial size, being formed in a fluctuation inside a metastable phase ($\tilde{r} - \tilde{r}_0(0) - 3\tilde{h}\tau/2 > 0$), begins to grow. Following (111) the gain in the free energy is

$$\delta F_{\text{seed}}^{\text{slab}} = \frac{4}{3}E_0l_0 - 2E_0l_0\tilde{h}\tilde{r}_0(\tau), \quad (115)$$

where $\tilde{r}_0(\tau) = \tilde{r}_0(0) + 3\tilde{h}\tau/2$.

For $n \neq 1$, seeds of stable phase of the under-critical size, being initially formed inside the metastable phase, are then dissolved, whereas seeds of the overcritical size grow. According to Eq. (113), the critical size of the seed is given by

$$r_0^{\text{cr}} = \frac{2(n-1)l_0}{3\tilde{h}} = \frac{(2\alpha_{31})^{1/2}2(n-1)}{3|\omega_0|\tilde{h}} \gg 1/|\omega_0|. \quad (116)$$

The critical size of the initial seed also can be found by minimization of the free energy. For $n = 3$ (when seeds are spherical droplets), as it follows from (111) the gain in the free energy is given by

$$\delta F_{\text{seed}}^{\text{drop}} = \frac{16\pi}{3} E_0 l_0^3 \tilde{r}_0^2(\tau) - \frac{8\pi}{3} E_0 \tilde{h} l_0^3 \tilde{r}_0^3(\tau). \quad (117)$$

Probability of the formation of a seed of the stable phase of the critical size inside the metastable phase is as follows $W \sim e^{-\delta F(r_0^{\text{cr}})/T}$ and the typical time needed to prepare a droplet seed is

$$t_W \sim (\Gamma \Lambda_0 \psi_0^2)^{-1} \exp \left[\frac{64\pi (2\alpha_{31})^{3/2} |\omega_0|^7}{3^4 \Lambda_0^2 h^2 T} \right]. \quad (118)$$

Weakly non-spherical solutions. Let initial seed of the stable phase is slightly non-spherical. Then \tilde{r}_0 depends not only on τ but also on angles θ and ϕ in spherical coordinates,

$$\tilde{r}_0(\tau, \theta, \phi) = \sum_{lm} \tilde{r}_0^{lm}(\tau) Y_{lm}(\theta, \phi), \quad (119)$$

where $Y_{lm}(\theta, \phi)$ are spherical functions. Assume \tilde{r}_0^{lm} for $l \geq 1$ be small. Then equation of motion for the seed renders

$$\chi'_\tau = \chi''_{\tilde{r}} + \frac{2}{\tilde{r}_0(\tau, \theta, \phi)} \chi'_{\tilde{r}} + 2\chi(1 - \chi^2) + \tilde{h} - \frac{\hat{l}^2}{\tilde{r}_0^2(\tau, \theta, \phi)}, \quad (120)$$

where \hat{l} is the operator of the angular momentum. The solution is as follows [187],

$$\chi = -\tanh(\tilde{r} - \tilde{r}_0(\tau, \theta, \phi)) + \tilde{h}/4 \quad (121)$$

and

$$\frac{d\tilde{r}_0^0(\tau)}{d\tau} = \frac{3\tilde{h}}{2} - \frac{2}{\tilde{r}_0^0(\tau)}, \quad \frac{d\tilde{r}_0^l(\tau)}{d\tau} = \frac{(2 - l(l+1))\tilde{r}_0^l(\tau)}{(\tilde{r}_0^0(\tau))^2} \quad (122)$$

with $l \neq 0$. From here

$$\tilde{r}_0^l(\tau) = \tilde{r}_0^l(0) \exp \left(\int \frac{(2 - l(l+1))}{[\tilde{r}_0^0(t')]^2} dt' \right) \quad (123)$$

and modes with $l > 1$ are damped with growing time. Thereby initially a weakly non-spherical seed becomes spherical with passage of time. Undamped first harmonic, $l = 1$, describes displacement of the seed as a whole. For $\tilde{h} \sim 1$ initially spherical seeds may acquire a non-spherical form, cf. [266, 105].

Strongly non-spherical configurations. Some configurations, which conserve their form during the first-order phase transition from metastable phase to the stable one, were found in [105]. For example, the seeds of the pyramidal form are growing following the law

$$\chi = -\tanh \left[\frac{|\tilde{x}| + |\tilde{y}| + |\tilde{z}|}{\sqrt{3}} - \frac{3\tilde{h}\tau}{2} \right] + \frac{\tilde{h}}{4}. \quad (124)$$

Such seeds grow with $\sqrt{3}$ times higher velocity than spherical droplets and slabs and, as slabs, pyramidal seeds have no critical size.

The cone-like seeds grow as

$$\chi = -\tanh \left[\frac{|\tilde{z}| + \tilde{\rho}}{\sqrt{2}} - \frac{3\tilde{h}\tau}{2} \right] + \frac{\tilde{h}}{4}, \quad (125)$$

where $\tilde{\rho} = \sqrt{\tilde{x}^2 + \tilde{y}^2}$. These seeds grow with $\sqrt{2}$ times higher velocity than spherical droplets and slabs and, as slabs and pyramidal seeds, they have no critical size.

Rod-like seeds grow as follows

$$\chi = \tanh \left[|\tilde{z}| - \tilde{z}_0 - \frac{3\tilde{h}\tau}{2} \right] \tanh [\tilde{\rho} - \tilde{\rho}_0(\tau)] + \frac{\tilde{h}}{4}, \quad (126)$$

where

$$\tilde{\rho}_0(\tau) + \frac{2}{3\tilde{h}} \ln \frac{\tilde{\rho}_0(\tau) - \tilde{\rho}_c}{\tilde{\rho}_0(0) - \tilde{\rho}_c} = \tilde{\rho}_0(0) + \frac{3\tilde{h}\tau}{2}, \quad (127)$$

$\tilde{\rho}_c = 2/(3\tilde{h})$, whereas it follows that $\rho_0(\tau) \simeq \tilde{\rho}_0(0) + \frac{3\tilde{h}\tau}{2}$ for $\rho_0(0) \gg \tilde{\rho}_c$. This solution describes the regions of stable phase $|\tilde{z}| - \tilde{z}_0 - \frac{3\tilde{h}\tau}{2} < 0$, $\tilde{\rho} - \tilde{\rho}_0(\tau) < 0$, and metastable phase $|\tilde{z}| - \tilde{z}_0 - \frac{3\tilde{h}\tau}{2} < 0$, $\tilde{\rho} - \tilde{\rho}_0(\tau) > 0$, and $|\tilde{z}| - \tilde{z}_0 - \frac{3\tilde{h}\tau}{2} > 0$, $\tilde{\rho} - \tilde{\rho}_0(\tau) < 0$.

The solution describing evolution of a parallelepiped-like seed is given by

$$\chi = -\tanh \left[|\tilde{x}| - \tilde{x}_0 - \frac{3\tilde{h}\tau}{2} \right] \tanh \left[|\tilde{y}| - \tilde{y}_0 - \frac{3\tilde{h}\tau}{2} \right] \tanh \left[|\tilde{z}| - \tilde{z}_0 - \frac{3\tilde{h}\tau}{2} \right] + \frac{\tilde{h}}{4}, \quad (128)$$

for $\tilde{x}_0, \tilde{y}_0, \tilde{z}_0 \gg 1$. This solution is applicable everywhere except the region where simultaneously $|\tilde{x}| - \tilde{x}_0 - \frac{3\tilde{h}\tau}{2} > 0$, $|\tilde{y}| - \tilde{y}_0 - \frac{3\tilde{h}\tau}{2} > 0$ and $|\tilde{z}| - \tilde{z}_0 - \frac{3\tilde{h}\tau}{2} > 0$, and, as other quasi-one dimensional configurations, this solution has no critical size.

There are also other approximate solutions describing evolution of seeds of a more whimsical form, which keep their initial form during the time evolution. Certainly, formation of such configurations in fluctuations is tiny, cf. [267], but in presence of various defects forming the centers of condensation these seeds may grow to the new phase.

3.3 Transitions between inhomogeneous configurations

3.3.1 Simple phenomenological model of phase transition to the state $k_0 \neq 0$

Let us consider the first-order phase transition described by the complex order parameter and simplifying consideration we take $\alpha_{01} = \alpha_1 = \alpha_2 = 0$ but $\alpha_{02} > 0, \alpha_4 < 0$. Then the equation describing dynamics of the order parameter is of the form given by Eq. (1). Let the free-energy density be

$$\delta\mathcal{F} = \psi^* \hat{L} \psi + \Lambda_0 |\psi|^4 / 2 - h e^{im\phi} \psi (\psi^* / \psi)^{1/2} - h e^{im\phi} \psi^* (\psi / \psi^*)^{1/2}. \quad (129)$$

For inhomogeneous configurations

$$\hat{L} = \omega_0^2 - \alpha_4 (\Delta + k_0^2)^2. \quad (130)$$

If transition arises between two inhomogeneous configurations then in the whole space \hat{L} has the form (130).

3.3.2 Transition between two one-axis configurations

In order to describe first-order phase transition between two one-axis configurations we take ψ in the form

$$\psi = \psi_0 \chi(t, \vec{r}) e^{i\vec{k}_0 \vec{r} + i\phi}, \quad \psi_0^2 = -\omega_0^2 / \Lambda_0, \quad (131)$$

where ϕ is as before the arbitrary constant phase, $\omega_0^2 < 0$, $\Lambda_0 > 0$. Then employing (130), (131) and (11) we obtain equation of motion

$$\partial_t \chi = 2\chi(1 - \chi^2) + \tilde{h} + \tilde{L}\chi, \quad \tilde{L} \simeq (\vec{n}\vec{\nabla})^2 - \tilde{\alpha}\tilde{\Delta}^2, \quad (132)$$

where $\tilde{\alpha} = \omega_0^2/(32k_0^4\alpha_4)$, $\tilde{h} = -2h/(\omega_0^2\psi_0)$, $\tilde{\nabla} = (\partial_{\tilde{x}}, \partial_{\tilde{y}}, \partial_{\tilde{z}})$, $\tilde{x}_i = x_i/\sqrt{8k_0^2\alpha_4/\omega_0^2}$, $\tilde{t} = -t\omega_0^2/(2\alpha_{02})$. If, as we suppose, $|\omega_0^2| \ll k_0^2$ and thereby $\tilde{\alpha} \ll 1$, the term $\tilde{\alpha}\tilde{\Delta}^2\chi$ can be neglected.

Let us consider now the case when the seed of the stable phase inside the metastable one has a form of the slab of the transverse size (in dimensionless units) $2\tilde{x}_0 \gg 1$. Then for $\tilde{h} \ll 1$ the required solution of Eq. (132) is

$$\chi = -\tanh[|\tilde{x}| - \tilde{x}_0 - 3\tilde{h}\tilde{t}/2] + \tilde{h}/4. \quad (133)$$

As we have discussed, in this approximation there is no critical size for slab-seeds to grow from metastable to stable phase. Generally speaking, a tiny critical size appears provided one takes into account a small $\tilde{\Delta}^2$ contribution, however this critical size is much smaller than that one ($\propto 1/h$) we considered above. So, we will ignore this effect. The solution (133) describes growing process of a slab of the stable phase ($\psi = a(1 + \tilde{h}/4)e^{ik_0\tilde{r}}$) formed within the metastable phase with $\psi = a(1 - \tilde{h}/4)e^{ik_0\tilde{r}}$. In the dimensionless variables the slab boundary grows with the speed $\tilde{v}_{\tilde{x}} = 3\tilde{h}/2$ in the $\vec{k}_0 \parallel x$ direction.

Let us assume now that an initially spherical seed was formed in a fluctuation inside the metastable one-dimensional system characterized by the order parameter $\psi = a(1 - \tilde{h}/4)e^{ik_0\tilde{r}}$, $\vec{k}_0 \parallel z$. Then the solution describing growth of the seed for $t \geq 0$ is as follows

$$\chi \simeq -\tanh[|\tilde{z}| - \sqrt{|\tilde{R}_0^2 - \tilde{\rho}^2}|\text{sgn}(\tilde{R}_0 - \tilde{\rho}) - 3\tilde{h}\tilde{t}/2] + \tilde{h}/4, \quad (134)$$

$\text{sgn}(x) = 1$ for $x > 0$ and -1 for $x < 0$. In this case there is no critical size of the seed $\propto 1/h$. The speed of the growth of the boundary (labeled below by subscript b) of the seed ($|\tilde{z}_b| - \sqrt{|\tilde{R}_0^2 - \tilde{\rho}_b^2}|\text{sgn}(\tilde{R}_0 - \tilde{\rho}_b) - 3\tilde{h}\tilde{t}/2 \simeq 0$) is different in z and x, y directions:

$$(\tilde{v}_{\tilde{z}})_{\tilde{\rho}_b} = 3\tilde{h}/2, \quad (\tilde{v}_{\tilde{\rho}})_{\tilde{z}_b} \simeq \frac{(3\tilde{h}/2)(3\tilde{h}\tilde{t}/2 - |\tilde{z}_b|)}{\sqrt{(3\tilde{h}\tilde{t}/2 - |\tilde{z}_b|)^2 + \tilde{R}_0^2}}. \quad (135)$$

Thus $\tilde{v}_{\tilde{z}} > \tilde{v}_{\tilde{\rho}}$, for all t . The elongation of the seed occurs in the \vec{k}_0 direction. Note that similar ‘‘battonets’’ have been observed in the A-smectic liquid crystals, cf. [25].

The rod with the order parameter of the one-dimensional symmetry (131) evolves as

$$\psi = ae^{ik_0z}[-\tanh[|\tilde{z}| - \tilde{z}_0 - 3\tilde{h}\tilde{t}/2] + \tilde{h}/4 - C_1\nu_3\exp[(\tilde{\rho} - \tilde{\rho}_0)/\tilde{l}_\perp]\cos[(\tilde{\rho} - \tilde{\rho}_0)/\tilde{l}_\perp + C_2]], \quad (136)$$

where $\nu_3 = \text{sgn}[\tilde{z}_0 + 3\tilde{h}\tilde{t}/2 - \tilde{z}]$, $\tilde{l}_\perp = \tilde{\alpha}^{1/4}$, $\tilde{\rho} < \tilde{\rho}_0$, i.e. it elongates only in the z direction.

Initially spherical seed of inhomogeneous stable phase of the symmetry (37) placed in the metastable medium of the same symmetry grows to the stable phase as

$$\psi = ae^{ik_0r}[-\tanh(\tilde{r} - \tilde{r}_0 - 3\tilde{h}\tilde{t}/2) + \tilde{h}/4]. \quad (137)$$

Initially spherical seed of inhomogeneous stable phase of the symmetry $e^{ik_0\rho}$ evolves to the expanding disk

$$\psi = ae^{ik_0\rho}[-\tanh(\tilde{\rho} - \sqrt{|\tilde{R}_0^2 - \tilde{z}^2}|\text{sgn}(\tilde{R}_0 - |\tilde{z}|) - 3\tilde{h}\tilde{t}/2) + \tilde{h}/4]. \quad (138)$$

A rod of inhomogeneous stable phase of the symmetry (36) placed in the metastable medium of the same symmetry grows to the stable phase as

$$\psi = ae^{ik_0\rho}[-\tanh(\tilde{\rho} - \tilde{\rho}_0 - 3\tilde{h}\tilde{t}/2) + \tilde{h}/4]. \quad (139)$$

In all considered cases there is no critical size $\propto 1/h$ for the initial seed.

Above we considered the dynamics of the first-order phase transition from metastable to stable phase in case of the complex field with the effectively one-dimensional ordering (purely one-dimensional e^{ik_0z} , spherical e^{ik_0r} , or cylindric $e^{ik_0\rho}$) in both phases. The same consideration holds in case of the real

order-parameter heaving the same ordering in both phases, however provided the h -term in (10) is also periodic with the same ordering, e.g., for $\phi = a_{\text{stan}}\chi(t, \vec{r}) \cos(\vec{k}_0 \vec{r})$ we choose

$$h = h_0 \cos(\vec{k}_0 \vec{r})$$

for $h_0 = \text{const.}$ In these cases the equation for $\chi(t, \vec{r})$ has the same form (132) and thus solutions for χ we have considered for the case of the complex field continue to hold after the replacement $h \rightarrow h_0$.

Above we focused on dynamics of the order parameter in case of the transition of the system from the metastable state to the stable one. Within the unstable, so called spinodal region, the perturbations grow exponentially. Spinodal instabilities may manifest themselves in experiments with heavy ions in some collision energy interval that corresponds to the first-order phase transition region of the QCD phase diagram. One of the possible signatures is a manifestation of fluctuations with a typical size $r \sim 1/p_m$, $p_m \lesssim m_\pi$, in the rapidity spectra, see Ref. [78] and discussion in Section 4. Also note that in condensed matter physics a glassing transition from a liquid to a glass state can be interpreted as the first-order phase transition occurring at a very high viscosity, when the system passes a spinodal region, or it is very rapidly overcooled [105]. Then, there may appear an order at several angström-scale, which transforms in a disorder at larger distances. Spinodal instabilities will be discussed in a more detail in next Section.

3.4 Transitions between homogeneous and inhomogeneous phases

If a phase transition arises between two homogeneous configurations then in the whole space \hat{L} has the form

$$\hat{L} = \omega_0^2 - \alpha_3 \Delta, \quad (140)$$

with $\alpha_3 > 0$. Situation is a more involved, if the transition occurs between homogeneous and inhomogeneous states. Then in a part of space \hat{L} should be taken in the form (140) and in the other part of space it is given by (130). The transition region from these regions is rather narrow $\delta r \sim 1/k_0$ being characterized by the minimal length scale in the given problem. Using this, instead of explicit description of the transition region one can employ the appropriate boundary conditions, cf. [184, 104].

For the description of the first-order phase transition to homogeneous state one arrives at the same Eq. (132) where now

$$\tilde{\hat{L}} = \tilde{\Delta}, \quad \tilde{x}_1 = x_i \sqrt{(-\omega_0^2)/(2\alpha_3)}, \quad (141)$$

and $\psi_0 = \sqrt{-\omega_0^2/\Lambda_0}$, $\tilde{h} = 2h/(-\omega_0^2\psi_0)$ and $\tilde{t} = -\omega_0^2/2\alpha_{02}$ have the same values as for the inhomogeneous phase transition, $\omega_0^2 < 0$, $\Lambda_0 > 0$.

For the three-axis system with the real order parameter of the form (60) we may also obtain Eq. (132), but where now

$$\tilde{\hat{L}} = -\tilde{\alpha}\tilde{\Delta}^2 + \tilde{\Delta}, \quad \tilde{x}_i = x_i/\sqrt{8k_{0i}^2\alpha_4/\omega_0^2}, \quad x_i = (x, y, z), \quad (142)$$

$\alpha_4 < 0$, $\omega_0^2 < 0$.

For $\tilde{\alpha} \ll 1$, i.e. in the vicinity of the critical point, the operators $\tilde{\hat{L}}$ given by Eq. (142) and (141) are of approximately the same form although presented in different variables. Thus using results obtained with (141) one may conclude that the seed of the metastable phase (60) of ellipsoidal form with $\tilde{\hat{L}}$ determined by Eq. (142) does not change the form during its expansion into the stable phase of the same type of the symmetry. It is described by Eq. (110) although in other variables. Initially spherical seed of the phase (142) gets ellipsoidal form during expansion. Similar description of the evolution of the system takes place, if the field is of the type (64). In this case $\tilde{\hat{L}} = \tilde{\Delta} - \tilde{\alpha}(\tilde{\partial}_x^4 + \tilde{\partial}_y^4 + \tilde{\partial}_z^4) \simeq \tilde{\Delta}$.

Transitions from the metastable phase of the symmetry (64) to the stable one of the symmetry (60), as well as from the metastable configuration of the type (60) to that of the symmetry (64), are described in the same manner, if parameters Λ_0 are the same in both cases, since \tilde{L} operators in both cases approximately coincide.

Now let us consider more specifically the case of the phase transition from the metastable homogeneous phase to the stable inhomogeneous phase. The case of equal surface energies of homogeneous and inhomogeneous phases can be studied analytically. The boundary conditions

$$\Re D^{-1}(k_0^2) = \Re D^{-1}(k^2 = 0), \quad (143)$$

$$(d\Re D^{-1}(k^2)/dk^2)_{k=k_0} = 0, \quad (144)$$

and

$$(d^2\Re D^{-1}(k^2)/d(k^2)^2)_{k=k_0} = (d^2\Re D^{-1}(k^2)/d(k^2)^2)_{k=0} \quad (145)$$

should be fulfilled. The conditions (143), (144) mean that $\Re D^{-1}(k^2)$ has the same minimal value at $k = k_0 \neq 0$ and $k_0 = 0$ and condition (145) means that surface energies of seeds of both phases are equal. Employing (132), (141) and (142) we need to require $\alpha_3 = -4k_0^2\alpha_4 > 0$. Further assume that conditions (143)–(145) are fulfilled.

Let initially the metastable homogeneous phase occupies the half space $x > 0$ and the one-axis inhomogeneous stable phase $\psi = ae^{ik_0x}$ occupies the half space $x < 0$ and let

$$\psi_{<} = a\chi_{<}(0, x)e^{ik_0x} \quad x < 0, \quad (146)$$

$$\psi_{>} = a\chi_{>}(0, x) \quad x > 0, \quad (147)$$

Both solutions $\chi_{<}(t, x)$ and $\chi_{>}(t, x)$ in the considered case have the same form

$$\chi = -\tanh(\tilde{x} - 3\tilde{h}\tilde{t}/2 - \tilde{x}_1) + \tilde{h}/4. \quad (148)$$

The order parameters are matched at $x = 0$ provided $\tilde{x}_1 \simeq -\tilde{h}/4$. Then $\psi_{<}(0, 0) = \psi_{>}(0, 0) = 0$, $\psi'_{<}(0, 0) = \psi'_{>}(0, 0) = 0$, since a smooth continuation of χ and since $ik_0\psi_{<}(0, 0) = 0$. The time dependent solution becomes

$$\psi_{<} = ae^{ik_0x}[-\tanh(\tilde{x} - 3\tilde{h}\tilde{t}/2 + \tilde{h}/4) + \tilde{h}/4], \quad (149)$$

$$\psi_{>} = a[-\tanh(\tilde{x} - 3\tilde{h}\tilde{t}/2 + \tilde{h}/4) + \tilde{h}/4]. \quad (150)$$

The one-axis crystal, $\psi_{<} \propto e^{ik_0x}$, grows from the surface with the passage of time following the law $x = 3ht/2$. The solution (149) continues to hold for the case, when the metastable phase occupying the half space $x > 0$ has the same symmetry as the stable phase $\psi = ae^{ik_0x}$ at $x < 0$ at $t = 0$.

Initially spherical seed with the order parameter $\psi_{<} \propto e^{ik_0r}$ appeared inside a metastable uniform matter evolves as

$$\psi_{<} = ae^{ik_0r}[-\tanh(\tilde{r} - 3\tilde{h}\tilde{t}/2 - \tilde{r}_0 + \tilde{h}/4) + \tilde{h}/4], \quad (151)$$

and

$$\psi_{>} = a[-\tanh(\tilde{r} - 3\tilde{h}\tilde{t}/2 - \tilde{r}_0 + \tilde{h}/4) + \tilde{h}/4]. \quad (152)$$

At the phase boundary $r = r_0 + 3ht/2 + h/4$ the order parameter ψ and its r -derivative are continuous quantities.

Therefore, provided conditions (143)–(145) are fulfilled, in dependence on the structure of the order parameter in the seed the metastable uniform phase either undergoes the first-order phase transition to the phase of the same symmetry or to the lattice.

4 Hydrodynamics of liquid–gas-type transition at small over-criticality. Nuclear liquid–gas and hadron–quark transitions

Further assume that the dynamics of a phase transition can be described using the variables n and s (or T), where n is the local baryon density, s is the local entropy density, T is the local temperature, cf. [61, 77, 78, 79]. Also, to proceed analytically assume that the system is rather close to the critical point of the phase transition. Refs. [268, 269, 270] demonstrated effect of the critical slowing down that limits the growth of the σ -field correlation length in the vicinity of the critical point. Some models speculate about explosive freeze-out assuming an increase of the bulk viscosity close to the critical point, see [271, 272]. Since all the processes in the vicinity of the critical point are slowed down, the velocity of a seed of a new phase prepared in the old phase, \vec{u} , is much smaller than the mean thermal velocity and one may use equations of non-relativistic non-ideal hydrodynamics: the Navier–Stokes equation, the continuity equation, and equation for the heat transport, even if one deals with violent heavy-ion collisions,

$$m^*n [\partial_t u_i + (\vec{u}\nabla)u_i] = -\nabla_i P + \nabla_k \left[\eta \left(\nabla_k u_i + \nabla_i u_k - \frac{2}{\nu} \delta_{ik} \text{div} \vec{u} \right) + \zeta \delta_{ik} \text{div} \vec{u} \right], \quad (153)$$

$$\partial_t n + \text{div}(n\vec{u}) = 0, \quad (154)$$

$$T \left[\frac{\partial s}{\partial t} + \text{div}(s\vec{u}) \right] = \text{div}(\kappa \nabla T) + \eta \left(\nabla_k u_i + \nabla_i u_k - \frac{2}{\nu} \delta_{ik} \text{div} \vec{u} \right)^2 + \zeta (\text{div} \vec{u})^2. \quad (155)$$

Here m^* is the baryon quasiparticle mass, P is the pressure. The quantities η and ζ are the shear and bulk viscosities, κ is the thermal conductivity, ν shows the geometry of the seed under consideration (droplets, rods, slabs).

All thermodynamical quantities can be expanded near a reference point (n_r, T_r) , which is assumed to be rather close to the critical point but outside the fluctuation region (determined by the value of the Gi number). The latter circumstance is important for the determination of the specific heat $c_{V,r}$ and transport coefficients, which may diverge in the critical point, whereas other quantities are smooth functions of n, T and calculating them one can put $n_r = n_{cr}, T_r = T_{cr}$.

The Landau free energy counted from the value at $n_r \simeq n_{cr}, T_r \simeq T_{cr}$ in the variables $\delta n = n - n_{cr}, \delta T = T - T_{cr}, \delta(\delta F_L)/\delta(\delta n) = P - P_f + P_{MC}$ can be presented as [61, 77, 78, 273]

$$\delta F_L = \int \frac{d^3x}{n_{cr}} \left\{ \frac{cm^*[\nabla(\delta n)]^2}{2} + \frac{\lambda m^{*3}(\delta n)^4}{4} - \frac{\lambda v^2 m^*(\delta n)^2}{2} - \epsilon \delta n \right\} + \delta F_L(k_0), \quad (156)$$

where $\epsilon = P_f - P_{MC} \simeq n_{cr}(\mu_i - \mu_f)$ is expressed through the (final) value of the pressure after the first-order phase transition has occurred, P_f , and the value of the pressure at the Maxwell construction, P_{MC} ; μ_i and μ_f are the chemical potentials of the initial and final configurations (at fixed P and T). The quantity $\epsilon \neq 0$, if one deals with a first-order phase transition, and $\epsilon = 0$, if a transition is of the second order. The maximum of the quantity ϵ is $\epsilon_m = 4\lambda v^3/(3\sqrt{3})$. For the description of phase transitions to the uniform state, $k_0 = 0$, one may retain only the term $\propto c[\nabla(\delta n)]^2$ in the expansion of the free energy in the density gradients, using $c > 0$. For the description of phase transitions to the inhomogeneous state, $k_0 \neq 0$, one should perform expansion retaining at least terms up to $\propto d[\Delta(\delta n)]^2$, assuming $c < 0$ and $d > 0$. Therefore the last term in (156) appears only, if $k = k_0 \neq 0$ [105, 273], like for the phase transition to the solid state, liquid crystal state, or a pion condensate state in a dense nuclear matter. Then for $k_0 \neq 0$ and $c < 0, d > 0$ we have

$$\delta F_L(k_0) = \int \frac{d^3x}{n_{cr}} \left\{ \frac{dm^*}{2} (\Delta \delta n)^2 - \left(\frac{cm^*k_0^2}{2} + \frac{dm^*k_0^4}{2} \right) (\delta n)^2 \right\}, \quad (157)$$

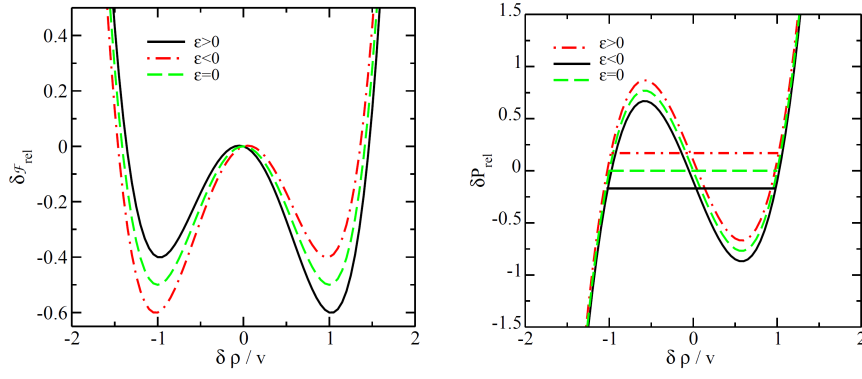


Figure 5: The Landau free-energy density $\delta\mathcal{F}_{\text{rel}} = \delta\mathcal{F}_L/\mathcal{F}_L(T_{cr}, \rho_{cr})$ and the value $\delta P_{\text{rel}} = \rho_{cr} \frac{\delta[F_L(T, \delta\rho)]}{\delta(\delta\rho)}|_T / P(T_{cr}, \rho_{cr})$, as functions of the order parameter $\delta\rho = m^*\delta n$ for the equation of state determined by Eq. (156), at $T < T_{cr}$. Dashed horizontal line ($\epsilon = 0$) in the right panel shows MC. Figure is adopted from [77].

where $k_0^2 = -\frac{c}{2d} > 0$ follows from minimization of $\delta F_L(k_0)$. In case of the phase transition to the homogeneous state one should put $k_0 = 0$, $d = 0$ (then $\delta F_L(k_0) = 0$) and $c > 0$. Then the first term $\propto c$ in Eq. (156) is associated with the positive surface tension, $\delta F_L^{\text{surf}} = \sigma S$, where S is the surface area of the seed.

The Landau free-energy density and pressure as functions of the order parameter $\delta\rho$ for the equation of state determined by Eq. (156) at $T < T_{cr}$ are shown in Fig. 5, cf. schematic Fig. 3 demonstrating isotherms $P(n)$ and Fig. 4 showing $T(n)$ dependence for the van der Waals equation of state discussed above in Section 3.1. For $\epsilon = 0$ two minima of the Landau free energy coincide and lie on the MC line on the plot $\delta P(1/\rho)$ (dashed horizontal line in the plot $\delta P(\delta\rho)$ in the right panel) describing thermal equilibrium of phases. At equilibrium the baryon chemical potentials of the vapor and liquid phases are equal, $\mu_{\text{eq,V}} = \mu_{\text{eq,L}}$. For $\epsilon \neq 0$ the interval of values $P(\delta\rho)$ from the point corresponding to the left local minimum of the Landau free energy to the point of the local maximum of the pressure describes a metastable supercooled vapor (SV) with $\mu_{\text{SV}} > \mu_{\text{eq,L}}$. The interval of values $P(\delta\rho)$ from the point corresponding to the right local minimum of the Landau free energy in the left panel to the point of the local minimum of the pressure in the right panel relates to a metastable overheated liquid (OL). In this interval $\mu_{\text{OL}} > \mu_{\text{eq,V}}$. The interval from maximum to minimum of $P(\delta\rho)$ shows unstable isothermal spinodal (ITS) region. If in the initial state $(\delta\rho)_i = \rho_i - \rho_{cr} = 0$, one deals with the spontaneous symmetry breaking and the second-order phase transition to the new state. For $(\delta\rho)_i = \rho_i - \rho_{cr} \neq 0$, $\epsilon > 0$ or $\epsilon < 0$, one deals with the first-order phase transition either from the metastable to the stable state or with the transition from spinodal region. For $\epsilon > 0$ (solid lines) the liquid state is stable and the vapor state is metastable (SV), and for $\epsilon < 0$ (dash-dotted lines) the liquid state is metastable (OL), whereas the vapor state is stable. The dynamics of the transition starting from a point within spinodal region for $\epsilon \neq 0$ (but small) is described similarly to that for the second-order phase transition, for $\epsilon = 0$. For the purely van der Waals equation of state (in this case $k_0 = 0$) one gets [77]:

$$v^2(T) = -4 \frac{\delta T n_{cr}^2 m^{*2}}{T_{cr}}, \quad \sigma = \sigma_0 \frac{|\delta T|^{3/2}}{T_{cr}^{3/2}}, \quad \sigma_0^2 = 32 m^* n_{cr}^2 T_{cr} c. \quad (158)$$

Applying operator div to Eq. (153) and expressing $\text{div } \vec{u}$ in Eq. (154) via $\partial_t n$, for small δn and u , keeping only linear terms in u , that is legitimate, since near the critical point processes develop slowly ($v^2 \propto -\delta T$), we rewrite Eq. (153) as

$$-\frac{\partial^2 \delta n}{\partial t^2} = \Delta \left[c \Delta \delta n + \lambda v^2 \delta n - \lambda m^{*2} (\delta n)^3 + \epsilon/m^* - (m^* n_{cr})^{-1} (\tilde{\nu} \eta_{cr} + \zeta_{cr}) \frac{\partial \delta n}{\partial t} \right] \quad (159)$$

$$+\Delta[-d\Delta^2\delta n + (ck_0^2 + dk_0^4)\delta n],$$

$\tilde{\nu} = 2(\nu - 1)/\nu$, cf. [96, 105, 77, 273]. Second line in Eq. (159) yields non-zero term only for the description of the condensation to the state $k_0 \neq 0$. With the help of the notation

$$\tilde{\omega}^2(\hat{k}^2) = -\lambda v^2 + c\hat{k}^2 + d\hat{k}^4 - ck_0^2 - dk_0^4 \quad (160)$$

Eq. (159) can be rewritten as

$$-\frac{\partial^2 \delta n}{\partial t^2} = \Delta \left[-\tilde{\omega}^2(\Delta)\delta n - \lambda m^{*2}(\delta n)^3 + \epsilon/m^* - (m^*n_{cr})^{-1}(\tilde{\nu}\eta_{cr} + \zeta_{cr})\frac{\partial \delta n}{\partial t} \right]. \quad (161)$$

Let us consider $T < T_{cr}$. In the dimensionless variables $m^*\delta n = v\psi$, $\tau = t/t_0$, $\xi_i = x_i/l$, $i = 1, \dots, \nu$, $\nu = 3$ for seeds of spherical geometry, Eq. (159) is presented as

$$-\beta \frac{\partial^2 \psi}{\partial \tau^2} = \Delta_\xi \left(\Delta_\xi \psi + 2\psi(1 - \psi^2) + \tilde{\epsilon} - \frac{\partial \psi}{\partial \tau} - \frac{\lambda v^2 d}{2c^2} \Delta_\xi^2 \psi + \frac{2(ck_0^2 + dk_0^4)}{\lambda v^2} \psi \right), \quad (162)$$

$$l = \left(\frac{2c}{\lambda v^2} \right)^{1/2}, \quad t_0 = \frac{2\tilde{\eta}_r}{\lambda v^2}, \quad \tilde{\epsilon} = \frac{2\epsilon}{\lambda v^3}, \quad \beta = \frac{c}{\tilde{\eta}_r^2}, \quad \tilde{\eta}_r = \frac{(\tilde{\nu}\eta_r + \zeta_r)}{m^*n_{cr}}.$$

It is important to notice that even for $k_0 = 0$ Eq. (162) differs in the form from the standard Ginzburg–Landau equation broadly exploited in the condensed matter physics, since Eq. (162) is of the second-order in time derivatives, whereas the standard Ginzburg–Landau equation is of the first order in time derivatives. The difference disappears, if one puts the bracketed-term in the r.h.s. of Eq. (162) to zero. This procedure is however not legitimate at least for description of the order parameter on an initial stage, since two initial conditions, such as $\delta n(t = 0, \vec{r}) = 0$ and $\partial_t \delta n(t, \vec{r})|_{t=0} \simeq 0$, should be fulfilled to describe a seed formed in a fluctuation. Thereby, at least there exists an initial stage of the dynamics of seeds ($t \lesssim t_{\text{init}}$), which is not described by the standard Ginzburg–Landau equation [61, 77]. The bracketed-term in the r.h.s. of Eq. (162) can indeed be put zero at large time, $\tau \gg 1$, if one considers an effectively very viscous medium, see below. In this case we arrive at Eqs. (105), (132) studied in Section 3.

The parameter β characterizes an inertia on an initial stage of evolution of the seeds, for $t \lesssim t_0\sqrt{\beta}$, cf. [77]. It is expressed in terms of the surface tension and the viscosity as

$$\beta = (32T_{cr})^{-1}[\tilde{\nu}\eta_r + \zeta_r]^{-2}\sigma_0^2 m^*. \quad (163)$$

The larger viscosity and the smaller surface tension, the effectively more viscous (inertial) is the fluidity of seeds. For $\beta \ll 1$ one deals with the regime of effectively viscous (inertial) fluidity and at $\beta \gg 1$ one deals with the regime of almost perfect fluidity. Estimates [77] show that for the nuclear liquid–vapor phase transition typically $\beta \sim 0.01$. For the quark–hadron transition $\beta \sim 0.02 - 0.2$, even for very low value of the ratio $\eta/s \simeq 1/(4\pi)$. The latter quantity characterizes fluidity of the matter at ultra-relativistic heavy-ion collisions [3]. Thus, as we argued, in case of the baryon-rich matter one deals with effectively very viscous (inertial) evolution of density fluctuations both in cases of the nuclear liquid–vapor and quark–hadron phase transitions.

In a process of a neutron star formation and cooling at $T > T_{\text{opac}} \sim 1$ MeV, when neutrino mean free path $\lambda_\nu < R_{\text{star}} \sim 10$ km, the viscosities η , ζ and the heat conductivity κ are determined by the most long-range neutrino processes [218, 96]. An overcritical pion-condensate drop reaches a size $R \sim 0.1$ km for $t \sim 10^{-3}$ sec. by the growth of the density mode. Then it may reach $R \sim (1 - 10)$ km for typical thermal transport time t_T varying from ~ 10 sec. up to several hours (rather than for typical collapse time $\sim 10^{-3}$ sec). A delay may appear owing to the neutrino heat transport to the surface (effect of thermal conductivity) that strongly depends on the value of the softening of the pion mode

responsible for the efficiency of the nucleon-nucleon interaction at $n > n_0$, being stronger for heaviest neutron stars [96]. One should also take into account that the bulk viscosity is significantly increased in presence of the soft modes [274, 275], e.g., near the pion condensation critical point [264]. Also notice that description of the dynamics of the pion-condensate phase transition is specific, since the transition occurs to the state $k_0 \neq 0$, see further discussion in Section 5.

Still, Eq. (162) should be supplemented by Eq. (155) for the heat transport, which owing to Eq. (154) after its linearization reads as

$$T_{cr} \left[\partial_t \delta s - s_{cr}(n_{cr})^{-1} \partial_t \delta n \right] = \kappa_r \Delta \delta T. \quad (164)$$

The variation of the temperature is related to the variation of the entropy density $s[n, T]$ by

$$\delta T \simeq T_{cr}(c_{V,r})^{-1} (\delta s - (\partial s / \partial n)_{T,cr} \delta n), \quad (165)$$

c_V is the density of the heat capacity.

The time scale for the relaxation of the entropy/temperature mode, following (164), is

$$t_T = R_{\text{seed}}^2 c_{V,r} / \kappa_r \propto R_{\text{seed}}^2, \quad (166)$$

i.e., relaxation time of the temperature/entropy is proportional to the surface area of the seed. Thus, interplay between viscosity, surface tension, and thermal conductivity effects is responsible for the typical time- and size- scales of fluctuations.

4.1 Stationary solutions

Now let us find stationary solutions of Eq. (159). For the condensation in the state $k_0 \neq 0$, $c < 0$, $d > 0$, and the gap $\tilde{\omega}^2(k^2)$ has a minimum for $k = k_0$. The phase transition arises for $\tilde{\omega}^2(k_0^2) < 0$. We find solution in the form [273]

$$m^* \delta n = a_{\text{stan}} [\cos(kx + \chi) + \frac{c_1 \tilde{\omega}^2(k^2)}{\tilde{\omega}^2(9k^2)} \cos(3kx + \chi) + \dots] + O(\epsilon), \quad (167)$$

where χ is arbitrary constant phase.

Setting (167) in Eq. (159) we find

$$a_{\text{stan}}^2 = -\frac{4}{3} \tilde{\omega}^2(k_0^2) / \lambda > 0, \quad c_1 = -1/3. \quad (168)$$

Minimization of the free energy in k yields $k = k_0$ and $\tilde{\omega}^2(k_0^2) = -\lambda v^2$. We have $\tilde{\omega}^2(k_0^2) > 0$ for $T > T_{cr}$ and $\tilde{\omega}^2(k_0^2) < 0$ for $T < T_{cr}$, $\tilde{\omega}^2(9k_0^2) = -\lambda v^2 + 16c^2/d \gg |\tilde{\omega}^2(k_0^2)|$. Thereby with appropriate accuracy we may use $m^* \delta n \simeq a_{\text{stan}} [\cos(k_0 x + \chi)]$ that yields

$$\delta F_L(k_0) \simeq -\lambda v^4 V_3 / (6m^* n) + O(\epsilon^2),$$

where V_3 is the volume of the system.

For the condensation in the uniform state $k_0 = 0$ we have [77]

$$\tilde{\omega}^2(k^2) = -\lambda v^2 + ck^2, \quad k^2 < \lambda v^2 / c, \quad c > 0. \quad (169)$$

Two spatially constant stationary solutions minimizing the free energy for $T < T_{cr}$ describe metastable and stable states:

$$\delta n_{\text{st}} \simeq \pm v / m^* + \epsilon / (2\lambda v^2 m^*). \quad (170)$$

The free energy corresponding to these solutions is given by

$$\delta F_L(k=0, k_0=0) \simeq -\frac{\lambda v^4 V_3}{4m^* n_{cr}} \left(1 \pm \frac{4\epsilon}{\lambda v^3}\right). \quad (171)$$

For $k \neq 0$ solutions in the form (167) are valid for $|\tilde{\omega}^2(k^2)| \ll \tilde{\omega}^2(9k^2)$, and $\tilde{\omega}^2(9k^2) > 0$, and they yield for $k_0 = 0$:

$$\delta F_L(k \neq 0, k_0=0) \simeq -\frac{\lambda v^4 (1 - ck^2/(\lambda v^2)) V_3}{6m^* n_{cr}}. \quad (172)$$

Although the minimum of the free energy for $k_0 = 0$ is given by (171) corresponding to solutions (170) obtained for $k = 0$, rather than to solutions of (167) corresponding to the free energy (172) at $k \neq 0$, nevertheless, as we will demonstrate below, solutions (167) characterized by $k \neq 0$ have a physical meaning in description of fluctuations in the spinodal region.

4.2 Dynamics of seeds at first-order phase transition from metastable state to stable state

Consider the limit of a high thermal conductivity, when in Eq. (159) the temperature can be put constant. Solution of Eq. (159) describing dynamics of the density fluctuation developing from the metastable state to the stable state is then presented in the form [78]

$$\delta n(t, r) \simeq \frac{v(T)}{m} \left[\mp \tanh \frac{r - R_{\text{seed}}(t)}{l} + \frac{\epsilon}{2\lambda v^3(T)} \right] + (\delta n)_{\text{cor}}. \quad (173)$$

The solution is valid for $|\epsilon/(\lambda v^3(T))| \ll 1$. Compensating correction $(\delta n)_{\text{cor}}$ is introduced to fulfill the baryon number conservation. Considering spatial coordinate r in the vicinity of a bubble/droplet boundary we get equation describing evolution of the seed size [77, 78]:

$$\frac{m^{*2} \beta t_0^2}{2l} \frac{d^2 R_{\text{seed}}}{dt^2} = m^{*2} \left[\pm \frac{3\epsilon}{2\lambda v^3(T)} - \frac{2l}{R_{\text{seed}}} \right] - \frac{m^{*2} t_0}{l} \frac{dR_{\text{seed}}}{dt}. \quad (174)$$

This equation reminds the Newton second law for a one-dimensional system, where the quantity $M = \frac{m^{*2} \beta t_0^2}{2l} \propto (T_{cr} - T)^{-3/2}$ has a meaning of a mass, $m^{*2} \left[\pm \frac{3|\epsilon|}{2\lambda v^3(T)} - \frac{2l}{R_{\text{seed}}} \right]$ is an external force and $-\frac{m^{*2} t_0}{l} \frac{dR_{\text{seed}}}{dt}$ is the friction force, with a viscous-friction coefficient proportional to an effective viscosity and inversely proportional to $\sqrt{T_{cr} - T}$. Following Eq. (174) a bubble of an overcritical size $R_{\text{seed}} > R_{cr} = 4l\lambda v^3(T)/(3|\epsilon|)$ of the stable “vapor” phase, or respectively a droplet of the stable “liquid” phase, been initially prepared in a fluctuation inside a metastable phase, then grow with increasing time. On an early stage of the evolution the size of the overcritical bubble/droplet $R_{\text{seed}}(t)$ (for $R_{\text{seed}} > R_{cr}$) grows with an acceleration. Then it reaches a steady growth regime with a constant velocity $u_{\text{as}} = \frac{3\epsilon l}{\lambda v^3(T) t_0} \propto |(T_{cr} - T)/T_{cr}|^{1/2}$. In the interior/exterior of the seed $\delta n \simeq \mp v(T)/m^*$. The correction $(\delta n)_{\text{cor}} \simeq v(T) R_{\text{seed}}^3(t)/(m^* R^3)$ is very small for $R_{\text{seed}}(t) \ll R_{\text{syst}}$, where R_{syst} is the radius of the whole system. In cases of the quark–hadron and nuclear liquid–vapor phase transitions in heavy-ion collisions $R_{\text{syst}}(t)$ is the radius of the expanding fireball. Usage of the isothermal approximation in Eq. (173) needs fulfillment of the inequality $t_\rho \sim \frac{R_{\text{seed}}}{u_{\text{as}}} \gg t_T$. For $\epsilon \sim \epsilon_m$ we get $t_\rho \sim (R/l_0)t_0$, and isothermal approximation is valid for $R_{\text{seed}} < R_{\text{fog}}$ (R_{fog} is typical radius of the seed at which $t_T \sim t_\rho$). For seeds with sizes $R > R_{\text{fog}}$, $t_T \propto R^2$ exceeds $t_\rho \propto R$ and growth of seeds is slowed down. Thereby, the number of seeds with the size $R \sim R_{\text{fog}}$ may increase with time (stage of a nuclear fog). Estimates [77, 78] show that for the hadron–quark phase transition $R_{\text{fog}} \sim 0.1 - 1$ fm and for the nuclear liquid–gas

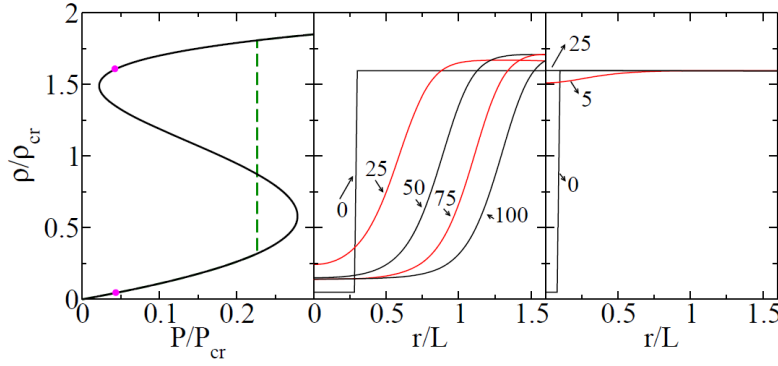


Figure 6: Isotherm for the pressure as a function of the density, with initial and final configurations shown by dots (left column). Dash vertical line corresponds to the MC on the curve $P(1/\rho)$. Initial state relates to stable vapor-phase disk in metastable overheated liquid. Middle column shows time evolution of the density profiles for the overcritical vapor disk. Right column, the same for initially undercritical vapor disks. Numbers near curves (in L) are time snapshots; $r = \sqrt{x^2 + y^2}$, $L = 30$ fm, $T_{cr} = 162$ MeV, $T/T_{cr} = 0.85$, $n/n_0 = 1.3$, $\eta \simeq 45 \text{ MeV/fm}^2$, for $\beta = 0.2$. Figure is adopted from [77].

transition $R_{\text{fog}} \sim 1 - 10 \text{ fm} \lesssim R_{\text{syst}}(t_{\text{f.o.}})$, where $R_{\text{syst}}(t_{\text{f.o.}})$ is the fireball size at the freeze-out time. Thus, thermal conductivity effects may manifest themselves in heavy-ion collision dynamics. In the clouds in terrestrial conditions the value R_{fog} , continuing to grow, may become so large that the gravity comes into play and there may arise the rain.

Substituting Eq. (173) to Eq. (164) for $T \simeq \text{const}$ (that is correct in linear approximation) we obtain

$$\delta s = \left(\frac{\partial s}{\partial n} \right)_T \left\{ \frac{v(T)}{m} \left[\pm \tanh \frac{r - R_{\text{seed}}(t)}{l} + \frac{\epsilon}{2\lambda_{cr} v^3(T)} \right] + (\delta n)_{\text{cor}} \right\}. \quad (175)$$

Note that for the description of the expanding fireball formed in heavy-ion collisions the approximation of a quasi-adiabatic expansion can be used even in presence of the weak first-order phase transition (for $\delta s \ll s$ and $\delta n \ll n$). The evolution of droplets/bubbles in metastable region can be considered at fixed size of the fireball provided expansion time $t_{\text{f.o.}} \gg (t_\rho, t_T)$.

The dynamics is characterized by the relations between various time-scales. The total time of the phase transition is given by

$$t_{\text{tr}} = t_W + t_\rho + t_T, \quad (176)$$

where $t_W \sim t_0 e^{\delta F(r_{cr})/T}$ is the typical time of the cooking of the initial seed of the overcritical size.

In Fig. 6 we show the dynamics of the stable vapor-phase disk in the metastable liquid surrounding for the parameter choice $T_{cr} = 162$ MeV, $n/n_{\text{sat}} = 1.3$, relevant for the hadron-sQGP phase transition. We take $T/T_{cr} = 0.85$ and compute the configuration for $\eta \simeq 45 \text{ MeV/fm}^2$ and for $\beta = 0.2$ (effectively large viscosity). The seed-vapor disk of an overcritical size is increasing in size (see the middle column), whereas the disk of an undercritical size (see the right column) is decreasing in size. Further details of calculations see in [77].

4.3 Evolution of bands ($d_{\text{sol}} = 1$) and two-dimensional seeds ($d_{\text{sol}} = 2$)

In Fig. 7 we show dynamics of liquid bands ($d_{\text{sol}} = 1$) in metastable vapor phase. Values $T/T_{cr} = 0.98$, $L = 30$ fm, $T_{cr} = 18.6$ MeV, $n_{cr}/n_0 = 0.42$, $\eta \simeq 3.2 \text{ MeV/fm}^2$ and $\beta \simeq 12.6$ (case of effectively small viscosity). These solutions are similar to slabs in $d = 3$. Left panel shows time evolution of a band of a large initial size ($R_0 = 0.3L$), whereas right panel demonstrates evolution of a band having initially rather small size ($R_0 = 0.1L$). In difference with disks (solutions with $d_{\text{sol}} = 2$) in both cases (for large

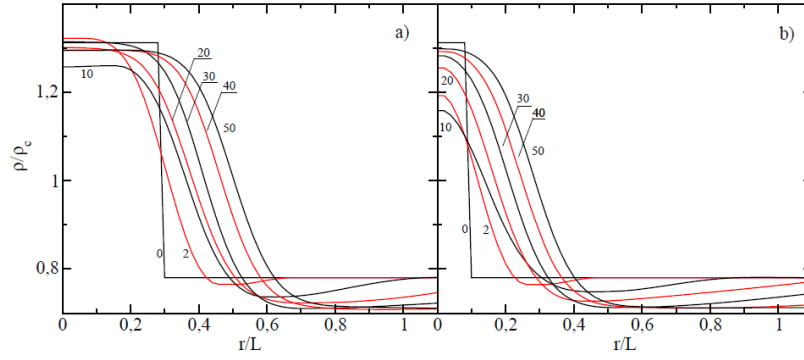


Figure 7: Evolution of bands ($d_{\text{sol}} = 1$) of initially large (left) and small (right) sizes, $r = |x|$. Parameters: $T/T_{cr} = 0.98$, $L = 30$ fm, $T_{cr} = 18.6$ MeV, $n_{cr}/n_0 = 0.42$, $\eta \simeq 3.2$ MeV/fm², for $\beta \simeq 12.6$ (effectively small viscosity). Figure is adopted from [77].

and small initial sizes of bands) dynamics looks similar: bands of the stable phase, being prepared in the metastable phase, undergo growth to the new phase. Nevertheless, we also see that during the shape reconstruction the slab first begins to dissolve and then grows. This peculiarity appeared since initial form of the density distribution that was exploited in numerical calculations deviates from the form given by analytical solution. Thus actually even for slabs there might exist a small critical size, that depends on peculiarities of the initial density profile. Slabs having sizes smaller than this critical size could then completely dissolve.

The probability to prepare a band in a fluctuation is tiny. However, bands of the stable phase could be formed near the system boundary, provided the latter is flat.

In Fig. 8 we demonstrate the law for the growing with time of the band boundary $R(t)$ (in the left panel) and the velocity of the boundary $u = dR/dt$ (in the right panel) for different values of the viscosity. As for discs, the band boundary is specified as the point, where the density reaches the critical value ($\rho = \rho_{cr}$). Results are presented for $T/T_{cr} = 0.98$, $L = 30$ fm. For small values of time (see Figure insertion) $R(t)$ obeys the quadratic law. Solid curve (case of effectively large viscosity, $\beta = 0.1$) shows the evolution of the slab-seed for $t > t_{\text{rec}} \sim 100$ fm, the reconstruction time increases as $t_{\text{rec}} \propto \sqrt{\beta}$. It is clearly demonstrated in the right panel, where the time dependence of the velocity of the seed growth is presented. As follows from the Figure, even for large times the velocity u does not obey the scaling law. The velocity of the seed surface still slowly increases with time. The asymptotic regime is reached at larger values of time (or for smaller β at values of time shown in Fig. 8). Another important issue is presence of the damped long-wave oscillations, which are clearly seen for all values of the effective viscosity. They occur at $t \lesssim t_{\text{rec}}$. Moreover, in case of an effectively small viscosity the short-wave quasi-periodic oscillations are clearly seen.

Finally, we would like to notice that obtained solution for $\beta \gg 1$ describing accelerated expansion of the seed and oscillations might be useful in application to the modeling of the accelerated expansion of the Universe with the formation of inhomogeneities.

4.4 Dynamics of fluctuations in unstable region

4.4.1 Growth of fluctuations of small amplitude

The phenomenon illustrating exponential growth of fluctuations in the spinodal region is the opening of the bottle of champagne. The dynamical trajectories of the expanding baryon-rich matter in the heavy-ion collisions and of the falling matter in supernova explosions, until a phase transition did not occur, can be characterized by approximately conserved entropy, whereas the volume V_3 and the temperature

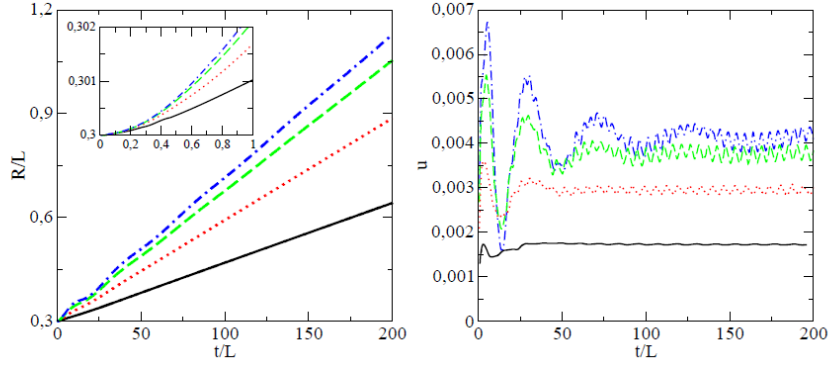


Figure 8: Solution $R(t)$ (left panel) and $u = dR/dt$ (right panel) for the band boundary for several values of the viscosity. Solid, dotted, dashed and dash-dotted lines are calculated for $\beta = 10^{-1}; 1; 10; 100$, $\delta\mathcal{T} = 0.02$, $L = 30$ fm. Figure is adopted from [77].

T are changed with the time. Adiabatic trajectories of the matter and different possibilities of occurring of the liquid–vapor type phase transition were shown in Fig. 4 on the plot of $T/T_{cr} = f(n/n_{cr})$. Note that in reality for the quark–hadron first-order phase transition the plot looks a bit different, since then T_{cr} increases with a decrease of the baryon density [276, 80, 81]. However this peculiarity does not change a general analysis.

Now let us consider evolution of fluctuations in the spinodal region. First, we find solutions of the linearized hydrodynamical equations, cf. [78]. Now “r”-reference point can be placed at arbitrary distance from the critical point, and assumption of a small over-criticality is not as essential. So, let us suppress the subscript “r”. Let us introduce

$$\delta n = \delta n_0 \exp[\gamma t + i\vec{k}\vec{r}] - \frac{\epsilon}{m^* \lambda v^2}, \quad \delta s = \delta s_0 \exp[\gamma t + i\vec{k}\vec{r}], \quad T = T_> + \delta T_0 \exp[\gamma t + i\vec{k}\vec{r}], \quad (177)$$

where $T_>$ is the temperature of the uniform matter. For $|\delta n| \gg |\frac{\epsilon}{m^* \lambda v^2}|$, i.e. for $|\epsilon| \ll |\epsilon_m|$, description of a fluctuation in spinodal region at the first-order phase transition and at the second-order phase transition are similar and we may put $\epsilon \rightarrow 0$.

For the case of a finite thermal conductivity, $\kappa \neq 0$, from Eqs. (164), (165) we obtain

$$\delta s_0 = \delta n_0 \frac{s}{n [1 + \kappa p^2 / (c_V \gamma)]} \left[1 + \frac{n \kappa p^2 (\partial s / \partial n)_T}{\gamma s c_V} \right]. \quad (178)$$

The increment, $\gamma(p)$, is determined by the linearized Eq. (159), where we put

$$\delta P = \left(\frac{\partial P}{\partial n} \right)_T \delta n + \left(\frac{\partial P}{\partial T} \right)_n \delta T. \quad (179)$$

Thus from linearized equations of the non-ideal hydrodynamics we find the increment, $\gamma(k)$,

$$\gamma^2 = -k^2 \left[\tilde{\omega}^2(k^2) + \tilde{\eta} \gamma + \frac{u_s^2 - u_T^2}{1 + \kappa k^2 / (c_V \gamma)} \right], \quad (180)$$

where $\tilde{\eta} = \frac{(\tilde{\nu}\eta + \zeta)}{m^* n}$ and quantity $\omega_0(k^2)$ is determined in Eq. (160). Eq. (180) has three solutions corresponding to the growth, damping and oscillation of the density- and thermal modes. It differs from the equation derived in [277] by presence of the surface tension term. General solutions can be found in [77, 78, 273].

4.4.2 Limit of a rather high thermal conductivity

Let us focus on the limit of a rather high thermal conductivity, cf. [77, 78], when the temperature of the seed can be put constant and we may deal with only one equation for the density mode (159). Thereby, let us present solutions for $\kappa k^2/(c_V |\gamma|) \gg 1$. Then

$$\gamma^2 = -k^2 [\tilde{\omega}^2(k^2) + \tilde{\eta}\gamma] , \quad (181)$$

from where we find two solutions for the density-modes,

$$\gamma_{1,2} = -\frac{k^2 \tilde{\eta}}{2} \pm \sqrt{\frac{k^4 \tilde{\eta}^2}{4} - k^2 \tilde{\omega}^2(k^2)} . \quad (182)$$

For $\tilde{\omega}^2(k^2) < 0$, that corresponds to the region of the phase transition, the upper-sign solution, $\gamma_1 > 0$, describes the growing mode and the lower sign solution, $\gamma_2 < 0$, describes the damping mode. For $k^2 \tilde{\eta}^2 / |\tilde{\omega}^2(k^2)| \ll 1$, we have

$$\gamma_1 \simeq \sqrt{-k^2 \tilde{\omega}^2(k^2)} - \frac{k^2 \tilde{\eta}}{2} + O(k^3) \quad (183)$$

for the growing mode. In the limit $k^2 \tilde{\eta}^2 / |\tilde{\omega}^2(k^2)| \gg 1$, we obtain

$$\gamma_1 \simeq -\tilde{\omega}^2(k^2)/\tilde{\eta} + O(\tilde{\omega}^4(k^2)/(k^2 \tilde{\eta}^3)) . \quad (184)$$

In case $k_0 = 0, c > 0$, for the most rapidly growing mode of a small amplitude (for $\gamma_m = \max\{\gamma_1\}$ corresponding to $k = k_m$) from (182) we find

$$\gamma_m \simeq \frac{\lambda v^2}{(2\sqrt{\beta} + 1)\tilde{\eta}} , \quad k_m^2 \simeq \frac{\lambda v^2 \sqrt{\beta}}{(2\sqrt{\beta} + 1)c} . \quad (185)$$

Note that the value $k_m \neq 0$ exists only because the dynamics is determined by the nonideal hydrodynamical equations, which resulted in the second-time-derivative Eq. (159), instead of the first-time-derivative Ginzburg–Landau equation, which yields $k_m = 0$, see also Eqs. (105)–(108) above.

For $k_0 \neq 0, c < 0, d > 0$ the most rapidly growing mode corresponds to $k \simeq k_0$, then $\tilde{\omega}^2(k_0^2) < 0$ and $|\tilde{\omega}^2(k_0^2)|$ as a function of k^2 is the largest.

Let us continue to study limit of a high thermal conductivity and consider now fluctuations in the system close to equilibrium. Assuming that ψ is close to its new equilibrium value, $\psi_{eq} \simeq \pm 1 + \tilde{\epsilon}/4$, we put $\psi = \psi_{eq} + \delta\psi$ in Eq. (162) and linearize the latter equation in $\delta\psi$:

$$-\beta \frac{\partial^2 \delta\psi}{\partial \tau^2} = \Delta_\xi \left(\Delta_\xi \delta\psi - 4\delta\psi - \frac{\partial \delta\psi}{\partial \tau} - \frac{\lambda v^2 d}{2c^2} \Delta_\xi^2 \delta\psi + \frac{2ck_0^2 + 2dk_0^4}{\lambda v^2} \delta\psi \right) . \quad (186)$$

Setting $\delta\psi = \text{Re}\{\psi_0 e^{\gamma_\psi \tau + i\vec{k}_\psi \vec{\xi}}\}$, where ψ_0 is an arbitrary but small real constant, we find

$$\gamma_\psi(k_\psi) = (2\beta)^{-1} \left(-k_\psi^2 \pm \sqrt{k_\psi^4 (1 - 4\beta) - 16\beta(k_\psi^2 - k_{0\psi}^2) + 2\beta^2 d(k_\psi^4 - k_{0\psi}^4)/c^2} \right) , \quad (187)$$

where $k_{0\psi}^2 = 2ck_0^2/(\lambda v^2)$.

In case $k_0 = 0, d = 0$ and for effectively large viscosity ($\beta \ll 1$) and for $k_\psi^2 > 16\beta$ there are only damped solutions. For $k_\psi^2 \gg 16\beta$:

$$\gamma_\psi^{(1)}(k_\psi) \simeq -(k_\psi^2 + 4), \quad \gamma_\psi^{(2)}(k_\psi) \simeq -k_\psi^2/\beta . \quad (188)$$

Fluctuations with large k rapidly dissolve with time. Existence of long living short-wave excitations is unlikely in the viscous medium. However there remain long-wave damped oscillations, for $k_\psi^2 < 16\beta$.

In case of effectively small viscosity ($\beta \gg 1$) we get

$$\gamma_\psi(k_\psi) = -(2\beta)^{-1} \left(k_\psi^2 \pm 4i\sqrt{\beta} k_\psi \sqrt{1 + k_\psi^2/4} \right), \quad (189)$$

that corresponds to oscillating slowly damped modes near the equilibrium state. Since $t_0\sqrt{\beta}$ does not depend on the viscosity and $t_0\beta \rightarrow \infty$ for $\eta, \zeta \rightarrow 0$, in case of the ideal fluid rapid oscillations continue till the energy is transported to the surface of the system (the process is governed by the heat transport) or till the energy is radiated away in the course of direct reactions. Thus in case of effectively small viscosity the stable phase is covered by fine ripples during some rather long period of time.

For $k_0 \neq 0$, $d > 0$ putting $k \simeq k_0$ in (187) we obtain

$$\gamma_\psi(k_\psi) = (2\beta)^{-1} \left(-k_\psi^2 \pm \sqrt{k_\psi^4(1 - 4\beta)} \right), \quad (190)$$

so both solutions are damped. Also, for $\beta > 1/4$ (small viscosity) besides the damping there are oscillations.

Now let us consider a general case ($k_0 = 0$ either $\neq 0$), and seek the solution of nonlinear equations (159), (162) in the form [273]

$$m^* \delta n = a_{\text{stan}} f(t) \left[\cos(kx + \chi) + \frac{c_1 \tilde{\omega}^2(k^2)}{\tilde{\omega}^2(9k^2)} \cos(3kx + \chi) + \dots \right] + O(\epsilon), \quad (191)$$

with $a_{\text{stan}}^2 = -\frac{4\tilde{\omega}^2}{3\lambda} > 0$ as in (167) but now with $f(t)$ satisfying equation

$$\partial_t^2 f = -k^2 \tilde{\omega}^2(k^2) f(1 - f^2) - k^2 \tilde{\eta} \partial_t f. \quad (192)$$

For $k^2 \tilde{\eta}^2 / |\tilde{\omega}^2(k^2)| \gg 1$, for $\beta \ll 1$ or $\tilde{\eta} \gg \sqrt{c}$, the term $\partial_t^2 f$ in the l.h.s. of Eq. (192) can be dropped and the amplitude

$$f(t) = \frac{f_0 e^{\gamma t}}{\sqrt{1 + f_0^2 e^{2\gamma t}}} \quad (193)$$

fulfils the resulting Eq. (192) with $\gamma = -\tilde{\omega}^2(k^2)/\tilde{\eta}$, $f_0/\sqrt{1 + f_0^2}$ shows the amplitude of the fluctuation at $t = 0$, f_0 is an arbitrary constant. For $k \sim k_m$ at $k_0 = 0$ this solution holds for $k_m^2 \tilde{\eta}^2 / |\tilde{\omega}^2(k_m^2)| \gg 1$. For $k = k_0 \neq 0$ the criterion of applicability is $k_0^2 \tilde{\eta}^2 / |\tilde{\omega}^2(k_0^2)| \gg 1$. In both cases $k_0 = 0$ and $k_0 \neq 0$ with the density distribution given by (191), (193) the free energy renders

$$\delta F_L(t) = -\frac{V_3 \tilde{\omega}^4(k^2)}{6\lambda m^* n} f^2(t) (2 - f^2(t)). \quad (194)$$

For $t \rightarrow \infty$ we have $f(t \rightarrow \infty) \rightarrow 1$ and δF_L reaches the minimum. For $k = k_0$ this value coincides with (172) given by the stationary solution.

In general case, Eq. (193) yields an interpolation between two approximate solutions of Eq. (192) valid for the limit cases $\gamma t \ll 1$ and $\gamma t \gg 1$. Replacing (193) in Eq. (192) we obtain then the same solutions (182) as in linear case.

Let first $k_0 = 0$. For $t \rightarrow \infty$ employing solution (193) at $\gamma = \gamma_m = \gamma(k_m)$ we find

$$\delta F_L(t \rightarrow \infty) = -\frac{\tilde{\omega}^4(k_m^2) V_3}{6\lambda m^* n}. \quad (195)$$

For the case of a large effective viscosity/inertia, $\beta \ll 1$, we obtain $\delta F_L(t \rightarrow \infty) \simeq -\frac{\lambda v^4 V_3}{6m^*n}$ that coincides with (172) but is still larger than the value given by (171). For the case of a small effective viscosity/inertia, $\beta \gg 1$, we find $\delta F_L(t \rightarrow \infty) \simeq -\frac{\lambda v^4 V}{24m^*n}$ that is much higher than the free energy given by both stationary solutions (171), (172). Thus one may expect that expression (195) either describes a metastable state or a state, which slowly varies on a time scale $t_k \gg t_\gamma \sim 1/\gamma_m$, reaching for $t \gg t_k$ the stationary state with the free energy given by (171).

To show the latter possibility consider the case $\beta \gg 1$ and assume k in solution (191) to be a slow function of time, i.e. $k = k(t)$, for typical time scale $t_k \gg t_\gamma$. One can see that for $R_{\text{seed}} \ll 1/k_m$ the quantity $k(t)$ satisfies equation $(d^2k/dt^2) = -k^2\tilde{\eta}(dk/dt)$ with the solution

$$k(t) = k_{00}[1 + 2\tilde{\eta}k_{00}^2t/3]^{-1/2} = k_m[1 + \tilde{\eta}\lambda v^2t/(3c)]^{-1/2} \quad (196)$$

for $k_{00} = k_m$ from (185), such as $k(t \rightarrow \infty) \rightarrow 0$ and the free energy for $t \rightarrow \infty$ indeed reaches the limit (171) provided we set $\cos \chi \simeq \frac{\sqrt{3}}{2} - \frac{\sqrt{3}m^*\tilde{\epsilon}}{8}$. From Eq. (196) we easily find that the typical time scale is $t_k \sim \beta t_0$ and we check that indeed $t_k \gg t_\gamma$. For $R_{\text{seed}} \gtrsim 1/k_m$ the solution (191) with (196) does not hold and should be modified.

For $\beta \ll 1$, $k_0 = 0$, Eq. (196) with slowly varying $k(t)$ does not hold. At realistic conditions, convection and sticking processes (at sizes $\sim l$) may be allowed, which destroy periodicity, and owing to these processes the system may finally reach the ground state with the free energy given by (171). Thus one possibility is that for the typical time $t \sim t_\gamma \sim t_0$ the quasiperiodic solution is formed with typical $k \simeq k_m$, corresponding to a metastable state with the free energy given by (172). Such a distribution is formed most rapidly. Another possibility is that for the typical time scale $t_{\text{hom}} > t_\gamma$ in the system of a large size an approximately homogeneous solution is developed. In the latter case to proceed consider the case $k \sim 1/R_{\text{syst}} \ll k_m$, where R_{syst} is the typical size of the system ($R_{\text{syst}} = R_{\text{f.o.}}$ for the fireball formed in heavy-ion collisions). The spatially homogeneous solution of equation

$$\Delta_\epsilon \psi + 2\psi(1 - \psi^2) + \tilde{\epsilon} = \partial_\tau \psi,$$

that follows from (162) in this case (as well as for seeds of a size $R_{\text{seed}} \ll R_{\text{syst}}$ at $\beta \ll 1$, as we have argued above), is given by

$$\psi(t) = \pm 1/\sqrt{1 + e^{-\tau}(1 - \psi_0^2)/\psi_0^2}, \quad (197)$$

where we for simplicity have put $\tilde{\epsilon} \rightarrow 0$. Typical time needed for the initial amplitude $\psi_0 \ll 1$ to grow to $\psi(t \rightarrow \infty) \simeq \pm 1$ is $t_{\text{hom}} \sim t_0 \ln(1/\psi_0^2) \gg t_\gamma$.

Thus, additionally to the homogeneous solution (197) we found some novel solutions describing evolution of fluctuations in the region of the instability. For $k = \text{const} \neq 0$ we found periodic solutions given by (191), (193). For $k = k_0 \neq 0$ the solution yields minimum of the free energy for $t \rightarrow \infty$. For $k_0 = 0$, $\beta \gg 1$, we found quasiperiodic solutions (191), (193) with $k = k(t)$ from (196), yielding minimum of the free energy for $t \rightarrow \infty$.

Above we considered the case of a large thermal conductivity. Discussion of cases of a small and zero thermal conductivity can be found in [77, 78].

4.4.3 First-order phase transition in the process of cooling

Although different aspects of the nucleation processes have been enlightened in many textbooks and reviews, cf. [278, 186, 279, 280, 281] and refs. therein, active investigations in this field are continued. If during the process of the cooling of the system characterized by the time t_{cool} the first-order phase transition to the inhomogeneous state starts from the metastable phase and chemical potentials in both phases are close to each other, the time for the preparation of the overcritical seed of stable phase, t_W ,

is very large. In case of a slow cooling, when $t_{\text{cool}} \gg t_W$, a monocrystal is formed. At a smaller value of t_{cool} , the resulting state contains crystal domains with different orientations of the wave vector \vec{k}_0 . After this state is formed, it undergoes an aging process, in which the domains coalesce to larger domains with a more energetically profitable structure. In the limit case, $t_{\text{cool}} \ll t_W$, the glassing transition either starts from a metastable region near the top of the energy barrier, cf. [282], or the system trajectory passes to the spinodal region [105] and then the polycrystal or glass-like state are formed, in which the directions of \vec{k}_0 change already at a short space-scale $l \sim 1/k_0$. The viscosity of the amorphous state is very large and after a long time in the aging process the matter transforms to the monocrystal.

In case of the nuclear matter, being of the main interest of the present review, a similar increase of the bulk viscosity should occur at densities $n > n_c^{(1)} \sim (0.5 - 0.8)n_0$ (in the liquid phase of the pion condensation) due to occurrence of the pion fluctuations with finite momenta $k \sim k_0 \sim p_{F,N}$, cf. [7, 273]. With increasing density, the bulk viscosity still increases reaching the maximum in the critical point of the pion condensation to the liquid-crystal or solid-like state (at $n = n_c^\pi$). In neutron star matter these effects may help to explain r -mode damping in rapidly rotating pulsars, cf. [263, 264]. Also note that the bulk viscosity should increase near the critical point of any first-order phase transition and it diverges in the critical point of the second-order phase transition. Such a critical opalescence phenomena should occur at the hadron-quark phase transition, cf. [283]. In addition, Ref. [284] suggested that in heavy-ion collisions the spike of the bulk viscosity near the critical point could trigger instabilities that rapidly break the system into evaporating clusters.

4.4.4 Sticking of domains

A supply of the material across the border of the seed occurring in the diffusion process during the seed growth to the stable phase from the metastable one requires a long time. So, near the seed there may appear a sparse space. In this case two domains of the stable phase formed nearby each other may undergo a sticking. Indeed the surface free energy due to the presence of the domain-domain boundary is estimated as $\delta F_{d-d} \sim R^2 l_\psi \omega_0^4 \tilde{h} / \Lambda_0$, at $\tilde{h} \ll 1$, whereas the surface energy at the domain-vacuum boundary is $\delta F_{d-v} \sim R^2 l_\psi \omega_0^4 / \Lambda_0 \gg \delta F_{d-d}$, cf. [105]. Thus the domain-domain surface energy is less than the domain-vacuum plus domain-vacuum surface energy. Thereby, there appears attractive sticking force $\sim (\delta F_{d-d} - \delta F_{d-v}) / l_\psi$, which permits sticking of the matter. Domains of a whimsical form can be formed during the sticking process. In case when quasi-one dimensional configurations are energetically favorable the domains are elongated. The processes of the sticking of seeds, formation of a larger-size domains and formation of monocrystal take a very long-time.

Finally, note that domain structures naturally appear in systems described by the vector-boson condensates such as ferromagnets and ferromagnetic superfluids and superconductors, cf. [26].

5 Pion condensation in dense and not too hot nuclear matter

5.1 Fermi liquid description of NN and πN interactions

Usually one supposes that nucleons and pions interact via pseudovector πNN coupling described by the Hamiltonian [95, 102, 96]:

$$H_{\pi NN}^{\text{p.v.}} = f_{\pi NN} \bar{\psi}_N \gamma^\mu \gamma_5 \partial_\mu (\vec{\tau} \vec{\pi}) \psi_N, \quad \mu = 0, 1, 2, 3. \quad (198)$$

Within the σ model one also uses pseudoscalar coupling [95, 102, 96]

$$H_{\pi NN}^{\text{p.s.}} = -ig \bar{\psi}_N \gamma_5 \vec{\tau} \vec{\pi} \psi_N, \quad g/2m_N \simeq f_{\pi NN} \simeq 1/m_\pi. \quad (199)$$

Both variants correspond to the same non-relativistic limit expression for the vertex

$$V_{\pi NN}^{n.rel} = -if_{\pi NN}\sigma_\alpha\tau_\beta\partial_\alpha\pi_\beta, \quad \alpha, \beta = 1, 2, 3, \quad (200)$$

γ^μ are Dirac matrices and $\vec{\sigma}$ and $\vec{\tau}$ are spin and isospin Pauli matrices.

Hamiltonian of $\pi N\Delta$ interaction is usually taken as

$$H_{\pi N\Delta} = f_{\pi N\Delta}\bar{\psi}_\Delta^\mu\vec{T}\partial_\mu\vec{\pi}\psi_N, \quad f_{\pi N\Delta} \simeq 2.15 f_{\pi NN}, \quad (201)$$

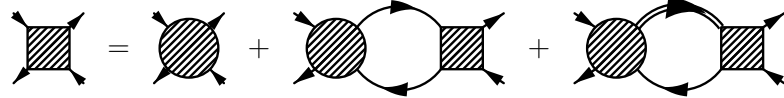
with appropriate non-relativistic limit expression for the vertex

$$V_{\pi N\Delta}^{n.rel} = -if_{\pi N\Delta}S_\alpha\partial_\alpha T_\beta\pi_\beta, \quad \alpha, \beta = 1, 2, 3, \quad (202)$$

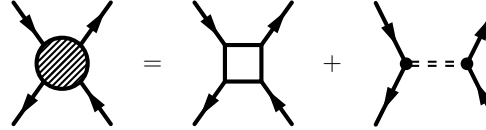
where \vec{S} and \vec{T} denote transition spin and isospin operators.

A more local part of the nucleon–nucleon interaction is due to exchanges of heavy mesons, like σ , ρ , Ω , being characterized by large ($\gg 1$) values of the coupling constants, cf. [10]. Methods of the perturbation theory do not work in this case. The Fermi-liquid approach with the explicit separation of the in-medium pion exchange was formulated by A. B. Migdal for description of the cold nuclear matter, cf. [95], and then it was generalized for description of equilibrium systems at finite temperatures [97, 96] and for nonequilibrium systems, cf. [99, 100, 6, 96, 7, 101]. In this approach the long-range (small momenta) processes are treated explicitly, whereas short-range (large momenta) ones are described by the local quantities approximated with the help of the phenomenological Landau–Migdal parameters.

At low excitation energies the retarded NN interaction amplitude is presented as follows



$$\text{shaded square} = \text{shaded circle} + \text{loop with shaded circle and shaded square} + \text{loop with shaded circle and shaded square} \quad (203)$$



$$\text{shaded circle} = \text{square loop} + \text{double line vertex} \quad (204)$$

The solid line, iG_N , stands for the nucleon quasiparticle, the double line, iG_Δ , for the dressed Δ isobar. For a higher excitation energy, the $\Delta\Delta^{-1}$ diagrams should be included [97, 96]. The doubly-dashed line shows the exchange by the free pion with inclusion of the residual s-wave πNN interaction and $\pi\pi$ scattering. The empty block in Eq. (204) is irreducible with respect to the particle–hole, Δ –nucleon hole and pion states. It is expressed via Landau–Migdal parameters as follows,

$$\Gamma_{\vec{n}\alpha\beta,\vec{n}'\gamma\delta}^\omega = F_{\vec{n},\vec{n}'}\delta_{\alpha\beta}\delta_{\gamma\delta} + G_{\vec{n},\vec{n}'}\vec{\sigma}_{\alpha\beta}\vec{\sigma}_{\gamma\delta}. \quad (205)$$

Due to the locality of the exchanges by massive mesons the momentum dependence of the values F and G is rather smooth. So, one usually assumes that F and G are functions dependent only on the direction of the momenta of incoming and outgoing nucleon and hole at the Fermi surface. The dimensionless amplitudes are $f_{\vec{n},\vec{n}'} = C_0^{-1}F_{\vec{n},\vec{n}'}$ and $g_{\vec{n},\vec{n}'} = C_0^{-1}G_{\vec{n},\vec{n}'}$, $C_0^{-1} = m_N^*(n_0)p_{F,N}(n_0)/\pi^2$ is the normalization factor – the density of states at the Fermi surface for $n = n_0$, m_N^* is the nucleon effective mass, $p_{F,N}$ is the nucleon Fermi momentum, \vec{n} and \vec{n}' are the directions of the fermion momenta before and after scattering. The amplitudes are expanded in the Legendre polynomials. In most cases it is sufficient to deal with zero and first harmonics, which can be extracted from the comparison with the data or they should be computed within some models. Most important role in nuclear physics problems is played by the zero harmonics.

The $N\Delta$ interaction is constructed analogously to that for NN . Information on the local part of the $N\Delta$ interaction is rather scarce. One usually supposes that the only important channel is the spin-isospin channel. Thereby,

$$(-i) \text{ (diagram: circle with four external arrows)} \simeq C_0 g'_{N\Delta} (\vec{\tau}_1 \vec{\tau}_2) (\vec{\sigma}_1 \vec{\sigma}_2) \quad (206)$$

Resummation of the diagrams shown in (203) in the pion channel yields the Dyson equation for the retarded pion full Green function $D^R = \text{Re}D^R - iA_\pi/2$,

$$\text{bold wavy line} = \text{thin wavy line} + \text{diagram: loop with shaded blob} + \text{diagram: loop with shaded blob} + \text{diagram: box labeled } \Sigma_{\text{res}}^R \text{ (207)}$$

Here the bold wavy line is the full pion Green function iD^R , thin wavy line is bare pion Green function iD_0^R , $-i\Sigma_{\text{res}}^R$ is a residual retarded pion self-energy including the contribution of all diagrams, which are not presented explicitly in (207), like the s-wave πN and $\pi\pi$ scattering. The full (retarded) vertex takes into account NN correlations

$$\text{diagram: shaded blob with two external arrows} = \text{diagram: vertex with two external arrows} + \text{diagram: loop with shaded blob and two external arrows} \quad (208)$$

Note that Eqs. (203)–(208) presented for the retarded quantities are valid not only for the ground state but also for the equilibrium matter at $T \neq 0$, as well as for the nonequilibrium matter, cf. [7].

In the matter of an arbitrary isospin composition the resummed NN interaction amplitude reads

$$\Gamma_{NN}^R = F + F' \vec{\tau}_1 \vec{\tau}_2 + (G + G' \vec{\tau}_1 \vec{\tau}_2) \vec{\sigma}_1 \vec{\sigma}_2 + f_{\pi NN}^2 T_\pi \vec{\sigma}_1 \vec{k} \cdot \vec{\sigma}_2 \vec{k}, \quad (209)$$

\vec{k} is the momentum transferred in the particle-hole channel. First three terms in Eq. (209) arise due to the loop resummation of the empty block graphs in Eq. (204), the last term in Eq. (209) is due to the contribution of the second diagram of Eq. (204). Amplitudes F , F' , G , G' , and T_π are expressed with the help of the dimensionless Landau–Migdal parameters f , f' , g , g' , related to the local NN interaction in the particle–hole channel [96]

$$\begin{aligned} F &= C_0 f \Gamma(f), \quad F' = C_0 f' \Gamma(f'), \\ G &= C_0 g \Gamma(g), \quad G' = C_0 g' \Gamma(g'), \\ T_\pi &= \Gamma^2(g') D_\pi^R(\omega, k) = \Gamma^2(g') / [\omega^2 - m_\pi^2 - k^2 - \Sigma^R(\omega, k)]. \end{aligned} \quad (210)$$

The Landau–Migdal parameters $f = (f_{nn} + f_{np})/2$, $f' = (f_{nn} - f_{np})/2$ in the scalar channel are expressed via the nucleon incompressibility and can be calculated already on the mean-field level, e.g., cf. the calculation in [285]. Calculation of the spin parameters $g = (g_{nn} + g_{np})/2$, $g' = (g_{nn} - g_{np})/2$ needs to go beyond the mean-field level, cf. [286, 287, 288, 289].

Resummation of Eq. (203) yields in the spin-isospin channel

$$\text{diagram: shaded square} = \left[\frac{C_0 g'}{1 - C_0 g' \text{ (loop diagram)}} + \text{diagram: vertex with two external arrows} \right] (\vec{\tau}_1 \vec{\tau}_2) (\vec{\sigma}_1 \vec{\sigma}_2) \quad (211)$$

Empirical value of $g'_{N\Delta} \simeq 0.1 - 0.2$ is rather small, cf. [290, 96, 291], whereas $g'_{\Delta\Delta}$ was estimated as $\simeq 0.8$, cf. [290, 96]. Thus with some accuracy one may for simplicity drop the contribution of the local $N\Delta$ interaction.

For $\omega \ll m_\pi$ and $k \lesssim p_{F,N}$ the main contribution to the pion self-energy is determined by the second diagram in r.h.s. of (207). Therefore one has

$$\Gamma(x) = \left[1 + 2x p_{F,N} \Phi^R(\omega, k, T) / p_{F,N}(n_0) \right]^{-1}, \quad (212)$$

$x = f, f', g, g', \Phi^R$ is the retarded Lindhard function

$$\Phi^R(\omega, k, T) = \Phi_1^R(\omega, \vec{k}, T) + \Phi_1^R(-\omega, -\vec{k}, T), \quad (213)$$

and at zero temperature [95]

$$\begin{aligned} \Phi_1^R(\omega, k, T=0) &= -\frac{m_N^{*2}}{2p_{F,N}k^3} \left[\frac{a^2 - b^2}{2} \ln \left(\frac{a+b}{a-b} \right) - ab \right], \\ a &= \omega - \frac{q^2}{2m_N^*}, \quad b = kv_{F,N}, \quad q^2 = \omega^2 - k^2, \end{aligned} \quad (214)$$

$v_{F,N} = p_{F,N}/m_N^*$. For low T the real part of the full Lindhard function in the limiting case of low frequencies yields [97, 96]

$$\text{Re}\Phi(\omega \ll kv_{F,N}, k \ll 2p_{F,N}, T \ll \epsilon_{F,N}) \simeq 1 - \frac{\omega^2 m_N^{*2}}{k^2 p_{F,N}^2} - \frac{\pi^2 T^2}{12 \epsilon_{F,N}^2} - \frac{k^2}{12 p_{F,N}^2}, \quad (215)$$

$\epsilon_{F,N} = p_{F,N}^2/m_N^*$.

There were found two sets of the parameters fitted to atomic-nucleus experiments, cf. [93], being $f \simeq 0.25$, $f' \simeq 1$, $g \simeq 0.5$, $g' \simeq 1$ and $f \simeq 0$, $f' \simeq 0.5-0.6$, $g \simeq 0.05 \pm 0.1$, $g' \simeq 1.1 \pm 0.1$. Uncertainties in numerical values appear due to attempts to get the best fit to experimental data in each specific case modifying the parametrization used for the residual part of the NN interaction. All of these numerical values of the parameters relate to the isospin-symmetric matter and the density $n \simeq n_0$, whereas there is no direct experimental information on their values for $n > n_0$ and for isospin-asymmetric matter. There exist various calculations of the Landau–Migdal parameters as functions of the density for the isospin-symmetric nuclear matter and for the purely neutron matter, cf. [286, 287, 288, 285] and references therein.

The spectrum of excitations with pion quantum numbers is determined by the spectral function $A_\pi = -2\Im D_\pi^R$. In the quasiparticle approximation the spectrum is given by

$$\Re D_\pi^{R-1}(\omega, k) \simeq \omega^2 - k^2 - \Re \Sigma^R(\omega, k) = 0.$$

In vacuum the pion dispersion law is $\omega(k) \equiv \omega_k = \sqrt{m_\pi^2 + \vec{k}^2}$. But the pion atom data can't be described with the free spectrum indicating that the pion branch of the spectrum behaves like $\omega(k) \simeq \sqrt{m_\pi^2 + \alpha_0 k^2}$, $\alpha_0 \simeq 0.4$ for $n \simeq n_0$ and for small momenta $k \lesssim m_\pi$, cf. [290, 292, 293, 294, 295, 296]. The main contribution to the pion polarization at $\omega \sim m_\pi$ is determined by the Δ term given by the third diagram in r.h.s. of (207). Besides the pion branch there is the Δ branch of the excitation with the pion quantum numbers. In vacuum it degenerates into the relation $\omega \simeq m_\Delta - m_N + k^2/(2m_\Delta)$. In the medium the Δ branch is modified. Analysis of the ${}^3\text{He}-t$ reaction on nuclei, cf. [297, 298, 299, 300], demonstrated agreement with the pion spectrum consisting of the medium-modified pion and Δ branches and with the assumption of the softening of these branches for $k \gtrsim 2m_\pi$.

The spectrum of quasiparticles $\pi^{\pm,0}$ in the isospin-symmetric matter and of π^0 also in asymmetric matter ($N \neq Z$) possesses three branches. For $n = n_0$ in the cold isospin-symmetric matter the spectrum is shown in Fig. 9. For $\omega \gtrsim m_\pi$ there exist mentioned above two quasi-branches: the pion branch and the Δ branch. For $\omega < m_\pi$ there is still the spin-sound branch (with $\omega \rightarrow 0$ when $k \rightarrow 0$). This branch appears owing to the nucleon-nucleon repulsive interaction determined in the Fermi liquid theory by the non-zero Landau parameters (see presence of the pole in (211) for $g' \neq 0$). In the lower hatched region, at $\omega < kv_{F,N}$ and $k \sim p_{F,N} = m_N^* v_{F,N}$, the pion width cannot be neglected. This is the region of the Landau damping. The pion spectral function is enhanced in this region of ω and k for $n > n_c^{(1)} \simeq (0.5-0.8)n_0$. Calculations [301, 302] taking into account pion and Δ width effects in a

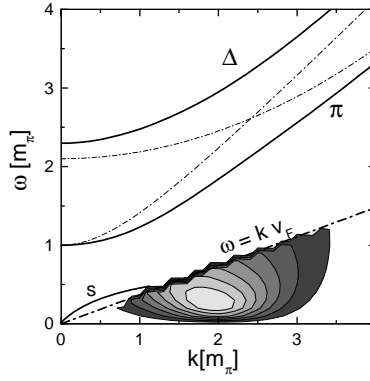


Figure 9: Pion spectrum in isospin-symmetric matter for $n = n_0$. Solid lines show quasiparticle branches of pion excitations in medium, computed neglecting effects of the particle widths. The contour plot depicts the spectral density of virtual pions. Thin dash-dotted lines are the dispersion laws for pions and Δ in the free space, thick dash-dotted line shows $\omega = kv_F$.

self-consistent approach resulted in some differences with the simplified quasiparticle spectrum shown in Fig. 9, compare this figure and Fig. 5 in [302]. These complications are however not of our interest in the present work.

The spectrum of π^+ and π^- in isospin-asymmetric matter is somewhat different. For purely neutron matter it can be found in [95, 96].

The pion excitations may decay to the nucleon particles and holes and Δ isobars and nucleon holes. For $\omega \lesssim m_\pi$ the main contribution to the pion self-energy is given by the nucleon particle-hole term. One obtains [303, 96, 304]

$$(\Im D_\pi^R)^{-1} = \beta T \ln \frac{e^\kappa + 1}{e^\kappa + e^{-\omega/T}}, \quad \beta = -\frac{f_{\pi NN}^2 q^2 m_N^{*2} \Gamma^2(g')}{k\pi}, \quad (216)$$

$\kappa = (\omega + q^2/(2m_N^*)^2 m_N^*/(2k^2 T) - \mu_N/T$. For $|\kappa| \gg T$, $\kappa < 0$, this expression simplifies as $-\Im \Sigma^R = \beta\omega$. Here μ_N is the nucleon chemical potential. Simplifying, one presents the spectral function for pions in the isospin-symmetric matter and for π^0 at arbitrary isospin composition as

$$A_\pi(\omega, k) \simeq \sum_i 2\pi Z_i \delta(\omega - \omega_i(k)) + \frac{2\beta_0 k \omega}{\tilde{\omega}^4(k) + \beta_0^2 k^2 \omega^2} \theta(\omega < p_F k/m_N), \quad (217)$$

$Z_i = \left[2\omega - \frac{\partial \Re \Sigma_\pi^R(\omega, k)}{\partial \omega}\right]_{\omega_i(k)}^{-1}$, and the sum is over the quasiparticle-like branches. The second term is due to virtual particle-hole modes. For $n = n_0$ in isospin-symmetric matter, with the help of Eq. (216) one estimates $\beta(n_0) = \beta_0 \simeq 0.7$.

5.2 Pion softening and pion condensation

The quantity [96, 306]

$$-\Re D_\pi^{R-1}(\mu_\pi, k^2, n, T) = \tilde{\omega}^2(k) = k^2 + m_\pi^2 + \Re \Sigma_\pi(\mu_\pi, k) - \mu_\pi^2, \quad (218)$$

has the meaning of the squared effective pion gap. For systems of a small size like atomic nucleus one should put $\mu_{\pi^+} = \mu_{\pi^-} = \mu_{\pi^0} = 0$. In case of the isospin-symmetric matter for $n = n_0$ one estimates $\tilde{\omega}^2(k_0(n_0)) \simeq 0.8 - 0.9$, cf. [96]. In the beta-equilibrium matter the pion chemical potentials ($\mu_{\pi^+} \neq \mu_{\pi^-} \neq 0$, $\mu_{\pi^0} = 0$) are determined from equilibrium conditions for the reactions involving pions [306]. The value μ_{π^-} follows from the condition of the chemical equilibrium with respect to the reactions

$n \leftrightarrow p\pi^-$ and $n \leftrightarrow pe\bar{\nu}$: $\mu_{\pi^-} = \mu_e = \varepsilon_{Fn} - \varepsilon_{Fp}$, where ε_{Fn} , ε_{Fp} are the Fermi energies of the neutron and proton.

In case of the isospin-symmetric matter the pion gap at $n > n_c^{(1)}$, $n_c^{(1)} \simeq (0.5 - 0.7)n_0$, gets a roton-like minimum at $k = k_0 \neq 0$ and near the minimum it behaves as

$$\tilde{\omega}^2(k) \simeq \tilde{\omega}^2(k_0) + \gamma_0(k^2 - k_0^2)^2/(4k_0^2) \quad (219)$$

with $\gamma_0 \sim 1$, $k_0 \simeq p_{F,N}$, cf. Eqs. (14), (39) used above. A typical density behavior of $\tilde{\omega}^2(k_0(n))$ for π^\pm, π^0 in isospin-symmetrical matter and for π^0 at $N \gg Z$ is demonstrated in Fig. 10. For $n > n_c^{(1)}$, when typical correlations in the spin channel are characterized by $k \sim k_0$, the nuclear matter can be treated as a liquid (or amorphous) phase of a quantum pion condensate [97, 98, 6, 96, 7]. With increasing density, $\tilde{\omega}^2(k_0(n))$ decreases, see line 1a. Various calculations done within the mean-field approximation (dropping fluctuation contribution to the pion self-energy) demonstrate that at $n > n_c^\pi$ the pion condensate with a liquid-crystal-like or a solid-like structure may occur by the second-order phase transition. In the isospin-symmetric matter the value n_c^π is the same for π^\pm and π^0 . In the isospin-asymmetric matter the value n_c^π depends on the sort of the pion. It is curious that numerical analysis [307] performed within the so called “variational theory of nuclear matter”, which employs the realistic two-nucleon potential in vacuum and then introduces the three-nucleon interactions, gave the value $n_c \simeq 2n_0$ for the critical density of the π^+, π^-, π^0 condensation in isospin-symmetric nuclear matter and the value $n_c^\pi \simeq 1.3n_0$ for the π^0 condensation in the purely neutron matter. Cooling of neutron stars is appropriately described in the “Nuclear medium cooling scenario” with taking into account of the pion softening effects [305, 99, 96] provided $n_c^\pi \gtrsim (2 - 2.5)n_0$, cf. [306, 308, 309, 310, 311] and references therein. At $n = n_c^\pi$, in the first-order phase transition due to the effect of fluctuations with $k \sim k_0 \sim p_{F,N}$ the classical pion field is developed. Line 1c shows a metastable phase in the system, where the ground state contains the pion condensate and line 1b demonstrates a possible saturation of the pion softening effect that could be, if the Landau–Migdal parameter g' increased with increase of the density. Line 3 corresponds to the presence of the pion condensate with a liquid-crystal-like or a solid-like structure and line 2 demonstrates behavior of the effective pion gap in presence of the condensate.

In the mean-field approximation the pion condensation for $n = n_c^\pi$ and $T = 0$ results in a negative contribution to the energy density

$$\delta E_\pi \simeq \tilde{\omega}^2(k_0(n))|\phi|^2 + \Lambda|\phi|^4/2 = -\frac{\tilde{\omega}^4(k_0(n))}{2\Lambda}\theta(-\tilde{\omega}^2),$$

where $\theta(x)$ is the step function, Λ is the constant of the effective $\pi\pi$ interaction in the medium [95]. Near the critical point $\tilde{\omega}^2(k_0(n)) \sim (n_c^\pi - n)/m_\pi$, if one neglects a jump of the effective pion gap due to quantum fluctuations, cf. [128, 96], and using $\Lambda \sim 1$ one estimates $\delta E_\pi \simeq -\alpha(n - n_c^\pi)^2/(n_c^\pi)^2$ with $\alpha \sim m_\pi^2$.

Finally, let us mention here that there exist two ways in the literature how one treats the pion condensation. One choice is to perform averaging of the initial Lagrangian over baryon degrees of freedom separating in such a way dressed pions, as we have done it above. Another in principle equivalent way is to perform averaging over the pion degrees of freedom to deal with the dressed baryons. In the latter case the pion condensation manifests in the appearance of the solid-like structure of baryons. Then one should find the structure yielding minimum of the free energy. Namely in such a way in [108, 109] it was demonstrated that the most energetically profitable among several structures, which were considered, is the so called (ALS) alternating-layer structure.

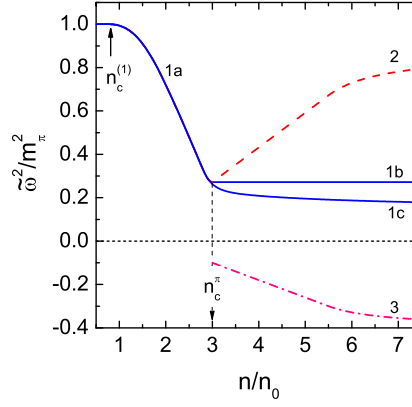


Figure 10: Typical density dependence of the effective pion gap for $\pi^{\pm,0}$ in isospin-symmetric matter and for π^0 in neutron star matter. The line 1a shows $\tilde{\omega}^2(k_0(n))$ for $n_c^{(1)} < n < n_c^\pi$. For $n > n_c^\pi$ the line 3 demonstrates the stable phase. Line 2 characterizes a softening of the spectrum of the pion excitations in presence of the pion condensate. Line 1c shows a metastable phase in the system, where the ground state contains the pion condensate and line 1b demonstrates artificially introduced saturation of the pion softening effect that could be, if the Landau–Migdal parameter g' increased with an increase of the density.

5.3 Fluctuations with $k_0 \neq 0$ and where soft pions are in atomic nuclei

5.3.1 Pion fluctuations

To be specific consider case of the isospin-symmetric matter. For $T \ll \epsilon_{F,N}$ and for $\omega < kv_{F,N}$, $k < 2p_{F,N}$, we have, see the tadpole diagram (75),

$$\frac{1}{2} < \hat{\phi}_{\pi-}^\dagger(\vec{k}) \hat{\phi}_{\pi-}(\vec{k}) + h.c. > = V_3 \int_0^\infty \frac{\beta \omega d\omega}{\pi [\tilde{\omega}^4(k) + \beta^2 \omega^2]} \left(\frac{1}{\exp(\omega/T) - 1} + \frac{1}{2} \right). \quad (220)$$

Here the contribution of fluctuations is included, and expansion of the Green function for small ω is as follows

$$-D^{R,-1}(\omega \ll m_\pi, k) \simeq \tilde{\omega}^2(k) - i\beta\omega, \quad (221)$$

$\beta = i(\partial \Sigma^R / \partial \omega)_{0,k_0} = \alpha_{02}(\omega_c = 0)$, see (14). The value β can be evaluated with the help of Eq. (216). Eq. (221) shows that the spectrum has the diffusion branch, like for paramagnon excitations in ^3He , cf. [312], (on complex plane) $\omega = -i\tilde{\omega}^2(k)/\beta$. For positive values of $\tilde{\omega}^2(k)$ this excitation branch corresponds to the Landau damping, since $\psi \sim \exp(-i\omega t) \rightarrow 0$ for $t \rightarrow \infty$ for such excitations. Due to this "complex plane branch", there arises the enhancement of the virtual pion sea resulting in enhancement of the pion distributions. Indeed, as one can see from Eqs. (217), (219), the pion spectral function has a pronounced maximum at pion energies $\omega \lesssim \tilde{\omega}^2(k)/\beta$.

In ^4He at the critical point one has $\omega_0^2 = \Lambda_0 = 0$, cf. [19]. This condition is required for presence of the so called Lifshitz point. Fluctuations in the phenomenological model of the phase transition to the state $k_0 \neq 0$ in the condensed matter systems described by the spectrum $\omega(p) = \Delta + (k - k_0)^2/m$ were first considered in [127]. The quantum fluctuations were studied in [128]. For nonrelativistic media usually the limit $T \gg |\omega_0^2|/\beta$ is realized. In relativistic systems, e.g., for consideration of the pion excitations in heavy-ion collisions, both the temperature regimes $T \lesssim |\omega_0^2|/\beta$ and $T > |\omega_0^2|/\beta$ are relevant [129, 97, 130, 132, 96]. With account of pion fluctuations with $k \sim k_0 \sim p_{F,N}$ the phase transition, being of the second order within the mean-field consideration, becomes of the first order.

As example, assuming

$$0 < \tilde{\omega}^2(k_0)/\beta(k_0) \ll T, \quad (222)$$

from Eq. (220) we obtain

$$\langle \hat{\phi}_{\pi-}^\dagger(\vec{k}) \hat{\phi}_{\pi-}(\vec{k}) \rangle_T \simeq VT/[2\tilde{\omega}^2(k)]. \quad (223)$$

Thus, the pion fluctuation contribution to the pion self-energy, being proportional to (223), has a sharp maximum at $k \simeq k_0 \sim p_{F,N}$. Integrating Eq. (223) over the phase space, in the approximation (222), one obtains

$$\Sigma_{F1}^R \simeq 5\Lambda(\omega \simeq 0, k_0) \int \frac{d^3k}{(2\pi)^3V} \langle \hat{\phi}_{\pi-}^\dagger(\vec{k}) \hat{\phi}_{\pi-}(\vec{k}) \rangle \simeq \frac{5\Lambda(\omega \simeq 0, k_0)k_0T}{4\pi\sqrt{2\gamma}\tilde{\omega}(k_0)}, \quad (224)$$

where Λ is the effective $\pi\pi$ in-medium interaction coupling constant and factor 5 includes possibility of π^+ , π^- and π^0 intermediate states.

As we have mentioned, a strong enhancement of the virtual pion sea at $k \sim k_0$ for $n > n_c^{(1)}$ can be treated as a liquid phase or as an amorphous phase of the pion condensation, cf. [132, 6, 7]. Due to this enhancement at $T \neq 0$ there arise essential contributions to thermodynamical characteristics such as the entropy, energy, pressure, etc., with important consequences for the description of heavy-ion collisions, cf. [100, 6, 7]. Contribution of a non-quasiparticle nature from thermal virtual pions of small energies $\omega \ll m_\pi$ and of momenta $k \sim p_{F,N}$ arising for $n > n_c^{(1)}$ can be estimated as follows [6, 7]

$$\begin{aligned} E_\pi^F &\simeq \xi T^{3/2}(n - n_{c1})^2 \theta(n - n_{c1})(nm_\pi^{7/2})^{-1}, \\ S_\pi^F/A &\simeq 3\xi T^{1/2}(n - n_{c1})^2 \theta(n - n_{c1})(nm_\pi^{7/2})^{-1}. \end{aligned} \quad (225)$$

These simplified expressions were introduced in Ref. [100] basing on the model [98, 130, 132]. The value $\Lambda(\omega \simeq 0, k_0)$ was estimated in [95] and [132]. It was shown that $\Lambda(\omega \simeq 0, k_0)$ crucially depends on the baryon-baryon correlation factor $\Gamma(g')$, which precise value is not too well known, especially for $n > n_0$. Therefore in [6, 7] this factor Λ was considered as extra phenomenological parameter, which enters the pre-factor ξ in Eq. (225) chosen to be $\simeq 0.4$ in [100, 6, 7], that allows to get the best fit of the heavy-ion collision data (differential pion and nucleon cross sections and some other characteristics) at energies $\lesssim 2$ GeV /A.

For $n > n_c^\pi$ the effective pion gap $\tilde{\omega}^2(k_0)$, being negative in a pion condensate state, depends on the assumed structure of the condensate field. Therefore for various pion condensate structures one should calculate $\tilde{\omega}^2(k_0)$, then find the structure, which corresponds to the minimum of the free energy, $F(n)$, for $\tilde{\omega}^2(k_0) < 0$, and to compare the resulting free energy with the free energy $F(n)$ of the state, corresponding to the branch $\tilde{\omega}^2(k_0) > 0$ at the given density. The liquid crystal-like or solid-like pion condensation starts at the density, when both the free energies coincide. It occurs by the first order phase transition for $n > n_c^\pi$, cf. [129, 97, 130, 132, 96]. Although for $n > n_c^\pi$ the stable system exists in the state $\tilde{\omega}^2(k_0) < 0$, it can remain for a while in the metastable state $\tilde{\omega}^2(k_0) > 0$. Which state is realized at the given time moment depends on the peculiarities of the dynamics of the system.

Above we considered the case of the p-wave pion condensation which appears owing to the strong p-wave pion-nucleon and pion- Δ isobar attractions increasing with increase of the baryon density, cf. [95, 96]. Also in some models, for instance in the model described by the Manohar-Georgi Lagrangian, there is a possibility that the pion condensate in dense isospin-symmetric baryon matter appears in the s-wave, cf. [103]. The kaon condensate may appear both in the s-wave, cf. [110, 10] and the p-wave, cf. [111, 112, 113]. In this case the s-wave interaction is stronger than in pion case. Possibilities of the s- and p-wave pion and kaon condensate phases make the $T - n$ diagram of the strongly interacting matter still more complicated.

Within the sigma model the $k_0 \neq 0$ condensates began to be studied in [206, 207, 208, 117, 107, 97, 106, 168]. References [206, 207, 208, 117, 97] considered the σ field together with the running π^\pm condensate wave, whereas Ref. [107] proposed the σ, π^0 condensate standing wave. Reference

[106] studied alternating layer structure of the pion condensate. Reference [313] suggested to consider possibility of the ferromagnetic neutron matter with a magnetization and a neutral pion condensation like the σ, π^0 condensate of Dautry and Neyman [107]. However, compared to the inhomogeneous phase with the alternating layer structure, the ferromagnetic phase turned out to be unfavored.

As it has been noted, cf. [314, 169], the QCD critical endpoint should be a Lifshitz point, where the normal, homogeneous and inhomogeneous chiral condensed phases meet. This configuration is similar to $\sigma\pi^0$ condensation, obtained in neutron matter within the sigma model of Dautry and Neyman [107], and with these phases one could expect a smooth transition from description of the nuclear $\sigma\pi N$ to the quark matter. However fluctuations with $k_0 \neq 0$ lead to the change of the phase transition from the second order to the first order, as we have discussed, cf. [134].

5.3.2 Where soft pions are in atomic nuclei

References [315, 316] analyzing experiments on (\vec{p}, \vec{n}) quasielastic polarization transfer and EMC and Drell–Yan ratios did not find any manifestation of pion softening effects and raised a principal question “where are the nuclear pions?” The answer is probably as follows, see [306] and also [317, 318].

The quantity $\tilde{\omega}^2(k_0)$ demonstrates how much the virtual nucleon particle–hole mode with the pion quantum numbers is softened at the given density. Typical momentum transferred in the two-nucleon reaction is $k \simeq p_{F,N}$. The ratio of the NN cross sections calculated with the help of the model of the free one-pion exchange (FOPE) and the model of the medium one-pion exchange (MOPE) is estimated as

$$R = \frac{\sigma[\text{FOPE}]}{\sigma[\text{MOPE}]} \simeq \frac{\Gamma^4(\omega \simeq 0, k \simeq p_{F,N})(m_\pi^2 + p_{F,N}^2)^2}{\tilde{\omega}^4(p_{F,N})}, \quad (226)$$

where Γ is the vertex dressing factor determined in (212). We estimate $|D_\pi(\omega \simeq 0, k \simeq p_{F,N})/(m_\pi^2 + p_{F,N}^2)|^2 \simeq 40$ for isospin-symmetric matter at $n = n_0$, whereas $\Gamma(n_0) \simeq 0.4$. Thereby, for $n \lesssim n_0$ one has $R \lesssim 1$, whereas already for $n = 2n_0$ this estimate yields $R \sim 10$. The contribution of a purely local interaction to the NN cross section is less than that of the soft pion. Thus, following (226) one can evaluate the NN interaction for $n > n_0$ with the help of the MOPE and with increasing density the MOPE contribution is increased. For small frequencies for $n_c^{(1)} < n < n_c^\pi$ one may use the presentation $D_\pi^{R,-1}(\omega \ll m_\pi, k \sim k_0) \simeq -\tilde{\omega}^2(k_0) - \gamma_0(k - k_0)^2 + i\beta\omega$, cf. Eq. (219). With the help of this expression we find that soft pions (with $\omega \ll m_\pi$) yield only a small contribution,

$$\delta S = \int_0^{kp_{F,N}/m_N^*} 2\omega A_\pi \frac{d\omega}{2\pi} = \frac{2}{\pi\beta} \left[\frac{kp_{F,N}}{m_N^*} - \arctan \frac{\beta kp_{F,N}}{m_N^* \tilde{\omega}^2(k)} \right], \quad (227)$$

to the full sum-rule, $S = \int_0^\infty 2\omega A_\pi \frac{d\omega}{2\pi} = 1$. An estimation yields $\delta S \simeq 0.05$ for $n = n_0$ and δS remains much less than unity (~ 0.1) even for $\tilde{\omega}^2(k_0) = 0$. So, pions are soft for $\tilde{\omega}(k_0) \ll m_\pi$, but their contribution to the sum-rule remains small.

On the other hand, a successful description of the data on the pion atoms [290, 96, 292, 293, 294, 295, 296, 103] requires a strong modification of the pion dispersion law $\omega \simeq \sqrt{m_\pi^2 + \alpha_0 k^2}$ with $\alpha_0 \simeq 0.4$ for $\omega \simeq m_\pi$ at $n = n_0$ involved in this problem. Analysis of the $^3\text{He}-t$ reaction on nuclei, cf. [297, 298, 299, 300], demonstrates agreement with two-branch pion spectrum consisting of the pion branch and the Δ branch and with the assumption of the softening of these branches for $k \gtrsim 2m_\pi$.

Summarizing, there are soft pions in atomic nuclei but the pion contribution to various quantities largely depends on the quantity under consideration, the density, the frequency and the momentum involved in the problem. For instance, virtual pions significantly contribute for $T \neq 0$. The momentum distribution function of π^- entering the detector at a sudden (prompt) break up of the piece of a hot

nuclear matter is given by [319, 6, 96, 7, 48]:

$$n_k^{\pi^-}(\text{virt}) = \int_0^\infty \frac{2\omega_k A_\pi d\omega}{2\pi(e^{\omega/T} - 1)} = 2\omega_k \int_0^\infty \frac{\beta\omega}{\tilde{\omega}^4(k) + \beta^2\omega^2} \frac{d\omega}{\pi(e^{\omega/T} - 1)} \simeq \frac{T\sqrt{m_\pi^2 + k^2}}{\tilde{\omega}^2(k)}, \quad (228)$$

where the second equality is valid for $0 < \tilde{\omega}^2(k_0) \ll \beta T$, cf. Eq. (73), $\omega_k = \sqrt{m_\pi^2 + k^2}$. This result shows a strong effect of thermal pion fluctuations with $k \sim k_0$ for $n_c^\pi > n > n_c^{(1)}$, i.e. in the liquid, better saying, the amorphous phase of the pion condensation. Also, such a fluctuations yield a large contribution to the bulk viscosity $\propto 1/\tilde{\omega}^3(k_0)$, cf. [264]. Thereby, in the vicinity of the critical point n_c^π , the nuclear matter for $T \neq 0$ behaves similarly to a glass, here, a pionic glass.

However, we should note that the result (228) exceeds significantly not only the free pion distribution

$$n_k^{\pi^-}(\text{free}) = 1/(e^{\sqrt{m_\pi^2 + k^2}/T} - 1), \quad (229)$$

but also the experimental result that follows from the study of the heavy-ion collisions. The solution of the puzzle [319, 96, 6, 7] is as follows: (i) At realistic conditions the freeze out for virtual pions with typical frequencies $\omega \ll m_\pi$ cannot be considered as sudden. Most of such virtual pions, existed for $n > n_c^{(1)}$, are “eaten” by nucleons during the freeze out stage, since the typical time of the latter is $\tau_{\text{f.o.}} > 1/m_\pi$. (ii) The freeze out density is estimated as $n_{\text{f.o.}} \lesssim n_c^{(1)}$, cf. [6, 7]. Thus contribution of the second term in (217) to the observable pion yield should be strongly suppressed, whereas the first term contributes significantly. This term describes the pions emitted from the π^- and Δ^- branches of the pion spectrum in Fig. 9. For them $\tau_{\text{f.o.}} < 1/|\omega(k, n_{\text{f.o.}}) - \sqrt{m_\pi^2 + k^2}|$, and the freeze out can be considered as sudden (at $n = n_{\text{f.o.}}$, $T = T_{\text{f.o.}}$) and thereby

$$n_k^{\pi^-}(\text{branches}) \simeq \sum_i \frac{2\sqrt{m_\pi^2 + k^2} Z_i}{(e^{\omega_i(k)/T_{\text{f.o.}}} - 1)}. \quad (230)$$

As it was demonstrated in [6, 7], the latter result well describes the experimental pion momentum distributions at heavy-ion collision energies $\lesssim 2 \text{ GeV} / A$. It significantly differs from (229), especially for low T . It should be noted that at the sudden transition the momentum of the pion excitation is conserved, whereas the energy is not conserved. Nevertheless the energy and momentum of the system as a whole is certainly conserved. The excess or deficit of the energy of the pion sub-system is compensated by the nucleon sub-system.

Note that the ideal pion gas approximation is up to now used in different kinetic and hydrodynamic codes. For example, the ideal hydrodynamical models employ both the sudden freeze-out and the ideal pion gas approximations, which are, generally speaking, incompatible. The equation of state including pion softening effects for $T \neq 0$ and $n > n_c^{(1)}$ unified with the model of the sudden freeze-out for nucleons and pions allowed to appropriately describe the Bevalac Berkeley and SIS GSI heavy-ion collision inclusive data at collision energies $\lesssim 2 \text{ GeV} / A$, cf. [6, 7].

A good moment to remind phrase of Albert Einstein “Raffiniert ist der Herr Gott, aber boshaft ist er nicht.”

5.4 Dynamics of pion-condensate phase transition

Let us now explain how the instability, which results in the pion condensation, develops dynamically. In a semiclassical scheme the dynamics of a mode is described by the solution of the quantum kinetic Kadanoff–Baym equation derived from the nonequilibrium Green function technique in the first-gradient order. The Boltzmann equation follows from the Kadanoff–Baym equation only in the limit of a weak interaction, cf. [320, 278]. The hydrodynamical equations with the transport coefficients expressed

in terms of the retarded Green functions also follow from the Kadanoff–Baym kinetic equation [321]. Actually, the first-gradient order quantum kinetic equation can be written in three forms: the original Kadanoff–Baym form, the Bottermans–Malfliet form [322], which is derived from the latter for configurations close to the thermal equilibrium and the non-local form [323, 324], which up to the second-gradient order coincides with the Kadanoff–Baym equation and up to the first-gradient order with the Bottermans–Malfliet form. In presence of the condensate, one needs to add equation of motion of the condensate field. Both equations are derived from the generating functional formulated on the Schwinger–Keldysh contour, cf. [325, 326, 327, 328].

Two Wigner transformed quantities, $F(t, \vec{r}, \omega, \vec{k}) = A_\pi(t, \vec{r}, \omega, \vec{k})f_\pi(t, \vec{r}, \omega, \vec{k})$, and

$$A_\pi(t, \vec{r}, \omega, \vec{k}) = \frac{\Gamma_\pi(t, \vec{r}, \omega, \vec{k})}{[\omega^2 - k^2 - m_\pi^2 - \Re \Sigma^R(t, \vec{r}, \omega, \vec{k})]^2 + \Gamma_\pi^2(t, \vec{r}, \omega, \vec{k})/4}, \quad (231)$$

where $\Gamma_\pi = -2\Im \Sigma_\pi^R$, completely determine the kinetic evolution of the given species. The spectral function given by (231) satisfies a general sum-rule [322]

$$\int_{-\infty}^{\infty} \omega A_\pi d\omega / 2\pi = 1. \quad (232)$$

In the isospin-symmetric nuclear matter π^+ , π^- and π^0 mesons have essentially the same distributions, $A_\pi(\omega, k) = -A_\pi(-\omega, k)$ that simplifies the scheme of the separation of particle and antiparticle contributions. Thereby one can work with the quantities related to one particle species at positive frequencies.

Above we extensively studied the dynamics of the condensate field. Now let us focus on the dynamics of the soft modes. Importance of taking into account width effects in description of the soft modes was emphasised in [329, 330]. As a specific example, let us consider the pion sub-system as a light admixture in a heavy nucleon environment, neglecting the feedback of the pions onto the nucleons ($m_\pi/m_N \simeq 1/7 \ll 1$), i.e., neglecting the contribution from in-medium pion fluctuations. Within the above approximations the quantum kinetic equation for the pion distribution, $f_\pi \ll f_N$, in homogeneous and equilibrated nucleon environment becomes [265]:

$$\frac{1}{2}\Gamma_\pi B_\mu^\pi \partial_X^\mu f_\pi = \Gamma_{in}^\pi - \Gamma_\pi f_\pi. \quad (233)$$

Here $\mu = 0, 1, 2, 3$, $X = (t, \vec{r})$, $\Gamma_{in}^\pi = i\Sigma_\pi^{-+}(f_N)$, B_μ^π is defined as

$$B_\mu^\pi = A_\pi \left[\left(2k_\mu - \frac{\partial \Re \Sigma_\pi^R}{\partial k^\mu} \right) - \Re D_\pi^{R,-1} \Gamma_\pi^{-1} \frac{\partial \Gamma_\pi}{\partial k^\mu} \right]. \quad (234)$$

The instability of the system can be discussed considering a weak perturbation, δf_π , of the equilibrium pion distribution, $f_\pi^{(0)} = [\exp(\omega/T) - 1]^{-1}$, in the rest frame of the system. Linearizing Eq. (233) we find

$$\frac{1}{2}B_\mu^\pi \partial_X^\mu \delta f_\pi + \delta f_\pi = 0, \quad (235)$$

with the solution

$$\delta f_\pi(t, \omega, k) = \delta f_0(\omega, k) \exp[-2t/B_0^\pi(\omega, k)], \quad (236)$$

where for simplicity the initial fluctuation $\delta f_0(p)$ of the pion distribution is assumed to be space-independent. Let us put $\omega \rightarrow 0$ and $k \sim k_0 \sim p_{F,N}$. This four-momentum region, being far from the pion mass shell, is the region, where the pion instability is expected to occur in isospin-symmetric nuclear matter. The real part of the pion self-energy, $\Re \Sigma_\pi^R$, is an even function of the pion energy ω while the width is an odd function proportional to ω for $\omega \rightarrow 0$, and, cf. [95, 96], one has $2\omega - \partial \Re \Sigma_\pi^R / \partial \omega \rightarrow 0$,

$\Gamma_\pi = \beta(k)\omega$ and $\beta(k) \sim m_\pi$ for $\omega \rightarrow 0$, $k \sim p_{F,N}$. Thus from Eq. (234) we get $B_0^\pi = \beta(k)/\tilde{\omega}^2(k)$ and therefore

$$\delta f_\pi(t, \omega = 0, \vec{k}) = \delta f_0(\omega = 0, \vec{k}) \exp \left[-2\tilde{\omega}^2(k)t/\beta(k) \right]. \quad (237)$$

This solution shows that for $\tilde{\omega}^2 > 0$ initial fluctuations are damped, whereas for $\tilde{\omega}^2 < 0$ they grow. Thus, the change of sign of $\tilde{\omega}^2(k_{0c})$ at $n = n_c^\pi$, $k_0 = k_{0c}$ leads to an instability of the virtual pion distribution at low energies and for momenta $k \simeq k_{0c}$. The solution (237) illustrates the important role of the width, $\Im \Sigma_\pi^R \neq 0$, in the quantum kinetic description. At neglected width in the quantum kinetic equation, one would fail to find the above instability.

Increase of the pion distribution δf_π is accompanied by a growth of the mean condensate field φ_π . Due to the latter, the increase of the virtual pion distribution slows down and finally stops, when the mean field reaches its stationary value. Therefore, a consistent treatment of the problem requires the solution of the coupled system of the quantum kinetic equation for the particle distribution function, the equation for the spectral function and the equation for the mean field. In presence of the condensate, Σ_π^R acquires an additional contribution $\Sigma_\pi^R(\varphi_\pi) = \Sigma_\pi^R(\varphi_\pi = 0) + \Lambda_{\text{eff}}|\varphi_\pi|^2 + O(\varphi_\pi^3)$, where Λ_{eff} denotes the total in-medium pion-pion interaction. Within the same order, the mean-field equation becomes

$$\left[\tilde{\omega}^2(k_{0c}) + \lambda_{\text{eff}}|\tilde{\varphi}_\pi|^2(t) + \frac{1}{2}\beta(k_{0c})\partial_t \right] \tilde{\varphi}_\pi(t) = 0. \quad (238)$$

Here we have assumed the simplest structure for the condensate field $\varphi_\pi = \tilde{\varphi}_\pi(t)\exp(i\vec{k}_{0c}\vec{r})$, where $\tilde{\varphi}_\pi(t)$ is a space-homogeneous real function, which varies slowly in time. Also one should do the replacement

$$\tilde{\omega}^2(k_{0c}) \rightarrow \tilde{\omega}^2(\varphi_\pi, k_{0c}) \equiv \tilde{\omega}^2(k_{0c}) + \Lambda_{\text{eff}} |\varphi_\pi|^2$$

in Eqs. (233) - (237) for the pion distribution.

The time dependence of $\tilde{\varphi}$ can qualitatively be understood inspecting the two limiting cases. At a short time scale the mean field is still small and one can neglect the $\Lambda_{\text{eff}}\tilde{\varphi}^2(t)$ term in Eq. (238). Then the mean field

$$\tilde{\varphi}_\pi(t) = \tilde{\varphi}_\pi(0) \exp \left[-2\tilde{\omega}^2(k_{0c})t/\beta(k_{0c}) \right] \quad (239)$$

grows exponentially with time, as well as the distribution function (237). Here $\tilde{\varphi}_\pi(0)$ is an initial small fluctuation of the field, which value is generated by the white noise.

At a larger time, the solution of Eq. (238) approaches the stationary limit $\tilde{\varphi}_\pi \rightarrow \tilde{\varphi}_\pi^{\text{stat}}$ with

$$(\tilde{\varphi}_\pi^{\text{stat}})^2 = -\tilde{\omega}^2(k_{0c})/\Lambda_{\text{eff}}(k_{0c}). \quad (240)$$

Since simultaneously $\tilde{\omega}^2(\varphi_\pi, k_{0c}) = \tilde{\omega}^2(k_{0c}) + \Lambda_{\text{eff}} |\varphi_\pi|^2 \rightarrow 0$, the change in the pion distribution δf_π will saturate. This stationary solution $\tilde{\varphi}_\pi^{\text{stat}}$ is stable. It can be seen from Eq. (238) linearized near the value $\tilde{\varphi}_\pi^{\text{stat}}$. Then we have

$$\tilde{\varphi}_\pi(t) = \tilde{\varphi}_\pi^{\text{stat}} - \delta\tilde{\varphi}_0 \exp \left[4\tilde{\omega}^2(k_{0c})t/\beta(k_{0c}) \right], \quad (241)$$

where the factor in the exponent is now negative. As $\tilde{\varphi}_\pi(0)$, the value $\delta\tilde{\varphi}_0$ is generated by the white noise term in the equation.

6 Fermion blurring and hot Bose condensation

6.1 System of strongly interacting light bosons – heavy fermions at $\mu_f = 0$

References [44, 41, 45] studied behavior of a system of strongly interacting heavy fermions at small (or zero) baryon chemical potential, μ_f , and light bosons, avoiding quasiparticle approximation. The

problem has application to the description of heavy-ion collisions at top RHIC and LHC energies. Description of the heated pion-nucleon vacuum (at zero total baryon charge) is in a sense analogous to the description of the electron-phonon interaction in doped semiconductors. In the latter case, even at zero temperature the tail of the electron wave function penetrates deeply into the band gap due to multiple electron-phonon collisions [331, 332]. In the nuclear problem, heavy nucleons and antinucleons may play the same role as electrons and holes, and light pions play role of massless phonons.

Let us first consider a hot system of two particle species. References [41, 45] treated the system in terms of the self-consistent two-particle irreducible (2PI) Φ derivable approximation scheme suggested by Baym [333]. The Φ functional is given by diagrams

$$i\Phi = \frac{1}{2} \text{ (fermion loop)} + \frac{1}{4} \text{ (boson loop)} + \dots, \quad (242)$$

Here both fermion (solid line) and boson (wavy line) Green functions are full Green functions, whereas vertices are bare. Simplifying consideration let us restrict ourselves by consideration of the simplest Φ (the first diagram (242)). Then the fermion self-energy

$$\text{fermion self-energy diagram} \quad (243)$$

enters the Dyson equation

$$\text{full fermion line} = \text{bare fermion line} + \text{fermion line with self-energy} \quad (244)$$

and the boson self-energy

$$\text{boson self-energy diagram} \quad (245)$$

enters the Dyson equation

$$\text{full boson line} = \text{bare boson line} + \text{boson line with self-energy} \quad (246)$$

Note that in a sense similar self-consistent approach was applied in [36] to the quark-gluon matter. For the chiral transition the authors found a crossover turning into a first order transition at a critical endpoint at the quark chemical potential $\mu_q/T_c \simeq 3$.

All the multi-particle re-scattering processes

$$\text{fermion self-energy} + \text{fermion self-energy with boson exchange} + \dots \quad (247)$$

are included in (244), whereas processes with crossing of boson lines (correlation effects) like

$$\text{crossing boson lines diagram} \quad (248)$$

are disregarded. Note that for πNN interaction each diagram with the one crossed boson line brings the suppression factor $\nu = \nu_\tau \nu_\sigma$ compared to the corresponding diagram with the same number of boson lines but without their crossing, cf. [44, 312, 41, 45]. In the non-relativistic approximation for nucleons, $\nu_\tau = 1/3$ is due to the non-commutation of the isospin τ matrices and $\nu_\sigma = 1/3$ is due to the non-commutation of the spin σ matrices. Each product $\tau_i \tau_i \tau_j \tau_j$ yields factor 9, whereas each product $\tau_i \tau_j \tau_i \tau_j$ yields factor 3. The same statement is valid for σ matrices. Concluding, one may retain only the first diagram (242) in Φ in this case with mentioned accuracy.

There are several temperature regimes [41]. The regime $T \ll \min\{m_b^2/m_f, T_{\text{bl.f}}\}$ corresponds to a *slightly heated hadron liquid*, m_b is the boson mass, m_f is the fermion mass, at $m_f \gg m_b$. $T_{\text{bl.f}}$ is the temperature, at which the gap between fermion-antifermion continua becomes completely blurred, see below. Typically $T_{\text{bl.f}}(g)$ is of the order of $\sim m_\pi$ for relevant values of the fermion-boson coupling constant g , $m_\pi = 140$ MeV is the pion mass. Bosons are almost free particles in this temperature regime but fermion distributions deviate from the Boltzmann law, obeying the Urbach rule, due to the multiple collisions of each fermion on bosons. At $m_b^2/m_f \lesssim T \ll \min\{T_{\text{bl.f}}, m_b\}$, if such interval indeed exists, the fermion mass shell is already partially blurred due to multiple re-scatterings of the fermion on bosons. Here we deal with (*a warm hadron liquid, partially blurred fermion continuum*). The quasiparticle approximation for fermions fails, if the fermion-boson coupling constant g is rather large (e.g., $g \sim 10$ for σ , ω and ρ meson – nucleon N and other baryon interactions). As the result, fermion distributions become essentially enhanced compared to the ordinary Boltzmann distribution. For realistic hadron parameters the regime of *a warm hadron liquid* can be realized only for pions, not for σ , ω and ρ due to their large masses. However the enhancement is not too strong for pions, since $g \sim 1$ (rather than $\gg 1$) in the latter case.

For $m_f \gg T \gtrsim T_{\text{bl.f}}$ the fermion effective mass significantly decreases and fermions become essentially relativistic particles. The hot hadron liquid comes to the regime of *the blurred fermion continuum*. The fermion sub-system represents then *a rather dense packing of fermion-antifermion pairs*. With further increase of the temperature, the boson effective masses substantially decrease. For $m_f \gg T \gtrsim m_b^*(T)$ (*hot hadron liquid, blurred boson continuum*), where $m_b^*(T, g)$ is the effective boson mass depending on g , rapid fermions abundantly produce effectively less massive and slower off-shell bosons and undergo multiple re-scatterings on them, as on quasi-static impurities. The fermion propagator completely loses the former quasiparticle pole shape it had in a dilute medium. The fermion-antifermion density, $n_{f\bar{f}}$ grows exponentially with the temperature in a wide temperature interval. Bosons rescatter on fermion-antifermion pairs and due to that become effectively less massive. At a temperature $T > T_{\text{cB}} > T_{\text{bl.f}}$, the effective boson mass may vanish and a hot Bose condensation may set in. We stress that the condensate may appear for the temperature larger than a critical temperature. Similarly, the condensate of the charged vector field in the form of the lattice may appear at a high magnetic field $H > H_c$, whereas condensation is absent for $H < H_c$, cf. [26, 334]. For realistic values of hadron parameters, the problem of the determination of $T_{\text{bl.f}}$, T_{cB} and $m_b^*(T)$ is the coupled-channel problem. Estimations show that T_{cB} proves to be close to $T_{\text{bl.f}}$.

6.2 Scalar boson – fermion coupling

To simplify derivations consider first example of the Yukawa interaction of spin 1/2 non-relativistic heavy fermion with a light relativistic scalar boson. The interaction Lagrangian is given by

$$L_{\text{int}} = g \bar{\psi} \phi \psi. \quad (249)$$

Examples of different couplings of relativistic fermions and bosons, including the Yukawa scalar boson-baryon interaction, the vector boson-baryon interaction and pion-nucleon one, can be found in [41].

6.2.1 Approximation of a soft thermal loop

For $m_f \gg m_b$, in a broad temperature range, boson occupations are essentially higher than fermion ones. Then, at such temperatures we may retain in (243) only terms proportional to boson occupations. Using this we find [41]:

$$\Sigma_f^R(p_f) \simeq \int g^2 \frac{d^3 p_b}{(2\pi)^3} \int_0^\infty \frac{d\omega_b}{2\pi} [G_f^R(p_f + p_b) + G_f^R(p_f - p_b)] A_b(p_b) f_b(\omega_b). \quad (250)$$

Dropping boson momentum p_b -dependence of the fermion Green functions G_f in (250), i.e., in the *soft thermal loop* (STL) approximation, Eq. (250) is simplified as

$$\Sigma_f^R(p_f) \simeq J \cdot G_f^R(p_f), \quad J = 2g^2 \int \frac{d^3 p_b}{(2\pi)^3} \int_0^\infty \frac{d\omega_b}{2\pi} A_b(p_b) f_b(\omega_b), \quad (251)$$

A_b and f_b are the boson spectral and distribution functions. At $T \gtrsim m_b^*(T)$ departure of the fermion energy from the mass shell, $\delta\omega_f \sim \sqrt{J}$, proves to be much larger than that for bosons, $\delta\omega_b \sim \max\{m_b - m_b^*(T), T\}$, and typical fermion momenta $p_f \sim \sqrt{2m_f T}$ are much higher than typical boson momenta $p_b \sim \max\{\sqrt{2m_b^*(T)T}, T\}$. Here $m_b^*(T)$ is an effective boson mass. At these conditions the STL approximation should be valid. Moreover, we assume that $\sqrt{2m_f T} \ll m_f$ and $\sqrt{J} \ll m_f$. At these conditions there is a broad region of temperatures, where fermions can be treated as non-relativistic particles. The latter approximation allows us to avoid the spin algebra. A general case was considered in [41].

As follows from (251), the quantity J can be expressed through the tadpole fluctuation diagram (75) where now the vertex yields the factor g^2 . The latter contribution describes fluctuations of virtual (off-mass shell) bosons, see Eq. (220). On the other hand, J can be interpreted as the density of quasi-static boson impurities. Due to multiple repetition of this diagram in the Dyson series for the fermion, J demonstrates *the intensity of the multiple quasi-elastic scattering* of the fermion on quasi-static boson impurities. In the kinetical description, with the multiply-repeated diagram (75) one describes the Landau–Pomeranchuk–Migdal effect, cf. [329, 330].

The Dyson equation for the retarded fermion Green function is greatly simplified in the STL approximation,

$$G_f^R = G_{0f}^R + G_{0f}^R J (G_f^R)^2, \quad (252)$$

with a simple analytical solution

$$G_f^R = \frac{\omega_f - \omega_p^f \pm \sqrt{(\omega_f - \omega_p^f)^2 - 4J}}{2J}, \quad \omega_p^f = m_f + \frac{p_f^2}{2m_f}. \quad (253)$$

In this problem it is convenient to count fermion energies from the mass shell.

Only negative sign solution satisfies the retarded property and should be retained. For $(\omega_f - \omega_p^f)^2 \gg 4J$ we recover the quasiparticle (pole-like) solution. Since then typical energies are $\omega_f - \omega_p^f \sim T$, the quasiparticle approximation for fermions proves to be valid only for low temperatures, $J \ll T^2$. Otherwise (for $J \gtrsim T^2$) fermion Green function is completely regular. The fermions become *blurred particles*. From (253), using relation $(G_f^R)^{-1} = \omega_f - \omega_p^f - \text{Re}\Sigma_f^R + i\Gamma_f/2$, for $4J > (\omega_f - \omega_p^f)^2$ we find

$$\begin{aligned} \text{Re}\Sigma_f^R &= \frac{\omega_f - \omega_p^f}{2}, \quad \Gamma_f = \sqrt{4J - (\omega_f - \omega_p^f)^2} \theta(4J - (\omega_f - \omega_p^f)^2), \\ A_f &= \frac{\sqrt{4J - (\omega_f - \omega_p^f)^2}}{J} \theta(4J - (\omega_f - \omega_p^f)^2). \end{aligned} \quad (254)$$

where the fermion spectral function, A_f , satisfies the exact sum-rule $\int_{-\infty}^\infty A_f d\omega/(2\pi) = 1$. Thus, although we used approximations, their consistency is preserved.

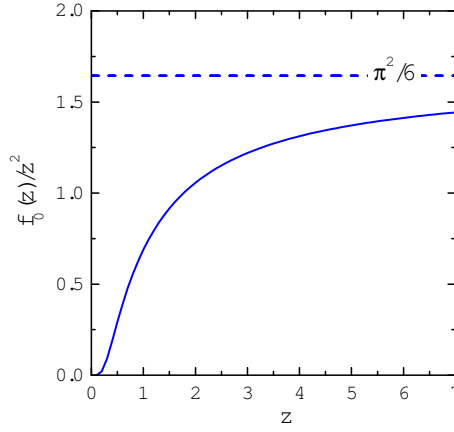


Figure 11: $f_0(z)/z^2$, cf. Eq. (256). Dash line demonstrates asymptotic behavior for $z \gg 1$.

6.2.2 Intensity of multiple scattering

Now we are able to evaluate the intensity of multiple scattering J . Assuming that in the energy-momentum and temperature region of our interest bosons are good quasiparticles we have [41, 45]

$$A_b = 2\pi\delta\left(\omega_b^2 - p_b^2 - m_b^2 - \text{Re}\Sigma_b^R(\omega_b, p_b)\right),$$

and find

$$J = \frac{g^2}{2\pi^2} \int_0^\infty \frac{p_b^2 dp_b}{[m_b^{*2}(T) + \beta_1 p_b^2 + \beta_2 p_b^4]^{1/2}} \frac{1}{\exp\left[(m_b^{*2}(T) + \beta_1 p_b^2 + \beta_2 p_b^4)^{1/2}/T\right] - 1},$$

where we adopted a simple form of the quasiparticle spectrum

$$\omega_b^2(p_b, T) \simeq m_b^{*2}(T) + \beta_1(T)p_b^2 + \beta_2 p_b^4 + \dots \quad (255)$$

Then for not too small positive value β_1 neglecting term β_2 one finds

$$J = \frac{g^2 T^2}{12\beta_1^{3/2}} r_s(z), \quad r_s(z) = \frac{6f_0(z)}{\pi^2 z^2}, \quad z = \frac{T}{m_b^*}. \quad (256)$$

Numerical evaluation of the integral (256) is demonstrated in Fig. 11, cf. [41]. In the limiting case of a high temperature typical values of the boson momenta $\sim T$ and

$$J \simeq \frac{g^2 T^2}{12\beta_1^{3/2}}, \quad \text{for } T \gg m_b^*(T). \quad (257)$$

Let us focus on the temperature region $T \gtrsim m_b^*(T)$, when J is not exponentially suppressed. For fermions in this case the quasiparticle approximation valid for $T^2 \gg 4J$ would work only for weak coupling $g \ll \beta_1^{3/4} \simeq 1$. Since we are interested in description of strongly interacting particles, when $g \gtrsim 1$, we deal with blurred fermions for $T \gtrsim m_b^*(T)$.

The quasiparticle boson density inside the system (compare with Eq. (228)) is given by

$$n_b = \int_0^\infty \frac{4\pi p^2 dp}{(2\pi)^3} \int_0^\infty \frac{d\omega}{2\pi} 2\omega A_b f_b \simeq \int_0^\infty \frac{p^2 dp}{2\pi^2} \frac{1}{e^{\sqrt{m_b^{*2} + \beta_1 p^2}/T} - 1}, \quad (258)$$

and for $T \gg m_b^*$ we find $n_b \simeq T^3 \zeta(3)/(\beta_1^{3/2} \pi^2)$, $\zeta(3) \simeq 1.202$.

6.2.3 Density of fermion-antifermion pairs

Let us continue to study the case of the strong interaction, $g \gtrsim 1$, and assume $m_b^*(T) \lesssim T \ll 5m_f\beta_1^{3/4}/g$, see [41, 45]. Then we can easily check that, on the one hand, conditions of the STL approximation are fulfilled and, on the other hand, fermions can be still treated as non-relativistic particles.

The 3-momentum fermion distribution is as follows

$$f_f^{(\pm)}(p_f) = \int_0^\infty \frac{d\omega_f}{2\pi} A_f^{(\pm)} f_f(\omega_f). \quad (259)$$

Substituting (254) into this expression we find the 3-momentum fermion distribution

$$f_f^{(\pm)}(p_f) = \int_{-2\sqrt{J}}^{2\sqrt{J}} \frac{d\xi}{\pi} \frac{\sqrt{4J - \xi^2}}{2J} \frac{1}{\exp[(\xi + \omega_p^f)/T] + 1}, \quad (260)$$

where the variable $\xi = \omega_f - \omega_p^f$ and $|\xi| < 2\sqrt{J} \ll m_f$. Doing further replacement $\xi = -2\sqrt{J} + Ty$ and using that $m_f \gg T$, we obtain

$$f_f^{(\pm)}(p_f) \simeq \frac{T^{3/2}}{\pi J^{3/4}} I\left(\frac{4\sqrt{J}}{T}\right) \exp\left[-\frac{\omega_p^f - 2\sqrt{J}}{T}\right] = F(T) f_{\text{Bol}}^{(\pm)}(p_f), \quad (261)$$

where $f_{\text{Bol}}^{(\pm)}(p_f) = e^{-\omega_p^f/T}$,

$$F(T) = \frac{T^{3/2}}{\pi J^{3/4}} I\left(\frac{4\sqrt{J}}{T}\right) \exp\left[\frac{2\sqrt{J}}{T}\right], \quad I(x) = \int_0^x dy e^{-y} \sqrt{y - y^2 x^{-1}}, \quad x = 4\sqrt{J}/T,$$

$I(x) \simeq \frac{\sqrt{\pi}}{2} (1 - \frac{3}{4x})$, for $x \gg 1$. As we have mentioned, for $g \gtrsim 1$ the condition of the validity of the quasiparticle approximation for fermions, $x \simeq 4\sqrt{J}/T \ll 1$, is not fulfilled at temperatures of our interest here.

For $z \gtrsim 1$, and $x \gg 1$ (i.e. for $g \gg 1$), we find

$$F(T) \simeq \frac{2^{1/2} 3^{3/4} \beta_1^{9/8}}{\pi^{1/2} g^{3/2} r_s^{3/4}} \exp\left[\frac{g r_s^{1/2}}{3^{1/2} \beta_1^{3/4}}\right]. \quad (262)$$

Integrating (261) in momenta we obtain the fermion (antifermion) density:

$$n_f^{(\pm)} \simeq F(T) n_{\text{Bol}}^{(\pm)}, \quad n_{\text{Bol}}^{(\pm)} \simeq N_f \left(\frac{m_f T}{2\pi}\right)^{3/2} \exp\left[-\frac{m_f}{T}\right], \quad N_f = 2. \quad (263)$$

We see that with growing parameter $\sqrt{J_s}/T$, i.e. with growing temperature, the density of fermion-antifermion pairs increases significantly compared to the standard Boltzmann value.

The result (261) can be interpreted with the help of the relevant quantity

$$m_f^*(T) = m_f - 2\sqrt{J}, \quad 2\sqrt{J} \ll m_f, \quad (264)$$

which has the meaning of *the effective fermion (antifermion) mass*. However, contrary to the usually introduced effective mass, the quantity (264) enters only the exponent in (261). We see that $m_f^*(T)$ decreases with increase of the intensity of the multiple scattering J , i.e., with growth of the temperature.

Typical (fermion blurring) temperature, when effective fermion mass decreases significantly, $\sqrt{J} \sim m_f$, is as follows

$$T \sim T_{\text{bl}} \sim \beta_1^{3/4} (T_{\text{bl}}) g^{-1} m_f r_s^{-1/2} (T_{\text{bl}}). \quad (265)$$

For $T \gtrsim T_{\text{bl}}$ the non-relativistic approximation for fermions, that we used, fails. However exponential increase of the density of fermion-antifermion pairs, that we have demonstrated, starts already for $T \ll T_{\text{bl}}$, in the region of validity of the non-relativistic approximation. Generalization to the relativistic case can be found in [41]. For $g \gg 1$ and $\beta_1 \simeq 1$ we obtain

$$T_{\text{bl}} \sim m_{\text{f}}/g \ll m_{\text{f}}. \quad (266)$$

Thus already for comparatively low temperatures the fermion vacuum becomes blurred due to strong interaction between light boson and heavy fermion sub-systems.

6.2.4 Boson quasiparticles

With the help of expression (253) we are able to calculate the boson self-energy (245),

$$\begin{aligned} \text{Re}\Sigma_{\text{b}}^R(\omega_{\text{b}}, p_{\text{b}}) &\simeq -2g^2 \text{Tr} \int \frac{d^4 p_{\text{f}}}{(2\pi)^4} [\text{Re}G_{\text{f}}^R(p_{\text{f}} + p_{\text{b}}) + \text{Re}G_{\text{f}}^R(p_{\text{f}} - p_{\text{b}})] \\ &\times \text{Im}G_{\text{f}}^R(p_{\text{f}}) f_{\text{f}}(\omega_{\text{f}}), \end{aligned} \quad (267)$$

$$\begin{aligned} \Gamma_{\text{b}}^R(\omega_{\text{b}}, p_{\text{b}}) &\simeq 4g^2 \text{Tr} \int \frac{d^4 p_{\text{f}}}{(2\pi)^4} \text{Im}G_{\text{f}}^R(p_{\text{f}} + p_{\text{b}}) \text{Im}G_{\text{f}}^R(p_{\text{f}}) \\ &\times [f_{\text{f}}(\omega_{\text{f}}) - f_{\text{f}}(\omega_{\text{f}} + \omega_{\text{b}})]. \end{aligned} \quad (268)$$

In the limit $x \gg 1$ (i.e., $g \gg 1$):

$$\text{Re}\Sigma_{\text{b}}^R(\omega_{\text{b}}, p_{\text{b}}) \simeq -\frac{4g^2 n_{\text{f}}^{(\pm)}}{\sqrt{J}} + \alpha(\omega_{\text{b}}^2 - \frac{1}{2}p_{\text{b}}^2), \quad \alpha = \frac{4g^2 n_{\text{f}}^{(\pm)}}{Jm_{\text{f}}}, \quad (269)$$

$$\Gamma_{\text{b}}^R/\text{Re}\Sigma_{\text{b}}^R = O(T^2/J) \quad (270)$$

and thereby $\beta_1 \simeq 1 + \alpha/2$ and at $T \sim T_{\text{bl}}$ we estimate $\beta_1 \simeq 1 + (m_{\text{b}}^2/m_{\text{f}}^2)$. Using (269) we recover the effective boson mass

$$m_{\text{b}}^{*2} \simeq m_{\text{b}}^2 - \frac{4g^2 n_{\text{f}}^{(\pm)}}{\sqrt{J}}. \quad (271)$$

The contribution $\propto \alpha$ has extra smallness for $m_{\text{f}} \gg m_{\text{b}}$ and dependence on it can be neglected.

We see that for temperatures $T < T_{\text{bl}}$ one has $|\text{Im}\Sigma_{\text{b}}^R/\text{Re}\Sigma_{\text{b}}^R| \ll 1$. Thus, at these temperatures bosons can be treated within the quasiparticle approximation. Although the value $\text{Re}\Sigma_{\text{b}}^R$ is exponentially small, we do not set $m_{\text{b}}^* = m_{\text{b}}$ and $\beta_1 \simeq 1$ because the boson corrections to some thermodynamic quantities, e.g., pressure, can be larger than the corresponding fermion contributions, cf. [45]. Moreover, following Ref. [41], which treated fermions in relativistic terms, at a somewhat higher temperature, $T > T_{\text{bl}}$, the value $-\text{Re}\Sigma_{\text{b}}^R$ sharply increases and the effective boson mass substantially decreases.

It proves to be that in thermodynamical quantities some interaction boson and fermion terms compensate each other. The resulting total pressure, energy density and the entropy are given by [45],

$$P_{\text{tot}} \simeq \frac{\pi^2 T^4}{90} - \frac{m_{\text{b}}^2 T^2}{24} + 2T n_{\text{f}}^{(\pm)}, \quad (272)$$

$$E_{\text{tot}} \simeq \frac{\pi^2 T^4}{30} - \frac{m_{\text{b}}^2 T^2}{24} + 2m_{\text{f}} n_{\text{f}}^{(\pm)}, \quad (273)$$

$$TS_{\text{tot}} = E_{\text{tot}} + P_{\text{tot}} \simeq \frac{2\pi^2 T^4}{45} - \frac{m_{\text{b}}^2 T^2}{12} + 2m_{\text{f}} n_{\text{f}}^{(\pm)}. \quad (274)$$

Finally we have arrived at the following picture. A hot system of strongly interacting ($g \gg 1$) light bosons and heavy fermions with zero chemical potentials at temperatures $T_{\text{bl}} > T \gtrsim m_b^*(T)$ represents a gas mixture of boson quasiparticles and blurred fermions. Blurred heavy fermions undergo rapid ($p_f \sim \sqrt{m_f T} \gg p_b \sim T$) Brownian motion in the boson quasiparticle gas. The density of blurred fermions is dramatically increased at $T \sim T_{\text{bl}}$ compared to the standard Boltzmann value. Thermodynamical quantities are such as for the quasi-ideal gas mixture of quasi-free fermion blurs and quasi-free bosons. Note however that the fermion distributions and the energy, pressure and entropy of the fermion blurs are much higher (by factor $F(T)$) than the corresponding quantities for the ideal Boltzmann gas.

6.2.5 Hot Bose condensation

For $T \gtrsim T_{\text{bl}}$ typical fermion momenta $\sqrt{2m_f T}$ continue to remain much smaller than the mass m_f . However non-relativistic approximation for fermions, that was for simplicity used above, fails since typical deviation of the fermion energy from the mass-shell becomes comparable with m_f . Nevertheless let us extrapolate our results to higher temperatures. From (271) we see that at $\sqrt{J}(T_{\text{HB}}) = 4g^2 n_f^{(\pm)}/m_b^2$ the squared effective boson mass reaches zero and it may become negative for $T > T_{\text{HB}}$. In Ref. [41] the phenomenon was dubbed the *hot Bose condensation*, since the condensate appears for the temperature larger than a critical temperature. As the consequence of the strong boson-fermion-antifermion interaction, the number of fermion degrees of freedom is dramatically increased that, on the other hand, results in the increase of the boson abundance. Bosons feel a lack of the phase space for energies and momenta $\sim T$ and a part of them is forced to occupy the coherent condensate state, thereby.

In Ref. [41] in relativistic framework it was found that the value T_{HB} lies in the vicinity of the value T_{bl} . Saturation of the condensate field arises for $T > T_{\text{HB}}$ due to the repulsive boson-boson interaction $L_{\text{int}} = -\Lambda\phi^4/4$ (with the coupling $\Lambda > 0$) as it happens in case of the pion condensation in dense nuclear matter. Further details see in [41, 45].

So, one could expect an anomalous enhancement of the boson (e.g. pion and kaon) production at low momenta ($p_b \lesssim T$) and an anomalous behavior of fluctuations, e.g. at LHC conditions, as a signature of the hot Bose condensation for $T > T_{\text{HB}}$, if a similar phenomenon occurred in a realistic problem including all relevant particle species.

6.3 Pseudo-vector boson – fermion coupling

6.3.1 Hot pion-nucleon vacuum. Nucleon blurring

Let us now consider light pseudo-scalar boson – spin $\frac{1}{2}$ heavy fermion system interacting via the pseudo-vector coupling (198). Let us further speak about π^+ , π^- , π^0 and nucleons and antinucleons. To easier demonstrate the key ideas we continue to consider fermions in non-relativistic approximation. For relativistic generalization see [41]. Due to the p-wave nature of the interaction, cf. (198), (200), one may employ in Eq. (255) the bare pion mass m_π instead of m_π^* , but $\beta_1 \neq 1$. Moreover, the quantity $\beta_1(T)$ decreases with increasing temperature and at $T > T_{1,\text{HB}}$ it can be that $\beta_1 < 0$. In the region of sufficiently small β_1 and of $\beta_1 < 0$ one should keep in (255) the higher order terms, at least the $\beta_2 k^4$ term. Eqs. (252), (253) continue to hold but now with the intensity of the multiple scattering J given by

$$J = 6f_{\pi NN}^2 \int \frac{\vec{q}^2 d^3 q d\omega}{(2\pi)^4} A_\pi n_\pi(\omega). \quad (275)$$

Assuming for a while that $\beta_1 > 0$ and not too small, in the limit case $T \gg m_\pi$ one finds

$$J(T \gg m_\pi) = J_{\text{lim}} = \frac{\pi^2 f_{\pi NN}^2 T^4}{10\beta_1^{5/2}(T)}. \quad (276)$$

This limiting expression works well already for $T \gtrsim m_\pi$, since numerical calculation shows that $J(T = m_\pi) \simeq 0.8J_{\text{lim}}$ and $J(T = 1.5m_\pi) \simeq 0.89J_{\text{lim}}$.

The temperature of the blurring of the fermion continuum evaluated within the non-relativistic approximation for fermions ($T_{\text{bl}}^{\text{n.r.}}$) follows from the relation $J = m_f^2/4$ (for $\mu_f = 0$), from where using (276) at the condition $\beta_1 > 0$ we estimate,

$$T_{\text{bl}}^{\text{n.r.}} = \frac{5^{1/4}(m_N)^{1/2}\beta_1^{5/8}(T_{\text{bl}}^{\text{n.r.}})}{2^{1/4}\pi^{1/2}f_{\pi NN}^{1/2}}. \quad (277)$$

Taking into account relativistic interactions results in a decrease of the value T_{bl} by the factor $1/(3 - \beta_1)^{1/4}$. Then for $\beta_1 = 1$ Ref. [41] estimated $T_{\text{bl}} \simeq 215$ MeV and for $\beta_1 = 0.5$, $T_{\text{bl}} \simeq 132$ MeV. Also, estimates [41] show that $n_{N\bar{N}}$ reaches $2n_{N\bar{N},\text{Bol}}$ already for $T \simeq 0.8m_\pi$.

With the expression similar to (267), but now for pseudovector coupling, we are able to recover the quantity entering the boson spectrum (255),

$$\beta_1(T) = 1 - \frac{4f_{\pi NN}^2 n_{N\bar{N}}}{\sqrt{J}}, \quad n_{N\bar{N}} \simeq \frac{m_N^{3/2} T^3 e^{-m_N^*/T}}{2^{3/2}\pi^2 J^{3/4}}, \quad (278)$$

where $m_N^* = m_N - 2\sqrt{J}$. For $\omega \ll T$ Ref. [41] found $\text{Im}\Sigma_b^R \simeq -\beta(k)\omega$, where the quantity

$$\beta(k) = \frac{4f_{\pi NN}^2 n_{N\bar{N}} k^2}{\pi^{1/2} J^{3/4} T^{1/2}}, \quad \text{for } 4\sqrt{J} \gg T, \quad (279)$$

controls the low-energy part of the spectrum (255). Note that in these estimates in the boson self-energy for $\beta_1 > 0$ we retained the term $\propto k^2$ and dropped terms of the higher order $\propto k^4$.

For temperatures $T > T_{1,\text{HB}}$ the value $\beta_1(T)$ may become negative. In refs [97, 98, 6, 96, 7] in the problem of the pion behavior in the dense and cold or warm matter the value of the density $n_c^{(1)}$, when there appears minimum in $\tilde{\omega}^2(k_0)$ at $k_0 \neq 0$, was called the critical density for the occurrence of the *liquid/amorphous phase of the pion condensation*. This phase exists till $n < n_c^\pi$. Here, for $T_{\text{HB}} > T > T_{1,\text{HB}}$ we may have a similar phenomenon [41]. There is no yet a long-ranged order in this temperature interval. However there arise many virtual boson excitations carrying finite momentum $|\vec{k}_0|$. Actual values of particle momenta are near a fixed value $|\vec{k}_0| \neq 0$, but directions of the momenta are randomly distributed.

At T close to T_{HB} at low ω , the boson spectrum gets a non-quasiparticle nature. The dispersion relation is then given by

$$i\beta(k)\omega \simeq \omega_0^2 + \beta_0(k - k_0)^2, \quad k_0 \neq 0, \omega_0^2, \beta, \beta_0 > 0, \quad (280)$$

where $\omega_0^2 = \tilde{\omega}^2(k_0) = m_\pi^2 + \text{Re}\Sigma_\pi^R(\omega = 0, k = k_0) \simeq m_\pi^2 - \beta_1^2/(4\beta_2)$. The value

$$k_0 \simeq \sqrt{-\beta_1/(2\beta_2)} \quad (281)$$

corresponds to the minimum of $\tilde{\omega}^2(k)$, $\beta_0 \simeq -2\beta_1 > 0$. The form of the spectrum (280) coincides with that we used above in the description of the pion behavior in the dense baryon matter. The boson spectral function has the form

$$A_\pi \simeq \frac{2\beta\omega}{[\omega_0^2 + \beta_0(k - k_0)^2]^2 + \beta^2\omega^2}. \quad (282)$$

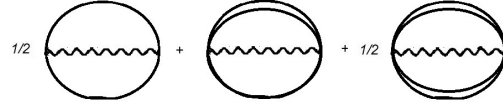
Replacing (282) in Eq. (275) and using for simplicity the limit $\beta T \gg \omega_0^2$, $\beta \equiv \beta(k_0)$, we calculate

$$J \simeq \frac{3f_{\pi NN}^2 k_0^4 T}{2\pi\sqrt{\beta_0}\omega_0}. \quad (283)$$

Thus we found an anomalous increase of the intensity of the multiple scattering for $\omega_0 \ll m_\pi$, i.e. the critical opalescence, as the precursor of the first order phase transition to the state of the hot Bose condensation. In difference with the case of the scalar bosons, here owing to a strong p-wave pion-nucleon attraction the phase transition may occur to the crystalline-like or liquid crystalline-like state similar to the case of the pion condensation in dense baryon matter studied in Section 5.

6.3.2 $\Delta\bar{\Delta}$ resonance matter

As we have mentioned, the Δ isobars play important role in nuclear interactions. With inclusion of the Δ -isobars the first diagram (242) should be replaced by



$$(284)$$

The number of $\Delta\bar{\Delta}$ pairs is estimated as

$$n_{\Delta\bar{\Delta}} \simeq 32 \int_0^\infty \frac{d\omega}{2\pi} \int \frac{d^3p}{(2\pi)^3} A_\Delta e^{-p_0/T} \simeq \frac{16J}{9\omega_\Delta^2} n_{N\bar{N}}, \quad (285)$$

where $\omega_\Delta = m_\Delta - m_N$, $A_\Delta = -2\Im G_\Delta^R$. Thus we estimate $n_{\Delta\bar{\Delta}}/n_{N\bar{N}} \gtrsim 1$ in the vicinity of the temperature $T = T_{bl}$. Strange/antistrange baryons also contribute on equal footing with nucleons/antinucleons and Δ and $\bar{\Delta}$. Thus the hot vacuum (system at $\mu_N = 0$) proves to be a matter consisting of blurred resonances.

6.3.3 Towards the description of the state of hot hadron porridge

We discussed simplified models, like the case of spin $\frac{1}{2}$ fermions (e.g., N , or N and Δ) and their antiparticles coupled with the scalar boson (σ), or with the pion. This is, of course, oversimplification. In reality nucleons couple with all mesons: σ , π , ω , ρ , K , etc. Also, higher lying baryon resonances, like Δ -isobar, $N^*(1440)$, hyperons, etc., interact with the nucleons, with each other and with mesons. Moreover, mesons interact with each other. Reference [41] dubbed such a state the *hot hadron porridge*, bearing in mind that the quasiparticle approximation fails and that for $T \gtrsim m_\pi$ the continuum is likely blurred for all relevant hadrons.

In realistic situation, also quark-gluon degrees of freedom are excited for $T \gtrsim m_\pi$. In a sense we deal with a quark-hadron duality, when similar effects follow both from the quark-gluon and the hadron descriptions. The role of quark-gluon fluctuations rises with increase of the temperature. More likely, the system comes to a strongly correlated hot hadron-quark-gluon mixed state, representing a hot hadron-quark-gluon porridge. Taking into account multiple scattering effects, the number of hadron degrees of freedom is significantly enhanced simulating at least partially the same effects, as those from deconfined quarks. It is not easy to perform calculations of such a system avoiding the double counting problems. Deconfinement, in a standard meaning, as the purely quark-gluon state without hadrons is likely not realized.

7 Non-pionic excitations in Fermi liquids and possible condensation of scalar quanta

7.1 Particle-hole amplitude and Landau-Migdal parameters

Let us consider the simplest case of a one-component Fermi liquid of non-relativistic fermions. Simplifying, we assume that the system is stable against pairing. References [70, 71] studied low-lying scalar excitation modes (density-density fluctuations) in cold normal Fermi liquids for various values and momentum behavior of the scalar Landau parameter f_0 in the particle-hole channel. In some density interval an interaction in the particle-particle channel is repulsive, $f_0(n) > 0$, and the system is, therefore, stable against pairing in the s-wave state. An induced p-wave pairing possible at the repulsion, cf. Ref. [335, 336, 337], can be precluded by the assumption that the temperature of the system is small but higher than the critical temperature for the pairing, $T_{c,p}^{\text{rep}}$.

The particle-hole scattering amplitude on the Fermi surface obeys the equation, cf. [18, 22, 23, 92, 70] and Eq. (203) above,

$$\begin{aligned} \hat{T}_{\text{ph}}(\vec{n}', \vec{n}; q) &= \hat{\Gamma}^\omega(\vec{n}', \vec{n}) \\ &+ \langle \hat{\Gamma}^\omega(\vec{n}', \vec{n}'') \mathcal{L}_{\text{ph}}(\vec{n}'', q) \hat{T}_{\text{ph}}(\vec{n}'', \vec{n}; q) \rangle_{\vec{n}''}, \end{aligned} \quad (286)$$

where \vec{n} and \vec{n}' are the directions of the fermion momenta before and after scattering and $q = (\omega, \vec{k})$ is the momentum transferred in the particle-hole channel. The brackets denote averaging over the momentum direction \vec{n} ,

$$\langle \dots \rangle_{\vec{n}} = \int \frac{d\Omega_{\vec{n}}}{4\pi} (\dots), \quad (287)$$

and the particle-hole propagator is

$$\mathcal{L}_{\text{ph}}(\vec{n}; q) = \int_{-\infty}^{+\infty} \frac{d\epsilon}{2\pi i} \int_0^{+\infty} \frac{dp p^2}{\pi^2} G_{\text{f}}(p_{\text{f}+}) G_{\text{f}}(p_{\text{f}-}), \quad (288)$$

where $p_{\text{f}\pm} = (\epsilon \pm \omega/2, p_{\text{F}} \vec{n} \pm \vec{k}/2)$ and p_{F} is the Fermi momentum. The quasiparticle contribution to the full Green function is given by

$$G_{\text{f}}(\epsilon, \vec{p}) = \frac{Z_{\text{qp}}^{\text{f}}}{\epsilon - \xi_{\vec{p}} + i0 \text{sign}\epsilon}, \quad \xi_{\vec{p}} = \frac{p^2 - p_{\text{F}}^2}{2m_{\text{f}}^*}. \quad (289)$$

Here m_{f}^* is the effective fermion mass, and the value Z_{qp}^{f} determines a quasiparticle weight in the fermion spectral density, $0 < Z_{\text{qp}}^{\text{f}} \leq 1$, which is expressed through the retarded fermion self-energy $\Sigma_{\text{f}}^R(\epsilon, p)$ as

$$Z_{\text{qp},\text{f}}^{-1} = 1 - (\partial \Re \Sigma_{\text{f}}^R / \partial \epsilon)_0.$$

The full Green function contains also a regular background part $G_{\text{f}}^{\text{reg}}$, which is encoded in the renormalized particle-hole interaction $\hat{\Gamma}^\omega$ in Eq. (286). The particle-hole (p-h) scattering amplitude on the Fermi surface is determined by the infinite series of p-h diagrams dressing the local interaction separated in scalar and spin channels as (205). We neglect the spin-orbit interaction, which is suppressed for small transferred momenta $k \ll p_{\text{F}}$.

On the Fermi surface $\Gamma_{0,1}$ are functions of the angle θ between momenta of incoming and outgoing fermions. Amplitudes $\Gamma_{0,1}^\omega$ (F and G in (205)) are expanded in Legendre polynomials, e.g.,

$$Z_{\text{qp},\text{f}}^2 N \Gamma_0^\omega(\theta) = f(\theta) = \sum_l (2l+1) f_l P_l(\cos \theta).$$

A similar expression exists in the spin channel. Here $N = \nu m_f^* p_F / \pi^2$ is the density of states at the Fermi surface. The Fermi momentum p_F is related to the total fermion density as $n = \nu p_F^3 / (3\pi^2)$ with $\nu = 1$ for one type of fermions and $\nu = 2$ for two types of fermions, like for the isospin-symmetric nuclear matter. Let us notice that here we use the normalization N different from C_0^{-1} employed in (205).

The Landau parameters f_l, g_l can be calculated or fitted from experiments. For instance, the scalar parameter f_0 is related to the incompressibility of the system

$$K = n d^2 E_f / dn^2 = (1 + f_0) p_F^2 / 3m_f^*,$$

where E_f is the energy density of the fermion system. Similarly, the square of the first-sound velocity is expressed as

$$u^2 = \frac{\partial P}{\partial \rho} = \frac{p_F^2}{3m_f m_f^*} (1 + f_0), \quad (290)$$

$P = n dE_f / dn - E_f$ is the pressure, ρ is the mass density. The positiveness of the incompressibility and of the first-sound velocity squared are assured by fulfillment of the Pomeranchuk stability condition $f_0 > -1$.

Solution of Eq. (286) is

$$\begin{aligned} \hat{T}_{\text{ph}}(\vec{n}', \vec{n}; q) &= T_{\text{ph},0}(q) \sigma'_0 \sigma_0 + T_{\text{ph},1}(q) (\vec{\sigma}' \vec{\sigma}), \\ T_{\text{ph},0(1)}(q) &= \frac{1}{1/\Gamma_{0(1)}^\omega - \langle \mathcal{L}_{\text{ph}}(\vec{n}; q) \rangle_{\vec{n}}}. \end{aligned} \quad (291)$$

The averaged particle-hole propagator is

$$\langle \mathcal{L}_{\text{ph}}(\vec{n}; q) \rangle_{\vec{n}} = -Z_{\text{qp},f}^2 N \Phi\left(\frac{\omega}{v_F k}, \frac{k}{p_F}, T\right), \quad (292)$$

where for $T \rightarrow 0$ the Lindhard function is

$$\Phi(\omega, k) = \frac{1}{2} + \sum_{i=\pm} (-i) \frac{z_i^2 - 1}{4(z_+ - z_-)} \ln \frac{z_i + 1}{z_i - 1}, \quad (293)$$

$z_\pm = \frac{\omega}{kv_F} \pm \frac{k}{2p_F}$, ω, k are the energy and momentum transferred in the particle-hole channel, $v_F = p_F / m_f^*$ is the Fermi velocity, cf. Eqs. (213), (214), (215).

7.2 Scalar excitations and condensation

7.2.1 Spectrum of scalar excitations

Solution of equation

$$f_0^{-1} = -\Phi(\omega, \vec{k}) \quad (294)$$

gives the spectrum of excitations in the scalar channel $\omega(k)$. A similar equation exists in the g -channel (with replacement $f_0 \rightarrow g_0$). Analytical properties of the solutions have been studied in [338, 339, 340].

Expanding the retarded particle-hole amplitude $T_{\text{ph},0}^R(q)$ near the spectrum branch [70],

$$T_{\text{ph},0}^R(q) \approx \frac{2\omega(k)V^2(k)}{(\omega + i0)^2 - \omega^2(k)}, \quad V^{-2}(k) = Z_{\text{qp},f}^2 N \frac{\partial \Phi}{\partial \omega} \Big|_{\omega(k)}, \quad (295)$$

we identify the quantity

$$D^R(\omega, k) = [(\omega + i0)^2 - \omega^2(k)]^{-1} \quad (296)$$

with the near-pole expansion of the retarded propagator of a *scalar boson* with the dispersion relation $\omega = \omega(k)$ and the quantity $V(k)$, as the effective vertex of the fermion-boson interaction. This scalar boson can be associated with a field operator $\hat{\phi}$ in the second quantization scheme.

For the repulsive interaction, $f_0(n) > 0$, there exists a real (zero sound) solution of this equation,

$$\omega = k v_F s(k/p_F), \quad s(k/p_F) \approx s_0 + s_2(k/p_F)^2, \quad k/p_F \ll 1, \quad (297)$$

where $s(x)$ is a function of $x = k/p_F$, which can be taken in the form $s(x) \approx s_0 + s_2 x^2 + s_4 x^4$, $s_0 > 1$, see [70]. The odd powers of x are absent, since $\Re\Phi$ is an even function of x . The zero-sound mode exists as a quasi-particle mode for frequencies much larger than the inversed fermion collision time, i.e. $\omega \gg \tau_{\text{col}}^{-1} \sim T^2/\epsilon_F$, ϵ_F is the Fermi energy, T is the temperature. In the opposite limiting case, $\omega \ll T^2/\epsilon_F$, the solution describes a hydrodynamic (first) sound. For $k > k_{\text{lim}}$, $k_{\text{lim}} \lesssim p_F$, for $s_2 < 1/(16(s_0 - 1))$ the spectrum branch enters the region with $\Im\Phi > 0$, and the zero sound becomes damped. For $s_2 > 1/(16(s_0 - 1))$ the dissipation appears as result of the decay of the quantum to two quanta of smaller momenta, see [70].

Above we assumed that f depends only on $\vec{n}\vec{n}'$. The results are, however, also valid, if the Landau parameter f is a very smooth function of x^2 , e.g., for

$$f_0(x) \approx f_{00} + f_{02}x^2, \quad (298)$$

where the parameter f_{02} is determined by the effective range of the fermion-fermion scattering amplitude and expansion is valid provided $|f_{00}| \gg |f_{02}|$ for relevant values $k/p_F < 1$. According to Ref. [341], in the case of atomic nuclei ($n \simeq n_0$), $f_{02} = -f_{00}r_{\text{eff}}^2 p_F^2/2$, and $0.5 \lesssim r_{\text{eff}} \lesssim 1\text{fm}$, as follows from the comparison with the Skyrme parametrization of the nucleon-nucleon interaction and with the experimental data. In the point $k = k_0$ corresponding to the minimum of $\omega(k)/k$ the group velocity of the excitation $v_{\text{gr}} = d\omega/dk$ coincides with the phase one $v_{\text{ph}} = \omega/k$. The quantity $\omega(k_0)/k_0$ coincides with the value of the Landau critical velocity u_L for the production of Bose excitations in the superfluid moving with the velocity $W > u_L$.

For isospin-symmetric nuclear matter $f_{00} > 0$ for $n > n_0$, $f_{00} < 0$ for lower densities, and in a certain density interval below n_0 one has $f_{00} < -1$, cf. Refs. [93, 64, 286, 342, 343, 285]. In the purely neutron matter one has $-1 < f_{00} < 0$ for $n \lesssim n_0$, cf. [344].

Let us assume $f_{02} = 0$. For $-1 < f_{00} < 0$, Eq. (293) has only damped solutions. In the density region where $f_0 < 0$ Eq. (293) has purely imaginary solution

$$\omega(k) \approx i(2kv_F/\pi) \left[z_f - k^2/12p_F^2 \right], \quad z_f = 1 - 1/|f_0|, \quad (299)$$

which is valid for $1 - |f_{00}| \ll 1$ and $k \ll p_F$.

For $f_0 < -1$, $z_f > 0$ and in some interval of momenta $\Im\omega(k) > 0$. The mode becomes exponentially growing (Pomeranchuk instability). The function $-i\omega(k)$ has a maximum at $k_m = 2p_F\sqrt{z_f}$ equal to

$$-i\omega_m = (8/3\pi)v_F p_F z_f^{3/2}. \quad (300)$$

For $T \neq 0$ corrections to these results are as follows: $1 + O(T^2/\epsilon_F^2)$. Usually this instability is treated as a spinodal instability resulting in the creation of aerosol-like mixture of droplets and bubbles. Reference [70] suggested a new alternative that at certain conditions the Pomeranchuk instability may lead to formation of a static Bose condensate of a scalar field.

The first-sound velocity squared follows from (290) after the replacement $f_0 \rightarrow f_{00}$. For $f_{00} < -1$, as the incompressibility, the first sound velocity $u^2 \propto 1 + f_{00}$ is negative. Thus, in the region $f_{00}(n) < -1$ the hydrodynamical first sound mode with the frequency $\omega = uk$ for $k \rightarrow 0$ proves to be unstable. Note once more that the first sound exists in the hydrodynamical (collisional) regime, i.e. for $\omega \ll \tau_{\text{col}}^{-1} \propto T^2$,

which is the opposite limit to the collision-less regime of the zero sound, i.e. $\omega \gg \tau_{\text{col}}^{-1}$. For the equation of state with the isotherms, $P_T(1/n)$, having a van der Waals form, the incompressibility and the square of the first-sound velocity prove to be negative in the spinodal region. After a while the system is separated, as a result of the spinodal instability, in a part, being in the vapor phase with the density n_V , and another part, being in the liquid phase with the density n_L . The corresponding chemical potentials at constant temperature and pressure are equal in the equilibrium state, $\mu_V = \mu_L$, forming the Maxwell line in the $P(1/n)$ dependence, see Fig. 3. The relative fraction of the vapor phase χ ($0 < \chi < 1$) is determined by the averaged density $\bar{n} = n_V\chi + n_L(1 - \chi)$. With a decrease of T , isotherms $P_T(n)$ may cross the line $P_T(n) = 0$ in two points for $n > 0$, one corresponds to a local maximum of the Landau free energy density and the other one to a local minimum of it. Collapsing to this minimum, the system becomes bound after a radiation of an energy excess, cf. [64, 65].

In the simplest case of ideal hydrodynamics the growing first-sound mode has the spectrum, cf. [61, 77, 78],

$$-i\omega = k\sqrt{|u_s^2| - ck^2}, \quad (301)$$

where $u = u_s$ is taken at fixed specific entropy, and c is a coefficient related to the surface tension of droplets of one phase in the other one as $\sigma \propto \sqrt{c}$. For a non-zero thermal conductivity the isothermal, $u = u_T$, and adiabatic, $u = u_s$, first-sound velocities are different, and u_T^2 becomes negative at a higher T than u_s^2 , see Ref. [78] and Fig. 4. After the replacement $u_s^2 \rightarrow u_T^2$, Eq. (301) holds also for the case of a large thermal conductivity and small viscosity. In the limit $T \rightarrow 0$ the isothermal and adiabatic first-sound velocities, u_T and u_s , coincide. Maximum of ω with respect to k is

$$-i\omega_m = v_F p_F (|f_{00}| - 1) / (6m_f \sqrt{c}). \quad (302)$$

The growth rate of the spinodal first-sound-like mode decreases with an increase of the surface tension of the droplets, whereas the growth rate of the collision-less zero-sound-like mode does not depend on the surface tension. For

$$\sqrt{c} > \frac{\pi |f_{00}|^{3/2}}{16m_f (|f_{00}| - 1)^{1/2}} \quad (303)$$

the zero-sound-like excitations (300) would grow more rapidly than excitations of the hydrodynamic mode (302). Note that the presence of the viscosity may additionally detain formation of the hydrodynamic modes.

As it has been noted, at first-order phase transitions in multi-component systems with charged constituents, like neutron stars, the resulting stationary state can be a mixed pasta state, where finite size effects (a surface tension and a charge screening) are very important, cf. Refs. [181, 180], contrary to the case of the one-component system, where the stationary state is determined by the Maxwell construction, cf. Ref. [64, 65]. For the isospin-symmetric nuclear matter at fixed temperature T , $T < T_c \simeq (15-20)$ MeV, there exists a spinodal region in the dependence $P(1/n)$ at nucleon densities below the nuclear saturation density, see Ref. [64, 65]. The liquid – vapor phase transition may occur in heavy-ion collisions. The nuclear fireball prepared in the course of a collision has a rather small size, typically less or of the order of the Debye screening length. Nevertheless, may be even in this case some features of the pasta phase could be manifested [8].

7.2.2 Condensation of scalar field

In a fermion system with a contact interaction in scalar channel one can introduce a collective scalar bosonic field by means of the Hubbard–Stratonovich transformation or by the formal replacement of the contact interaction to the exchange by a heavy scalar boson [70, 71]. The effective Lagrangian

density of a static scalar complex condensate field, taken in the simplest form $\phi = \phi_0 e^{-i\omega_c t + i\vec{k}_0 \vec{r}}$, can be presented as follows

$$\mathcal{L}_\phi = -\text{sgn}(f_0)[(\Gamma_0^\omega)^{-1} + Z_{\text{qp},f}^2 N \Phi(\omega_c, k_0)]|\phi_0|^2 - \frac{1}{2}\Lambda(\omega_c, k_0)|\phi_0|^4, \quad (304)$$

where the self-interacting term is determined by the integral of four fermion Green functions evaluated in [345, 346]. Energetically preferable is the state $\omega_c = 0$, cf. [70], then

$$\Lambda(0, k_0) \approx Z_{\text{qp},f}^4 \lambda (1 + k_0^2/2p_F^2) \quad (305)$$

for $k_0 \ll p_F$ with $\lambda = \nu/(\pi^2 v_F^3)$, cf. general Eq. (9) with neglected h term. Variation of the Lagrangian in ϕ_0 yields equation

$$-Z_{\text{qp},f}^2 N \tilde{\omega}^2(k_0) \phi_0 - \Lambda(0, k_0) |\phi_0|^2 \phi_0 = 0.$$

The quantity $\tilde{\omega}^2(k_0) = |f_0(k_0)|^{-1} - \Re \Phi(0, k_0)$ plays now a role of an effective gap in the excitation spectrum. The amplitude of the condensate field $|\phi_0|$ and the Bose condensate energy-density term become

$$|\phi_0|^2 = -\frac{N \tilde{\omega}^2(k_0)}{Z_{\text{qp},f}^2 \lambda} \left(1 + \frac{k_0^2}{2p_F^2}\right)^{-1}, \quad E_b = -\frac{N^2 \tilde{\omega}^4(k_0)}{2\lambda} \left(1 + \frac{k_0^2}{2p_F^2}\right)^{-1}. \quad (306)$$

The inhomogeneous condensation proves to be more energetically favorable compared to the homogeneous one, if

$$f_{02} \leq f_{02}^{\text{cr}} = -f_{00}^2/3 - f_{00}/4, \quad (307)$$

otherwise there appears condensate with $k_0 = 0$, further details see in [70].

In the presence of the condensate the incompressibility becomes, $K = K_f + K_b$, $K_b = n \frac{d^2 E_b}{dn^2}$, and, therefore, the scalar Landau parameter changes to

$$f_0 \rightarrow f_0^{\text{tot}} = f_0 + f_0^b = f_0 + 3m_f^* K_b [f_0^{\text{tot}}]/p_F^2. \quad (308)$$

Here f_0 and f_0^b are functions of k_0 , which should be found from the energy minimization. In case of a weak condensate (for $|f_0 + 1| \ll 1$) one can use $E_b[f_0^{\text{tot}}] \approx E_b[f_0]$. For a developed condensate the perturbative analysis does not work and one should solve Eq. (308) self-consistently.

7.2.3 Possibility of dilute metastable scalar condensate states

The spectrum of excitations on top of the condensate is described by the equation

$$Z_{\text{qp},f}^2 N [-|f_0^{\text{tot}}(k)|^{-1} + \Phi(\omega, k)] - \delta \Sigma_\phi = 0,$$

where $\delta \Sigma_\phi = 2\Lambda(\omega, k) |\phi_0|^2$ includes the interaction of excitations with the condensate. Making use expression for $|\phi_0|$, one presents the spectrum in the form [70, 71]

$$\omega \approx i \frac{2}{\pi} \tilde{\omega}^2(k_0) k v_F$$

for $-1 \ll \tilde{\omega}^2(k_0) < 0$. We see that excitations are damped, i.e., in the presence of the condensate the Fermi liquid becomes free from the Pomeranchuk instability of the zero-sound-like modes.

The particle-hole interaction also changes in the presence of the condensate. There appears a new term in equation for the p-h amplitude, which can be included in the renormalized local interaction as

$$1/f_{\text{ren},0} = 1/f_0^{\text{tot}}(k_0) + 2\tilde{\omega}^2(k_0).$$

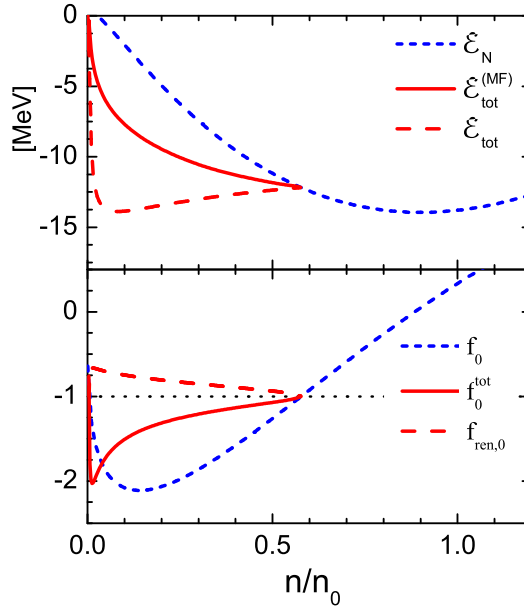


Figure 12: Energy per particle (upper panel) and the scalar Landau parameter (lower panel) as functions of the nucleon density in a piece of isospin-symmetric nuclear matter with and without the condensate. The figure is adopted from [70, 71].

For homogenous condensate with $k_0 = 0$ we have $\tilde{\omega}^2(0) = -z_f = -1 - 1/f_0^{\text{tot}}$ and consequently $f_{\text{ren},0} = -f_0^{\text{tot}}/(2f_0^{\text{tot}} + 1)$. Thus, if originally $f_0 < -1$ and therefore $f_0^{\text{tot}} < -1$, the renormalized interaction yields $-1 < f_{\text{ren},0} < -1/2$. Hence, in the Fermi liquid with the condensate the first-sound modes are stable. Knowing the value $f_{\text{ren},0}$ one can reconstruct the energy density $E_{\text{tot}}(n)$ of the Fermi liquid from the differential equation

$$d^2 E_{\text{tot}}(n)/dn^2 = 2\epsilon_F(1 + f_{\text{ren},0})/(3n), \quad (309)$$

which solution should continuously match the original energy density E_f at the values of the density, where $f_0 = -1$. Note that the energy density includes both mean-field and quadratic-fluctuation contributions. Note also that the results are valid, if on the one hand ϕ_0 is rather small and on the other hand fluctuations on the top of the condensate yield a yet smaller contribution, since the self-interaction of excitations on top of the condensate and feedback of fluctuations on the mean field were disregarded.

Let us demonstrate how the scheme works on example of the isospin-symmetric nuclear matter. References [70, 71] considered a system of 125 nucleons, which energy per particle, $\mathcal{E}_N = E_N/n - m_N$, contains the volume and surface parts. The volume part satisfies standard properties of the nuclear saturation: the density $n_0 = 0.16\text{fm}^{-3}$, the energy per particle $\mathcal{E}_0 = -16\text{MeV}$ and the nuclear incompressibility $9K_f = 285\text{MeV}$. The inclusion of the surface term shifts the saturation density to $0.9n_0$ and the energy per particle to -13.9MeV . Values \mathcal{E}_N and f_0 are shown in Fig. 12 by short-dash lines. We see that $f_0 < -1$ in some density interval. With this f_0 we solve Eq. (308) and obtain f_0^{tot} and $\mathcal{E}_{\text{tot}}^{(\text{MF})} = \mathcal{E}_N + E_b[f_0^{\text{tot}}]/n$ shown by solid lines. Finally, long-dashed lines show the renormalized Landau parameter $f_{\text{ren},0}$ and the corresponding energy per particle $\mathcal{E}_{\text{tot}}(n) = E_{\text{tot}}(n)/n$ with E_{tot} determined by Eq. (309). We see that because of the condensate formation *a new metastable dilute nuclear state* may appear (in our example at density $0.081n_0$ with the binding energy 13.8MeV).

8 Condensation of Bose excitations in nonuniform state in uniformly moving media

8.1 Physical picture and general phenomenological treatment

The spectrum of excitations in the ^4He is schematically shown in Fig. 13 a). During a long time it was thought that the superfluidity is destroyed, if the superfluid moves uniformly with the speed \vec{W} such that $|\vec{W}|$ is larger than the Landau critical velocity $u_L = \min(\omega(k)/k)$ with respect to a wall. The wall singles out the laboratory frame, with respect to which the motion is defined. Equivalently one can consider motion of a massive body with the speed $-\vec{W}$ in the superfluid, cf. [20]. In case of the spectrum shown in Fig. 13 a) the local minimum of the frequency is reached at $k = k_0 \neq 0$. The criterion $W < u_L$ is usually called the necessary condition for the superfluidity. However Pitaevskii [347] demonstrated that in case of the superfluid ^4He moving in the capillary with $W > u_L$ (in a nonrelativistic motion) there may appear additional condensate of excitations with $k = k_0 \neq 0$. In [348] the consideration was generalized for different media including relativistic systems provided the spectrum of excitations has the form shown in Figs. 13 a) or b). Both uniformly moving and rotating bodies were considered. The spectrum of zero-sound excitations in Fermi liquids has the form shown in Fig. 13 b), see discussion in Section 7. Possibility of the condensation of the Bose excitations with $k_0 \neq 0$ in the moving Fermi liquids was considered in [304]. It was shown that Cherenkov-like radiation of strongly interacting excitations may form a Bose condensate with a non-zero wave vector. Explicit results were presented for pions and for various types of zero sounds in moving nuclear matter. Then Ref. [349] studied a possibility of the condensation of excitations with $k_0 \neq 0$ (levons) in cold Bose gases. Condensation of excitations with $k_0 \neq 0$ in moving ^4He and superconductors was studied in [350]. The results might be applicable to the description of various bosonic systems like superfluid ^4He , ultra-cold atomic Bose gases, charged pion and kaon condensates in rotating neutron stars, and various superconducting fermionic systems with the pairing, like proton and color-superconducting components in compact stars, metallic superconductors, and neutral fermionic systems with the pairing, like the neutron component in compact stars and ultracold atomic Fermi gases. The photon Cherenkov radiation and shock waves in supersonic fluxes (e.g., shock wave appearing when an airplane overcomes sound velocity) are related phenomena. However in open systems produced excitations may run away instead of forming of the condensate.

The key idea of the phenomenon is as follows [347, 348]: when a medium moves with a velocity as a whole with respect to a laboratory frame (respectively a wall) with a velocity higher than u_L , it may become energetically favorable to transfer part of its momentum from particles of the moving medium to a Bose condensate of excitations with non-zero momentum $k_0 \neq 0$. This would happen, if the spectrum of excitations is soft in some region of momenta. References [347, 349, 351] studied the condensation of excitations at $T = 0$ assuming the conservation of the flow velocity. Alternatively, [348, 304, 70, 350] considered systems under other conditions, namely assuming conservation of the momentum (or angular momentum for rotating systems), for $T \neq 0$ in [350].

Let a system, having spectrum of Bose excitations of the form shown in Fig. 13 a) or b) moves initially as a whole with the constant velocity $|\vec{W}_{\text{in}}| \ll c$ relatively the flat wall. In absence of the excitations occupying the state $\omega(k_0)$ the density of the kinetic energy of the moving fluid in the reference frame of the wall is $E_{\text{in}}^{\text{kin}} = \rho \vec{W}_{\text{in}}^2/2$, where $\rho = M/V_3$, M is the total mass of the system and V_3 is its volume. Assume that appearance of the condensate of Bose excitations of the form of the running plane wave,

$$\phi' = \phi'_0 e^{-i\omega(\vec{k}_0)t + i\vec{k}_0 \vec{r}}, \quad (310)$$

can be energetically profitable, where ϕ'_0 is a real quantity. Then, after appearance of the condensate of excitations with $k = k_0$ a part of the momentum $\vec{k}_0 \phi'_0{}^2$ belongs to the condensate of excitations. The

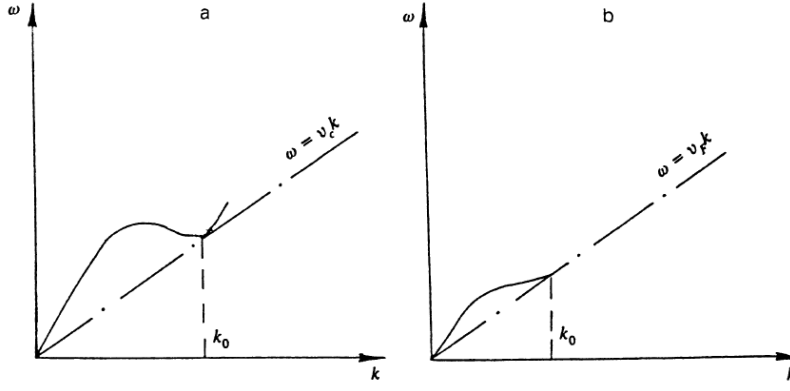


Figure 13: (a) Spectrum of Bose phonon-roton excitations in superfluid helium. (b) Zero sound branch of the spectrum in Fermi liquids.

conservation of the momentum reads as

$$\rho \vec{W}_{\text{in}} = \rho_M \vec{W}_{\text{fin}} + \vec{k}_0 \phi_0'^2, \quad (311)$$

where assuming that the momentum of the condensate is $\vec{k}_0 \phi_0'^2$ we simplifying consideration disregarded the retardation effects.

The kinetic energy of the system after appearance of the condensate of excitations becomes

$$E_{\text{fin}}^{\text{kin}} = \rho \vec{W}_{\text{fin}}^2 / 2 + \omega(k_0) \phi_0'^2 + \Lambda \phi_0'^4 / 2, \quad (312)$$

where the term $\Lambda \phi_0'^4 / 2$ describes self-interaction of the condensate of excitations. Also, simplifying consideration we disregarded interaction of the (“daughter”) condensate of excitations with the “mother” condensate existed already in the resting system. The latter interaction is disregarded in [347, 348, 304, 349] but was then taken into account in [350].

After substitution of \vec{W}_{fin} from (311) to (312) the difference $E_{\text{fin}}^{\text{kin}} - E_{\text{in}}^{\text{kin}}$ renders

$$\delta E^{\text{kin}} = E_{\text{fin}}^{\text{kin}} - E_{\text{in}}^{\text{kin}} = -[\vec{k}_0 \vec{W}_{\text{in}} - \omega(k_0)] \phi_0'^2 + \tilde{\Lambda} \phi_0'^4 / 2, \quad (313)$$

where $\tilde{\Lambda} = \Lambda + k_0^2 / \rho$. It is energetically favorable to take $\vec{k}_0 \parallel \vec{W}$ in order the condensate would decrease the initial velocity of the system. After minimization of (313) in the amplitude of the field ϕ_0' we arrive at the final results

$$\phi_0'^2 = \frac{k_0 (W_{\text{in}} - u_L)}{2 \tilde{\Lambda}} \theta(W_{\text{in}} - u_L), \quad (314)$$

$$\delta E^{\text{kin}} = -\frac{k_0^2 (W_{\text{in}} - u_L)^2}{2 \tilde{\Lambda}} \theta(W_{\text{in}} - u_L). \quad (315)$$

Thus we see that for $W_{\text{in}} > u_L = \omega(k_0) / k_0$ formation of the condensate of excitations with $k = k_0$ becomes energetically profitable. A part of the initial momentum of the system moving as a whole is transported to the inhomogeneous condensate of excitations. As it follows from (311) and (314), in the limit $\tilde{\Lambda} \rightarrow 0$ for arbitrary initial velocity U_{in} (in nonrelativistic system, which was considered) the resulting velocity tends to u_L .

Note that in absence of the wall or in absence of any interaction, due to the Galilean invariance of the moving and resting reference frames excitations are not produced and the condensation cannot occur. In presence of the wall excitations are produced near the walls.

8.2 Condensation of zero-sound-like excitations with a non-zero momentum and frequency in a moving Fermi liquid

8.2.1 Condensation in rectilinearly moving Fermi liquid

Let us apply the constructed scheme to the analysis of a possibility of the condensation of zero-sound-like excitations with a non-zero momentum and frequency in a moving Fermi liquid. As in Refs. [348, 304], we consider a fluid element of the medium with the mass density ρ moving with a non-relativistic constant velocity \vec{W} . The quasiparticle energy $\omega(k)$ in the rest frame of the fluid is determined from the dispersion relation

$$\Re D_\phi^{-1}(\omega, k) = 0. \quad (316)$$

We continue to employ the complex scalar condensate field described by the simplest running-wave probe function, cf. Eq. (310), and the general expression for the Lagrangian density (9), but now for the condensate of excitations, neglecting \hbar term.

The appearance of the condensate with a finite momentum \vec{k}_0 , frequency $\omega = \omega(k_0)$ and an amplitude ϕ_0 leads to a change of the fluid velocity from \vec{W} to \vec{W}_{fin} , as it is required by the momentum conservation

$$\rho \vec{W} = \rho \vec{W}_{\text{fin}} + \vec{k}_0 Z_{\text{qp,b}}^{-1} |\phi_0|^2, \quad (317)$$

where $\vec{k}_0 Z_{\text{qp,b}}^{-1} |\phi_0|^2$ is the density of the momentum of the condensate of the boson quasiparticles with the quasiparticle weight

$$Z_{\text{qp,b}}^{-1}(k_0) = \left[\frac{\partial}{\partial \omega} \Re D_\phi^{-1}(\omega, k) \right]_{\omega(k_0), k_0} > 0, \quad (318)$$

at taking into account the retardation effects. If in the absence of the condensate of excitations the energy density of the liquid element was $E_{\text{in}} = \rho \vec{W}^2/2$, then in the presence of the condensate of excitations, which takes a part of the momentum, the energy density becomes

$$E_{\text{fin}} = \frac{1}{2} \rho W_{\text{fin}}^2 + \omega(k_0) Z_{\text{qp,b}}^{-1} |\phi_0|^2 + \frac{1}{2} \Lambda(\omega(k_0), k_0) |\phi_0|^4. \quad (319)$$

Here the last two terms appear because of the classical field of the condensate of excitations. The gain in the energy density due to the condensation, $\delta E = E_{\text{fin}} - E_{\text{in}}$, is equal to

$$\delta E = -[\vec{W} \vec{k}_0 - \omega(k_0)] Z_{\text{qp,b}}^{-1}(k_0) |\phi_0|^2 + \frac{1}{2} \tilde{\Lambda} |\phi_0|^4, \quad (320)$$

where

$$\tilde{\Lambda} = \Lambda(\omega(k_0), k_0) + (Z_{\text{qp,b}}^{-1}(k_0))^2 k_0^2 / \rho. \quad (321)$$

For $\omega = 0$, $\Lambda(0, k_0)$ is calculated explicitly, cf. Eq. (305). Note that above equations hold also for $\Lambda = 0$.

The condensate of excitations is generated for the velocity of the medium exceeding the Landau critical velocity, $W > u_L = \omega(k_0)/k_0$, where the direction of the condensate vector \vec{k}_0 coincides with the direction of the system velocity, $\vec{k}_0 \parallel \vec{W}$, and the magnitude k_0 is determined by the equation $\omega(k_0)/k_0 = d\omega(k_0)/dk$. The gain in the energy density after the formation of the classical condensate field with the amplitude ϕ_0 and the momentum k_0 is then

$$\delta E = -Z_{\text{qp,b}}^{-1}(k_0) [W k_0 - \omega(k_0)] \phi_0^2 + \frac{1}{2} \tilde{\Lambda} \phi_0^4. \quad (322)$$

The amplitude of the condensate field is found by minimization of the energy. From (322) one gets

$$\phi_0^2 = Z_{\text{qp,b}}^{-1}(k_0) \frac{W k_0 - \omega(k_0)}{\tilde{\Lambda}} \theta(W - u_L). \quad (323)$$

The resulting velocity of the medium becomes

$$W_{\text{fin}} = u_L + \frac{(W - u_L)\theta(W - u_L)}{1 + [Z_{\text{qp,b}}^{-1}(k_0)]^2 k_0^2 / [\Lambda(\omega(k_0), k_0)\rho]}. \quad (324)$$

For a small Λ , we have $W_{\text{fin}} = u_L + O(\Lambda)$.

For the repulsive interaction $f_0 > 0$ there is real zero-sound branch of excitations $\omega_s(k) \approx kv_F(s_0 + s_2 x^2 + s_4 x^4)$, where the parameters s_i depend on the coupling constants f_{00} and f_{02} , cf. Eqs. (298), (297) and [70]. The ratio $\omega_s(k)/(kv_F)$ has a minimum at $k_0 = p_F \sqrt{-s_2/(2s_4)}$ provided f_{02} is smaller than $f_{\text{crit},02} = -f_{00}^2/[12(s_0^2 - 1)^2]$. The Landau critical velocity of the medium is equal to $u_L/v_F = \omega_s(k_0)/(v_F k_0) \approx s_0 - s_2^2/(2s_4)$. The quasiparticle weight of the zero-sound mode (318) is now

$$Z_{\text{qp,b}}^{-1}(k_0) = \frac{Z_{\text{qp,f}}^2 N}{k_0 v_F} \frac{\partial \Phi(s, x)}{\partial s} \Big|_{\frac{\omega_s(k_0)}{v_F k_0}, \frac{k_0}{p_F}}. \quad (325)$$

The amplitude of the condensate field (323) can be written as

$$\phi_0^2 = Z_{\text{qp,b}}^{-1}(k_0) k_0 \frac{W - u_L}{\tilde{\Lambda}} \theta(W - u_L). \quad (326)$$

The energy density gained owing to the condensation of the excitations is

$$\delta E = -k_0^2 (Z_{\text{qp,b}}^{-1}(k_0))^2 \frac{(W - u_L)^2}{2\tilde{\Lambda}} \theta(W - u_L). \quad (327)$$

For a small Λ , Eqs. (326), (327) are simplified as

$$\begin{aligned} \phi_0^2 &= \rho(W - u_L) Z_{\text{qp,b}}(k_0) k_0^{-1} \theta(W - u_L), \\ \delta E &= -\frac{\rho}{2} (W - u_L)^2 \theta(W - u_L). \end{aligned} \quad (328)$$

Finally we note that the Landau parameter $f_0(k_0)$ should be recalculated with taking into account of the condensate in the moving Fermi liquid, except the vicinity of the critical point, where the corrections are small and can be neglected.

The instability condition for the mode with $\vec{W} \vec{k}_0 > \omega(k_0)$, which was found at hand of the energy balance in Eq. (320), can be obtained differently. We may transfer the description in the laboratory frame, shifting variables [304] $\Phi(\omega, k, n) \rightarrow \Phi(\omega - \vec{k} \vec{W}, k, n)$. Then from Eqs. (291), (292) it follows that the imaginary part of Φ changes its sign for $\omega < \vec{k} \vec{W}$. Thus, the instability first arises for modes with $\omega < kW$ at $\vec{k} \parallel \vec{W}$, like in case of the Cherenkov radiation. Excitations with the momentum $k = k_0$ start to populate the spectral branch $\omega(k)$, when the minimum $\omega(k)$ touches the value $\vec{k} \vec{W}$ (the condition of the coincidence of the group and phase velocities).

8.2.2 Condensation in two interpenetrating dilute streams of fermions

Now let us consider two interpenetrating dilute streams of fermions, which are supposed to interact very weakly. This model may have a number of physical applications – as example let us mention a possible manifestation of pion instabilities and Cherenkov-like radiation in peripheral heavy-ion collisions, cf. [304, 352].

Let us consider a peripheral nucleus-nucleus ($A + A$) collision in the reference frame associated with one of the nuclei (the target frame). For a momentum of the excitation k there exists a minimal value of the projectile momentum, p_{lab} , above which the product of two momentum Fermi distributions, $n_F(\vec{p})$, of target and projectile fermions vanishes $n_F(\vec{p}) n_F(\vec{p} + \vec{p}_{\text{lab}} + \vec{k}) = 0$. Then excitations from one Fermi

sphere cannot overlap with the ground state distribution in the other Fermi sphere. This condition is satisfied already for the laboratory energy $E_{\text{lab}} \gtrsim 160 \text{ MeV}/A$. All the results obtained above continue to hold after the replacement

$$f_0(n)\Phi(\omega, k, n) \rightarrow f_0(n/2)[\Phi(\omega, k, n/2) + \Phi(\omega - \vec{k}\vec{W}, k, n/2)].$$

For example, for $\vec{k} \perp \vec{V}$ we have

$$f_0(n)\Phi(\omega, k, n) \rightarrow 2f_0(n/2)\Phi(\omega, k, n/2)$$

and for $\omega = 0$, $k \ll 2p_F$ we arrive at the simple replacement $f_0(n)\Phi(\omega, k, n) \rightarrow 2f_0(n_0/2)$. For a smooth density dependent value f_0 it further reduces to $f_0\Phi(0, k, n) \simeq f_0 \rightarrow 2f_0$. If so, the Pomernanchuk instability would arise already for the values of $f_0(n)$ essentially larger than -1 ; e.g., in the just considered simplified case of a smooth $f_0(n)$ function the instability would occur for $f_0(n) < -1/2$ rather than for $f_0(n) < -1$. The instability could provoke a growth of the scalar condensate field ϕ with $\vec{k}_0 \perp \vec{p}_{\text{lab}}$ in the course of peripheral heavy-ion collisions.

Application of the same model of two interpenetrating beams to the pion modes for $\vec{k} \perp \vec{W}$, cf. [352, 353], leads us to the replacement

$$\Phi(\omega, k, n) \rightarrow 2\Phi(\omega, k, n/2)$$

and for $\omega = 0$, $k \ll 2p_F$ we arrive at the replacement $\Phi(\omega, k, n) \rightarrow 2$ for $\vec{k} \perp \vec{p}_{\text{lab}}$. Since the nucleon particle-hole term of the pion polarization function is $\Re\Sigma^R \propto -p_F(n)k^2$ for $\omega = 0$, $k \ll 2p_F$ and $p_F \propto n^{1/3}$, with the above modification $p_F(n)\Phi \rightarrow 2p_F(n/2)$ we get effectively 4 times larger density and much stronger pion-nucleon attraction compared to the equilibrium case. So, there arises question about a possibility to observe pion condensate with $k_0 \neq 0$ in peripheral heavy-ion collisions.

8.2.3 Vortices

Above we focused our consideration on the cases where either the vortices are absent (as in a narrow capillary [347]) or they leave the system (in open systems), or the presence of vortices supports a common rigid motion of the normal and superfluid components [20] (e.g., as in systems with charged components [354], or in rotating systems, like neutron stars [355]).

In case of He-II moving in a narrow capillary vortices do not appear, see [347, 356]. For a rectilinearly moving superfluids, as well as for the rotating superfluids, there may appear excitations of the type of vortex rings and other structures, cf. [357, 350]. The energy of the vortex ring is estimated, cf. [19, 358], as $\epsilon^{\text{vort}} = 2\pi^2\hbar^2|\psi|^2R m^{*-1}\ln(R/l_0)$, and the momentum is $p^{\text{vort}} = 2\pi^2\hbar|\psi|^2R^2$, where ψ is the complex order parameter, $m^* = 1/(2\alpha_3)$ is the coefficient near the gradient squared term in the Lagrangian density, cf. (14), for nonrelativistic particles m^* has the sense of the effective mass of the particle, R is the radius of the vortex ring and $l_0 \sim 1/\sqrt{|T - T_c|}$ is the coherence length. Thus, $u_{c1} = \epsilon^{\text{vort}}/p^{\text{vort}} = \hbar(R_{\text{tr}}m^*)^{-1}\ln(R_{\text{tr}}/l_0)$ is the Landau critical velocity for the vortex production, where in the absence of impurities R_{tr} is the transverse size of the system. For a system of distributed impurities moving together with the fluid, R_{tr} is a typical distance between the defects. We recovered dependence on \hbar only to remind that vortices have quantum origin. Vortices are pinned to the impurities and move together with them and the superfluid. In an open clean system moving with the velocity $W > u_{c1}$ the vortex rings are pushed to infinity by the Magnus and Iordanskii forces. Note that for spatially extended systems the value u_{c1} proves to be lower than the Landau critical velocity u_L . The flow moving with the velocity W at $W \geq u_{c1}$ can be considered as metastable, since the vortex creation probability is hindered by a large potential barrier, and formation of a vortex takes a long time [359, 360]. The vortex production rate increases, however, strongly when W approaches u_L . For a motion in a pipe

the vortices are captured by the pipe wall, forming after a while a stationary sub-system in the frame of the walls. Periodic solitonic solutions of the Gross-Pitaevskii equation were studied in [361]. This situation might be rather similar to that of a condensate moving in a periodic potential, produced by the spatial variations of the order parameter of the condensate of excitations [349]. Since in the exterior regions of the vortices the superfluidity persists, the consideration of the condensation of excitations for $W > u_L$ remains applicable, cf. [350]. Note that in He-II under a high external pressure the value u_L decreases and at some conditions becomes lower than u_{c1} , see [362], and in the interval $u_L < W < u_{c1}$ there are no vortices. Therefore for $u_L < W < u_{c1}$ the condensate of excitations with $k_0 \neq 0$ is not influenced by the vortices related to the mother condensate, cf. [350].

Above we considered vortices appearing on the ground of the uniform mother condensate (at $k_0 = 0$). If the mother condensate is characterized by the wave vector $\vec{k}_0 \neq 0$, the form of the vortices is different. Instead of vortex filaments there may appear vortex sheets, see [96]. The same relates to the daughter condensate of excitations.

Finally, let us notice that in superconducting systems vortices, if formed, are involved in a common motion with the superconducting sub-system due to the appearance of a tiny London field [354] distributed throughout the medium, that supports the condition $W = 0$. In rotating superfluids vortices appear at rotation frequency $\Omega > \Omega_{c1} = \frac{\hbar}{m^* R^2} \ln(R/l_0)$, where for the spherical system R is the size of the system (transversal size for the cylindrical system), and their number grows with an increase of Ω . When the density of vortices becomes sufficiently large, they form the Abrikosov lattice, cf. [20], forcing, thereby, the superfluid and normal components to move as a rigid body, i.e. with $W \rightarrow 0$.

9 Quantum and finite size effects in nonequilibrium particle distributions

9.1 Bose–Einstein condensation of relativistic bosons at a dynamically fixed particle number

The heavy-ion collision experiments at SPS, RHIC and LHC energies demonstrated that at midrapidity a baryon-poor medium is formed [363, 364, 365, 366, 367] with pion number exceeding the baryon/antibaryon one more than by the order. To describe such a matter authors of the hadron resonance gas model, e.g., cf. Ref. [37] and references therein, assume that hadrons are produced at the hadronization temperature T_{had} after cooling of an expanding quark-gluon fireball. At the temperature of the chemical freeze-out, T_{chem} , all inelastic processes cease and for lower temperatures only elastic processes are possible. In this model the chemical potentials of the conserving baryonic, electric and strangeness charges are fitting parameters. The hadron resonance gas state is assumed to be a mixture of ideal gases of all stable hadrons and resonances. At the sudden break up of the system at the same temperature T_{chem} mesons, e.g. pions, are assumed to be in the ideal pion gas state at the thermal equilibrium at $\mu = 0$. Fitting the ratios of the measured particle yields at collision energies $\sqrt{s_{NN}} > 20$ the authors found values $T \simeq T_{\text{had}} \simeq T_{\text{chem}} \simeq (155 - 160)$ MeV. Sometimes, repulsive interactions are modelled with an “excluded volume” prescription, which is however inherently a low density approach.

Authors of a chemical nonequilibrium approach [38, 39] performed the analysis of top SPS and LHC data on mean particle multiplicities assuming a sudden decay of the quark-gluon medium into hadrons streaming then towards detector without a hadron re-scattering phase, i.e. keeping information on the value $T \simeq T_{\text{had}} \simeq T_{\text{chem}} \simeq T_{\text{kin}}$, where $T = T_{\text{kin}}$ is the temperature of the kinetic (thermal) freeze-out, when the system breaks up. For the best fits the authors used all particle distributions, including those for pions, with non-zero fugacities determined by the values of the quark fugacities. They extracted smaller values $T_{\text{chem}} \simeq (140 - 145)$ MeV than [37] and values of the pion chemical potentials μ_π to be rather close to m_π . Note that following [39] at $T = T_{\text{chem}}$ about 80% of pions are hidden in

hadron resonances producing “secondary pions” at the freeze-out. The later ones contribute to the total number of pions and to the extracted values μ_π together with primary pions from the ideal gas state. The lattice QCD calculations [40] found that the temperature of a hypothetical critical point of a chiral phase transition should not exceed a value of $132 + 3 - 6$ MeV.

We considered the behavior of the baryon-poor equilibrium hot hadronic medium in Section 6, where an important role of strong interaction effects was demonstrated. Strongly interacting baryons prove to be blurred at temperatures $T \sim T_{\text{bl}} \lesssim m_\pi$ and we discussed a possibility of the hot Bose condensation for $T > T_{\text{HB}} > T_{\text{bl}}$. In Section 5.3.2 we demonstrated influence of the in-medium effects on the particle distributions at assumption of the sudden freeze out, further details see in [319, 6, 96, 7, 48].

Spectra of pions produced in experiments at SPS, RHIC and LHC proved to be approximately exponential at intermediate transverse momenta, $2m_\pi \lesssim p_T \lesssim 7m_\pi$, but show a significant enhancement at low transverse momenta $p_T \lesssim m_\pi$. Already first attempts to fit the pion p_T distributions in heavy-ion collisions at 200 AGeV by ideal gas expressions required usage of the pion chemical potential $\mu_\pi \simeq (120 - 130)$ MeV, cf. [368, 369]. Subsequent analyzes of the SPS data [370, 371], employing the method proposed in [372] of extraction of the pion freeze-out density from the mid-rapidity particle densities and the femtoscopic radii, supported statement about significant enhancement of pion distributions at small transverse momenta. Using the results of the first pion femtoscopy experiments, the value of the density of the pion system at the kinetic freeze-out was estimated as $n_\pi \sim (1 - 6)n_0$. Subsequent estimates, cf. [373, 51], yielded values $n_\pi \sim (0.8 - 2.5)n_0$ for the pion production at LHC energies. Analysis [37] extracted the fireball volume $V_3 = 5280 \pm 410 \text{ fm}^{-3}$ that corresponds to the pion density $n_\pi \sim 2.5n_0$.

Estimates [374, 375] showed that at temperatures $T \simeq (130 - 140)$ MeV the rate of the pion absorption becomes smaller than the rate of the re-scattering. During subsequent pion fireball expansion from the chemical freeze-out state, when $T = T_{\text{chem}}$, till a kinetic freeze-out state, at which T reaches the value $T_{\text{kin}} < T_{\text{chem}}$, the total pion number can be considered as approximately fixed, see [374, 375, 376]. Estimates [373, 377, 378, 379] gave the value $T_{\text{kin}} \simeq (100 - 120)$ MeV.

Recently, the ALICE Collaboration observed a significant suppression of three and four pion Bose–Einstein correlations in Pb-Pb collisions at $\sqrt{s_{NN}} = 2.76$ TeV at the LHC [380, 381]. This can be interpreted as there is a considerable degree of coherent pion emission in relativistic heavy-ion collisions [382, 383]. Analysis [384] indicated that about 5% of pions could stem from the Bose–Einstein condensate. Also, a discussion of a possibility of the Bose–Einstein condensation in heavy-ion collisions at LHC energies can be found in the review [385].

As it was mentioned, Section 6.3.1 considered description of the equilibrium strongly interacting pion enriched matter at a rather high temperature. Now we assume that such a matter exists for $T_c > T > T_{\text{chem}}$, where T_c is the pseudo-critical temperature of the deconfinement crossover transition. Now we will focus on the description of the expanding pion fireball in the regime $T_{\text{kin}} < T(t) < T_{\text{chem}}$.

Actually, the problem is a more general. Above we considered various examples of the Bose condensation in equilibrium systems. In ^4He at $T = 0$ all particles are in the condensate state and their number is fixed. At $T \neq 0$ a part of particles is in the condensate and a part is in “normal” excitations. In this case only the total number of the condensate- and over-condensate- particles is fixed. Similar situation occurs for the ordinary metallic superconductors, where at $T \neq 0$ only a part of fermions is paired. The pairs form the Bose condensate with not fixed particle number. In case of the p-wave neutral pion, π^0 , condensation in baryonic matter there appears condensate of virtual particles, the number of neutral relativistic bosons in the equilibrium system is not fixed. The same relates to the $\pi^{\pm,0}$ condensate in the isospin-symmetrical finite-size systems. In these cases there arise static π^0 and $\pi^{\pm,0}$ condensate fields, respectively. In the electrically neutral neutron star matter it is energetically profitable to produce the π^\pm condensate with a net negative electric charge. An excess of the charged π^- condensate particles together with electrons and μ^- muons compensate the positive charge of the protons [96]. These problems have been considered in the given review.

In case of the Bose–Einstein condensation of nonrelativistic bosons in equilibrium matter one deals with fixed averaged number of bosons determined by the value of their chemical potential, cf. [17]. However the Bose–Einstein condensation may also develop in nonequilibrium systems at some conditions. For instance, let a system of Bose particles is rapidly cooled down below the value T_c during the typical time $\tau_{\text{cool}} \ll \tau_{\text{abs}}$, where T_c is the critical temperature of the Bose–Einstein condensation and τ_{abs} is the time characterizing the absorption of bosons. We assume that thermalization occurs in elastic processes at typical time scale $\tau_T \lesssim \tau_{\text{cool}}$. In this case the system on a time scale $t \ll \tau_{\text{abs}}$ is characterized by the dynamically fixed particle number. Such a kind of the Bose–Einstein condensation was studied in [46, 47, 48, 49, 50, 51, 52, 53, 54, 55] and other works on example of pions produced in ultra-relativistic heavy-ion collisions. On the time scale $t \ll \tau_{\text{abs}}$ the dynamical behavior of the pion Bose–Einstein condensate is described by the equations of the two-fluid hydrodynamics similarly to the description of superfluids at $T \neq 0$. Note that descriptions of the hydrodynamical evolution of the Bose–Einstein condensate in approximation of the ideal gas and the self-interacting gas are essentially different, cf. [386, 275]. Both cases were considered in [46]. A number of subsequent works continued to study the Bose–Einstein condensation of the ideal pion gas, e.g., cf. [387, 51]. Behavior of the interacting pion gas was studied in the $\lambda\phi^4$ and the σ models for $\lambda > 0$, cf. [46, 47, 48, 50, 52, 53, 54, 55], and in the model with the Weinberg interaction [49].

The condensate component and the normal component do not interact provided the velocity of the expansion of the pion fireball W is low, $W < u_{c1} \sim [l \ln(R/l_0)]/R$, where R is the typical size of the fireball (transversal size in case of one-dimensional Bjorken flux) and $l_0 \ll R$ is the correlation (coherence) length associated with the pion condensate field, estimated in [48, 50]. For $W > u_{c1}$ the vortex filaments and rings are produced. Reference [46] suggested to seek such a pion soliton-like inhomogeneities in heavy-ion collisions. In presence of rotation in the interval of rotation frequencies $\Omega_{c1} < \Omega < \Omega_{c2}$, $\Omega_{c1} \sim l_0 \ln(R/l_0)/R^2$, $\Omega_{c2} \sim 1/l_0 \sim (10^{21} - 10^{22})\text{Hz}$, there may appear the Abrikosov lattice of vortices. Recall however that although this picture is similar to that occurs in case of superfluids and superconductors, in case of pions there exist dissipative processes and the pion Bose–Einstein condensation may occur only for $t \ll \tau_{\text{abs}}$.

The pion Bose–Einstein condensation in the Hartree approximation was studied in [49, 52, 55]. Pions acquire effective mass $m_\pi^*(T) > m_\pi$. The critical temperature for the self-interacting pion gas, at which $\mu_\pi(T_{\text{BEC}}) = m^*(T_{\text{BEC}})$, is smaller than that would be for the ideal gas. At T_{BEC} there occurs the second-order phase transition. However already for $T = T_{\text{BEC}}^{\text{ind}} > T_{\text{BEC}}$, at which $\mu_\pi(T_{\text{BEC}}^{\text{ind}})$ reaches the free pion mass m_π , there may occur the first-order phase transition to the state of the “induced Bose–Einstein condensation.” A role of inelastic reactions $\pi^0\pi^0 \leftrightarrow \pi^-\pi^+$, which however conserve the net pion number, was also discussed. The Lagrangian of the pion system describing not only elastically interacting pions but also permitting processes $\pi^0\pi^0 \leftrightarrow \pi^-\pi^+$ but not permitting other inelastic reactions was studied in [52, 55].

The kinetics of the Bose–Einstein condensation of photons in totally ionized plasma and shock waves of photons were considered in [388] with the help of the kinetic equation for photons in electron gas derived in [389]. Then kinetics of the Bose–Einstein condensation in nonrelativistic systems was studied in a number of works, cf. [390, 391, 392]. In relativistic systems kinetics of the Bose–Einstein condensation of pions was considered in [48, 50, 54]. Reference [50] employed the Boltzmann equation (previously generalized to deal with high boson occupations $f(p) > 1$), Ref. [48] used framework of the quantum kinetic Kadanoff–Baym equation and Ref. [54] considered the theoretical background provided by the Zubarev formalism of the nonequilibrium statistical operator [393, 394]. Following [50], if the initial state is appropriately overpopulated by pions undergoing predominantly elastic collisions, then the self-interacting pions at low energies, $10^{-2}m^* \lesssim |\omega - m^*| \ll m^*$, enter the region of a nonlinear Kolmogorov turbulence. For nonrelativistic bosons the stationary state can be realized, characterized by the distribution function $f(\epsilon) \propto \epsilon^{-7/6}$ at constant flux of particles to the low energies, where $\epsilon \ll m$ is the nonrelativistic particle energy, cf. [390]. With a time passage, for still lower particle energies a self-

similar solution is formed $f(\epsilon) \propto \epsilon^{-1.24}$, which is then destroyed at the formation of the Bose–Einstein condensate for $t > \tau_{\text{BEC}}$, cf. [391, 392]. A similar picture holds in case of relativistic self-interacting pions forming the pion Bose–Einstein condensate [50]. For $t > \tau_{\text{BEC}}$ the solution of the corresponding Boltzmann equation for the pion distribution should be supported by the solution of additional equation for the condensate field. This problem can be adequately considered, e.g., within Zubarev formalism of the nonequilibrium statistical operator, cf. [54].

The higher is the pion multiplicity the more probable is to observe effects related to the pion Bose–Einstein condensation [46, 50]. The fluctuation effects are increased in the vicinity of the critical point of any phase transition, cf. discussion in Sects. 2.1.2 and 2.4.2. In particular, second-order phase transitions are accompanied by fluctuations of the order parameter observed in various critical opalescence phenomena in equilibrium systems [395]. If the system crosses the spinodal instability border at a first order phase transition, fluctuations begin to grow exponentially, cf. [61, 77, 78, 8] and Section 4.4.

In case of the nonequilibrium matter the normalized variance of the density is expressed in terms of the structure factor [74],

$$S(\vec{q} \rightarrow 0, t, \vec{r}) = (\langle \hat{n}^2 \rangle - n^2)/n = \int_{-\infty}^{\infty} dq_0 [-i\Sigma_{-+}^{00}(q_0, \vec{q} \rightarrow 0, t, \vec{r})]/(2\pi), \quad (329)$$

where $\mu, \nu = 0, 1, 2, 3$, $-i\Sigma_{-+}^{\mu\nu}(q, t, \vec{r})$ is the Wigner transform of the 4-current–4-current auto-correlation function expressed in terms of the nonequilibrium diagram technique [329, 330], $\hat{n}(t, \vec{r})$ is the density operator, the local density is $\langle \hat{n}(t, \vec{r}) \rangle$. In the thermal equilibrium $S(\vec{q} \rightarrow 0) = T/(\partial\mu/\partial n)_T$.

In the ideal gas approximation the normalized variance of the number of produced pions diverges at the critical point of the Bose–Einstein condensation, cf. [387]. In experiments at SPS energies a growth of the normalized variance for the pion number with an increase of the collision energy and the number of produced pions was reported in Ref. [396]. Also an enhancement of the normalized variance with an increase of the pion multiplicity was observed for pp collisions [397, 398] in the energy range (50–70) GeV. However, a care should be taken comparing expectations for the thermal fluctuation characteristics with results of actual measurements, which incorporate background contributions, the dependence on the center-of-mass energy, other dynamical effects, collision centrality, kinematic cuts, etc.

The most simple and still relevant description of fluctuations in a quasi-equilibrium system formed in heavy-ion collisions can be performed employing the grand-canonical ensemble formulation, since usually only a part of the system, typically around mid-rapidity, is considered. Thus energy and conserved quantum numbers may be exchanged with the rest of the system, which serves as a heat bath. Although in the time interval between chemical and kinetic freeze-outs the total number of pions remains fixed, an exchange of particles between pion species continues owing to the $2 \leftrightarrow 2$ reactions. Thus, if pions are measured in experiments with incomplete geometry and/or in a restricted momentum range, then the elastic pion-pion reactions and processes of the type $\pi^0\pi^0 \leftrightarrow \pi^+\pi^-$ change populations of pions of different isospin species and in different momentum bins. Therefore, there exists a kind of thermodynamic reservoir for the sub-system of pions, which reach the detector later, and the grand-canonical formulation can be relevant in such a situation. If one measures correlations between pions emitted at different angles and in various momentum bins, one may get an information about the state of the pion fireball at the kinetic freeze-out. Self-consistent account for a pion-pion interaction in the Hartree approximation demonstrated that variance of the pion number in the system with an equal averaged number of pion species remains finite at the critical temperature [52] as well as the skewness and kurtosis [399]. A suppression of fluctuation effects occurs also due to the finiteness of the system, cf. [387, 55]. Nevertheless, they remain to be enhanced near the critical point of the Bose–Einstein condensation. In [55] it was shown that in the case of the system with equal averaged numbers of isospin species, the variance of the charge, $Q = N_+ - N_-$, diverges at $T \rightarrow T_{\text{BEC}}$, whereas variances of

the total particle number, $N = N_+ - N_-$, and of a relative abundance of charged and neutral pions, $G = (N_+ - N_-)/2N_0$, remain finite in the critical point. Thus, the appearance of a significant increase of particle number fluctuations could be considered as a signal that the pion system formed in heavy-ion collisions is approaching the critical point of the Bose–Einstein condensation. However to avoid a possible misunderstanding let us notice that the cumulants of the net baryon/charge distributions are increased in the vicinity of the critical point in case of other second-order phase transitions. Also recall about the dynamical slowing-down effect for the near-critical fluctuations in the dynamical systems, cf. [268, 77].

9.2 Breaking of potential box filled by particles

Comparison with the data obtained at RHIC and LHC for proton-proton, proton-nucleus, and nucleus-nucleus collisions demonstrates that nucleon and pion distribution functions (for $p_\perp > 1$ GeV) follow the power laws, although at intermediate transverse momenta ($2m_\pi \lesssim p_\perp \lesssim 1$ GeV) these particles follow thermal equilibrium distributions and for $p_\perp \lesssim m_\pi$ the pion distributions are enhanced. The parton model for scattering of point particles yields

$$\frac{d\sigma}{dyd^2p_\perp} \propto p_\perp^{-n} \quad (330)$$

with $n = 4$, as it follows from the dimensional analysis, cf. [400]. However, scale breaking and realistic parton distribution functions in the projectile and target increase n significantly for hadrons, whereas $n \simeq 4.5$ to 5.5 for jets. In [401, 402] these features were attributed to the Tsallis distributions. Let us demonstrate that strongly nonequilibrium particle distributions can be also characterized by power-law high-momentum tails.

Let us discuss a toy quantum mechanical model, when one can easily find nucleon and pion distributions. Assume that nucleons of one species are placed into the box with infinite walls,

$$U = \begin{cases} \infty, & r < R \\ 0, & r > R \end{cases} \quad (331)$$

and occupy stationary states, e.g., with $l = 0, m = 0, n = 1, \dots, N$, where N is the total number of nucleons of fixed spin and species. These distributions essentially differ from the thermal equilibrium distributions. If the nucleon gas is so rare that collisions can be neglected, the initial distributions can be considered as not changed at the time scale of our interest.

9.3 Nucleon distributions

Now let us assume that the walls are suddenly removed. Let us find the nucleon distributions in the momentum space. For this aim we need the nucleon ψ function in the momentum representation

$$\psi_{nlm}(\vec{p}) = \int_0^R \psi_{nlm}(\vec{r}) \psi_{\vec{p}}^*(\vec{r}) r^2 dr d\Omega, \quad (332)$$

where $\psi_{\vec{p}}(\vec{r}) = \exp(i\vec{p}\vec{r})/(2\pi)^{3/2}$ is the eigen function of the $\hat{\vec{p}}$ operator. From Eq. (332) it follows that

$$\int |\psi_{nlm}(\vec{p})|^2 d^3p = \int |\psi_{nlm}(\vec{r})|^2 d^3x, \quad dN/[d^3p/(2\pi)^3] = (2\pi)^3 \sum_{nlm} |\psi_{nlm}(\vec{p})|^2, \quad (333)$$

$\sum_{nlm} 1 = N$, where the sum is taken over the occupied states, i.e. $l = m = 0$ in our case. Replacing

$$\psi_{n00}(\vec{r}) = A_{n0} \frac{\sin(k_n r)}{r} Y_{00}, \quad k_n = \pi n/R, \quad A_{n0} = (2/R)^{1/2}, \quad Y_{00} = 1/(4\pi)^{1/2} \quad (334)$$

in Eq. (332) one obtains

$$\psi_{n00}(\vec{p}) = \frac{(-1)^{(n+1)} R^{1/2} n \sin(pR)}{\pi^2 p (n^2 - \xi^2)}, \quad \xi = pR/\pi. \quad (335)$$

The momentum distribution of the nucleons (of fixed spin) is as follows

$$n_p^N = dN / [V_3 d^3p / (2\pi)^3] = \frac{\sin^2(pR) J}{(pR)^2}, \quad (336)$$

where

$$J = \frac{6}{\pi^2} \sum_{n=1}^N \frac{n^2}{(n^2 - \xi^2)^2}, \quad (337)$$

and V_3 is the volume of the box. In the limit case $\xi \ll 1$, $N \gg 1$, we have

$$n_p^N \simeq \frac{\sin^2(pR)}{(pR)^2} \simeq 1 - \frac{(pR)^2}{3}. \quad (338)$$

Thus, for $pR \ll 1$ we get $n_p^N \simeq 1$. In the limit $\xi \gg N \gg 1$ we obtain an oscillating solution

$$n_p^N \simeq \frac{2\pi^2 N^3 \sin^2(pR)}{(pR)^6}. \quad (339)$$

One can see from (338) and (339) that nucleon distributions behave in this nonequilibrium quantum model quite differently compared to the quasi-equilibrium thermal distribution. Quantum effects are important for $p \lesssim \pi N/R \lesssim N^{2/3} m_\pi$, where the system size is $R \sim N^{1/3}/m_\pi$. Also, Eq. (339) demonstrates a power-law tail at very large momenta $p \gg \pi N/R \sim N^{2/3} m_\pi$, whereas thermal distributions show exponential behaviour $\sim \exp(-\epsilon_p/T)$, cf. [319, 403, 96]. Another peculiarity of the distribution (339) is the presence of oscillations (factor $\sin^2(pR)$).

9.4 Pion distributions

Now with obtained nucleon distributions let us calculate the pion distributions. Supposing that the number of pions is much smaller than the number of nucleons, i.e. $N_\pi \ll N$, we may neglect the back reaction of the light pion sub-system on the heavy nucleon sub-system. The pion distribution yields

$$n_k^{\pi^-} = \frac{-i\Sigma_{\pi^-}^{+-}(t, \omega, \vec{k})}{A_{\pi^-}(t, \omega, \vec{k})} = \frac{\int_{\epsilon_0}^{\infty} d\epsilon_p n_{\epsilon_p+\omega}^N (1 - n_{\epsilon_p}^N)}{\int_{\epsilon_0}^{\infty} d\epsilon_p (n_{\epsilon_p}^N - n_{\epsilon_p+\omega}^N)}, \quad (340)$$

where $\Sigma_{\pi^-}^{+-}$ is the π^- self-energy expressed in terms of the nonequilibrium diagram technique, cf. [326], and we assumed that the pion self-energy is determined by the diagram (245). With the help of Eq. (339) we get

$$A_\pi = -2\Im\Sigma_\pi^R \simeq \frac{\alpha N^3 \pi^2}{4m_N^3 R^6} \left(\frac{1}{\epsilon_0^2} - \frac{1}{(\epsilon_0 + \omega)^2} \right), \quad (341)$$

and

$$-i\Sigma_\pi^{+-} \simeq \frac{\alpha N^3 \pi^2}{4m_N^3 R^6} \frac{1}{(\epsilon_0 + \omega)^2}, \quad (342)$$

with $\alpha = -f_{\pi NN}^2 q^2 m_N^{*2} / \pi k$, and

$$\epsilon_0 \simeq (\omega + q^2/2m_N^*)^2 m_N^* / 2k^2. \quad (343)$$

The condition $\xi \gg N$ is satisfied, if $\epsilon_0 \gg N^2 \pi^2 / m_N R^2$. Thus we obtain

$$n_k^{\pi^-}(t, \omega, k) \simeq \frac{\epsilon_0^2(\omega)}{2\epsilon_0(\omega)\omega + \omega^2} \quad (344)$$

for the virtual pion distribution characterized by disconnected values ω, k . Setting $\omega = \omega_k$ we find π^- distribution at infinity,

$$n_k^{\pi^-}(\text{free}) \simeq \frac{\epsilon_0^2(\omega_k)}{2\epsilon_0(\omega_k)\omega_k + \omega_k^2}, \quad \omega_k = (m_\pi^2 + k^2)^{1/2}. \quad (345)$$

Both Eqs. (344) and (345) are quite different from the thermal equilibrium distributions (229), (230), (258). Instead of exponentially suppressed thermal distributions we obtained enhanced pion distributions.

From Eq. (345) we see a pronounced enhancement of the pion distribution at small momenta,

$$n_k^{\pi^-}(\text{free}) \rightarrow m_\pi m_N^* / 4k^2, \quad (346)$$

for $k \rightarrow 0$, whereas for thermal distribution one would rather have $n_k^{\pi^-}(\text{free}) \rightarrow \text{const}$ for $k \rightarrow 0$. Introducing the value $T_c m_N / 8 \simeq 0.8 m_\pi$, we present Eq. (346) in the form $n_k^{\pi^-}(\text{free}) = 2m_\pi T_c / k^2$. Such a behaviour is typical for the thermal Bose distribution at small momenta characterized by the pion chemical potential $\mu_\pi = m_\pi$ and the temperature T_c , corresponding to the critical point of the Bose–Einstein condensation. Please note that enhancement of the soft pion production is required in order to describe experimental pion differential cross sections in a broad interval of heavy-ion collision energies, from GSI to LHC energies, cf. [50, 52, 55].

For the momenta ($m_N \gg k \gg m_\pi$) we have $n_k^{\pi^-}(\text{free}) \simeq (m_N^*)^2 / 4k^2$, whereas in ultrarelativistic limit ($k \gg m_N$) we get $n_k^{\pi^-}(\text{free}) \simeq (m_N^*)^4 / 4k^4$ and the pion number (N^{π^-}) is converged. Thus we see that the pion momentum distribution is characterized by three different slopes at $k \lesssim m_\pi$, $m_N \gtrsim k \gg m_\pi$ and $k \gg m_N$. Inclusion of the Δ isobars into consideration can be done with the help of the replacement $\omega \rightarrow \pm\omega - \omega_\Delta$. It does not bring about new peculiarities to the problem.

10 Conclusion

Description of the phase diagram of the strongly interacting matter with possible phase transitions between various phases is the great challenge for the researchers during many years. In nuclear physics microscopic description of the transition from the quark-gluon degrees of freedom to the hadron ones is absent due to absence of the solution of the confinement problem. In spite of intensive experimental studies of nonequilibrium nuclear matter have been performed on accelerators new and more trick measurements are required. A hope to get new exciting results is connected with commissioning of the NICA and FAIR facilities in the nearest future and with astrophysical studies. In this situation it is reasonable to employ methods borrowed from the condensed matter physics with its much wider experimental facilities.

Phenomenological methods like the Ginzburg–Landau theory are widely used together with various semi-phenomenological and microscopic descriptions, such as the theory of finite Fermi systems, chiral perturbation theory, etc. Methods for description of inhomogeneous phases and phase transitions in nuclear systems to the states characterized by the non-zero wave vectors are less developed. Dynamics of the phase transitions and the structure formation are still less studied.

This manuscript deals with a broad range of problems associated with phase transitions in various systems characterized by the strong interaction between particles and with formation of structures, focusing on hadron systems. In Section 2 we started with a general phenomenological mean-field

model constructed for the description of phase transitions of the first and the second order to the homogeneous, $k_0 = 0$, and inhomogeneous, $\vec{k}_0 \neq 0$, states, the latter transition may occur even in case, when the interaction is translation-invariant. First we studied the phase transitions within the mean-field approximation and then focus was made on the role of long-range fluctuations of the order parameter. These fluctuations are especially strong in case of the phase transition to the state $\vec{k}_0 \neq 0$ due to their large phase-space volume. Their inclusion results in that the phase transition to the state $\vec{k}_0 \neq 0$ necessarily becomes the transition of the first order. Especially strong are fluctuations at $T \neq 0$.

Various specific features of the phase transitions to the state $\vec{k}_0 \neq 0$ are then considered such as the anisotropic spectrum of excitations, a possibility of formation of various structures including running and standing waves, three-axis structures, the chiral waves, pasta states, etc. The Higgs effect is specific for $\vec{k}_0 \neq 0$ due to the anisotropy. The Goldstone mode remains even in case of the charged running wave condensate. In case of the pasta mixed phase attention is focused on the charge screening effects resulting in that the hadron–quark and kaon condensate equations of state are closer to those described by the Maxwell construction than by the homogeneous Gibbs conditions. Next, a formal transition to hydrodynamical variables is performed. Derived equation for the phase of the order parameter is formally similar to Navier-Stokes equation of non-ideal hydrodynamics. Such an analogy can be helpful, since one may use well developed methods of hydrodynamics.

In Section 3 focus is made on description of the dynamics of the order parameter at the phase transitions to the states with $\vec{k}_0 = 0$ and $\vec{k}_0 \neq 0$. In case of the first-order phase transition, seeds of the form of slabs of any size of the stable phase inside the metastable one grow to the stable state, whereas rods and droplets of under-critical size are melt and overcritical seeds grow. In case of the phase transition from homogeneous state to the inhomogeneous state the seeds of some specific strongly non-spherical form may grow to the new phase at any their initial size, similar to the slabs. In case of the phase transition from the inhomogeneous state to the inhomogeneous state the dynamics has specific features. For example, initially spherical seeds change their form during the time evolution. Also, we discussed specificity of the transitions between homogeneous and inhomogeneous phases.

In Section 4 the non-ideal hydrodynamical description of the phase transitions of the liquid–vapor type was studied. In nuclear physics the phase transition of the liquid–gas type occurs in heavy-ion collision reactions with isospin-symmetric nuclei at very low collision energies ($\lesssim 100$ GeV/A). Following [61, 77, 78, 80, 81] it was also conjectured that the hadron–quark phase transition might be of the liquid–gas type. It was argued that the ordinary Ginzburg–Landau model is not applicable for description of an initial inertial stage of the seeds. Dynamics is determined by the inertial/viscous parameter β proportional to the surface tension and inversely proportional to the viscosity. Stages of the nuclear rain and fog were discussed. Then we focused on the dynamics of seeds in the spinodal region. At this stage quasi-periodic structures are developed, see Fig. 8. Crucial role played by the transport coefficients was emphasized. Linear and nonlinear dynamical stages were considered as for transitions to the homogeneous liquid state as to inhomogeneous state. Effect of the cooling of the system, aging of materials and sticking of domains were discussed.

The specific example of the pion condensation phase transition to the $\vec{k}_0 \neq 0$ state in dense, cold and warm nuclear matter was considered in Section 5. First, the Fermi-liquid description of the nuclear systems with explicit separation of the soft pion mode was performed according [95, 96]. Then we focused on peculiarities of the π condensate phase transition. Actually, due to strong fluctuations of the pion field with $k_0 \neq 0$, cf. [129, 97, 98, 132, 133], already for $n > n_c^{(1)} \simeq (0.5 - 0.8)n_0$ there appears, so called liquid or amorphous phase of the pion condensate, cf. [132, 6, 7]. For $n > n_c > n_c^{(1)}$ by the first-order phase transition there appears the p-wave pion condensate with the liquid-crystalline-like or solid-like structure. We focused on the discussion of the fluctuations with $k_0 \neq 0$ at $T \neq 0$ and their contribution to thermodynamical quantities and observable pion distributions. The pion mass-width effect is very essential, since it drives the phase transition. Following [265] we considered dynamics of the pion condensate transition.

Then in Section 6 the high temperature – small baryon chemical potential system was studied, when baryons become completely blurred in the sense that their Green function loses information about the quasiparticle pole due to multiple re-scatterings on virtual boson impurities. In dynamics this is similar to the Landau-Pomeranchuk-Migdal effect. For $T > T_{\text{bl}}$, with $T_{\text{bl}} \lesssim m_\pi$, the number of nucleon-antinucleon pairs increases appreciably compared to the standard Boltzmann result. Light bosons, e.g., pions, may condense either in $\vec{k}_0 = 0$ or $\vec{k}_0 \neq 0$ states. This phenomenon can be called the hot Bose condensation, since it may occur for $T > T_{\text{HB}}$ slightly exceeding the value T_{bl} . Number of bosons is significantly increased due to the increase of the number of nucleon-antinucleon pairs for $T \sim T_{\text{bl}}$ contributing to the nucleon-antinucleon loops. Then we focused on the example of the pion-nucleon sub-system, then included Δ degrees of freedom and demonstrated that probably Δ contribute even stronger than nucleons. We argued that at $T \sim m_\pi$ one may speak about the state of a hot hadron porridge, when many hadron species contribute on equal footing. The resulting state is rather dense and hot, so quarks and gluons may also contribute significantly.

In Section 7 the phenomena of the Pomeranchuk instability and the condensation of the scalar collective modes were studied. The latter phenomenon may result in appearance of a metastable nuclear state in dilute nuclear matter, as was conjectured in [70].

In Section 8 we considered condensation of the Bose collective excitations in the $\vec{k}_0 \neq 0$ state in rectilinearly moving media with the speed larger than the critical Landau velocity. The condensation of scalar quanta and the pion condensation with $\vec{k}_0 \neq 0$ in peripheral heavy ion collisions can be considered as one of possible observable effects, cf. [352].

In Section 9 we started with a possibility of the Bose-Einstein condensation of bosons characterized by the dynamically fixed particle number, i.e., when inelastic processes can be neglected at the typical time of the evolution of the system. The consideration was then applied to the description of the pion production in heavy-ion collisions at ultrarelativistic energies. Then, on the example of the sudden break up of the box filled by nucleons we discussed a specificity of the purely nonequilibrium effects in production of nucleons and pions and oscillations in the nucleon distributions.

Finally note that the structure formations at the rotation and in magnetic fields, α Bose condensation, as well as many other relevant problems, were not considered in the given review. These problems should be discussed elsewhere.

Acknowledgments. Fruitful discussions with E. E. Kolomeitsev are acknowledged.

References

- [1] E. V. Shuryak, Quantum Chromodynamics and the Theory of Superdense Matter, Phys. Rept. **61**, 71 (1980).
- [2] E. Shuryak, What RHIC experiments and theory tell us about properties of quark–gluon plasma? Nucl. Phys. A **750**, 64 (2005).
- [3] P. Romatschke and U. Romatschke, Viscosity information from relativistic nuclear collisions: How perfect is the fluid observed at RHIC?, Phys. Rev. Lett. **99**, 172301 (2007).
- [4] F. Karsch, K. Redlich and A. Tawfik, Thermodynamics at non-zero baryon number density: a comparison of lattice and hadron resonance gas model calculations, Phys. Lett. B **571**, 67 (2003).
- [5] W. Reisdorf et al. [FOPI Collaboration], Systematics of pion emission in heavy ion collisions in the 1 A- GeV regime, Nucl. Phys. A **781**, 459 (2007).
- [6] D. N. Voskresensky, Thermodynamic model of nucleus-nucleus collision process, Sov. J. Nucl. Phys. **50**, 983 (1989).

- [7] D. N. Voskresensky, Many particle effects in nucleus-nucleus collisions, Nucl. Phys. A **555**, 293 (1993).
- [8] K. A. Maslov and D. N. Voskresensky, RMF models with σ -scaled hadron masses and couplings for the description of heavy-ion collisions below 2 A GeV, Eur. Phys. J. A **55**, 100 (2019).
- [9] T. Klähn, D. Blaschke, S. Typel, E. N. E. van Dalen, A. Fässler, C. Fuchs, T. Gaitanos, H. Grigorian, A. Ho and E. E. Kolomeitsev, *et al*, Constraints on the high-density nuclear equation of state from the phenomenology of compact stars and heavy-ion collisions, Phys. Rev. C **74**, 035802 (2006).
- [10] N. K. Glendenning, *Compact stars: Nuclear physics, particle physics and general relativity* (Springer-Verlag New York, 2000).
- [11] E. Witten, Cosmic separation of phases, Phys. Rev. D **30**, 272 (1984).
- [12] A. De Rujula and S. L. Glashow, Nuclearites – a novel form of cosmic radiation, Lett. to Nature (London) **312**, 734 (1984).
- [13] S. Bogdanov, A. J. Dittmann, W. C. G. Ho, F. K. Lamb, S. Mahmoodifar, M. C. Miller, S. M. Morsink, T. E. Riley, T. E. Strohmayer and A. L. Watts, *et al*. Constraining the Neutron Star Mass-Radius Relation and Dense Matter Equation of State with NICER. III. Model Description and Verification of Parameter Estimation Codes, Astrophys. J. Lett. **914**, L15 (2021).
- [14] S. Blacker, N. U. F. Bastian, A. Bauswein, D. B. Blaschke, T. Fischer, M. Oertel, T. Soultanis and S. Typel, Constraining the onset density of the hadron-quark phase transition with gravitational-wave observations, Phys. Rev. D **102**, 123023 (2020).
- [15] P. Senger, Exploring terra incognita in the phase diagram of strongly interacting matter–experiments at FAIR and NICA, Phys. Scripta **97**, 6, (2022).
- [16] P. W. Anderson, *Basic Notions of Condensed Matter Physics*, (Westview Press, 1997).
- [17] L. D. Landau and E. M. Lifshitz, *Statistical Physics*, Vol. 5 (Butterworth-Heinemann, 3rd ed. 1980).
- [18] E. M. Lifshitz and L. P. Pitaevskii, *Statistical Physics, Part 2* (Pergamon, 1980).
- [19] V. L Ginzburg and A. A. Sobyenin, Superfluidity of helium II near the λ point, Sov. Phys. Usp. **19**. 773 (1976).
- [20] D. R. Tilley and J. Tilley, *Superfluidity and Superconductivity* (IoP Publishing, Bristol, 1990).
- [21] A. J. Leggett, *Quantum liquids, Bose condensation and Cooper pairing in condensed matter systems*, (Oxford Univ. Press, 2006).
- [22] D. Pines and Ph. Nozieres, *The Theory of Quantum Liquids* (W.A. Benjamin, New York, 1966).
- [23] G. Baym and Ch. Pethick, *Landau Fermi-liquid Theory* (Wiley-VCH, Weinheim, 2nd. Edition, 2004).
- [24] L. Pitaevskii and S. Stringari, *Bose-Einstein condensation and superfluidity*, (Oxford Univ. Press, 2016).
- [25] S. Chandrasekhar, *Liquid crystals*, (Cambridge Univ. Press 1992).

- [26] D. N. Voskresensky, Vector-boson condensates, spin-triplet superfluidity of paired neutral and charged fermions, and $3P_2$ pairing of nucleons, Phys. Rev. D **101**, 056011 (2020).
- [27] K. von Klitzing, G. Dorda and M. Pepper, Phys. Rev. Lett. **45**, 494 (1980).
- [28] M. Z. Hasan and C. L. Kane, Colloquium: Topological insulators, Rev. Mod. Phys. **82**, 3045 (2010).
- [29] D. N. Voskresensky, To the question about superconductivity of the pionic condensate, Sov. J. Nucl. Phys. **32**, 629 (1980).
- [30] C. S. Fischer, QCD at finite temperature and chemical potential from Dyson-Schwinger equations, Prog. Part. Nucl. Phys. **105**, 1 (2019).
- [31] O. Philipsen, Lattice constraints on the QCD chiral phase transition at finite temperature and baryon density, Symmetry **13**, 2079 (2021).
- [32] J. N. Guenther, An overview of the QCD phase diagram at finite T and μ , 38th Intern. Symposium on Lattice Field Theory (2022), PoS LATTICE, 2021, 013 (2022).
- [33] L. Ya. Glozman, O. Philipsen and R. D. Pisarski, Chiral spin symmetry and the QCD phase diagram, arXiv: 2204.05083.
- [34] P. Senger, Studies of dense nuclear matter at NICA, NUPECC Long Range Plan 2017, [arXiv: 2005.13856 [nucl-ex]].
- [35] C. S. Fischer and J. A. Mueller, Chiral and deconfinement transition from Dyson-Schwinger equations, Phys. Rev. D **80**, 074029 (2009).
- [36] C. S. Fischer, J. L  cker and J. A. M  ller, Chiral and deconfinement phase transitions of two-flavour QCD at finite temperature and chemical potential, Phys. Lett. B **702**, 438 (2011).
- [37] A. Andronic, P. Braun-Munzinger, K. Redlich and J. Stachel, Decoding the phase structure of QCD via particle production at high energy, Nature **561**, 321 (2018).
- [38] J. Letessier and J. Rafelski, Hadron production and phase changes in relativistic heavy-ion collisions, Eur. Phys. J. A **35**, 221 (2008).
- [39] M. Petran, J. Letessier, V. Petracek and J. Rafelski, Hadron production and quark-gluon plasma hadronization in Pb-Pb collisions at $\sqrt{s_{NN}} = 2.76$ TeV, Phys. Rev. C **88**, 034907 (2013).
- [40] H. T. Ding, P. Hegde, O. Kaczmarek, F. Karsch, A. Lahiri, S. T. Li, S. Mukherjee, H. Ohno, P. Petreczky, C. Schmidt and P. Steinbrecher (HotQCD Collaboration), Chiral phase transition temperature in (2+1)-flavor QCD, Phys. Rev. Lett. **123**, 062002 (2019).
- [41] D. N. Voskresensky, Hadron liquid with a small baryon chemical potential at finite temperature, Nucl. Phys. A **744**, 378 (2004).
- [42] C. Rohrhofer, Y. Aoki, G. Cossu, H. Fukaya, C. Gatttringer, L. Y. Glozman, S. Hashimoto, C. B. Lang and S. Prelovsek, Symmetries of spatial meson correlators in high temperature QCD, Phys. Rev. D **100**, 014502 (2019).
- [43] C. Rohrhofer, Y. Aoki, L. Y. Glozman, and S. Hashimoto, Phys. Lett. B **802**, 135245 (2020).
- [44] A. M. Dyugaev, Properties of a hot hadron vacuum, JETP Lett. **58**, 886 (1993).

- [45] D. N. Voskresensky, Thermodynamics of resonances and blurred particles, Nucl. Phys. A **812**, 158 (2008).
- [46] D. N. Voskresensky, On the possibility of Bose condensation of pions in ultrarelativistic collisions of nuclei, JETP **78**, 793 (1994).
- [47] E. E. Kolomeitsev and D. N. Voskresensky, Bose-Einstein condensation of pions in ultrarelativistic nucleus-nucleus collisions and spectra of kaons, Phys. Atom. Nucl. **58**, 2082 (1995).
- [48] D. N. Voskresensky, D. Blaschke, G. Röpke and H. Schulz, Nonequilibrium approach to dense hadronic matter,” Int. J. Mod. Phys. E **4**, 1 (1995).
- [49] E. E. Kolomeitsev, B. Kämpfer and D. N. Voskresensky, Hot and dense pion gas with finite chemical potential, Acta Phys. Polonica B **27**, 3263 (1996).
- [50] D. N. Voskresensky, Kinetic description of a pion gas in ultrarelativistic collisions of nuclei: turbulence and Bose condensation, Phys. Atom. Nucl. **59**, 2015 (1996).
- [51] V. Begun, W. Florkowski and M. Rybczynski, Explanation of hadron transverse-momentum spectra in heavy-ion collisions at $\sqrt{s_{NN}} = 2.76$ TeV within a chemical nonequilibrium statistical hadronization model, Phys. Rev. C **90**, 014906 (2014).
- [52] E. E. Kolomeitsev and D.N. Voskresensky, Fluctuations in non-ideal pion gas with dynamically fixed particle number, Nucl. Phys. A **973**, 89 (2018).
- [53] E. Nazarova, Ł. Juchnowski, D. Blaschke and T. Fischer, Low-momentum pion enhancement from schematic hadronization of a gluon-saturated initial state, Particles **2**, 140 (2019).
- [54] D. Blaschke, G. Röpke, D. N. Voskresensky and V. G. Morozov, Nonequilibrium pion distribution within the Zubarev approach, Particles **3**, 380 (2020).
- [55] E. E. Kolomeitsev, D. N. Voskresensky and M. E. Borisov, Charge and isospin fluctuations in a non-ideal pion gas with dynamically fixed particle number, Eur. Phys. J. A **57**, 145 (2021).
- [56] J. P. Blaizot, F. Gelis, J.F. Liao, L. McLerran and R. Venugopalan, Bose–Einstein condensation and thermalization of the quark–gluon plasma, Nucl. Phys. A **873**, 68 (2012).
- [57] Z. Xu, K. Zhou, P. Zhuang and C. Greiner, Thermalization of gluons with Bose-Einstein condensation, Phys. Rev. Lett. **114**, 182301 (2015).
- [58] S. Tsutsui, J. P. Blaizot and Y. Hatta, Thermalization of overpopulated systems in the 2PI formalism, Phys. Rev. D **96**, 036004 (2017).
- [59] R. Lenkiewicz, A. Meistrenko, H. van Hees, Kai Zhou, Zhe Xu and C. Greiner, Kinetic approach to a relativistic BEC with inelastic processes, Phys. Rev. D **100**, 091501(R) (2019).
- [60] B. Harrison and A. Peshier, Bose-Einstein Condensation from the QCD Boltzmann Equation, Particles, **2**, 231 (2019).
- [61] V. V. Skokov and D. N. Voskresensky, Hydrodynamical description of a hadron-quark first-order phase transition, JETP Lett. **90**, 223 (2009), arXiv: 0811.3868.
- [62] G. Röpke, L. Münchow and H. Schulz, On the phase stability of hot nuclear matter and the applicability of detailed balance equations, Phys. Lett. B **110**, 21 (1982).

- [63] G. Röpke, L. Münchow and H. Schulz, Particle clustering and Mott transitions in nuclear matter at finite temperature: (i) method and general aspects, Nucl. Phys. A **379**, 536 (1982).
- [64] H. Schulz, D.N. Voskresensky and J. Bondorf, Dynamical aspects of the liquid-vapor phase transition in nuclear systems, Phys. Lett. B **133**, 141 (1983).
- [65] P. Chomaz, M. Colonna and J. Randrup, Nuclear spinodal fragmentation, Phys. Rept. **389**, 263 (2004).
- [66] J. Margueron and P. Chomaz, A unique spinodal region in asymmetric nuclear matter, Phys. Rev. C **67**, 041602 (2003).
- [67] C. Ducoin, P. Chomaz and F. Gulminelli, Role of isospin in the nuclear liquid–gas phase transition, Nucl. Phys. A **771**, 68 (2006).
- [68] A. R. Raduta and F. Gulminelli, Isospin dependent thermodynamics of fragmentation, Phys. Rev. C **75**, 044605 (2007).
- [69] INDRA Collaboration (B. Borderie et al.), Phase transition dynamics for hot nuclei, Phys. Lett. B **782**, 291 (2018).
- [70] E. E. Kolomeitsev and D. N. Voskresensky, Scalar quanta in Fermi liquids: zero sounds, instabilities, Bose condensation, and a metastable state in dilute nuclear matter, Eur. Phys. J. A **52**, 362 (2016).
- [71] E. E. Kolomeitsev and D. N. Voskresensky, Zero-sound condensate in a Fermi liquid, Phys. Part. Nucl. **48**, 897 (2017).
- [72] G. Röpke, N. U. Bastian, D. Blaschke, T. Klahn, S. Typel and H. H. Wolter, Cluster virial expansion for nuclear matter within a quasiparticle statistical approach, Nucl. Phys. A **897**, 70 (2013).
- [73] G. Röpke, D. Blaschke, Y. B. Ivanov, I. Karpenko, O. V. Rogachevsky and H. H. Wolter, Medium effects on freeze-out of light clusters at NICA energies, Phys. Part. Nucl. Lett. **15**, 225 (2018).
- [74] G. Röpke, D. N. Voskresensky, I. A. Kryukov and D. Blaschke, Fermi liquid, clustering, and structure factor in dilute warm nuclear matter, Nuclear Phys. A **970**, 224 (2018).
- [75] Xin-Hui Wu, Si-Bo Wang, A. Sedrakian and G. Röpke, Composition of nuclear matter with light clusters and Bose–Einstein condensation of α Particles, Journ. of Low Temperature Phys. **189**, 133 (2017).
- [76] K. Fukushima and T. Hatsuda, The phase diagram of dense QCD, Rept. Prog. Phys. **74**, 014001 (2011).
- [77] V. V. Skokov and D. N. Voskresensky, Hydrodynamical description of first-order phase transitions: Analytical treatment and numerical modeling, Nucl. Phys. A **828**, 401 (2009).
- [78] V. V. Skokov and D. N. Voskresensky, Thermal conductivity in dynamics of first-order phase transition, Nucl. Phys. A **847**, 253 (2010).
- [79] D. N. Voskresensky and V. V. Skokov, Viscosity and thermal conductivity effects at first-order phase transitions in heavy-ion collisions, Phys. Atom. Nucl. **75**, 770 (2012).
- [80] J. Steinheimer and J. Randrup, Spinodal density enhancements in simulations of relativistic nuclear collisions, Phys. Rev. C **87**, 054903 (2013).

- [81] J. Steinheimer and J. Randrup, Spinodal amplification and baryon number fluctuations in nuclear collisions at NICA, *Eur. Phys. J. A* **52**, 239 (2016).
- [82] J. Fang, H. Pais, S. Avancini and C. Providencia, Larger and more heterogeneous neutron star crusts: A result of strong magnetic fields, *Phys. Rev. C* **94**, 062801 (2016).
- [83] J. Fang, H. Pais, S. Pratapsi, S. Avancini, J. Li and C. Providencia, Effect of strong magnetic fields on the crust-core transition and inner crust of neutron stars, *Phys. Rev. C* **95**, 045802 (2017).
- [84] L. McLerran and R. D. Pisarski, Phases of dense quarks at large N_c , *Nucl. Phys. A* **796**, 83 (2007).
- [85] G. Baym, T. Hatsuda, T. Kojo, P. D Powell, Yifan Song, and T. Takatsuka, From hadrons to quarks in neutron stars: a review, *Rep. Prog. Phys.* **81**, 056902 (2018).
- [86] L. D. Landau, The theory of a Fermi liquid, *JETP* **3**, 920 (1957).
- [87] L. D. Landau, Oscillations in a Fermi liquid, *JETP* **5**, 101 (1957).
- [88] A. B. Migdal, The momentum distribution of interacting Fermi particles, *JETP* **5**, 333 (1957).
- [89] V. M. Galitsky and A. B. Migdal, Application of quantum field theory methods to the many body problem, *JETP* **7**, 96 (1958).
- [90] L. D. Landau, On the theory of the Fermi liquid, **8**, 70 (1959).
- [91] A. B. Migdal, The theory of a Fermi Liquid consisting of two kinds of particles. Application to the nucleus, *Sov. Phys. JETP* **16**, 1366 (1963).
- [92] A. B. Migdal, *Theory of Finite Fermi Systems and Properties of Atomic Nuclei* (Wiley and Sons, New York, 1967).
- [93] A. B. Migdal, *Teoria Konechnykh Fermi System i Svoistva Atomnykh Yader* (Nauka, Moscow, 1983) [in Russian].
- [94] I. Ya. Pomeranchuk, On the stability of a Fermi liquid, *Sov. Phys. JETP* **8**, 361 (1958).
- [95] A. B. Migdal, Pion fields in nuclear matter, *Rev. Mod. Phys.* **50**, 107 (1978).
- [96] A. B. Migdal, E. E. Saperstein, M. A. Troitsky and D. N. Voskresensky, Pion degrees of freedom in nuclear matter, *Phys. Rept.* **192**, 179 (1990).
- [97] D. N. Voskresensky and I. N. Mishustin, Polarization operator of pions at finite temperatures, *Sov. J. Nucl. Phys.* **35**, 667 (1982).
- [98] A. M. Dyugaev, Crystalline and liquid phases of a pion condensate, *JETP Lett.* **35**, 420 (1982).
- [99] D. N. Voskresensky and A. V. Senatorov, Description of nuclear interaction in Keldysh's diagram technique and neutrino luminosity of neutron stars, *Sov. J. Nucl. Phys.* **45**, 411 (1987).
- [100] D. N. Voskresensky and A. V. Senatorov, Pion degrees of freedom in nucleus nucleus collisions, *Sov. J. Nucl. Phys.* **48**, 71 (1988).
- [101] E. E. Kolomeitsev and D. N. Voskresensky, Superfluid nucleon matter in and out of equilibrium and weak interactions, *Phys. Atomic Nuclei*, **74**, 1316 (2011).
- [102] T. E. O. Ericson and W. Weise, *Pions and nuclei* (Int. Ser. Monogr. Phys. **74**, 1988).

- [103] D. N. Voskresensky, S-wave pion condensation in symmetric nuclear matter, *Phys. Rev. D* **105**, 116007 (2022).
- [104] D. N. Voskresensky, The phase transition to an inhomogeneous condensate state, *Phys. Scripta* **29**, 259 (1984).
- [105] D. N. Voskresensky, Quasiclassical description of condensed systems by a complex order parameter, *Phys. Scripta* **47**, 333 (1993).
- [106] T. Muto, R. Tamagaki and T. Tatsumi, A chiral symmetry approach to meson condensations, *Prog. Theor. Phys. Suppl.* **112**, 159 (1993).
- [107] F. Dautry and E. M. Nyman, Pion condensation and the σ -model in liquid neutron matter, *Nucl. Phys. A* **319**, 323 (1979).
- [108] T. Takatsuka, K. Tamiya, T. Tatsumi and R. Tamagaki, Solidification and pion condensation in nuclear medium. Alternating layer spin structure with one-dimensional localization accompanying π^0 condensate, *Prog. Theor. Phys.* **59**, 1933 (1978).
- [109] T. Takatsuka, R. Tamagaki and T. Tatsumi, Characteristic aspects of pion condensed phases, *Prog. Theor. Phys. Suppl.* **112**, 67 (1993).
- [110] N. Glendenning, Phase transitions and crystalline structures in neutron star cores, *Phys. Rept.* **342**, 393 (2001).
- [111] E. E. Kolomeitsev, B. Kämpfer and D. N. Voskresensky, Kaon polarization in nuclear matter, *Nucl. Phys. A* **588**, 889 (1995).
- [112] E. E. Kolomeitsev and D. N. Voskresensky, Negative kaons in dense baryonic matter, *Phys. Rev. C* **68**, 015803 (2003).
- [113] E. E. Kolomeitsev, B. Kämpfer and D. N. Voskresensky, The impact of kaon polarization in nuclear matter on the K^- production in heavy ion collisions, *Int. J. Mod. Phys. E* **5**, 313 (1996).
- [114] D. N. Voskresensky, On the possibility of the condensation of the charged rho meson field in dense isospin asymmetric baryon matter, *Phys. Lett. B* **392**, 262 (1997).
- [115] E. E. Kolomeitsev and D. N. Voskresensky, Relativistic mean-field models with effective hadron masses and coupling constants, and ρ^- condensation, *Nucl. Phys. A* **759**, 373 (2005).
- [116] E. E. Kolomeitsev, K. A. Maslov and D. N. Voskresensky, Charged ρ -meson condensation in neutron stars, *Nucl. Phys. A* **970**, 291 (2018).
- [117] D. N. Voskresensky and I. N. Mishustin, The nature of a pi- condensate first order transformation at finite temperature, *JETP Lett.* **28**, 449 (1978).
- [118] G. Baym, Pion condensation at finite temperature. 1. Mean field theory, *Nucl. Phys. A* **352**, 355 (1981).
- [119] A. Larkin and A. Varlamov, *Theory of fluctuations in superconductors* [BOOK] 2005, books.google.com.
- [120] M. Stein, A. Sedrakian, Xu-Guang Huang and John W. Clark, BCS-BEC crossovers and unconventional phases in dilute nuclear matter, *Phys. Rev. C* **90**, 065804 (2014).

- [121] R. D. Pisarski, V. V. Skokov and A. M. Tsvelik, Fluctuations in cool quark matter and the phase diagram of quantum chromodynamics, *Phys. Rev. D* **99**, 074025 (2019).
- [122] D. N. Voskresensky, Thermal color superconducting fluctuations in dense quark matter, [arXiv:nucl-th/0312016 [nucl-th]].
- [123] D. N. Voskresensky, Fluctuations of the color-superconducting gap in hot and dense quark matter, *Phys. Rev. C* **69**, 065209 (2004).
- [124] T. Nishimura, T. Kunihiro and M. Kitazawa, Anomalous enhancement of dilepton production as a precursor of color superconductivity, *PTEP*, **2022**, 093D02 (2022).
- [125] B. O. Kerbikov, Precritical soft photon emission from quark matter, *Phys. Rev. D* **102**, 096022 (2020).
- [126] B. I. Halperin, T. C. Lubensky and Shang-keng Ma, First-order phase transitions in superconductors and smectic-A liquid crystals, *Phys. Rev. Lett.* **32**, 292 (1974).
- [127] S. A. Brazovskii, Phase transition of an isotropic system to a nonuniform state, *JETP* **41**, 85 (1975).
- [128] A. M. Dyugaev, Nature of phase transition in case of π -condensation, *JETP Lett.* **22**, 83 (1975).
- [129] D. N. Voskresensky and I. N. Mishustin, Thermal fluctuations of pion field near π -condensate critical point, *JETP Lett.* **34**, 303 (1981).
- [130] A. M. Dyugaev, Effects occurring near the critical points of phase transitions in a Fermi liquid as illustrated by pion condensation, *JETP* **56**, 567 (1982).
- [131] K. Kolehmainen and G. Baym, Pion condensation at finite temperature. 2. Simple models including thermal excitations of the pion field, *Nucl. Phys. A* **382**, 528 (1982).
- [132] A. M. Dyugaev, Precondensate phenomena in nuclear matter, *Sov. J. Nucl. Phys.* **38**, 680 (1983).
- [133] H. Schulz and D. N. Voskresensky, Pion fluctuations in relativistic heavy ion reactions and the π^-/Z ratio, *Phys. Lett. B* **141**, 37 (1984).
- [134] S. Karasawa, T. G. Lee and T. Tatsumi, Brazovskii–Dyugaev effect on the inhomogeneous chiral transition in quark matter, *Prog. Theor. Exp. Phys.*, **4**, 043D02 (2016).
- [135] R. D. Pisarski, F. Rennecke, A. Tsvelik, and S. Valgushev, The Lifshitz regime and its experimental signals, *Nucl. Phys. A* **1005**, 121910 (2021).
- [136] D. Blaschke, H. Grigorian, A. Khalatyan and D. N. Voskresensky, Exploring the QCD phase diagram with compact stars, *Nucl. Phys. B Proc. Suppl.* **141**, 137 (2005).
- [137] Y. B. Ivanov, A. S. Khvorostukhin, E. E. Kolomeitsev, V. V. Skokov, V. D. Toneev and D. N. Voskresensky, Lattice QCD constraints on hybrid and quark stars, *Phys. Rev. C* **72**, 025804 (2005).
- [138] M. Okamoto, T. Maruyama, K. Yabana and T. Tatsumi, Nuclear “pasta” structures in low-density nuclear matter and properties of the neutron-star crust, *Phys. Rev. C* **88**, 025801 (2013).

- [139] A. Ayriyan, N. U. Bastian, D. Blaschke, H. Grigorian, K. Maslov and D. N. Voskresensky, Robustness of third family solutions for hybrid stars against mixed phase effects, *Phys. Rev. C* **97**, 045802 (2018).
- [140] K. Maslov, N. Yasutake, A. Ayriyan, D. Blaschke, H. Grigorian, T. Maruyama, T. Tatsumi and D. N. Voskresensky, Hybrid equation of state with pasta phases and third family of compact stars, *Phys. Rev. C* **100**, 025802 (2019).
- [141] H. Dinh Thi, A. F. Fantina and F. Gulminelli, Properties of pasta phases in catalyzed neutron stars, *arXiv* 2206.07969.
- [142] A. B. Migdal, Stability of vacuum and limiting fields, *Zh. Eksp. Teor. Fiz.* **61**, 2209 (1971).
- [143] A. B. Migdal, Meson condensation and anomalous nuclei, *Phys. Lett. B* **52**, 172 (1974).
- [144] D. N. Voskresensky, G. A. Sorokin and A. I. Chernoutsan, Charge distribution in anomalous nuclei, *JETP Lett.* **25**, 465 (1977).
- [145] M. Shahrbafe, D. Blaschke, S. Typel, G. R. Farrar and D. E. Alvarez-Castillo, Sexaquark dilemma in neutron stars and its solution by quark deconfinement, *Phys. Rev. D* **105**, 103005 (2022).
- [146] V. A. Gani, M. Y. Khlopov and D. N. Voskresensky, Double charged heavy constituents of dark atoms and superheavy nuclear objects, *Phys. Rev. D* **99**, 015024 (2019).
- [147] A. Sedrakian and J. W. Clark, Superfluidity in nuclear systems and neutron stars, *EPJ A* **55**, 167 (2019).
- [148] P. Fulde and A. Ferrell, Superconductivity in a strong spin-exchange field, *Phys. Rev.* **135**, A550 (1964).
- [149] A. Larkin and Y. Ovchinnikov, Inhomogeneous state of superconductors, *JETP* **20**, 762 (1965).
- [150] A. Sedrakian and D. H. Rischke, Phase diagram of chiral quark matter: From weakly to strongly coupled Fulde-Ferrell phase, *Phys. Rev. D* **80**, 074022, (2009).
- [151] K. A. Maslov, E. E. Kolomeitsev and D. N. Voskresensky, Solution of the hyperon puzzle within a relativistic mean-field model, *Phys. Lett. B* **748**, 369 (2015).
- [152] A. Drago, A. Lavagno, G. Pagliara and D. Pigato, Early appearance of Δ isobars in neutron stars, *Phys. Rev. C* **90**, 065809 (2014).
- [153] E. E. Kolomeitsev, K. A. Maslov and D. N. Voskresensky, Delta isobars in relativistic mean-field models with σ -scaled hadron masses and couplings, *Nucl. Phys. A* **961**, 106 (2016).
- [154] A. R. Raduta, M. Oertel and A. Sedrakian, Proto-neutron stars with heavy baryons and universal relations, *Monthly Notices*, **499**, 914 (2020).
- [155] A. Sedrakian and A. Harutyunyan, Delta-resonances and hyperons in proto-neutron stars and merger remnants, *arXiv* 2202.12083.
- [156] K. D. Marquez, H. Pais, D. P. Menezes and C. Providencia, Delta baryons in neutron stars, *arXiv* 2206.02935.
- [157] B. C. Barrois, Superconducting quark matter, *Nucl. Phys. B* **129**, 390 (1977).

- [158] D. Bailin and A. Love, Superfluidity and superconductivity in relativistic fermion systems, *Phys. Rept.* **107**, 325 (1984).
- [159] K. Rajagopal and F. Wilczek, *At the frontier of particle physics*, (World Scientific, Singapore, vol. 3, p. 2061, 2001).
- [160] M. Alford, K. Rajagopal, S. Reddy and F. Wilczek, Minimal color-flavor-locked–nuclear interface, *Phys. Rev. D* **64**, 074017 (2001).
- [161] M. G. Alford, J. A. Bowers, and K. Rajagopal, Crystalline color superconductivity, *Phys. Rev. D* **63**, 07401 (2001).
- [162] M. G. Alford, A. Schmitt, K. Rajagopal, and T. Schäfer, *Rev. Mod. Phys.* **80**, 1455 (2008).
- [163] K. Iida and G. Baym, The superfluid phases of quark matter: Ginzburg-Landau theory and color neutrality, *Phys. Rev. D* **63**, 074018 (2001), Erratum: [*Phys. Rev. D* **66**, 059903 (2002)].
- [164] M. Kitazawa, K. Koide, T. Kunihiro, and Y. Nemoto, Precursor of color superconductivity in hot quark matter, *Phys. Rev. D* **65**, 091504 (2002).
- [165] M. Kitazawa, K. Koide, T. Kunihiro and Y. Nemoto, Pre-critical phenomena of two-flavor color superconductivity in heated quark matter – diquark-pair fluctuations and non-Fermi liquid behavior, *PTP*, **114**, 117 (2005).
- [166] R. Anglani, R. Casalbuoni, M. Ciminale, N. Ippolito, R. Gatto, M. Mannarelli, and M. Ruggieri, Crystalline color superconductors, *Rev. Mod. Phys.* **86**, 509 (2014).
- [167] M. Mannarelli, Meson condensation, *Particles* **2**, 411 (2019).
- [168] E. Nakano and T. Tatsumi, Chiral symmetry and density waves in quark matter, *Phys. Rev. D* **71**, 114006 (2005).
- [169] S. Carignano, M. Buballa and B. J. Schaefer, Inhomogeneous phases in the quark-meson model with vacuum fluctuations. *Phys. Rev. D* **90**, 014033 (2014).
- [170] M. Buballa and S. Carignano, Inhomogeneous chiral condensates. *Prog. Part. Nucl. Phys.* **81**, 39, (2015).
- [171] Tong-Gyu Lee, E. Nakano, Y. Tsue, T. Tatsumi and B. Friman, Landau-Peierls instability in a Fulde-Ferrell type inhomogeneous chiral condensed phase, *Phys. Rev. D* **92**, 034024 (2015).
- [172] M. S. Grønli and T. Brauner, Competition of chiral soliton lattice and Abrikosov vortex lattice in QCD with isospin chemical potential, *Eur. Phys. J. C* **82**, 354 (2022).
- [173] F. Canfora, S. Carignano, M. Lagos, M. Mannarelli and A. Vera, Pion crystals hosting topologically stable baryons, *Phys. Rev. D* **103**, 076003 (2021).
- [174] P. Adhikari and J. O. Andersen, Quark and pion condensates at finite isospin density in chiral perturbation theory, *Eur. Phys. J. C* **80**, 1028 (2020).
- [175] N.K. Glendenning, First-order phase transitions with more than one conserved charge: consequences for neutron stars, *Phys. Rev.* **D46**, 1274 (1992).
- [176] D. G. Ravenhall, C. J. Pethick and J. R. Wilson, Structure of matter below nuclear saturation density, *Phys. Rev. Lett.* **50**, 2066 (1983).

- [177] C. P. Lorenz, D. G. Ravenhall and C. J. Pethick, Neutron star crusts, Phys. Rev. Lett. **70**, 379 (1993).
- [178] G. Watanabe, K. Iida and K. Sato, Thermodynamic properties of nuclear “pasta” in neutron star crusts, Nucl. Phys. A **676**, 455 (2000).
- [179] D. N. Voskresensky, M. Yasuhira and T. Tatsumi, Charge screening at first order phase transitions, Phys. Lett. B **541**, 93 (2002).
- [180] D. N. Voskresensky, M. Yasuhira and T. Tatsumi, Charge screening at first order phase transitions and hadron quark mixed phase, Nucl. Phys. A **723**, 291 (2003).
- [181] T. Maruyama, T. Tatsumi, D. N. Voskresensky, T. Tanigawa and S. Chiba, Nuclear pasta structures and the charge screening effect, Phys. Rev. C **72**, 015802 (2005).
- [182] T. Maruyama, T. Tatsumi, D.N. Voskresensky, T. Tanigawa, T. Endo and S. Chiba, Finite size effects on kaonic pasta structures, Phys. Rev. C **73**, 035802 (2006).
- [183] Toshiki Maruyama, S. Chiba, H.-J. Schulze and T. Tatsumi, Quark deconfinement transition in hyperonic matter, Phys. Lett. B **659**, 192 (2008).
- [184] D. N. Voskresensky and N. Y. Anisimov, Properties of a pion condensate in a magnetic field, JETP **51**, 13 (1980).
- [185] V. Skokov, A. Y. Illarionov and V. Toneev, Estimate of the magnetic field strength in heavy-ion collisions, Int. J. Mod. Phys., A **24**, 5925 (2009).
- [186] A. Onuki, *Phase transition dynamics*, Cambridge Univ. Press, 2002.
- [187] A. Z. Patashinsky and B. I. Shumilo, Theory of relaxation of metastable states, JETP **50**, 712 (1979).
- [188] P. Kovtun, Lectures on hydrodynamic fluctuations in relativistic theories, J. Phys. A **45**, 473001 (2012).
- [189] S. Jeon and U. Heinz, Introduction to Hydrodynamics, Int. J. Mod. Phys. E **24**, 1530010 (2015).
- [190] M. Nahrgang, M. Bluhm, T. Schäfer and S. A. Bass, Diffusive dynamics of critical fluctuations near the QCD critical point, Phys. Rev. D **99**, 116015 (2019).
- [191] M. Bluhm, et al, Dynamics of critical fluctuations: Theory – phenomenology – heavy-ion collisions, Nucl. Phys. A **1003**, 122016 (2020).
- [192] D. N. Voskresensky, “*Stability of vacuum and phase transformations*”, (Moscow, MEPhI 1988) [in Russian].
- [193] E. Lake, T. Senthil and A. Vishwanath, Bose-Luttinger liquids, Phys. Rev. B **104**, 014517 (2021).
- [194] G. Basar and G. V. Dunne, Self-consistent crystalline condensate in chiral Gross-Neveu and Bogoliubov-de Gennes systems, Phys. Rev. Lett. **100**, 200404 (2008).
- [195] G. Basar and G. V. Dunne, A twisted kink crystal in the chiral Gross-Neveu model, Phys. Rev. D **78**, 065022 (2008).

- [196] G. Basar, G. V. Dunne and M. Thies, Inhomogeneous condensates in the thermodynamics of the chiral NJL(2) model, *Phys. Rev. D* **79**, 105012 (2009).
- [197] R. D. Pisarski, Remarks on nuclear matter: how an ω_0 condensate can spike the speed of sound, and a model of Z(3) baryons, *Phys. Rev. D* **103**, L071504 (2021).
- [198] R. D. Pisarski and F. Rennecke, Signatures of moat regimes in heavy-ion collisions, *Phys. Rev. Lett.* **127**, 152302 (2021).
- [199] N. Y. Anisimov and D. N. Voskresensky, Superconductivity of pion condensate, *Sov. J. Nucl. Phys.* **30**, 612 (1979).
- [200] V. L. Ginzburg, Theory of superdiamagnets, **30**, 345 (1979).
- [201] P. M. Chaikin and T. Lubensky, *Principles of Condensed Matter Physics* (Cambridge University Press: Cambridge, UK, 2010).
- [202] D. R. Nelson and J. Toner, Bond-orientational order, dislocation loops, and melting of solids and smectic-A liquid crystals, *Phys. Rev. B* **24**, 363 (1981).
- [203] A. B. Migdal, N. A. Kirichenko and G. A. Sorokin, Pi- condensation in a finite system and properties of nuclei, *Phys. Lett. B* **50**, 411 (1974).
- [204] M. A. Baranov, Theoretical progress in many-body physics with ultracold dipolar gases, *Phys. Rep.* **464**, 71 (2008).
- [205] K. Maeda, T. Hatsuda and G. Baym, Antiferrosmectic ground state of two-component dipolar Fermi gases – an analog of meson condensation in nuclear matter, *Phys. Rev. A* **87**, 021604(R) (2013).
- [206] D. K. Campbell, R. F. Dashen and J. T. Manassah, Chiral symmetry and pion condensation. 1. Model dependent results, *Phys. Rev. D* **12**, 979 (1975).
- [207] D. K. Campbell, R. F. Dashen and J. T. Manassah, Chiral symmetry and pion condensation. 2. General formalism, *Phys. Rev. D* **12**, 1010 (1975).
- [208] G. Baym, D. Campbell, R. F. Dashen and J. Manassah, A simple model calculation of pion condensation in neutron matter, *Phys. Lett. B* **58**, 304 (1975).
- [209] D. V. Deryagin, D. Y. Grigoriev and V. A. Rubakov, Standing wave ground state in high density at large N_c , *Int. J. Mod. Phys. A* **7**, 659 (1992).
- [210] E. Shuster and D. T. Son, On finite-density QCD at large N_c , *Nucl. Phys. B* **573**, 434 (2000).
- [211] T. Kojo, Y. Hidaka, L. McLerran and R. D. Pisarski, Quarkyonic chiral spirals, *Nucl. Phys. A* **843**, 37 (2010).
- [212] D. Nickel, Inhomogeneous phases in the Nambu–Jona-Lasinio and quark-meson model, *Phys. Rev. D* **80**, 074025 (2009).
- [213] D. Müller, M. Buballa and J. Wambach, Dyson–Schwinger study of chiral density waves in QCD, *Phys. Lett. B* **727**, 240 (2013).
- [214] B. D. Serot and J. D. Walecka, The Relativistic Nuclear Many Body Problem, *Adv. Nucl. Phys.* **16**, 1 (1986).

- [215] G. Grinstein and R. A. Pelcovits, Anharmonic effects in bulk smectic liquid crystals and other "one-dimensional solids", *Phys. Rev. Lett.* **47**, 856 (1981).
- [216] G. Baym, B. L. Friman and G. Grinstein, Fluctuations and long-range order in finite-temperature pion condensates, *Nucl. Phys. B* **210**, 193 (1982).
- [217] D. N. Voskresensky, A. V. Senatorov, B. Kämpfer and H. J. Haubold, A possible explanation of the second neutrino burst in SN1987A, *Astrophys. Space Sci.* **138**, 421 (1987).
- [218] H. J. Haubold, B. Kampfer, A. V. Senatorov and D. N. Voskresensky, A tentative approach to the second neutrino burst in SN1987A, *Astron. Astrophys.* **191**, L22 (1988).
- [219] P. Galeotti and G. Pizzella, New analysis for the correlation between gravitational wave and neutrino detectors during SN1987A, *Eur. Phys. J. C* **76**, 426 (2016).
- [220] A. B. Migdal, A. I. Chernoutsan and I. N. Mishustin, Pion condensation and dynamics of neutron stars, *Phys. Lett.* **83B**, 158 (1979).
- [221] M. Prakash, I. Bombaci, M. Prakash, P. J. Ellis, J. M. Lattimer and R. Knorren, Composition and structure of protoneutron stars, *Phys. Rept.* **280**, 1 (1997).
- [222] I. Iosilevskiy, Non-congruent phase transitions in cosmic matter and in the laboratory, *Acta Phys. Polon. Supp.* **3**, 589 (2010).
- [223] M. Hempel, V. Dexheimer, S. Schramm and I. Iosilevskiy, Noncongruence of the nuclear liquid-gas and deconfinement phase transitions, *Phys. Rev. C* **88**, 014906 (2013).
- [224] Y. B. Ivanov, V. N. Russkikh and V. D. Toneev, Relativistic heavy-ion collisions within 3-fluid hydrodynamics: Hadronic scenario, *Phys. Rev. C* **73**, 044904 (2006).
- [225] G. Baym, H. Bethe and Ch. Pethick, Neutron star matter, *Nucl. Phys. A* **175**, 225 (1971).
- [226] J. W. Negele and D. Vautherin, Neutron star matter at sub-nuclear densities, *Nucl. Phys. A* **207**, 298 (1973).
- [227] V. Thorsson, M. Prakash and J.M. Lattimer, Composition, structure and evolution of neutron stars with kaon condensates, *Nucl. Phys. A* **572**, 693 (1994).
- [228] T. Tatsumi, Kaon condensation and neutron stars, *Prog. Theor. Phys. Suppl.* **120**, 111 (1995).
- [229] N. K. Glendenning and J. Schaffner-Bielich, First order kaon condensate, *Phys. Rev. C* **60**, 025803 (1999).
- [230] M. Christiansen, N. K. Glendenning and J. Schaffner-Bielich, Surface tension between a kaon condensate and the normal nuclear matter phase, *Phys. Rev. C* **62**, 025804 (2000).
- [231] H. Heiselberg, C. J. Pethick and E. F. Staubo, Quark matter droplets in neutron stars, *Phys. Rev. Lett.* **70**, 1355 (1993).
- [232] T. Klähn, D. Blaschke, F. Sandin, C. Fuchs, A. Fässler, H. Grigorian, G. Röpke and J. Trümper, Modern compact star observations and the quark matter equation of state, *Phys. Lett. B* **654**, 170 (2007).
- [233] S. Reddy, G. F. Bertsch and M. Prakash, First order phase transitions in neutron star matter: droplets and coherent neutrino scattering, *Phys. Lett. B* **475**, 1 (2000).

- [234] H. Sonoda, G. Watanabe, K. Sato, T. Takiwaki, K. Yasuoka and T. Ebisuzaki, The impact of nuclear pasta on neutrino transport in collapsing cores, *Phys. Rev. C* **75**, 042801 (2007).
- [235] N. Yasutake, T. Maruyama and T. Tatsumi, Amorphous state in the mixed phase of quark-hadron phase transition in protoneutron stars, *Phys. Rev. D* **86**, 101302 (2012).
- [236] P. N. Alcain, P. A. Giménez Molinelli and C. O. Dorso, Beyond nuclear pasta: Phase transitions and neutrino opacity of new pasta phases, *Phys. Rev. C* **90**, 065803 (2014).
- [237] Cheng-Jun Xia, Toshiki Maruyama, N. Yasutake and T. Tatsumi, Nuclear pasta structures at high temperatures, *Phys. Rev. D* **106**, 063020 (2022).
- [238] J. A. Pons, S. Reddy, P. J. Ellis, M. Prakash and J. M. Lattimer, Kaon condensation in proto-neutron star matter, *Phys. Rev., C* **62**, 035803 (2000).
- [239] M. Yasuhira and T. Tatsumi, Protoneutron stars with kaon condensation and their delayed collapse, *Nucl. Phys. A* **690**, 769 (2001).
- [240] H. Heiselberg, C. J. Pethick and E. F. Staubo, Quark matter droplets in neutron stars, *Phys. Rev. Lett.* **70**, 1355 (1993).
- [241] T. Norsen and S. Reddy, First order kaon condensation in neutron stars: Finite size effects in the mixed phase, *Phys. Rev. C* **63**, 065804 (2001).
- [242] Cheng-Jun Xia, Toshiki Maruyama, N. Yasutake, T. Tatsumi and Ying-Xun Zhang, Nuclear pasta structures and symmetry energy, *Phys. Rev. C* **103**, 055812 (2021).
- [243] G. Lugones and A. G. Grunfeld, Vector interactions inhibit quark-hadron mixed phases in neutron stars, *Phys. Rev. D* **104**, L101301 (2021).
- [244] C. J. Pethick and A. Y. Potekhin, Liquid crystals in the mantles of neutron stars, *Phys. Lett. B* **427**, 7 (1998).
- [245] C. J. Pethick, Z. Zhang and D. N. Kobyakov, Elastic properties of phases with nonspherical nuclei in dense matter, *Phys. Rev. C* **101**, 055802 (2020).
- [246] Zhao-Wen Zhang and C. J. Pethick, Proton superconductivity in pasta phases in neutron star crusts, *Phys. Rev. C* **103**, 055807 (2021).
- [247] C. J. Horowitz, M. A. Perez-Garcia, D. K. Berry, and J. Piekarewicz, Dynamical response of the nuclear pasta in neutron star crusts, *Phys. Rev. C* **72**, 035801 (2005).
- [248] C. J. Horowitz and D. K. Berry, The shear viscosity and thermal conductivity of nuclear pasta, *Phys. Rev. C* **78**, 035806 (2008).
- [249] G. Watanabe, H. Sonoda, Toshiki Maruyama, K. Sato, K. Yasuoka, and T. Ebisuzaki, Formation of nuclear “pasta” in supernovae, *Phys. Rev. Lett.* **103**, 121101 (2009).
- [250] Toshiki Maruyama, G. Watanabe and S. Chiba, Molecular dynamics for dense matter, *Prog. Theor. Exp. Phys.* **2012**, 01A201 (2012).
- [251] A. S. Schneider, C. J. Horowitz, J. Hughto and D. K. Berry, Nuclear “pasta” formation, *Phys. Rev. C* **88**, 065807 (2013).

- [252] P. Alcaín and C. Dorso, Dynamics of Fragment Formation in Neutron Rich Matter, *Phys. Rev. C* **97**, 015803 (2018).
- [253] J. A. Lopez, C. O. Dorso and G. A. Frank, Properties of nuclear pastas, *Front. Phys. (Beijing)* **16**, 24301 (2021).
- [254] A. S. Khvorostukhin, V. D. Toneev and D. N. Voskresensky, Viscosity coefficients for hadron and quark-gluon phases, *Nucl. Phys. A* **845**, 106 (2010).
- [255] A. S. Khvorostukhin, V. D. Toneev and D. N. Voskresensky, Viscosity of hadron matter within relativistic mean-field based model with scaled hadron masses and couplings, *Phys. Atom. Nucl.* **74**, 650 (2011).
- [256] P. Chakraborty and J. I. Kapusta, Quasi-particle theory of shear and bulk viscosities of hadronic matter, *Phys. Rev. C* **83**, 014906 (2011).
- [257] A. S. Khvorostukhin, V. D. Toneev and D. N. Voskresensky, Shear and bulk viscosities for pure glue matter, *Phys. Rev. C* **83**, 035204 (2011).
- [258] A. S. Khvorostukhin, V. D. Toneev and D. N. Voskresensky, Relaxation time ansatz and shear and bulk viscosities of gluon matter, *Phys. Rev. C* **84**, 035202 (2011).
- [259] A. S. Khvorostukhin, V. D. Toneev and D. N. Voskresensky, Remarks concerning bulk viscosity of hadron matter in relaxation time ansatz, *Nucl. Phys. A* **915**, 158 (2013).
- [260] M. Albright and J. I. Kapusta, Quasiparticle theory of transport coefficients for hadronic matter at finite temperature and baryon density, *Phys. Rev. C* **93**, 014903 (2016).
- [261] P. Chakraborty and J. I. Kapusta, Departure from equilibrium of the quasiparticle distribution functions in high-energy nuclear collisions, *Phys. Rev. C* **95**, 014907 (2017).
- [262] X. G. Den, P. Danielewicz, Y. G. Ma, H. Lin and Y. X. Zhang, Impact of fragment formation on shear viscosity in the nuclear liquid-gas phase transition region, *Phys. Rev. C* **105**, 064613 (2022).
- [263] E. E. Kolomeitsev and D. N. Voskresensky, Mechanism of r-mode stability in young rapidly rotating pulsars, *Eur. Phys. J. A* **50**, 180 (2014).
- [264] E. E. Kolomeitsev and D. N. Voskresensky, Viscosity of neutron star matter and r -modes in rotating pulsars, *Phys. Rev. C* **91**, 025805 (2015).
- [265] Y. B. Ivanov, J. Knoll, H. van Hees and D. N. Voskresensky, Soft modes, resonances and quantum transport, *Phys. Atom. Nucl.* **64**, 652 (2001).
- [266] Yu. N. Devyatko and V. N. Tronin, Nucleation of new phase in irradiated metals, *Fiz. Mettals*, **63**, 635 (1987) [in Russian].
- [267] P. C. Hohenberg and J. B. Swift, Metastability in fluctuation-driven first-order transitions: Nucleation of lamellar phases, *Phys. Rev. E* **52**, 1828 (1995).
- [268] B. Berdnikov and K. Rajagopal, Slowing out of equilibrium near the QCD critical point, *Phys. Rev. D* **61**, 105017 (2000).
- [269] C. Nonaka and M. Asakawa, Hydrodynamical evolution near the QCD critical end point, *Phys. Rev. C* **71**, 044904 (2005).

- [270] C. Nonaka and M. Asakawa, Critical end point and its consequences, Nucl. Phys. **A774**, 753 (2006).
- [271] O. Scavenius, A. Dumitru and A.D. Jackson, Explosive decomposition in ultrarelativistic heavy-ion collisions, Phys. Rev. Lett. **87**, 182302 (2001).
- [272] G. Torrieri, B. Tomasik and I. Mishustin, Bulk-viscosity-driven clusterization of quark-gluon plasma and early freeze-out in relativistic heavy-ion collisions, Phys. Rev. **C77**, 034903 (2008).
- [273] D. N. Voskresensky, Evolution of quasiperiodic structures in a onn-ideal hydrodynamic description of phase transitions, Universe **6**, 42 (2020).
- [274] L. I. Mandelstam and M. A. Leontovich, To the theory of the second sound, Zh. Eksp. Teor. Fiz. **7**, 438 (1937).
- [275] L. D. Landau and E. M. Lifshitz, *Fluid Mechanics* (Pergamon Press, Oxford, 1987).
- [276] J. Randrup, Phase transition dynamics for baryon-dense matter, Phys. Rev. C **79**, 054911 (2009).
- [277] C. J. Pethick and D. G. Ravenhall, Growth of instability in a normal Fermi liquid, Ann. Phys. **183**, 131 (1988).
- [278] E. M. Lifshiz and L. P. Pitaevskii, *Physical Kinetics*, (Pergamon press, 1981).
- [279] J. W. P. Schmelzer (Ed.), *Nucleation theory and applications*, Wiley-VCH Verlag GmbH & Co. KGaA, 2005.
- [280] J. I. Kapusta and C. Gale, *Finite-temperature field theory. Principles and applications*, Cambridge Univ. Press, 2006.
- [281] V. V. Slezov, *Kinetics of first-order phase transitions* Wiley-VCH Verlag GmbH & Co. KGaA, 2009.
- [282] J. W. P. Schmelzer and T. V. Tropin, Theory of crystal nucleation of glass-forming liquids: Some new developments, Int. J. Appl. Glass Sci. **13**, 171 (2022).
- [283] B. O. Kerbikov, Critical acoustics and singular bulk viscosity of quark matter, arXiv:1806.09872.
- [284] G. Torrieri, B. Tomasik and I. Mishustin, Bulk-viscosity-driven clusterization of quark-gluon plasma and early freeze-out in relativistic heavy-ion collisions, Phys. Rev. C **77**, 034903 (2008).
- [285] K. A. Maslov, E. E. Kolomeitsev and D. N. Voskresensky, Relativistic mean-field models with scaled hadron masses and couplings: hyperons and maximum neutron star mass, Nucl. Phys. A **950**, 64 (2016).
- [286] S. O. Backman, G. E. Brown and J. A. Niskanen, The nucleon nucleon interaction and the nuclear many body problem, Phys. Rept. **124**, 1 (1985).
- [287] J. W. Holt, G. E. Brown, Jason D. Holt and T. T. S. Kuo, Nuclear matter with Brown-Rho-scaled Fermi liquid interactions, Nucl. Phys. A **785**, 322 (2007).
- [288] D. Gambacurta, U. lombardo and W. Zuo, The Landau-Migdal parameters from the Brueckner theory, Phys. Atom. Nucl., **74**, 1424 (2011).

- [289] J. Speth, S. Krewald, F. Grümmer, P.-G. Reinhard, N. Lyutorovich and V. Tselyaev, Landau–Migdal vs. Skyrme, Nucl. Phys. A **928**, 17 (2014).
- [290] M. A. Troitsky and N. I. Chekunaev, Isotopic shift of levels of πn atom, Yad. Fiz. **33**, 1300 (1981).
- [291] Toshio Suzuki and Hideyuki Sakai, The Landau-Migdal parameters, g'_{NN} and $g'_{N\Delta}$, Phys. Lett. B **455**, 25 (1999).
- [292] J. Delorme, M. Ericson and T. E. O. Ericson, “To condense or not to condense? That is the question,” Phys. Lett. B **291**, 379 (1992).
- [293] T. E. O. Ericson, “Anomalous chiral effects in media,” Phys. Lett. B **321**, 312 (1994).
- [294] E. E. Kolomeitsev, N. Kaiser and W. Weise, Chiral dynamics of deeply bound pionic atoms, Phys. Rev. Lett. **90**, 092501 (2003).
- [295] E. E. Kolomeitsev, N. Kaiser and W. Weise, Chiral dynamics and pionic 1s states of Pb and Sn isotopes, Nucl. Phys. A **721**, 835 (2003).
- [296] E. Friedman and A. Gal, Extracting $\Sigma_{\pi N}$ from pionic atoms, arXiv: 2008.03147.
- [297] V. F. Dmitriev and T. Suzuki, Spin-isospin dependent response function of nuclear matter at high excitation energies, Nucl. Phys. A **438**, 697 (1985).
- [298] V. F. Dmitriev, The (He-3, T) Reaction on nuclei in the Delta isobar region, Sov. J. Nucl. Phys. **46**, 435 (1987).
- [299] T. Hennino, B. Ramstein, D. Bachelier, J. L. Boyard, C. Ellegaard, C. Gaarde, J. Gosset, J. C. Jourdain, J. S. Larsen, M. C. Lemaire, et al., Coherent pions in charge exchange reactions, Phys. Lett. B **303**, 236 (1993).
- [300] K. Snepken and C. Gaarde, Cascade simulation of a Delta isobar propagating in a nucleus, Phys. Rev. C **50**, 338 (1994).
- [301] C. L. Korpa and R. Malfliet, Self-consistent delta-hole model at nonzero temperature, Phys. Rev. C **52**, 2756 (1995).
- [302] C. L. Korpa, M. F. M. Lutz and F. Riek, Covariant and self consistent vertex corrections for pions and isobars in nuclear matter, Phys. Rev. C **80**, 024901 (2009).
- [303] D. N. Voskresensky and A. V. Senatorov, Pion excitations in a nucleonic medium may be persistent to the luminosity of neutron stars, JETP Lett. **40**, 1212 (1984).
- [304] D. N. Voskresensky, Exponential growth and possible condensation of the particle-hole excitations in moving hot Fermi liquids, Phys. Lett. B **358**, 1 (1995).
- [305] D. N. Voskresensky and A. V. Senatorov, Emission of Neutrinos by Neutron Stars, Sov. Phys. JETP **63**, 885 (1986).
- [306] D. N. Voskresensky, Neutrino cooling of neutron stars: Medium effects. In *Physics of Neutron Star Interiors* (Springer: Berlin/Heidelberg, Germany, 2001; pp. 467–503).
- [307] A. Akmal, V. R. Pandharipande and D. G. Ravenhall, Equation of state of nucleon matter and neutron star structure, Phys. Rev. C **58**, 1804 (1998).

- [308] D. Blaschke, H. Grigorian and D. N. Voskresensky, Cooling of neutron stars: Hadronic model, *Astron. Astrophys.* **424**, 979 (2004).
- [309] H. Grigorian and D. N. Voskresensky, Medium effects in cooling of neutron stars and 3P(2) neutron gap, *Astron. Astrophys.* **444**, 913 (2005).
- [310] H. Grigorian, D. N. Voskresensky and D. Blaschke, Influence of the stiffness of the equation of state and in-medium effects on the cooling of compact stars, *Eur. Phys. J. A* **52**, 67 (2016).
- [311] H. Grigorian, D. N. Voskresensky and K. A. Maslov, Cooling of neutron stars in nuclear medium cooling scenario with stiff equation of state including hyperons, *Nucl. Phys. A* **980**, 105 (2018).
- [312] A. M. Dyugaev, Contribution to the theory of liquid 3-He, *Sov. Phys. JETP*, **43**, 1247 (1976).
- [313] K. Hashimoto, Possibility of ferromagnetic neutron matter, *Phys. Rev. D* **91**, 085013 (2015).
- [314] D. Nickel, How many phases meet at the chiral critical point? *Phys. Rev. Lett.* **103**, 072301 (2009).
- [315] G. F. Bertsch, L. Frankfurt and M. Strikman, Where are the nuclear pions?, *Science* **259**, 773 (1993).
- [316] G. E. Brown, M. Buballa, Z. B. Li and J. Wambach, Where the nuclear pions are, *Nucl. Phys., A* **593**, 295 (1995).
- [317] D. N. Voskresensky, On manifestation of in-medium effects in neutron stars and heavy-ion collisions, *Universe* **4**, 28 (2018).
- [318] D. N. Voskresensky, Pion softening and pion condensation, *Phys. Atom. Nucl.* **83**, 188 (2020).
- [319] A. V. Senatorov and D. N. Voskresensky, Pion dynamics in heavy ion collisions, *Phys. Lett. B* **219**, 31 (1989).
- [320] L. P. Kadanoff and G. Baym, *Quantum Statistical Mechanics*, (Benjamin, New York, 1962).
- [321] D. N. Voskresensky, Hydrodynamics of Resonances, *Nucl. Phys. A* **849**, 120 (2011).
- [322] W. Botermans and R. Malfliet, Quantum transport theory of nuclear matter, *Phys. Rept.* **198**, 115 (1990).
- [323] Y. B. Ivanov and D. N. Voskresensky, Nonlocal form of quantum off-shell kinetic equation, *Phys. Atom. Nucl.* **72**, 1168 (2009).
- [324] E. E. Kolomeitsev and D. N. Voskresensky, Time delays and advances in classical and quantum systems, *J. Phys. G* **40**, 113101 (2013).
- [325] Y. B. Ivanov, J. Knoll and D. N. Voskresensky, Selfconsistent approximations to nonequilibrium many body theory, *Nucl. Phys. A* **657**, 413 (1999).
- [326] Y. B. Ivanov, J. Knoll and D. N. Voskresensky, Resonance transport and kinetic entropy, *Nucl. Phys. A* **672**, 313 (2000).
- [327] J. Knoll, Y. B. Ivanov and D. N. Voskresensky, Exact conservation laws of the gradient expanded Kadanoff-Baym equations, *Annals Phys.* **293**, 126 (2001).

- [328] Y. B. Ivanov, J. Knoll and D. N. Voskresensky, Selfconsistent approach to off-shell transport, Phys. Atom. Nucl. **66**, 1902 (2003).
- [329] J. Knoll and D. N. Voskresensky, Nonequilibrium description of bremsstrahlung in dense matter (Landau-Pomeranchuk-Migdal effect), Phys. Lett. B **351**, 43 (1995).
- [330] J. Knoll and D. N. Voskresensky, Classical and Quantum Many-Body Description of Bremsstrahlung in Dense Matter, Annals Phys. **249**, 532 (1996).
- [331] D. Dunn, Urbach's rule in an electron-phonon model, Phys. Rev. **174**, 855 (1968).
- [332] B. I. Shklovskii and A. L. Efros, *Electronic properties of Doped Semiconductors*, (Springer-Verlag, N.Y., 1984).
- [333] G. Baym, Self-consistent approximations in many-body systems, Phys. Rev. **127**, 1391 (1962).
- [334] M. N. Chernodub, Electromagnetic superconductivity of vacuum induced by strong magnetic field, Lect. Notes Phys. **871**, 143 (2013).
- [335] D. Fay and A. Layzer, Superfluidity of low-density fermion systems, Phys. Rev. Lett. **20**, 187 (1968).
- [336] M. Yu. Kagan and A. V. Chubukov, Possibility of a superfluid transition in a slightly nonideal Fermi gas with repulsion, JETP Lett. **47**, 614 (1988).
- [337] M. Yu. Kagan, *Modern Trends in Superconductivity and Superfluidity* (Springer, Heidelberg, 2013).
- [338] V. A. Sadovnikova and M. G. Ryskin, Behavior of solutions to the pion dispersion equation in the complex frequency plane, Phys. Atom. Nucl. **64**, 440 (2001).
- [339] V. A. Sadovnikova, Investigation of zero-frequency solutions to the pion dispersion equation, Phys. Atom. Nucl. **70**, 989 (2007).
- [340] V. A. Sadovnikova, Structure functions generated by zero sound excitations, arXiv: 2004.04971 [nucl-th].
- [341] E. E. Saperstein and S. V. Tolokonnikov, The Migdal jump in the nucleon momentum distribution in nuclear matter is determined by the spin-isospin response function, JETP Lett. **68**, 553 (1998).
- [342] J. Speth, S. Krewald, F. Grümmer, P.-G. Reinhard, N. Lyutorovich and V. Tselyaev, Landau-Migdal vs. Skyrme, Nucl. Phys. A **928**, 17 (2014).
- [343] T. Matsui, Fermi-liquid properties of nuclear matter in a relativistic mean-field theory, Nucl. Phys. A **370**, 365 (1981).
- [344] J. Wambach, T. L. Ainsworth, and D. Pines, Quasiparticle interactions in neutron matter for applications in neutron stars, Nucl. Phys. A **555**, 128 (1993).
- [345] E. G. Brovman and Yu. Kagan, Singularities of multitail ring diagrams for Fermi systems, JETP **36**, 1025 (1972).
- [346] E. G. Brovman and A. Kholas, A general method for integration of many-point ring diagrams for Fermi systems, JETP **39**, 924 (1974).

- [347] L. P. Pitaevskii, Layered structure of superfluid ^4He with supercritical motion, JETP Lett. **39**, 511 (1984).
- [348] D. N. Voskresensky, Condensate with a finite momentum in a moving medium, JETP **77**, 917 (1993).
- [349] G. Baym and C. J. Pethick, Landau critical velocity in weakly interacting Bose gases, Phys. Rev. A **86**, 023602 (2012).
- [350] E. E. Kolomeitsev and D. N. Voskresensky, Condensate of excitations in moving superfluids, PTEP, **2017**, 023D01 (2017).
- [351] L. A. Melnikovsky, Bose-Einstein condensation of rotons, Phys. Rev. B **84**, 024525 (2011).
- [352] H. J. Pirner and D. N. Voskresensky, Where to look for pion condensation in heavy ion collisions, Phys. Lett. B **343**, 25 (1995).
- [353] D. N. Voskresensky, Comments on manifestation of in-medium effects in heavy-ion collisions, Eur. Phys. J. A **52**, 223 (2016).
- [354] J. Sauls, *Timing Neutron Stars*, Eds. H. Ögelman and E. P. J. van den Heuvel, Kluwer Academic Publishers, Dordrecht, 1989, pp. 457-490.
- [355] S. Shapiro and S. A. Teukolsky, *Black Holes, White Dwarfs and Neutron Stars: The Physics of Compact Objects*, Wiley, N.Y., 1983.
- [356] F. Ancilotto, F. Dalfovo, L. P. Pitaevskii and F. Toigo, Density pattern in supercritical flow of liquid ^4He , Phys. Rev. B **71**, 104530 (2005).
- [357] A. F. Andreev and M. Yu. Kagan, Hydrodynamics of rotating superfluid liquid, Sov. Phys. JETP **59**, 318 (1984).
- [358] I. M. Khalatnikov, *An Introduction to the Theory of Superfluidity*, Benjamin, N.Y., 1965.
- [359] V. Iordanskii, Vortex ring formation in a superfluid, Sov. Phys. JETP **48**, 708 (1965).
- [360] J. S. Langer and M.E. Fisher, Intrinsic critical velocity of a superfluid, Phys. Rev. Lett. **19**, 560 (1967).
- [361] T. Tsuzuki, Nonlinear waves in the Pitaevskii-Gross equation, J. Low Temp. Phys. **4**, 441 (1971).
- [362] P. V. E. McClintock and R. M. Bowley, *The Landau critical velocity*, Progress in Low Temp. Phys., Vol. XIV, Ed. by W.P. Halperin, Elsevier Sci. B.V., 1995.
- [363] S. V. Afanasiev et al. [NA49 Collab.], Energy dependence of pion and kaon production in central Pb+Pb collisions, Phys. Rev. C **66**, 054902 (2002).
- [364] C. Alt et al. [NA49 Collab.], Pion and kaon production in central Pb+Pb collisions at 20A and 30A GeV: Evidence for the onset of deconfinement, Phys. Rev. C **77**, 024903 (2008).
- [365] T. K. Nayak, Heavy ions: results from the large hadron collider. Pramana **79**, 719 (2012).
- [366] B. Abelev et al. [ALICE Collab.], Pion, kaon, and proton production in central Pb-Pb collisions at $\sqrt{s_{NN}} = 2.76$ TeV, Phys. Rev. Lett. **109**, 252301 (2012).

- [367] L. Adamczyk et al. [STAR Collab.], Bulk properties of the medium produced in relativistic heavy-ion collisions from the beam energy scan program, *Phys. Rev. C* **96**, 044904 (2017).
- [368] M. Kataja and P. V. Ruuskanen, Nonzero chemical potential and the shape of the p_T distribution of hadrons in heavy-ion collisions, *Phys. Lett. B* **243**, 181 (1990).
- [369] I. N. Mishustin, L. N. Satarov, J. Maruhn, H. Stöcker and W. Greiner, Pion production and Bose-enhancement effects in relativistic heavy-ion collisions, *Phys. Lett. B* **276**, 403 (1992).
- [370] D. Ferenc, U. Heinz, B. Tomasik, U. A. Wiedemann and J. G. Cramer, Universal pion freeze-out phase-space density. *Phys. Lett. B* **457**, 347 (1999).
- [371] B. Tomasik and U. Heinz, Flow effects on the freeze-out phase-space density in heavy-ion collisions. *Phys. Rev. C* **65**, 031902(R) (2002).
- [372] G. F. Bertsch, Meson phase-space density in heavy-ion collisions from interferometry, *Phys. Rev. Lett.* **72**, 2349 (1994); [Erratum *Phys. Rev. Lett.* **77**, 789 (1996)].
- [373] D. Teaney, Chemical freezeout in heavy ion collisions arXiv:nucl-th/0204023.
- [374] J. L. Goity and H. Leutwyler, On the mean free path of pions in hot matter, *Phys. Lett. B* **228**, 517 (1989).
- [375] P. Gerber, H. Leutwyler and J. L. Goity, Kinetics of an expanding pion gas, *Phys. Lett. B* **246**, 513 (1990).
- [376] C. M. Hung and E. V. Shuryak, Equation of state, radial flow and freezeout in high-energy heavy ion collisions, *Phys. Rev. C* **57**, 1891 (1998).
- [377] S. Pratt and K. Haglin, Hadronic phase space density and chiral symmetry restoration in relativistic heavy ion collisions, *Phys. Rev. C* **59**, 3304 (1999).
- [378] I. Melo and B. Tomasik, Reconstructing the final state of Pb+Pb collisions at $\sqrt{s_{NN}} = 2.76$ TeV, *J. Phys. G* **43**, 015102 (2016).
- [379] D. Prorok, Single freeze-out, statistics and pion, kaon and proton production in central Pb-Pb collisions at $\sqrt{s_{NN}} = 2.76$ TeV, *J. Phys. G* **43**, 055101 (2016).
- [380] B. Abelev et al. [ALICE Collaboration], Two- and three-pion quantum statistics correlations in Pb-Pb collisions at $\sqrt{s_{NN}} = 2.76$ TeV at the CERN Large Hadron Collider, *Phys. Rev. C* **89**, 024911 (2014).
- [381] J. Adam et al., [ALICE Collaboration], Multipion Bose–Einstein correlations in pp, p-Pb, and Pb-Pb collisions at energies available at the CERN Large Hadron Collider, *Phys. Rev. C* **93**, 054908 (2016).
- [382] S. V. Akkelin, R. Lednicky and Yu. M. Sinyukov, Correlation search for coherent pion emission in heavy ion collisions, *Phys. Rev. C* **65**, 064904 (2002).
- [383] C. Y. Wong and W. N. Zhang, Chaoticity parameter λ in Hanbury–Brown–Twiss interferometry. *Phys. Rev. C* **76**, 034905 (2007).
- [384] V. Begun and W. Florkowski, Bose–Einstein condensation of pions in heavy-ion collisions at the CERN Large Hadron Collider (LHC) energies. *Phys. Rev. C* **91**, 054909 (2015).

- [385] E. Shuryak, Strongly coupled quark-gluon plasma in heavy-ion collisions. *Rev. Mod. Phys.* **89**, 035001 (2017).
- [386] S. J. Putterman, *Superfluid hydrodynamics*, North-Holland Series in Low Temperature Physics. Volume 3, 1974.
- [387] V. V. Begun and M. I. Gorenstein, Bose–Einstein condensation in the relativistic pion gas: thermodynamic limit and finite size effects, *Phys. Rev. C* **77**, 064903 (2008).
- [388] Ya. B. Zeldovich and E. V. Levich, Bose condensation and shock waves in photon spectra, *Sov. Phys. JETP* **28**, 1287 (1969).
- [389] A. S. Kompaneets, The establishment of thermal equilibrium between quanta and electrons, *Sov. Phys. JETP* **4**, 730 (1957).
- [390] Yu. M. Kagan, V. V. Svistunov and G. V. Shlyapnikov, Kinetics of Bose condensation in an interacting Bose gas, *Sov. Phys. JETP* **74**, 279 (1992).
- [391] D. V. Semikoz and I. I. Tkachev, Kinetics of Bose condensation, *Phys. Rev. Lett.* **74**, 3093 (1995).
- [392] D. V. Semikoz and I. I. Tkachev, Condensation of bosons in kinetic regime, *Phys. Rev. D* **55**, 489 (1997).
- [393] D. N. Zubarev, *Nonequilibrium Statistical Thermodynamics*; Nauka: Moscow, Russia, 1971.
- [394] D. N. Zubarev, V. Morozov and G. Röpke, *Statistical Mechanics of Nonequilibrium Processes*; Akademie Verlag: Berlin, Germany, Volume I, II, 1996.
- [395] L. D. Landau, E. M. Lifshitz and L. P. Pitaevskii, *Electrodynamics of continuous media*, Vol. 8 (Pergamon Press, Oxford, 1984).
- [396] T. Anticic et al., [NA49 Collaboration], Phase-space dependence of particle-ratio fluctuations in Pb+Pb collisions from 20 A to 158AGeV beam energy. *Phys. Rev. C* **89**, 054902 (2014).
- [397] E. Kokoulina, Neutral pion fluctuations in pp collisions at 50 GeV by SVD-2. *Prog. Theor. Phys. Suppl.* **193**, 306 (2012).
- [398] V. N. Ryadovikov, Fluctuations of the number of neutral pions at high multiplicity in pp interactions at 50 GeV, *Phys. At. Nucl.* **75**, 989 (2012).
- [399] E. E. Kolomeitsev, M. E. Borisov and D. N. Voskresensky, Particle number fluctuations in a non-ideal pion gas. *EPJWeb Conf.* **182**, 02066 (2018).
- [400] J. I. Kapusta, Perspective on Tsallis statistics for nuclear and particle physics, *Intern. J. Modern Phys.* **30**, 2130006 (2021).
- [401] C.-Y. Wong and G. Wilk, Tsallis fits to spectra and multiple hard scattering in collisions at the LHC, *Phys. Rev. D* **87**, 114007 (2013).
- [402] C.-Y. Wong, G. Wilk, L. J. L. Cirto and C. Tsallis, From QCD-based hard-scattering to nonextensive statistical mechanical descriptions of transverse momentum spectra in high-energy pp and $p\bar{p}$ collisions, *Phys. Rev. D* **91**, 114027 (2015).
- [403] D. N. Voskresensky and O. V. Oreshkov, In medium effects in momentum distributions of nucleons in nucleus-nucleus collisions and the so called entropy puzzle, *Sov. J. Nucl. Phys.* **50**, 820 (1989).